

Copyright

By

Widianto

2006

**The Dissertation Committee for Widiyanto certifies that this is the approved
version of the following dissertation:**

**Rehabilitation of Reinforced Concrete Slab-column Connections
for Two-way Shear**

Committee:

Oguzhan Bayrak, Supervisor

Eric B. Becker

John E. Breen

James O. Jirsa

Sharon L. Wood

**Rehabilitation of Reinforced Concrete Slab-column Connections
for Two-way Shear**

by

Widianto, B.Sc., M.S.E.

Dissertation

Presented to the Faculty of the Graduate School of

The University of Texas at Austin

in Partial Fulfillment

of the Requirements

for the Degree of

Doctor of Philosophy

The University of Texas at Austin

August 2006

Dedication

*For my Mom and Dad
with all my love and respect*

Acknowledgements

This dissertation is part of the research project “Punching Shear Upgrade of Reinforced Concrete Flat Plates”, sponsored by National Science Foundation (NSF). The experimental work of this research project was conducted at the Phil M. Ferguson Structural Engineering Laboratory (FSEL) of The University of Texas at Austin. I express my gratitude to NSF for providing financial support to this research project.

I would like to extend my sincere appreciation to my dissertation committee. In particular, I would like to gratefully acknowledge the inspiration and the leadership provided by Prof. Oguzhan Bayrak as my supervisor. His advice and encouragement were invaluable in all stages of the research. Dr. Bayrak, thank you for all that you have taught me, not only about research but also about life in general. I would also like to thank Prof. James O. Jirsa. His assistance on this project and his insights have helped me significantly and he was always available to answer my questions. Dr. Jirsa, thank you also for your advice related to my job searching process. And I will always remember that you joined us in pouring concrete. I also gratefully acknowledge an extraordinary effort of the other members of my dissertation committee to improve the quality of my work. Dr. John Breen, Dr. Sharon Wood, and Dr. Eric Becker, thank you very much for all suggestions and detailed reviews of my dissertation. All of you viewed the work with a unique perspective.

I would like to extend my gratitude to my fellow students and co-workers at FSEL. I am especially indebted to Ying Tian and Jaime Argudo, with whom I worked together in the research projects related to slab-column connections sponsored by NSF. Ying and Jaime, thank you so much for sharing various research activities and teaching me many things. I am also grateful to Sarah Orton who taught me about an installation of fiber reinforced polymers (FRP) and helped me to stitch the FRP stirrups for one of the repaired specimens. I would also like to thank the undergraduate research assistants who contributed significantly to this project: Andrew Chronister, Gary Lehman, and Royce Owens.

The support staff at the FSEL has been very helpful in many ways. I thank the lab technicians: Blake Stasney, Dennis Phillip, Mike Bell, Eric Schell, and Mike Wason for their knowledge and assisting me in many phases of the experimental work. I thank the office staff: Barbara Howard, Ella Schwartz, Regina Forward, and Hortensia Peoples for making many details run smoothly.

Finally, I would like to express my heartfelt appreciation to my parents who made all of my education possible. Mom and Dad, your love, support, and encouragements during this academic phase in my life have been the cornerstone of this accomplishment. And I thank many friends who have supported me during my doctoral work, especially Thadea Silvana.

August 10, 2006

Rehabilitation of Reinforced Concrete Slab-column Connections for Two-way Shear

Publication No. _____

Widianto, Ph.D.

The University of Texas at Austin, 2006

Supervisor: Oguzhan Bayrak

Even though a reinforced concrete flat-plate structural system is an economical structural system, it is prone to brittle shear failure at slab-column connections, which may result in the progressive collapse of a building. For that reason, connections with insufficient two-way shear strength may need to be rehabilitated and rehabilitation can be a cost-effective alternative to replacement. This study focused on the rehabilitation of slab-column connections in existing structures built in the mid 20th century. The main objectives of this study were to develop efficient strengthening methods for deficient connections that do not

satisfy current code requirements and to develop efficient post-earthquake repair methods for connections that experience seismic-damage.

Experimental research on seven 2/3-scale interior slab-column connections was conducted to quantify the effects of low flexural reinforcement ratio and earthquake-damage. The efficiency of various rehabilitation techniques on improving the two-way shear strength of connections was also investigated. The test results show that two-way shear strength was sensitive to the slab top reinforcement ratio within the $(c+3h)$ region, where c is the column dimension and h is the slab thickness. The damage induced by lateral displacement cycles up to 1.25% lateral drift did not affect the two-way shear capacity of the specimens tested.

Three alternatives for repairing and strengthening slab-column connections that were experimentally evaluated are as follows:

The first alternative is the installation of steel collars on the column under the slab. In addition to increasing the deformation capacity, the two-way shear strength and the post-punching capacity under gravity loading, the installation of steel collars increased the lateral load capacity and prevented punching shear failure under reversed cyclic lateral loading.

The second alternative is the installation of external Carbon Fiber Reinforced Polymers (CFRP) stirrups. The installation of externally installed stirrups increased the deformation capacity and the two-way shear strength. In addition to enlarging the failure surface, which increased the number of flexural reinforcement contributing to the residual capacity following a punching shear

failure, a tightly knit array of CFRP stirrups helped to prevent stripping out of the tensile flexural reinforcement. For those reasons, the installation of CFRP stirrups was effective to increase the post-punching capacity.

And the third alternative is the application of well-anchored CFRP sheets on the tension side of the slab. The application of CFRP sheets increased the flexural capacity of the connection, limited the width of flexural cracks, and therefore increased the two-way shear strength. However, the deformation capacity was reduced. After punching shear failure occurred, the well-anchored CFRP sheets acted as tension bands and allowed the slab to carry substantial shear force through larger deformations. CFRP anchors were very effective to prevent delamination of CFRP sheets.

Guidelines for the evaluation and rehabilitation of existing slab-column connections are given. These guidelines are based on the results of the tests conducted in this study and on the synthesis of the literature review conducted as part of this project.

Table of Contents

CHAPTER 1 INTRODUCTION.....	1
1.1 GENERAL.....	1
1.1.1 <i>Common characteristics of flat-plate structural systems.....</i>	<i>1</i>
1.1.2 <i>Failures of flat-plate structures</i>	<i>3</i>
1.2 MOTIVATION.....	13
1.3 SCOPE.....	15
1.4 OBJECTIVES.....	17
1.5 ORGANIZATION	18
CHAPTER 2 LITERATURE REVIEW	20
2.1 GENERAL.....	20
2.2 SLAB COLUMN CONNECTIONS: FAILURE MODE.....	22
2.2.1 <i>Flexural strength of the slab</i>	<i>24</i>
2.3 PREVIOUS RESEARCH ON TWO-WAY SHEAR RESISTANCE OF SLABS	26
2.3.1 <i>Early research.....</i>	<i>26</i>
2.3.2 <i>Shear strength of flat-plates & research conducted in the USA</i>	<i>27</i>
2.3.2.1 Richart (1948).....	27
2.3.2.2 Hognestad (1953)	28
2.3.2.3 Elstner and Hognestad (1956)	29
2.3.2.4 Whitney (1957).....	30
2.3.2.5 Moe (1961)	31
2.3.2.5.1 Design considerations.....	34
2.3.2.6 ACI-ASCE Committee 326 (1962).....	34
2.3.2.7 Guralnick and LaFraugh (1963)	36
2.3.2.8 Magura and Corley (1969).....	37
2.3.2.9 Criswell (1970, 1974)	37

2.3.2.10	ACI-ASCE Committee 426 (1977).....	39
2.3.2.11	Hawkins and Mitchell (1979)	39
2.3.2.12	Moehle et al. (1988).....	39
2.3.2.13	ACI-ASCE Committee 352 (1988).....	39
2.3.3	<i>Shear strength of flat-plates and research conducted outside the US</i>	40
2.3.3.1	Yitzhaki (1966).....	40
2.3.3.2	Regan (1981), Regan and Braestrup (1985)	40
2.3.3.3	Nolting (1984)	41
2.3.3.4	Rankin and Long (1987).....	41
2.3.3.5	Yamada et al. (1992).....	44
2.3.3.6	Strip model (Alexander and Simmonds 1992).....	44
2.3.3.7	Gardner (1995, 1996), Gardner and Shao (1996)	49
2.3.3.8	Sherif and Dilger (1996).....	50
2.4	ACI DESIGN PROVISIONS: FLAT-PLATE SLAB-COLUMN CONNECTIONS.....	51
2.4.1	<i>Provisions for two-way shear strength</i>	51
2.4.1.1	Joint Committee of 1924	51
2.4.1.2	ACI 318-41, ACI 318- 47, ACI 318-51.....	51
2.4.1.3	ACI 318-56.....	52
2.4.1.4	ACI 318-63.....	52
2.4.2	<i>ACI design provisions for two-way shear strength: Observations of Alexander and Hawkins (2005).....</i>	54
2.4.3	<i>Provisions related to unbalanced moment transfer under gravity loads</i>	55
2.4.3.1	Calculation of unbalanced moment	55
2.4.3.2	Concentration of reinforcement.....	56
2.4.4	<i>Seismic provisions for flat-plate structures</i>	58
2.5	DIFFERENT BUILDING CODES PROVISIONS FOR TWO-WAY SHEAR STRENGTH OF INTERIOR SLAB-COLUMN CONNECTIONS.....	59
2.5.1	<i>American Concrete Institute Code (ACI 318-05).....</i>	61
2.5.2	<i>Canadian Standard (CSA-A 23.3-04)</i>	61
2.5.3	<i>Building code provisions: Comparison.....</i>	62

2.6	EFFECT OF FLEXURAL REINFORCEMENT ON PUNCHING SHEAR.....	63
2.6.1	<i>Flexural reinforcement ratio</i>	63
2.6.2	<i>Concentration of reinforcement towards the column or loaded area</i>	64
2.6.3	<i>Compression steel</i>	65
2.7	RESIDUAL CAPACITY AFTER PUNCHING SHEAR FAILURE.....	66
2.8	FIBER REINFORCED POLYMERS (FRP).....	68
2.8.1	<i>Characteristics of FRP used for structural rehabilitation</i>	69
2.8.2	<i>Structural performance of FRP under elevated temperatures</i>	71
2.8.3	<i>FRP sheets versus steel plate</i>	71
2.8.4	<i>Debonding of FRP</i>	72
2.9	PREVIOUS RESEARCH ON STRENGTHENING AND REPAIR OF SLAB-COLUMN CONNECTIONS FOR TWO-WAY SHEAR.....	77
2.9.1	<i>Strengthening methods</i>	78
2.9.1.1	Adding steel bars, steel rods, and shear bolts.....	78
2.9.1.2	Steel jacketing.....	81
2.9.1.3	Externally installed CFRP stirrups.....	83
2.9.1.3.1	Monotonic concentric load tests.....	84
2.9.1.3.2	Monotonic eccentric load tests.....	87
2.9.1.3.3	Reversed cyclic load tests.....	88
2.9.1.4	Increasing column size.....	90
2.9.1.5	Applying FRP sheets or strips.....	94
2.9.2	<i>Repair methods</i>	103
2.9.2.1	Insertion of steel bolts.....	103
2.9.2.2	Steel jacketing.....	104
2.9.2.3	Substitution of the damaged concrete (concrete patching).....	107
2.9.2.4	Substitution of the damaged concrete and installation of the steel beams.....	109
2.9.2.5	Substitution of the damaged concrete, injection of epoxy, and steel jacketing.....	110
2.9.2.6	Epoxy repair.....	112
2.9.2.7	Increasing column size.....	112

2.10 SUMMARY	121
2.10.1 <i>Behavior of connection, previous research, recommendations, and code provisions on two-way shear strength</i>	121
2.10.2 <i>Rehabilitation</i>	124
CHAPTER 3 EXPERIMENTAL PROGRAM	128
3.1 GENERAL.....	128
3.2 DESIGN OF TEST SPECIMENS.....	129
3.2.1 <i>Prototype structure</i>	129
3.2.2 <i>Test specimens</i>	132
3.3 TEST SPECIMENS AND PARAMETERS	136
3.4 SPECIMEN CONSTRUCTION	140
3.5 MATERIAL PROPERTIES	149
3.5.1 <i>Concrete</i>	149
3.5.2 <i>Steel reinforcing bars</i>	150
3.5.3 <i>CFRP</i>	151
3.5.4 <i>Epoxy</i>	151
3.6 TEST SETUP.....	152
3.7 INSTRUMENTATION.....	156
3.7.1 <i>Strain measurements</i>	156
3.7.2 <i>Load measurements</i>	158
3.7.3 <i>Displacement measurements</i>	159
3.7.4 <i>Data acquisition and monitoring</i>	160
3.8 TEST PROCEDURE.....	161
3.8.1 <i>Specimen installation</i>	161
3.8.2 <i>Changing boundary conditions</i>	165
3.8.3 <i>Rehabilitation</i>	165
3.8.4 <i>Cutting the specimen</i>	166
3.9 SUMMARY	168

CHAPTER 4 EXPERIMENTAL RESULTS AND DISCUSSION.....	169
4.1 GENERAL.....	169
4.2 SPECIMENS G0.5 AND G1.0.....	169
4.3 SPECIMENS RCG0.5 AND RCG1.0.....	171
4.3.1 Components of steel collars.....	172
4.3.2 Rehabilitation process.....	174
4.3.3 Failure surfaces.....	183
4.3.3.1 RcG0.5.....	183
4.3.3.2 RcG1.0.....	188
4.4 SPECIMEN L0.5.....	192
4.5 SPECIMEN LG0.5.....	199
4.6 SPECIMEN LRSTG0.5.....	202
4.6.1 Rehabilitation process.....	202
4.6.2 Actual hole locations and critical shear perimeter.....	207
4.6.3 Failure surface.....	208
4.7 LRSHG0.5.....	212
4.7.1 Rehabilitation process.....	212
4.7.2 CFRP strain.....	222
4.7.3 Failure surface.....	224
4.8 SPECIMEN LG1.0.....	231
4.9 SPECIMEN RCL1.0.....	234
4.9.1 Behavior during a simulated seismic test.....	236
4.9.2 Failure surface.....	242
4.10 SUMMARY OF TEST RESULTS AND DISCUSSION.....	246
4.10.1 Concentric punching shear test.....	246
4.10.1.1 Two-way shear strength.....	247
4.10.1.1.1 Undamaged, unstrengthened specimens (Effect of flexural reinforcement ratio).....	253
4.10.1.1.2 Effect of seismic damage.....	255
4.10.1.1.3 Effectiveness of steel collars.....	256

4.10.1.1.4	Effectiveness of externally installed CFRP stirrups.....	256
4.10.1.1.5	Effectiveness of well-anchored CFRP sheets	257
4.10.1.2	Residual capacity after punching shear failure	258
4.10.1.2.1	Effect of flexural reinforcement ratio on residual capacity.....	260
4.10.1.2.2	Effect of seismic damage on residual capacity	260
4.10.1.2.3	Effectiveness of steel collars on residual capacity	261
4.10.1.2.4	Effectiveness of externally installed CFRP stirrups on residual capacity	261
4.10.1.2.5	Effectiveness of well-anchored CFRP sheets on residual capacity	262
4.10.1.2.6	Effectiveness of top slab reinforcing bars on residual capacity	262
4.10.2	<i>Simulated seismic tests</i>	263
4.10.2.1	Effect of flexural reinforcement ratio	263
4.10.2.2	Effectiveness of steel collars	264

CHAPTER 5 EVALUATION AND REHABILITATION GUIDELINES . 267

5.1	GENERAL.....	267
5.2	EVALUATION.....	268
5.2.1	<i>Damage level</i>	270
5.3	REHABILITATION.....	271
5.3.1	<i>General considerations for gravity loads</i>	271
5.3.2	<i>General considerations for seismic loads</i>	272
5.3.3	<i>General considerations for rehabilitation using FRP</i>	273
5.4	REHABILITATION USING STEEL COLLARS.....	275
5.4.1	<i>General</i>	275
5.4.2	<i>Size</i>	276
5.4.3	<i>Stiffness</i>	276
5.4.4	<i>Clamping force</i>	277
5.5	REHABILITATION USING EXTERNALLY INSTALLED CFRP STIRRUPS	278
5.5.1	<i>General</i>	278
5.5.2	<i>Spacing of stirrups</i>	279
5.5.3	<i>Strength calculations</i>	279

5.5.3.1	Shear strength inside the CFRP-reinforced zone	280
5.5.3.2	Shear strength outside the CFRP-reinforced zone	282
5.5.4	<i>Proposed rehabilitation design procedure</i>	282
5.5.5	<i>Example calculations – Specimen LRstG0.5</i>	285
5.6	REHABILITATION USING EXTERNALLY INSTALLED CFRP SHEETS	286
5.6.1	<i>General</i>	286
5.6.2	<i>CFRP Anchors</i>	287
5.6.2.1	Position	287
5.6.2.2	Cross-sectional area	289
5.6.2.3	Depth	289
5.6.3	<i>Length of the CFRP sheets</i>	289
5.6.4	<i>Area of the CFRP sheets</i>	289
5.6.5	<i>Verification using experimental results</i>	294
5.7	SUMMARY	295
CHAPTER 6 SUMMARY AND CONCLUSIONS.....		296
6.1	GENERAL.....	296
6.2	SUMMARY	296
6.3	CONCLUSIONS	298
6.3.1	<i>General behavior of connections in older structures</i>	298
6.3.2	<i>Effect of flexural reinforcement ratio</i>	299
6.3.3	<i>Estimation of the capacity of existing connections</i>	300
6.3.4	<i>Effect of seismic damage</i>	301
6.3.5	<i>Residual capacity after punching shear failure</i>	301
6.3.6	<i>Rehabilitation</i>	302
6.3.6.1	Installation of steel collars on the column under the slab	302
6.3.6.2	Installation of external CFRP stirrups	303
6.3.6.3	Application of well-anchored CFRP sheets	303
6.4	RECOMMENDATIONS FOR FUTURE RESEARCH	304

APPENDIX A CRACK PATTERNS	306
A.1 GENERAL.....	306
A.2 SPECIMEN G0.5	306
A.2.1 Top surface.....	306
A.3 SPECIMEN RCG0.5	308
A.3.1 Top surface.....	308
A.3.2 Bottom surface	308
A.4 SPECIMEN G1.0	309
A.4.1 Top surface.....	309
A.5 SPECIMEN RCG1.0	310
A.5.1 Top surface.....	310
A.5.2 Bottom surface	310
A.6 SPECIMEN L0.5.....	311
A.6.1 Top surface.....	311
A.6.2 Bottom surface	313
A.7 SPECIMEN LG0.5.....	315
A.7.1 Simulated seismic test, top surface	315
A.7.2 Simulated seismic test, bottom surface	316
A.7.3 Punching shear test, top surface	317
A.8 SPECIMEN LRSTG0.5	318
A.8.1 Simulated seismic test, top surface	318
A.8.2 Simulated seismic test, bottom surface	319
A.8.3 Punching shear test, top surface	320
A.8.4 Punching shear test, bottom surface	321
A.9 SPECIMEN LRSHG0.5.....	321
A.9.1 Simulated seismic test, top surface	321
A.9.2 Simulated seismic test, bottom surface	323
A.9.3 Punching shear test, top surface	323
A.10 SPECIMEN LG1.0.....	324

<i>A.10.3</i>	<i>Punching shear test, top surface</i>	326
A.11	SPECIMEN RCL1.0	327
<i>A.11.1</i>	<i>Simulated seismic test, top surface</i>	327
<i>A.11.2</i>	<i>Simulated seismic test, bottom surface</i>	327
References		328

List of Tables

Table 2.1 Criswell’s test results	38
Table 2.2 Code provisions for basic two-way shear strength.....	60
Table 2.3 Percent increase in ultimate capacities of the strengthened specimens	106
Table 3.1 Prototype structure designed using different ACI codes	130
Table 3.2 Test program	137
Table 3.3 Concrete cylinder compressive strength.....	150
Table 3.4 CFRP properties	151
Table 4.1 Failure loads and stresses	249
Table 4.2 Residual capacity after punching shear failure.....	260
Table 5.1 Relative effectiveness of different rehabilitation techniques.....	272
Table 5.2 Geometric and material properties of specimen LRstG0.5	285
Table 5.3 Geometric and material properties of specimen LRshG0.5.....	294

List of Figures

Figure 1.1 Flat-plate structures.....	2
Figure 1.2 Punching shear failure at an interior connection (Feld 1964)	4
Figure 1.3 Punching shear failure at a connection with an opening (Feld 1964)	4
Figure 1.4 Columns remained standing after the progressive collapse (Feld 1964).....	5
Figure 1.5 Incipient punching shear failure (Rosenblueth and Meli 1986).....	7
Figure 1.6 Complete collapse of a waffle-flat-plate structure (EERI 1997).....	8
Figure 1.7 Punching shear failure in post-tensioned slab (Mitchell et al. 1990)	9
Figure 1.8 Collapse of Bullock’s Department Store (EERI 1997)	10
Figure 1.9 Close-up of a slab-column joint at Bullock’s Department Store (Mitchell et al. 1995) 10	
Figure 1.10 Seismic-damaged interior connections	11
Figure 1.11 Sampoong Department Store collapse	12
Figure 2.1 Behavior of slab-column connections.....	23
Figure 2.2 Typical yield-line pattern.....	25
Figure 2.3 Test results used in Moe’s statistical analysis (1961)	33
Figure 2.4 Test on nine panels of three-quarters scale of a flat-plate structure	36
Figure 2.5 Criswell’s test specimen	38
Figure 2.6 Typical yield-line pattern.....	43
Figure 2.7 Geometry of radial strips (Alexander 1999)	45
Figure 2.8 FBD of one-half radial strip (Alexander and Simmonds 1992)	46
Figure 2.9 Simplified FBD of radial strip	46
Figure 2.10 FBD of a concentrically loaded interior connection (Afhami et al. 1998).....	48
Figure 2.11 Ultimate capacity of slab-column connection (Alexander and Hawkins 2005).....	55
Figure 2.12 Different assumptions for pattern loading.....	56
Figure 2.13 Two-way shear strength according to different building code provisions	62

Figure 2.14 Generic characteristics of FRP (http://www.shef.ac.uk/~ccc/frp/what_is_frp.htm) ..	69
Figure 2.15 Details of U-anchor (Khalifa et al. 1999).....	75
Figure 2.16 Details of CFRP anchors (Burr 2004).....	75
Figure 2.17 Fiber anchors (Teng et al. 2000)	76
Figure 2.18 NEFMAC anchors (Mostafa 2005).....	77
Figure 2.19 Installation of reinforcing bars (Hassanzadeh and Sundqvist 1998).....	78
Figure 2.20 Shear reinforcement using steel rods and shear bolts (El-Salakawy et al. 2003).....	79
Figure 2.21 Strengthening using shear bolts (Adetifa and Polak 2005)	80
Figure 2.22 Effectiveness of shear bolts (Adetifa and Polak 2005)	81
Figure 2.23 Details of steel jacketing (Martinez et al. 1994)	82
Figure 2.24 Test results of Martinez et al. (1994)	83
Figure 2.25 Concentric loading test setup (Binici 2003).....	84
Figure 2.26 CFRP stitching (Binici 2003).....	85
Figure 2.27 Concentric loading test results for pattern A (Binici 2003)	86
Figure 2.28 Concentric loading test results for pattern B (Binici 2003).....	86
Figure 2.29 Eccentric loading test results (Binici 2003)	87
Figure 2.30 Test setup (Stark 2003).....	89
Figure 2.31 Backbone curves (Stark 2003).....	90
Figure 2.32 Shotcrete column head (Hassanzadeh and Sundqvist 1998).....	91
Figure 2.33 Steel collars (Hassanzadeh and Sundqvist 1998).....	91
Figure 2.34 Column capital and post punching geometry (Luo and Durrani 1994).....	92
Figure 2.35 Test setup and details of specimens (Luo and Durrani 1994).....	93
Figure 2.36 Effect of GFRP on ultimate capacity (Chen and Li 2000).....	95
Figure 2.37 Debonding failure of CFRP strengthened slab (Limam et al. 2003).....	96
Figure 2.38 CFRP sheet layout and failure surface (Harajli and Soudki 2003)	97
Figure 2.39 CFRP sheets applied around the slab opening (Casadei et al. 2003)	98
Figure 2.40 Seismic strengthening using CFRP sheets (Johnson and Robertson 2004)	99

Figure 2.41 CFRP shear studs (Johnson and Robertson 2004)	101
Figure 2.42 Strengthening of edge connection with FRP sheets (El-Salakawy et al. 2004)	102
Figure 2.43 Combination of FRP sheets and steel bolts (El-Salakawy et al. 2004)	103
Figure 2.44 Steel bolts configurations (Ramos et al. 2000)	104
Figure 2.45 Repair using steel jacketing (Ebead and Marzouk 2002).....	106
Figure 2.46 Details of concrete patching (Ospina et al. 2001)	108
Figure 2.47 Steel beam as a column head (Ramos et al. 2000).....	109
Figure 2.48 Seismic repair using steel jacketing (Farhey et al. 1995).....	111
Figure 2.49 Installation of steel collars after 1985 Mexico City Earthquake (Iglesias 1986)	113
Figure 2.50 Details of column capital (Martinez et al. 1994).....	114
Figure 2.51 Details of CFRP sheets application.....	115
Figure 2.52 Repair using CFRP strips (Mosallam and Mosalam 2003).....	116
Figure 2.53 Flexural strengthening using CFRP strips (Ebead and Marzouk 2004).....	117
Figure 2.54 Load-deformation response and failure surface of the CFRP-strengthened specimen (Ebead and Marzouk 2004)	118
Figure 2.55 Connection repaired by a combination of CFRP and steel bolts (Ebead 2002)	119
Figure 2.56 Earthquake-damaged connection and application of CFRP sheets (Robertson and Johnson 2001).....	120
Figure 3.1 Notation for minimum length requirement of slab reinforcement	131
Figure 3.2 Top mat of 0.5% flexural reinforcement within (c+3h)	133
Figure 3.3 Top mat of 1.0% flexural reinforcement within (c+3h)	134
Figure 3.4 Bottom mat of flexural reinforcement	135
Figure 3.5 Specimen notation.....	137
Figure 3.6 Typical displacement protocol.....	138
Figure 3.7 Formwork	141
Figure 3.8 Column reinforcing cage.....	142
Figure 3.9 Discontinued bottom flexural reinforcement	143

Figure 3.10 Slab reinforcement with 0.5% steel within (c+3h).....	144
Figure 3.11 Slab reinforcement with 1.0% steel within (c+3h).....	145
Figure 3.12 Concrete placement: slab and lower column	146
Figure 3.13 Compacting concrete	147
Figure 3.14 Construction joint at slab-column connection.....	147
Figure 3.15 Concrete placement: upper column.....	148
Figure 3.16 Lifting a specimen from the formwork	149
Figure 3.17 Schematic of the test setup.....	154
Figure 3.18 Test setup: Simulated seismic test	155
Figure 3.19 Test setup: Punching shear test	156
Figure 3.20 Typical strain gage locations used in simulated seismic tests.....	157
Figure 3.21 Typical strain gage locations used in punching shear tests	158
Figure 3.22 Load and displacement measurements.....	159
Figure 3.23 Linear potentiometers	160
Figure 3.24 Position of vertical struts: simulated seismic test.....	162
Figure 3.25 Installation of a test specimen	163
Figure 3.26 Position of vertical struts: punching shear test.....	164
Figure 3.27 Schematic of the cuts	167
Figure 3.28 Saw cutting the specimen.....	167
Figure 4.1 Failure surface of specimen G0.5	170
Figure 4.2 Failure surface of specimen G1.0	171
Figure 4.3 Components of the collars	173
Figure 4.4 Collar after installation	174
Figure 4.5 Concrete surface before and after preparation	175
Figure 4.6 Roughening the column surface.....	176
Figure 4.7 Installation of the shorter steel tubes.....	178

Figure 4.8 After installation of the shorter steel tubes	178
Figure 4.9 Installation of the longer steel tubes	179
Figure 4.10 Installation of the angles	180
Figure 4.11 Gap fillers	181
Figure 4.12 Mixing epoxy	182
Figure 4.13 Pouring epoxy into cracks.....	182
Figure 4.14 Significant vertical deflection at failure of RcG0.5	184
Figure 4.15 Top view of the failure surface of RcG0.5.....	185
Figure 4.16 Bottom view of the failure surface of RcG0.5	186
Figure 4.17 Angles of punching cones of G0.5 and RcG0.5.....	187
Figure 4.18 Cracks filled with epoxy	188
Figure 4.19 Top view of the failure surface of RcG1.0.....	190
Figure 4.20 Bottom view of the failure surface of RcG1.0	191
Figure 4.21 Angles of punching cones of G1.0 and RcG1.0.....	192
Figure 4.22 Lateral displacement excursions	193
Figure 4.23 Lateral load versus drift response of L0.5.....	194
Figure 4.24 Top failure surface of L0.5	197
Figure 4.25 Bottom failure surface of L0.5	198
Figure 4.26 Punching cone of L0.5	199
Figure 4.27 Damage in specimen LG0.5 at 1.25% drift.....	200
Figure 4.28 Failure surface after punching shear test.....	201
Figure 4.29 Externally installed CFRP stirrups.....	203
Figure 4.30 Surface preparation	205
Figure 4.31 Concrete surface before and after grinding and chamfering	206
Figure 4.32 Actual hole locations	208
Figure 4.33 Significant vertical displacement at failure of LRstG0.5.....	210
Figure 4.34 Failure surfaces of LRstG0.5	211

Figure 4.35 Failure surface of LRstG0.5.....	212
Figure 4.36 Surface preparation before the application of CFRP sheets.....	216
Figure 4.37 Concrete surfaces before and after surface preparation	217
Figure 4.38 Cracks were sealed with silicone	218
Figure 4.39 Installation of CFRP sheets.....	219
Figure 4.40 Preparation and installation of CFRP anchors	220
Figure 4.41 After installation of CFRP sheets and CFRP anchors.....	221
Figure 4.42 CFRP strain profile along the West-East sheet	223
Figure 4.43 CFRP strain profile across the North-South sheet	224
Figure 4.44 Top view of failure surface of LRshG0.5	227
Figure 4.45 Close-up view of CFRP anchors at failure.....	228
Figure 4.46 Bottom view of failure surface of LRshG0.5.....	229
Figure 4.47 Failure surface of LRshG0.5.....	230
Figure 4.48 CFRP anchor.....	230
Figure 4.49 Damage in specimen LG1.0 at 1.25% drift.....	232
Figure 4.50 Punching shear failure surfaces of LG1.0	233
Figure 4.51 Epoxy pouring after punching shear failure of LG1.0	235
Figure 4.52 After epoxy pouring in RcL1.0.....	235
Figure 4.53 RcL1.0 just before the test	236
Figure 4.54 Lateral force versus drift of RcL1.0.....	238
Figure 4.55 One-way shear failure of RcL1.0.....	239
Figure 4.56 Flexural cracks and concentration of rotation at 3.25% drift	240
Figure 4.57 Close-up view of the collars at 3.25% drift.....	241
Figure 4.58 Bottom slab surface of RcL1.0 at the end of the test	242
Figure 4.59 Failure surface on the West side of LG1.0 and RcL1.0	244
Figure 4.60 Failure surface on the North side of LG1.0 and RcL1.0	246
Figure 4.61 Results of the punching shear tests	247

Figure 4.62 Estimated strength from building codes versus measured strength.....	250
Figure 4.63 Estimated strength from researchers versus measured strength.....	253
Figure 4.64 Reinforcing bar strains.....	255
Figure 4.65 Lateral load versus drift of specimens LG1.0 and L0.5.....	264
Figure 4.66 Lateral load versus drift of specimens LG1.0 and RcL1.0.....	265
Figure 5.1 Flowchart for evaluation and rehabilitation.....	268
Figure 5.2 Damage after reversed cyclic displacements up to 1.25% drift.....	271
Figure 5.3 Simplified free-body diagram of steel collars.....	277
Figure 5.4 Design procedure for rehabilitation using external CFRP stirrups.....	284
Figure 5.5 Recommended details of CFRP sheets and anchors.....	288
Figure 5.6 Design procedure for rehabilitation using external CFRP sheets.....	291
Figure 5.7 Procedure for calculating M_o	292
Figure 5.8 Procedure for calculating M_F	293

CHAPTER 1

Introduction

1.1 GENERAL

1.1.1 Common characteristics of flat-plate structural systems

Flat-plate structural systems consist of slabs with a uniform thickness that are supported directly on columns without any beams, drop panels, or column capitals (Figure 1.1). The use of flat-plate structural systems was common for office and residential construction up to substantial heights in the period around 1950-1960 (FEMA 1997). Durrani et al. (1995) indicated that in the central and eastern regions of the United States (US), there are many older flat-slab buildings designed and detailed to resist gravity loads only. They further stated that these buildings are typically 5 to 15 stories high and do not have shear walls except for the elevator shafts and stairwells. The floor slabs in these buildings can be categorized as lightly reinforced and the slab-column connections do not have the appropriate reinforcement details for seismic resistance. Sherif and Dilger (1996) reported that most slabs in flat plate structures have a flexural reinforcement ratio of less than 1%. Moehle (1996) indicated that in western US, gravity load carrying system is commonly ignored for resisting seismic forces. However, the gravity load carrying system must be designed to carry the gravity loads under the design lateral deformations. Structural drawings of several flat-plate structures located in western US, examined as part of this research, show that those structures have roughly about 0.5% flexural reinforcement ratio in the column strip and do not have shear reinforcement.



Figure 1.1 Flat-plate structures

Flat-plate structures offer several advantages over other reinforced concrete structural systems. Advantageous characteristics of flat-plate systems are as follows:

- Providing more clear space for given story heights;
- Reducing the required total story height. In areas of absolute height restrictions, flat-plate structures may enable one to have an additional floor for approximately every 10 floors, as compared with slabs supported

on beams. Lower building heights also result in reductions of wind load and building weight, which may reduce the cost of foundation (Park and Gamble 2000).

- Minimizing obstacles to the location of mechanical and electrical services;
- Requiring relatively simple formwork, leading to reduction in construction cost and time. Gardner and Shao (1996) indicated that in extreme cases, a new floor can be cast every 2 or 3 days.

The greatest disadvantage of flat-plate structural systems is the risk of brittle punching shear failure at slab-column connections. Punching failure, or two-way shear failure, is associated with a particular collapse mechanism in which the column together with an attached portion of the slab pushes through the surrounding slab. The likelihood of punching shear failures at slab-column connections is higher when lateral forces due to wind or earthquake loadings cause substantial unbalanced moments to be transferred between the slab and the column. Regan (1981) indicated that the shear failure at an interior connection may significantly increase the shear demand at neighboring connections and result in larger load eccentricities because of the inequality of the residual spans. He further pointed out that a failure initiated at one connection can easily spread horizontally. Once this happens the slab falls onto the next lower floor where the extra loading is magnified by dynamic effects. In short, a punching shear failure in one connection can lead to the progressive collapse of an entire structure.

1.1.2 Failures of flat-plate structures

There have been several cases of punching shear failure of connections in flat-plate structures during and after construction. Several failures of flat-plate structures initiated by punching shear failure are presented in this section.

A typical punching shear failure surface on the top side of an interior slab-column connection is shown in Figure 1.2. The failure surface intersects the bottom side of the slab right at the slab-column intersection, as shown in Figure 1.3. It should be noted that the opening adjacent to the column (Figure 1.3), interrupts continuity of reinforcement and reduces the concrete contribution to shear strength.



Figure 1.2 Punching shear failure at an interior connection (Feld 1964)

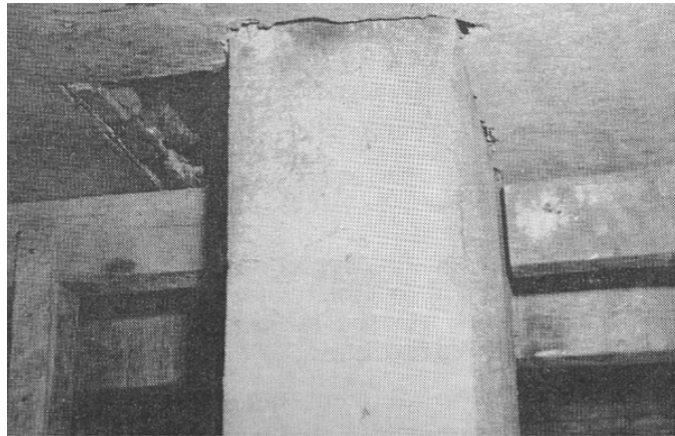


Figure 1.3 Punching shear failure at a connection with an opening (Feld 1964)

On October 3, 1956, the progressive collapse of a flat-plate office building in Jackson, Michigan occurred when concrete had been placed in the fourth floor that was shored to the second floor (Feld 1964). At failure, the second floor was only several weeks old. Almost all columns remained standing full height after the collapse (Figure 1.4). It can also be seen from Figure 1.4 that there were only very few reinforcing bars projecting from the free-standing columns at the floor levels.



Figure 1.4 Columns remained standing after the progressive collapse (Feld 1964)

On January 25, 1971, a sixteen-story flat-slab apartment building at 2000 Commonwealth Avenue, Boston, Massachusetts collapsed when concrete was being placed on the mechanical room above the main roof (Granger et al. 1971). Workers said that the progressive collapse was initiated by a punching shear failure of an interior slab-column connection on the roof. Granger et al. (1971) indicated that the failure was likely preceded and aggravated by flexural yielding in the roof slab. The contributing factors to failure were as follows: (i) premature

removal of formwork, (ii) very low early-age concrete strength because of cold temperatures, (iii) poor workmanship in placing rebars, (iv) insufficient length of rebars, and (v) insufficient slab thickness.

On March 2, 1973, a 30-story apartment building, the Skyline Center at Bailey's Crossroads, Alexandria, Virginia collapsed during construction (Kaminetzky 1991). The collapse was triggered by a punching shear failure at an interior column on the 23rd floor due to premature removal of formwork between the 22nd and 23rd floors.

On March 27, 1981, a five-story apartment building in Cocoa Beach, Florida, collapsed when workers were finishing the concrete at the fifth floor (Kaminetzky 1991). Several factors contributed to the failure: (i) insufficient two-way shear strength because punching shear was not checked in design, (ii) a construction error that resulted in a reduction of the effective depth, and (iii) inadequate reshoring. Kaminetzky (1991) also reported that there were sufficient warnings in the form of excessive slab deflections and "*spider cracks*" at the slab-column connections before the collapse. However, those warnings were not regarded.

Many punching shear failures also occurred during strong ground motions. ACI-ASCE Committee 426 (1974) reported that punching shear failure at slab-column connections were observed in the 1964 Alaska, 1967 Venezuela, and 1971 San Fernando earthquakes.

In the 1985 Mexico City Earthquake, the common failure mode for waffle-flat-plate structures was shear failure at slab-column connections (Meli 1986, Meli and Avila 1989, Rodriguez and Diaz 1989). Rosenblueth and Meli (1986) reported that 91 waffle-flat-plate structures collapsed and 44 others were severely damaged in the 1985 Mexico City Earthquake. Figures 1.5 and 1.6 show an incipient punching shear failure at an interior slab-column connection and a

complete collapse of a waffle-flat-plate structure, respectively, after the 1985 Mexico City Earthquake. It is interesting to note that there were only very few flexural reinforcing bars passing through the column (Figure 1.6) and that these bars could not provide secondary resistance once punching failure occurred.

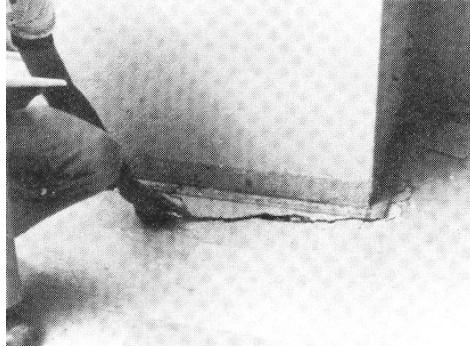


Figure 1.5 Incipient punching shear failure (Rosenblueth and Meli 1986)



Figure 1.6 Complete collapse of a waffle-flat-plate structure (EERI 1997)

Figure 1.7 shows the incipient punching shear failure in one of the interior slab-column connections in Baybridge Office Plaza, Emeryville, after the 1989 Loma Prieta Earthquake. The floor slabs were two-way post-tensioned flat-plates with post-tensioned beams only around the perimeter of the building.



Figure 1.7 Punching shear failure in post-tensioned slab (Mitchell et al. 1990)

In the 1994 Northridge Earthquake, punching shear failure caused the progressive collapse of Bullock's Department Store in the Northridge Fashion Center (Figure 1.8). The close-up view of one of the connections at a lower level after the collapse is shown in Figure 1.9. As can be observed in Figure 1.9, only the top reinforcing bars in one direction passed through the column. These top bars were not effective in preventing progressive collapse after punching shear failure because the top bars ripped out of the top surface of the slab (Mitchell et al. 1995). Figure 1.10 shows interior connection damages in a flat-slab building structure that was “red-tagged” following the 1994 Northridge Earthquake (Sabol 1994). The damage followed the outline of the drop panel and exposed flexural rebars in many locations. Vertical offsets of the slab on the order of 0.5 to 0.75 inches were observed in severely damaged connections.



Figure 1.8 Collapse of Bullock's Department Store (EERI 1997)



*Figure 1.9 Close-up of a slab-column joint at Bullock's Department Store
(Mitchell et al. 1995)*

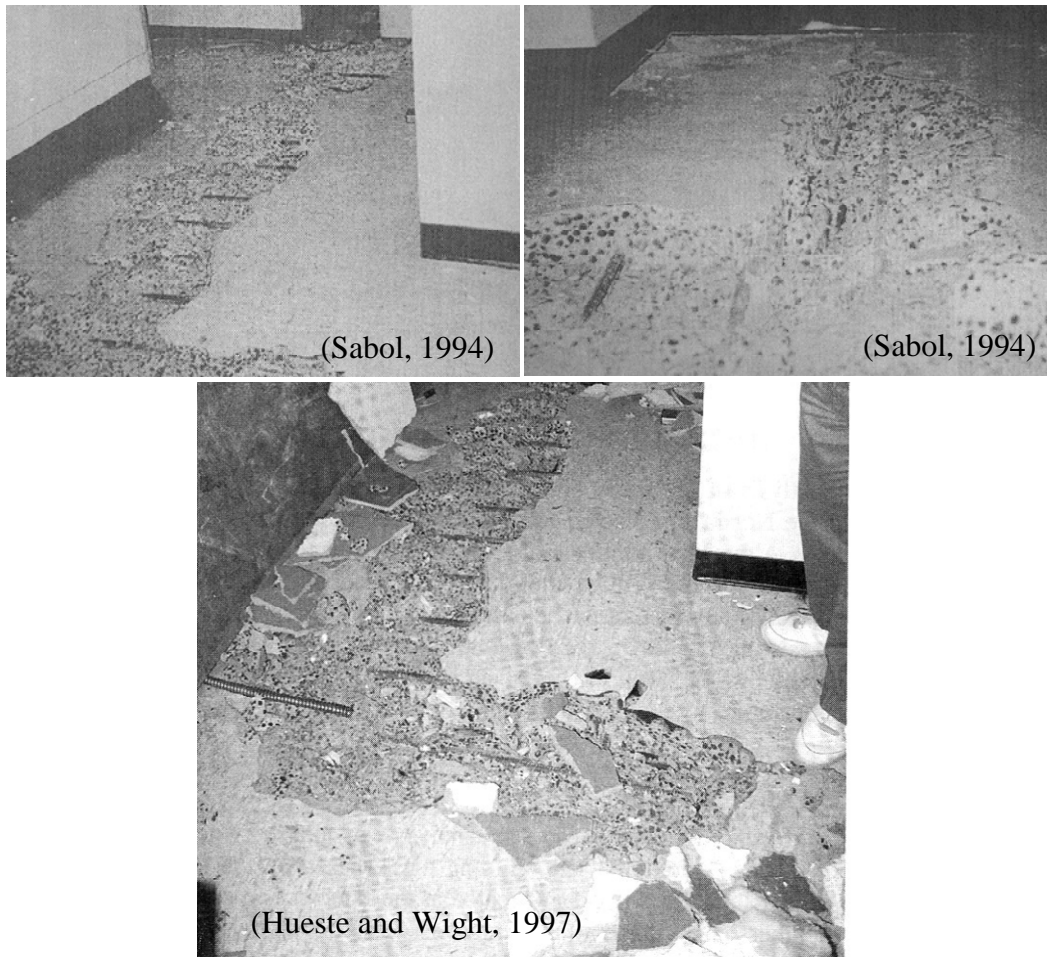


Figure 1.10 Seismic-damaged interior connections

Punching shear failure has also occurred under gravity loads. On June 29 1995, the north wing of the Sampoong Department Store, Seoul, South Korea collapsed (Figure 1.11) due to punching shear failure of an interior connection on the fifth floor (Gardner et al. 2002). The building was a 5-story flat-plate building with 0.47% flexural reinforcement ratio in slab-column connections. The most important causes of the collapse were the reduced slab depth and the excessive loads applied to the building due to change of use of the fifth floor from a roller

skating rink to a restaurant, which increased the dead loads by 35% (Gardner et al. 2002).



(<http://esl.fis.edu/students/projects/disaster/sampoong.htm>)



(Gardner et al. 2002)

Figure 1.11 Sampoong Department Store collapse

All flat-plate structures failing in a progressive collapse initiated by punching shear failure have clearly demonstrated the possible disastrous consequences of a punching shear failure. Several factors that may cause a deficiency in two-way shear strength (which can result in a punching shear failure) are as follows:

- Low concrete strengths during construction
- Improper procedures for form removal and reshoring during construction
- The need to install new service ducts or pipes that require openings in the slabs adjacent to the column
- Design errors or construction deficiencies
- Significant shear and moment transfers during strong ground motions
- Partial loss of the concrete contribution to shear strength due to cracking, spalling, and delamination of the concrete cover because of damage during strong ground motions or corrosion of reinforcing bars
- Increase of gravity loads due to the change of building use

1.2 MOTIVATION

This research was motivated by the following observations:

1. Punching shear failure of a slab-column connection in flat-plate structures may result in progressive collapse of the entire structure.
2. Many punching shear failure cases over the years, including Sampoong Department Store that occurred recently, indicate that two-way shear strength of slab-column connections and the mechanics of punching shear failure have not been well understood. Park and Gamble (2000) indicated that the actual behavior of the failure region of a cracked slab is extremely complex and design provisions used are thus derived from empirical

simplifications of the real behavior. Bari (2000) reported that there are no guidelines at the theoretical level of punching shear failure and there are significant variations among different empirical treatments. As a result, current building code design procedures may not be able to accurately predict the punching shear strength of slabs in all situations (Li 2000).

3. Flat-plate structures built in the mid 20th century do not conform to current code requirements of shear reinforcement, integrity steel (Binici 2003), and concentration of flexural reinforcement over the column because code provisions have changed. Since the changes in the code provisions are intended to produce a safer structure based on experimental test results and lessons learned from failures, many flat-plate structures that were built in the mid 20th century and are currently still in service do not have a safety margin that is intended by current code provisions. Simple, effective, reliable, and economical rehabilitation methods are therefore needed to encourage owners to rehabilitate their structures so that the intended safety margin can be achieved.
4. There are many flat-plate structures located in seismic regions that were designed considering gravity loads only. During strong ground motions, sufficient slab-column ductility is needed. Punching failures that occurred in many flat-plate structures during previous earthquakes shows that the connections in flat-plate structures built in the mid 20th century do not have sufficient ductility. Therefore, post-earthquake repair methods that can increase the two-way shear strength under gravity loads and improve connection ductility under reversed cyclic loads are needed.
5. Strengthening or repairing can be a cost-effective alternative to replacement and may provide the best solution (El-Salakawy et al. 2003). However, guidelines and experimental data about rehabilitation techniques

are not widely available. In addition, most guidelines and data that are currently available are based on experimental studies that were conducted on relatively small-scale specimens. The test results from the small-scale specimens may not represent the behavior of actual structures because two-way shear strength is sensitive to the size of connection (Regan 1981, Bazant and Cao 1987, Menetrey 1995, 1996).

1.3 SCOPE

This study is part of the two research projects sponsored by the National Science Foundation (NSF) on reinforced concrete slab-column connections. The two projects are as follows:

1. Gravity Load Capacity of Earthquake Damaged Slab-column Connections
2. Punching Shear Upgrade of Reinforced Concrete Flat Plates

This dissertation focuses on the rehabilitation of slab-column connections. The study was conducted under the framework and objectives of the second project listed above.

This study is limited to interior flat-plate slab-column connections without shear reinforcement and does not include edge and corner connections. It is believed that interior slab-column connections are more critical in punching shear than edge and corner connections in a properly designed multibay flat-plate structure with approximately equal reinforcement ratios at all connections (Gardner and Shao 1996). Tests on multipanel flat-plate structures have also shown that under a uniform load, the first shear failure occurred at an interior connection, at the time when the edge and corner connections remained relatively intact (Guralnick and LaFraugh 1963, Tankut 1969, Dilger and Sherif 1993, and Gardner and Shao 1996). In addition, as presented in Section 1.1.2, the collapses

of a flat-plate office building in Jackson, a 16-story flat-slab apartment building in Boston, the 30-story Skyline Center in Alexandria, and Sampoong Department Store were initiated by a punching shear failure at an interior connection.

As part of this investigation, experimental testing was conducted on isolated interior slab-column connections. However, the boundary conditions and the support locations of the isolated connections were determined based on non-linear finite element analyses (Tian 2006) so that the force distribution in the isolated connections can reasonably match that in the continuous prototype structure. Gardner and Shao (1996) concluded that punching tests on isolated slab-column connections could represent the punching shear behavior of the interior connections in continuous slab systems. Guralnick and LaFraugh (1963) showed that deflections, crack patterns, distribution of service load moments, mode of failure, and capacity of their 3-bay by 3-bay continuous flat-plate test structure were in close agreement with corresponding observations for companion isolated connection specimens.

This dissertation only covers thin concrete slabs, which is typical in flat-plate structures (span to depth ratio l/d between 25 and 35). The behavior of thick slabs (for blast loading applications or the end slabs of concrete reactor vessels, with l/d of about 5), in which the size effect may be significant, is outside the scope of this dissertation.

This dissertation focuses on rehabilitation of slab-column connections in existing structures built in the mid 20th century. Methods for enhancing shear capacity of connections in new construction using shear reinforcement are outside the scope of this research project and discussed elsewhere (Hawkins 1974, Hawkins et al. 1975, Seible et al. 1980, Van der Voet et al. 1982, Regan 1985, Ghali and Hammill 1992, Marzouk and Jiang 1997, Gomes and Regan 1999, Alander 2000, Beutel and Hegger 2000, Broms 2000, Megally and Ghali 2000,

Pilakoutas and Ioannou 2000, Regan and Samadian 2001, Beutel and Hegger 2002, Robertson et al. 2002, El-Ghandour et al. 2003, Pilakoutas and Li 2003, Polak et al. 2005).

1.4 OBJECTIVES

The main objectives of this research study are as follows:

1. To develop efficient strengthening methods for deficient flat-plate slab-column connections that do not satisfy current code requirements.
2. To develop efficient post-earthquake repair methods for flat-plate slab-column connections that have experienced prior seismic-damage.

In order to develop an efficient strengthening method, typical characteristics of slab-column connections in flat-plate structures built in the mid 20th century, the mechanics of punching shear failure, and the two-way shear strength of existing slab-column connections must be known first. For these reasons, a comprehensive literature review on building code provisions related to design of flat-plate structures, on the mechanics of punching shear failure, and on previous research and recommendations related to two-way shear strength of connections was conducted.

In order to study the effectiveness of post-earthquake repair techniques, the effect of earthquake-damage on two-way shear strength must be evaluated first. Since the results of the test conducted on typical lightly-reinforced slab-column connections showed that the effect of earthquake-damage on two-way shear strength is not significant and the effect of flexural reinforcement ratio is much more significant, this study also examines the effect of flexural reinforcement ratio on two-way shear strength. Therefore, in addition to the two main objectives listed above, the indirect objective of this study is to evaluate the

effect of earthquake-damage and flexural reinforcement ratio on two-way shear strength of slab-column connections.

In order to develop efficient rehabilitation methods, a comprehensive literature review on different techniques for strengthening and repairing slab-column connections was performed. Three alternatives for strengthening and repairing slab-column connections, which are believed to be practical and efficient but have not been extensively researched, are as follows:

1. Installing steel collars underneath the slab to increase the critical shear perimeter;
2. Stitching fiber reinforced polymer strips through drilled holes as external stirrups; and
3. Installing fiber reinforced polymer sheets on the tension surface of the slab as external flexural reinforcement.

In order to evaluate the performance of those three alternatives, an experimental study on seven two-third scale interior slab-column connections was conducted at the Ferguson Structural Engineering Laboratory at the University of Texas at Austin.

1.5 ORGANIZATION

The results of an experimental study on strengthening and repair of flat-plate slab-column connections for two-way shear are presented in this dissertation. The organization of this dissertation is as follows:

A comprehensive literature review is presented in Chapter 2. The topics covered in the literature review include the general behavior of slab-column connections related to punching shear, previous research, recommendations, and building code provisions related to two-way shear strength of interior slab-column

connections, and rehabilitation techniques for improving the punching shear resistance. Questions that arose after conducting a comprehensive literature review and that are addressed in this research are also presented.

Details of the experimental program are discussed in Chapter 3. Design and construction of seven specimens are presented. The properties of materials used in this study are reported. Ten different tests that were performed on those seven specimens to quantify the effects of low flexural reinforcement ratios, earthquake damage, and the efficiency of various rehabilitation techniques on two-way shear strength are described. Test setup and instrumentation are discussed.

Details of the test procedure, behavior, failure surfaces, and rehabilitation methods for all specimens are presented in Chapter 4. Test results for all specimens are presented and compared. The measured capacity of unstrengthened, undamaged connections is compared with the estimated capacities through the use of the code provisions. The effects of flexural reinforcement ratio and seismic damage on two-way shear strength, and the effectiveness of different rehabilitation methods on improving the two-way shear strength of slab-column connections are discussed.

Guidelines for the evaluation and rehabilitation of existing slab-column connections are presented in Chapter 5. Important design considerations for each one of the three rehabilitation techniques studied in this research are discussed.

The significant results of the experimental study are summarized in Chapter 6. Conclusions from this study are presented. And future research needs are discussed.

Crack patterns for all specimens are presented in Appendix A.

CHAPTER 2

Literature Review

2.1 GENERAL

A comprehensive literature review is presented in this chapter. The topics covered in this literature review include: (i) the mechanics of punching shear failure, (ii) previous research, recommendations, and building code provisions on two-way shear strength of interior slab-column connections, (iii) Fiber Reinforced Polymers (FRP) as an emerging material for structural rehabilitation, and (iv) repair and strengthening techniques for improving punching shear resistance. The purposes of literature review presented in this chapter are as follows:

- To understand the mechanics of punching shear failure, including the effect of flexural reinforcement on the two-way shear strength, so that the most effective rehabilitation method can be developed.
- To summarize different recommendations of researchers and various code provisions for estimating the two-way shear strength of interior slab-column connections. These recommendations and code provisions are evaluated to study whether they can be used for evaluating the capacity of existing structures. In rehabilitation, more accurate estimations of the actual strength of existing structural members may result in more efficient and economical rehabilitation. In many cases, the code provisions may not be suitable for evaluation purposes because they are mainly intended for a conservative design of new structures. If the code provisions are unconservative for estimating the capacity of existing structures,

understanding the development of code provisions may provide an explanation.

- To review the American Concrete Institute (ACI) Code provisions related to the design of flat plate structures for gravity loads. Recognizing the changes made to the code provisions over the years is useful for:
 - i. Understanding typical structural details of existing structures that require rehabilitation and the differences between old details and current details.
 - ii. Understanding the deficiencies related to the two-way shear strength that may be present in structures built several decades ago so that the most effective rehabilitation technique can be developed.
- To evaluate effectiveness of different techniques for strengthening and repairing slab-column connections. This information is important for:
 - i. Developing rehabilitation techniques evaluated in this research, including the use of FRP as an emerging material for structural rehabilitation.
 - ii. Providing readers with a general overview of different rehabilitation techniques that may help in developing a solution specific to a given structure.

The literature review chapter is organized as follows: Failure mode of slab-column connections, and definition of punching shear and flexural failures are presented in Section 2.2. Previous research and recommendations on two-way shear strength of interior slab-column connections without shear reinforcement subjected to concentric gravity loads are reported in Section 2.3. The historic development of ACI Code provisions for two-way shear-strength (since 1924) is presented in Section 2.4. Various building codes' provisions for two-way shear

strength of interior slab-column connections are given in Section 2.5. Opinions of many researchers about the effect of flexural reinforcement on punching shear strength are summarized in Section 2.6. Discussion on residual capacity after punching shear failure is presented in Section 2.7. Information on FRP as an emerging material for structural rehabilitation is reported in Section 2.8. Previous research on strengthening and repair of slab-column connections for two-way shear are presented in Section 2.9. An overview of the literature review conducted as part of this research project is presented in Section 2.10.

2.2 SLAB COLUMN CONNECTIONS: FAILURE MODE

A reinforced concrete slab-column connection can reach its capacity and fail in two modes: punching shear or widespread flexural yielding of longitudinal reinforcement (Dragosavic and Van den Beukel 1974, Rankin and Long 1987, Polak 2005). Punching shear failure is a local brittle failure of the slab-column connection in which the column together with an attached portion of slab pushes through the slab. Widespread yielding of longitudinal reinforcement is also described as formation of a complete yield-line mechanism. Independent of whether the connections fail in punching shear or a complete formation of yield-line mechanism, *failure always occurs when the loaded area punches through the slab, pushing ahead of it a plug of concrete which has the form of a truncated cone or pyramid with a minimum cross-section at least as large as the loaded area* (ACI-ASCE Committee 326 1962).

Even though some researchers explicitly classified the failure mode of slab as punching shear failure and flexural failure (Yitzhaki 1966, Gesund and Kaushik 1970, Criswell 1974), many researchers did not explicitly differentiate between the punching shear and flexural failure. Gesund and Kaushik (1970)

conducted a systematic investigation into the relationship between the calculated flexural strength P_{flex} and the measured failure load P_{test} of the slabs under concentric loading. They found that the arithmetic mean of P_{flex}/P_{test} for 106 alleged punching shear failures was 1.02, with a standard deviation of 0.25. Regan and Braestrup (1985) indicated that a substantial proportion of the test results reported in the literature as punching shear failures exhibited ultimate loads that did not differ significantly from the flexural capacities.

Most failures in slab-column connections look the same: the column together with a portion of the slab pushed through the slab. This resemblance is believed to be the cause of why almost all failures were called punching failure. In reality, the column may punch through the slab before or after a widespread yielding of longitudinal reinforcement (Afhami et al. 1998).

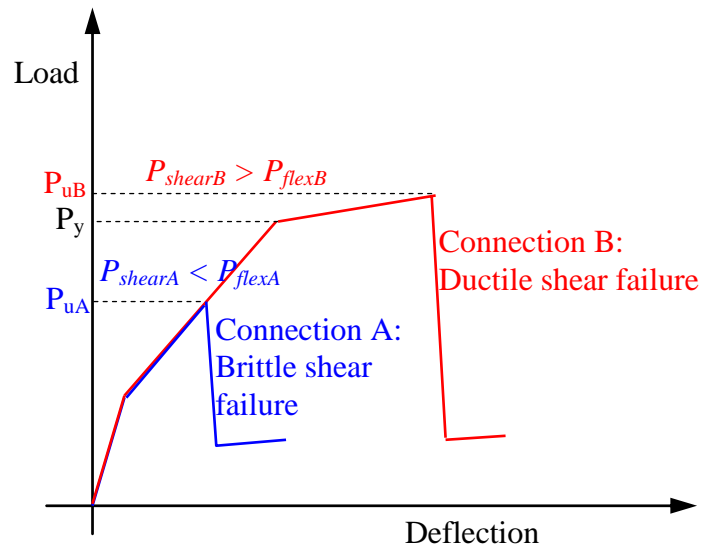


Figure 2.1 Behavior of slab-column connections

Figure 2.1 shows typical load-deflection curves for flat-plate slab-column connections subjected to concentric loads. The shear and flexural capacities of the connections are P_{shear} and P_{flex} , respectively, and the ultimate load carrying

capacity of the connections is P_u . In connection A, P_{shearA} is less than P_{flexA} , whereas in connection B, P_{shearB} is larger than P_{flexB} . At failure, connection B exhibits more deformation than connection A. Afhami et al. (1998) indicated that when $P_{shear} < P_{flex}$, loss of bond between the reinforcement and its surrounding concrete causes a brittle punching shear failure. And when $P_{shear} > P_{flex}$, the spread of yielding away from the column reduces the force gradient in the reinforcement and the connection exhibits larger deformations prior to failure. Shehata and Regan (1989) described a ductile shear failure (connection B) as primarily flexural, with punching being a secondary phenomenon. Even though flexural reinforcement has yielded, punching failure always results in a significant drop in load carrying capacity, as shown in Figure 2.1.

For connections of normal proportions and with usual amounts of flexural reinforcement, a complete yield-line mechanism will precede punching shear failure. The ultimate load carrying capacity of such connections may be equal to their flexural capacity, which is smaller than their two-way shear capacity. (Chen and Li 2005).

2.2.1 Flexural strength of the slab

Hognestad (1953) and Elstner and Hognestad (1956) indicated that the ultimate flexural strength of the slab could be estimated by the yield-line theory. They further stated, “... *The yield-line theory assumes that yielding of the tension reinforcement is concentrated across certain lines in the slab plane called the yield lines. The locations of the yield lines depend primarily on loading and boundary conditions...*” A typical yield-line pattern for a single panel, simply-supported slab-column connection with and without a concentration of flexural reinforcement over the column and subjected to a concentrated load at center is shown in Figure 2.2. The ultimate capacity of simply supported plates routinely

exceeds the estimated load from yield-line theory due to membrane forces, boundary restraints, and second order effects which allow the slab to act as a folded plate (Elstner and Hognestad 1956, Criswell 1974, Afhami et al. 1998).

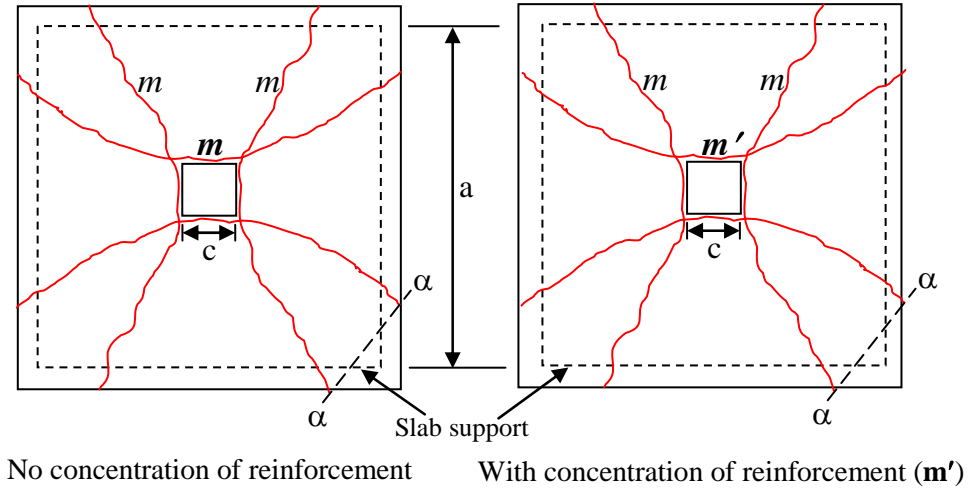


Figure 2.2 Typical yield-line pattern

For square slabs supported along four edges with the corners permitted to lift by rotating about the α - α axes, the ultimate flexural strength P_{flex} is:

Without concentration of reinforcement:

$$P_{flex} = 8m \left(\frac{1}{1 - \frac{c}{a}} - 3 + 2\sqrt{2} \right) \quad (2.1)$$

With concentration of reinforcement over the column:

$$P_{flex} = 8m \left(\frac{1}{1 - \frac{c}{a}} - 3 + 2\sqrt{2} + \frac{\frac{m'}{m} - 1}{\frac{a}{c} - 1} \right) \quad (2.2)$$

where:

$$m = \rho f_y d^2 \left(1 - 0.59 \left(\rho \frac{f_y}{f_c'} \right) \right) \quad (2.3)$$

ρ is the tensile flexural reinforcement ratio, a is the distance between supports of the slab specimen (for continuous structures, $a \approx 0.4L$, where L is the clear span length (Rankin and Long 1987)), c is the dimension of the square column, d is the effective depth, f_y is the yield strength of flexural reinforcement, and f_c' is the concrete strength of the slab.

2.3 PREVIOUS RESEARCH ON TWO-WAY SHEAR RESISTANCE OF SLABS

Previous research and recommendations on two-way shear strength of interior slab-column connections without shear reinforcement and subjected to concentric gravity loads are presented in this section. Research and recommendations are grouped in three sub-sections: (i) early research as an initial development, (ii) research performed in the United States, particularly those related to ACI provisions, (iii) research conducted outside of the United States. Summary of previous research and recommendations on this topic is also reported in Tankut (1969), Faulkes (1974), Regan and Braestrup (1985), Van Dusen (1985), Li (2000), and Zaghoul (2002).

2.3.1 Early research

Li (2000) reported that in the early 1900's, Morsch proposed the following expression for the calculation of nominal shear stress, v :

$$v = \frac{V}{bd} \quad (2.4)$$

where V is the applied shear force, b is the perimeter of the loaded area, and d is the effective depth.

Based on his test results of 114 wall footings and 83 column footings, Talbot (1913) expanded Eq. (2.4) by saying $b=4(c+2d)$, where c is the column dimension. He observed that the shear failure surfaces were approximately at a 45-degree angle and the failure surfaces extended from the intersection of slab-column on the compression side to the level of the tensile flexural reinforcement at a distance d away from the column face. He also found that an increase in the percentage of flexural reinforcement resulted in an increase in the shear strength of the slab.

As reported by ACI-ASCE Committee 326 (1962), Graf (1933) concluded that the flexural cracking had some influence on shear strength. Graf proposed:

$$v = \frac{V}{4ch} \quad (2.5)$$

where h is the slab thickness.

2.3.2 Shear strength of flat-plates & research conducted in the USA

2.3.2.1 Richart (1948)

Richart (1948) tested 24 wall footings and 132 column footings supported on a bed of steel springs simulating soil pressure. Most of the specimens tested by Richart were 7-ft square footings. Richart found that the reinforcing steel in the footings with 0.2% and 0.4% flexural reinforcement ratio yielded before punching failure occurred. These footings developed extensive cracking and finally failed in diagonal tension at relatively low shear stresses v ($2.4\sqrt{f_c'}$ - $3.4\sqrt{f_c'}$, evaluated at the critical section d -away from the column face). He referred to this punching shear failure as a secondary failure (after the yielding of flexural reinforcement). He explained that the secondary failure occurred because yielding of the steel produced large cracks, which then reduced the concrete section resisting shear. He

also found that the footings with $\rho=0.56\%$ and $\rho=0.75\%$ clearly failed in diagonal tension, at shear stress (v) levels that varied between $2.9\sqrt{f_c'}$ and $4.3\sqrt{f_c'}$ (evaluated at the critical section d -away from the column face).

2.3.2.2 Hognestad (1953)

Hognestad (1953) concluded that the majority of the footings failed after local yielding of the flexural reinforcement, but before reaching the ultimate flexural load from a yield-line analysis. He recognized that the flexural and shear strength were interrelated and introduced the parameter $\phi_o = \frac{V_{shear}}{V_{flex}}$ where V_{shear} is the ultimate shear capacity of the slab and V_{flex} is the ultimate flexural capacity. Based on Richart's footing test results (1948), Hognestad proposed the following empirical equation:

$$v = \frac{V}{bjd} = \left(0.035 + \frac{0.07}{\phi_o} \right) f_c' + 130 \text{ psi} \quad (2.6)$$

where $j=7/8$, f_c' is concrete cylinder strength in [psi], and ϕ_o is:

$$\phi_o = \frac{A + \sqrt{A^2 + 0.28BC}}{2BC} \quad (2.7)$$

$$A = 0.035 + \frac{130}{f_c'} \quad (2.8)$$

$$B = \frac{V_{flex}}{7/8 d 4c f_c'} \quad (2.9)$$

$$V_{flex} = \frac{8a}{(a-c)^2} A_s d f_y \left(1 - \frac{1}{2} \frac{\rho f_y}{f_c'} \right) \quad (2.10)$$

$$C = \frac{a^2 - (c + 2d)^2}{a^2} \quad (2.11)$$

where a is the width of the slab or footing.

The limits for Eq.(2.6) are:

$$0.38 \leq \frac{d}{c} \leq 1.14$$

$$2000 \text{ psi} \leq f_c' \leq 5000 \text{ psi}$$

2.3.2.3 *Elstner and Hognestad (1956)*

Elstner and Hognestad (1956) found that the final failure of slabs with flexural reinforcement ratios that varied from 1.15% to 3.7% was by the column punching through the slab (when shear stresses v were evaluated at a distance $d/2$ away from the column, v varied from $4\sqrt{f_c'}$ to $7.4\sqrt{f_c'}$). In most cases, such punching occurred after initial yielding of the reinforcement in the vicinity of the column. However, a flexural failure was observed for the slabs with 0.5% and 1.0% flexural reinforcement (when v were evaluated at a distance $d/2$ away from the column, v varied from $2.1\sqrt{f_c'}$ to $3.5\sqrt{f_c'}$).

After re-analyzing Richart's test results (1948), Elstner and Hognestad indicated that v computed at the column face was a better measure of shear strength than that computed at a distance d away from the column faces. They also revised the earlier Hognestad empirical formula (Eq. (2.6)) as follows:

$$v = \frac{V}{bjd} = \frac{333 \text{ psi}}{f_c'} + \frac{0.046}{\phi_o} \quad (2.12)$$

where $j=7/8$. They also found that a concentration of 50% of the flexural reinforcement directly over a column did not increase the shear strength and compression reinforcement had no effect on the ultimate shear strength.

2.3.2.4 Whitney (1957)

Whitney (1957) reviewed Richart's (1948) and Elstner and Hognestad's (1956) test results. He indicated that the conventional shear formula ($v = \frac{V}{bjd} = k(f_c')$) was not suitable for use because the shear strength is not a simple function of concrete strength, but depends largely on the amount of flexural reinforcement and its efficiency. He critiqued the conventional shear formula because it was too conservative for cases with large ρ and relatively unsafe with light ρ . He also found that using the critical section at a distance $d/2$ away from the column face (instead of d away) gave the most consistent results for all slab depths.

Whitney proposed the following expression:

$$v = \frac{V}{bd} = 100 \text{ psi} + 0.75 \frac{m_u}{d^2} \sqrt{\frac{d}{l_s}} \quad (2.13)$$

where $b=4(c+d)$ (critical shear perimeter is at a distance $d/2$ away from the loaded area), l_s is the shear span, and m_u is the ultimate moment capacity per unit width of slab near the column defined as follows (Whitney 1957):

For under-reinforced slabs:

$$m_u = \rho d^2 f_y \left(1 - \frac{\rho f_y}{1.7 f_c'} \right) \quad (2.14)$$

For over-reinforced slabs:

$$m_u = \frac{d^2 f_c'}{3} \quad (2.15)$$

The customary term j was omitted from Eq. (2.13) because the value of v was calculated empirically and the average value for the full depth was considered to be as good as any other.

Whitney explained that there were two different types of failure: gradual and sudden. The gradual type of failure occurred after flexural reinforcement yielded and caused excessive cracking that eventually reduced the shear strength until the column punched through the slab. The sudden type of failure occurred before any of flexural reinforcement yielded. This sudden failure could be caused by over-reinforcement in flexure (resulting in destruction of the compression zone around the column) or bond/anchorage failure (because of insufficient embedment length or very close spacing of the reinforcing bars). In explaining a mechanism of failure, Whitney indicated that the horizontal component of the shear force on the “pyramid of rupture” must be resisted by the flexural reinforcement passing through the pyramid. This horizontal component is limited by the yield strength of flexural reinforcement. As the reinforcement yields, three failure mechanisms can happen: (i) flexural cracks extend up from the steel into the pyramid until they finally precipitate a shear failure, (ii) if the slab is over-reinforced, the compression zone around the column crushes and results in sudden punching, or (iii) if the steel is not properly anchored, it slips and permits sudden punching.

ACI-ASCE Committee 326 (1962) commented that since the test results of specimens with relatively high flexural strengths were omitted in the study leading to Eq. (2.13), this equation could only apply in cases of nearly balanced design (i.e. when ϕ_o is close to unity). It can be seen from Eq. (2.13) that v can be increased by increasing ρ inside the pyramid of rupture. Shifting the flexural reinforcement from the outside of the pyramid to the inside also increases ρ inside the pyramid of rupture, and hence increases v .

2.3.2.5 Moe (1961)

Since tensile strength is generally assumed proportional to $\sqrt{f_c'}$, Moe suggested that the shear strength was proportional to $\sqrt{f_c'}$ instead of f_c' in order

to reflect the fact that shear failures are controlled primarily by tensile splitting. Based on the test results of the slabs with varying degrees of concentration of the flexural reinforcement inside the pyramid of rupture, Moe found that V_{flex} is a better indicator of the shear strength than m_u , which was used by Whitney (Eq. (2.13)). However, Moe indicated that the magnitude of V_{flex} had in itself no direct physical relation to the mechanism of failure. Rather, it reflected several other important influences, such as distribution of cracking, amount of the elongation of the tensile reinforcement, magnitude of the compressive stresses in the critical section, and the depth of neutral axis at failure.

Moe believed that the interaction between shear and flexural strength could be approximated by a straight line as follows:

$$\frac{V}{V_o} + C \frac{V}{V_{flex}} = 1 \quad (2.16)$$

He assumed that $V_o = Abd\sqrt{f_c'}$, where b is the critical shear perimeter at a distance of $d/2$ away from the loaded area. Moe also believed that the shear strength is sensitive to c/d ratio and he assumed a linear variation.

Based on a statistical analysis of 37 slab and 106 footing test results (shown in Figure 2.3) of Richart (1948), Elstner and Hognestad (1956), and his own tests, Moe proposed Eq. (2.17). All slab and footings were 7'×7' or smaller, and had the flexural reinforcement ratios that varied between 0.39% and 3.7%.

Only the specimens that were believed to have failed in shear were included in Moe's statistical analysis and are shown in Figure 2.3. All 106 footing test results that are included in Figure 2.3 are Richart's (1948, discussed in Section 2.3.2.1). From 156 footing tests conducted by Richart, 50 tests that were excluded from Moe's statistical analysis are as follows:

- 6 tests did not provide information on the yield strength of steel.
- 6 tests were believed to show bond failure.

- 22 tests (with $0.2\% \leq \rho \leq 0.4\%$) were believed to show flexural failure.

From 38 slab tests conducted by Elstner and Hognestad (1956), only 34 test results were included in Moe's statistical analysis. 4 slabs (with $0.5\% \leq \rho \leq 1.0\%$ and v varied from $2.1\sqrt{f_c'}$ to $3.5\sqrt{f_c'}$ when they were evaluated at a distance $d/2$ away from the column face) that were believed to have failed in flexure were excluded from Moe's statistical analysis.

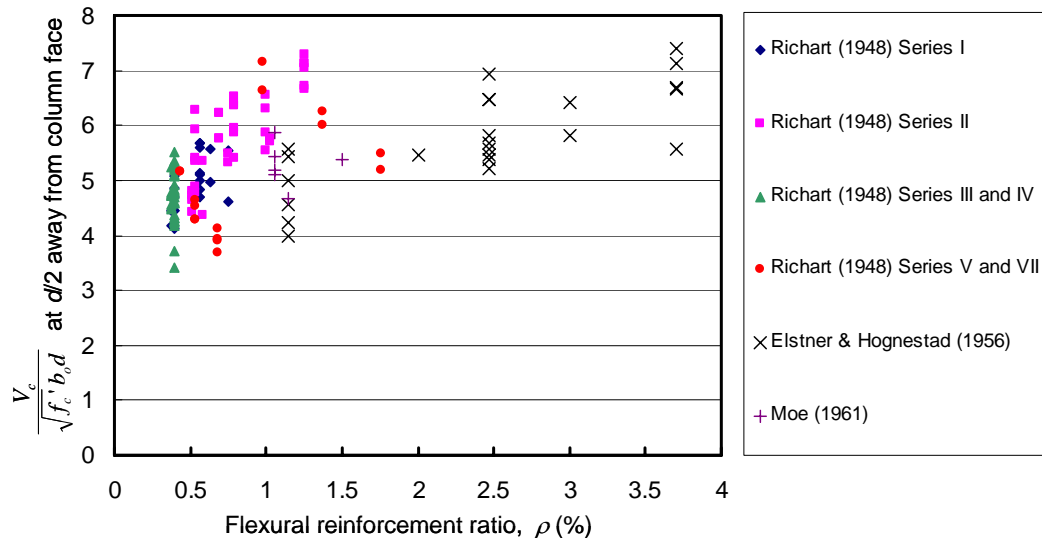


Figure 2.3 Test results used in Moe's statistical analysis (1961)

$$v = \frac{V}{bd} = \frac{15\sqrt{f_c'} \left(1 - 0.075 \frac{c}{d}\right)}{1 + 5.25 \frac{bd\sqrt{f_c'}}{V_{flex}}} \quad (2.17)$$

where V_{flex} is the shear force at the calculated ultimate flexural capacity of the slab by using the yield-line theory. Using a definition of $\phi_o = \frac{V}{V_{flex}}$, Eq. (2.17) can be re-organized as follows:

$$v = \frac{V}{bd} = \left[15 \left(1 - 0.075 \frac{c}{d} \right) - 5.25 \phi_o \right] \sqrt{f_c'} \quad (2.18)$$

The most important contribution of Moe stems from his effort to explicitly include the effect of flexural reinforcement through the term V_{flex} .

2.3.2.5.1 Design considerations

Based on the ultimate strengths of slabs and footings obtained from relatively short duration tests and considering the average strength, rather than the minimum, Moe also developed design equations. Since slabs failing in flexure resisted loads considerably greater than the flexural capacity as computed using the yield line theory, Moe assumed $V=1.1V_{flex}$ as the point of balanced design (i.e. the value at which the flexural and shear strengths are equal).

In order to ensure that the flexural failure always governs over the shear failure, Moe proposed that v must be limited to the following values:

$$v = \left(9.23 - 1.12 \frac{c}{d} \right) \sqrt{f_c'} \quad \text{for } c/d \leq 3 \quad (2.19)$$

$$v = \left(2.5 + 10 \frac{d}{c} \right) \sqrt{f_c'} \quad \text{for } c/d > 3 \quad (2.20)$$

Those design recommendations (Eqs. (2.19) and (2.20)) were developed on the basis of tests on slabs and footings with c/d ratios between 0.9 and 3.1.

2.3.2.6 ACI-ASCE Committee 326 (1962)

ACI-ASCE Committee 326 (1962) reviewed Moe's equation (Eq. (2.18)) and believed that ϕ_o could be eliminated from Eq. (2.18) by substituting $\phi_o=1.0$ because in a practical design, V_{shear} should exceed V_{flex} (i.e. $\phi_o \geq 1.0$). This simplification resulted in the following equation:

$$v = \frac{V}{bd} = \left(9.75 - 1.125 \frac{c}{d} \right) \sqrt{f_c'} \quad (2.21)$$

However, the committee believed that Eq. (2.21) could not be applied for all cases encountered in practical design because of the following illogical reasons:

- (i) When the load was applied to a slab over a very small area (i.e. b and c/d were very small), v would approach $4\sqrt{f_c'}$ but V would approach zero.
- (ii) When c/d was large (i.e. columns with drop panels), v would approach zero.

Based on the available test results, ACI-ASCE Committee 326 then proposed the following equation:

$$v = \frac{V}{bd} = 4 \left(\frac{d}{c} + 1 \right) \sqrt{f_c'} \quad (2.22)$$

where b is the periphery of the loaded area. In order to avoid an open interpretation on the value of c for irregular columns or columns with openings, and to propose the design recommendation that was consistent with the ACI 318-56 concept, the committee simplified Eq. (2.22) into the following equation:

$$v = \frac{V}{b_o d} = 4 \sqrt{f_c'} \quad (2.23)$$

where b_o is the critical section located at a distance $d/2$ from the loaded area. In the discussion of the paper by ACI-ASCE Committee 326, Diaz de Cossio (1962) considered that the lower limit of $4\sqrt{f_c'}$ at $d/2$ from the loaded area was reasonable and on the safe side for most common cases. Diaz de Cossio's test results of 22 one-way slabs (reinforced in tension only) with ρ values varying between 1.85% and 2.81% had the average v (measured at $d/2$ away from the loaded area) of $3.65\sqrt{f_c'}$ with a coefficient of variation of 7.4%. However, he believed that actual two-way slabs with significantly larger width-to-depth ratio than that of his specimens would have higher strengths than those measured in his

tests. Hence, it can be seen that upon its adoption $4\sqrt{f_c'}$ was not a lower limit to the measured strengths, but more like an average stress.

ACI-ASCE Committee 326 also believed that concentration of reinforcement over the column had advantages in flexure, (i.e. increasing the slab stiffness and reducing the stresses in the flexural reinforcement in the vicinity of the column) and therefore should be encouraged. However, the committee felt that such encouragement should not be tied to the design requirements for shear.

2.3.2.7 Guralnick and LaFraugh (1963)

Guralnick and LaFraugh (1963) tested a three-quarter scale flat-plate test specimen (Figure 2.4), having overall dimensions 45×45 ft and consisting of nine 15×15 ft panels arranged three-by-three. The amounts of top flexural reinforcement in all interior connections were 0.69% in the column strip and 1.4% within the $(c+3h)$ region.

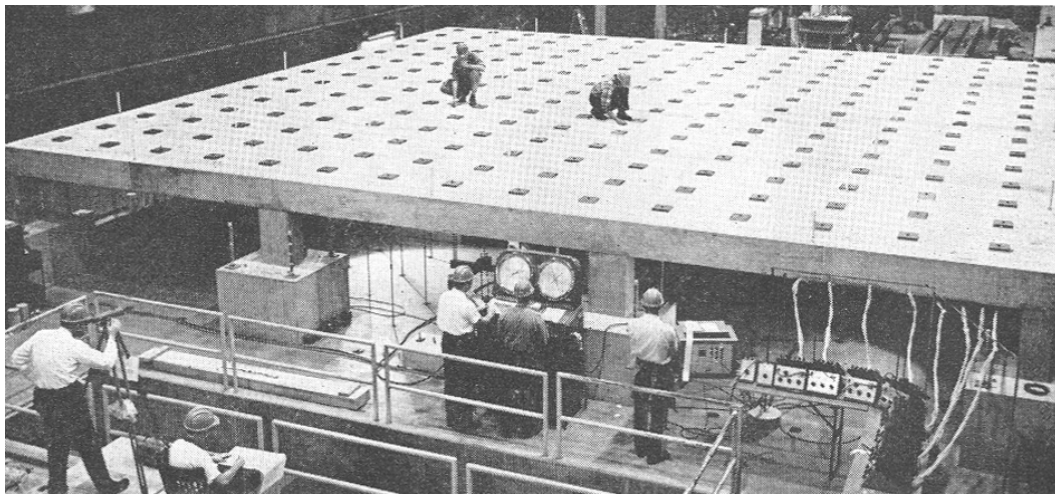


Figure 2.4 Test on nine panels of three-quarters scale of a flat-plate structure

Failure occurred when one of interior columns punched through the slab at a load of 85% of the two-way shear capacity computed using ACI 318-1963 (i.e.

$0.85 \times 4\sqrt{f_c'}b_o d$). The measured failure load of the test structure was 1.05 times the predicted yield-line failure load. Immediately before failure, the average steel strain at the four faces of the column was about 0.01, which was seven times greater than the yield strain.

2.3.2.8 Magura and Corley (1969)

Magura and Corley (1969) reported the results of the test conducted on the waffle slab roof of the Rathskeller Building in the 1964-1965 New York World's Fair. The roof of the structure was a 2-foot-thick waffle slab supported on columns, about 30 feet on centers. The building was designed to meet the provisions of the ACI 318-1956 and the roof was designed for a live load of 300 psf and an average computed dead load of 220 psf.

In one of the tests, Connection C4 (one of the interior connections that had the flexural reinforcement ratios within the column strip of 0.45% and 1.8% in North-South and East-West directions, respectively) was loaded concentrically up to failure. Connection C4 failed in shear, before reaching its flexural capacity. The structure behaved “elastically” until failure occurred. The connection failed at a load that was 16% greater than that estimated using ACI 318-1963. However, the measured failure load was 20% lower than that estimated using Moe's equation (Eq. (2.17)).

2.3.2.9 Criswell (1970, 1974)

Criswell tested several connections (Figure 2.5) with low flexural reinforcement ratios and some of his test results are summarized in Table 2.1. Criswell found that a punching failure could occur at loads considerably below the ACI Code values. V_u of the connections with $\rho=0.75\%$ were about the same as V_{flex} , whereas V_u with $\rho=1.5\%$ were lower than V_{flex} .

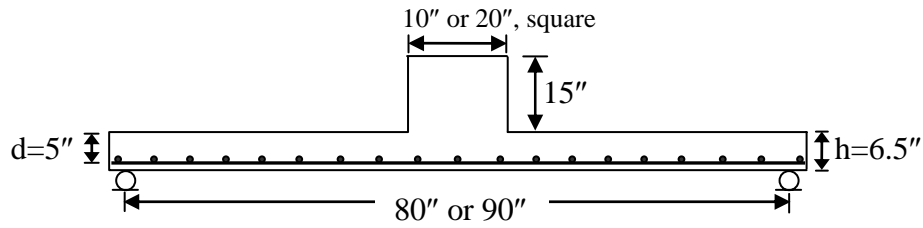


Figure 2.5 Criswell's test specimen

Table 2.1 Criswell's test results

Specimen	Measured c/d	ρ	V_u / V_{ACI}	V_u / V_{flex}
S2075-1	2.1	0.79%	0.85	1.02
S2075-2	2.1	0.78%	0.83	0.95
S4075-1	4.0	0.75%	0.62	1.01
S4075-2	4.1	0.77%	0.56	0.99
S4150-1	4.1	1.50%	0.92	0.89
S4150-2	4.1	1.50%	0.92	0.87

V_u : Observed failure load

V_{ACI} : Calculated failure load using ACI Code

V_{flex} : Calculated failure load using yield line theory

Criswell indicated that since the ACI 318-1963 and Moe's (1961) equations were derived using only test results with $\phi_o < 1.0$ and failing primarily in shear, the applicability of those equations to the connections with $\rho = 0.75\%$, which failed in flexure, was questionable. Criswell stated, "... The strengths of the connections with smaller ρ values were primarily controlled by the flexural capacity even though a punching failure did develop before the connections displayed large ductility. Such failures could be considered as flexural-shear or secondary shear failure..."

2.3.2.10 ACI-ASCE Committee 426 (1977)

ACI-ASCE Committee 426 indicated that v at failure for lightly-reinforced slabs with a square column could be less than $4\sqrt{f'_c}$ if the slabs developed large deflections prior to the punching failure.

2.3.2.11 Hawkins and Mitchell (1979)

Hawkins and Mitchell (1979) reported that if a slab was properly designed according to ACI 318-77 concepts, the flexural strength could be slightly less than the shear strength and therefore the ACI 318-77 provisions attempted to define the punching shear strength for the onset of large rotations. The design based on ACI 318-77 was conservatively presumed to correspond to $\phi_o=1.0$, because if $\phi_o<1.0$, the shear strength exceeded $4\sqrt{f'_c}$. Hawkins and Mitchell indicated that if a connection is forced to develop rotations larger than those at which the flexural capacity is first reached, a punching failure occurs unless the shear stress is limited to $2\sqrt{f'_c}$ or shear reinforcement is provided.

2.3.2.12 Moehle et al. (1988)

Moehle et al. (1988) recommended that the shear strength of a connection be reduced to three-quarters of the value given by ACI 318 (for both basic formula and with large critical shear area) if extensive yielding is anticipated.

2.3.2.13 ACI-ASCE Committee 352 (1988)

ACI-ASCE Committee 352 reported that connections subjected to widespread flexural yielding exhibited shear strengths lower than those failing in shear prior to flexural yielding because in-plane restraint significantly decreases when the flexural reinforcement yields. The committee recommended a reduction factor C_v of 0.75 in cases where flexural yielding is anticipated.

2.3.3 Shear strength of flat-plates and research conducted outside the US

2.3.3.1 Yitzhaki (1966)

Yitzhaki indicated that the punching resistance depends mainly on the reinforcement strength as in the case of flexural strength. He showed that the effect of the concrete strength on punching resistance V_u can be expressed in terms of $\left(1 - \frac{\omega}{2}\right)$ factor and accordingly proposed the following expression:

$$V_u = 8 \left(1 - \frac{\omega}{2}\right) d^2 (149.3 + 0.164 \rho f_y) \left(1 + 0.5 \frac{c}{d}\right) \quad [\text{k}] \quad (2.24)$$

in [inch] and [ksi], where $\omega = \rho \frac{f_y}{f_c}$.

2.3.3.2 Regan (1981), Regan and Braestrup (1985)

Considering several parameters affecting two-way shear resistance of the slab-column connections V_u , Regan proposed the following empirical equation:

$$V_u = K_a K_{sc} \xi_s \sqrt[3]{100 \rho f_{cube}} 2.69 d (\Sigma c + 7.85 d) \quad [\text{N}] \quad (2.25)$$

in [mm] and [MPa], where:

K_a : factor to account for different concrete density ($K_a=0.13$ for normal density concrete and $K_a=0.105$ for lightweight aggregate concrete)

$$K_{sc} = 1.15 \sqrt{4\pi \frac{\text{column area}}{(\text{column perimeter})^2}} \quad (2.26)$$

$$\xi_s = \sqrt[4]{\frac{300}{d}} \quad (2.27)$$

ρ : the average of the percentages of tensile reinforcement in two orthogonal directions within the column strip

f_{cube} : the compressive strength of concrete determined by cube tests

Σc : the perimeter of the column

2.3.3.3 *Nolting (1984)*

Nolting (1984) related the behavior in punching to flexural conditions represented by the slab moments at the column face calculated by elastic plate theory. He proposed Eq. (2.28) to estimate the punching load of concentrically loaded slabs.

$$V_u = 4.75\sqrt{\rho f_c'} d^2 \alpha_o \quad [\text{N}] \quad (2.28)$$

in [mm] and [MPa], where:

$$\alpha_o = \left(0.65 + 9.4 \frac{c}{l}\right) - \left(2.2 + 70 \frac{c}{l}\right) \frac{d}{l} \quad (2.29)$$

c = diameter of column (for non-circular column, an equivalent circular column with the same area is used)

l = longer span of flat slab structural system. (for an isolated interior connection, $l/0.46$ is used)

2.3.3.4 *Rankin and Long (1987)*

Rankin and Long (1987) indicated that punching strength can be classified as either flexural or shear, depending on whether failure was initiated by the yielding of reinforcement (flexure), crushing of the concrete (flexure), or by internal diagonal cracking (shear). They concluded that punching strength V_p should be equal to the lesser of the flexural punching strength V_{flex} (Eq. (2.30)) and shear punching strength V_{shear} (Eq. (2.35)).

Although punching failure occurs finally by the concrete shearing in the highly stressed compression zone adjacent to the column, the ultimate

deformations depend primarily on the flexural characteristics of the slab. Rankin and Long suggested that all slabs with a reinforcement index $\rho \frac{f_y}{f_c'} < 0.1$ could be predicted to punch after flexural yielding. The lower the reinforcement ratio, the more the spread of yielding approaches the full yield-line pattern. Conversely, in heavily reinforced slabs, yielding becomes more localized and the failure mode approaches that of localized compression failure of concrete around the column. Thus depending on the slab ductility, the flexural punching strength must be somewhere between the yield-line capacity and the load causing localized compression failure. This highlights the importance of recognizing both the flexural and shear modes of punching failure for the normal range of reinforcement levels in flat slab structures.

In order to produce more economical and safer designs of flat slab structures, Rankin and Long recommended that both the flexural and shear modes of punching failure in future code provisions should be recognized. Rankin and Long stated, “... For a slab of a given span/depth ratio, the flexural punching strength can be increased effectively by increasing the percentage of flexural reinforcement until the mode of punching failure becomes shear at which point the strength of the concrete becomes more important...”

Flexural strength of the connection shown in Figure 2.6 is:

$$V_{flex} = \left\{ k_{yl} - \left(k_{yl} - \frac{k_b}{r_f} \right) \frac{M_b}{M_{bal}} \right\} M_b \geq \frac{k_b}{r_f} M_{bal} \quad (2.30)$$

where:

k_{yl} : factor for overall yielding considering corner lift-up (similar to Eq. (2.1))

$$k_{yl} = 8 \left(\frac{s}{a-c} - 3 + 2\sqrt{2} \right) \quad (2.31)$$

k_b : ratio of applied load to internal bending moment at column periphery (derived from finite element analyses)

$$k_b = \frac{25}{\left(\ln\left(\frac{2.5a}{c}\right)\right)^{1.5}} \quad (2.32)$$

r_f : column shape factor ($r_f = 1$ for circular columns ; $r_f = 1.15$ for square columns)

M_b : flexural capacity of connection

$$M_b = \rho f_y d^2 \left(1 - 0.59 \left(\rho \frac{f_y}{f_c'}\right)\right) \quad (2.33)$$

M_{bal} : flexural capacity of connection with ρ_{bal} (balanced failure: $V_{flex} = V_{shear}$)

$$M_{bal} = 0.333 f_c' d^2 \quad (2.34)$$

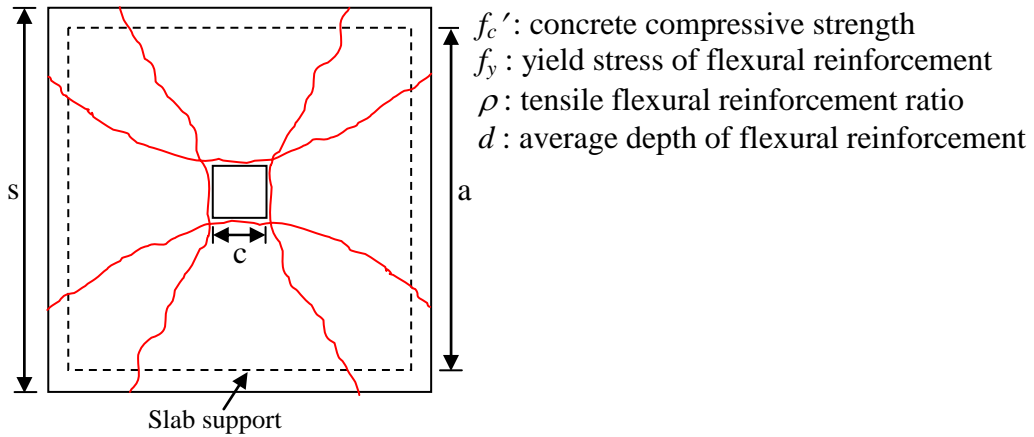


Figure 2.6 Typical yield-line pattern

Rankin and Long reported that the shear mode of punching failure could be precipitated by internal diagonal tension cracking prior to the development of yielding of the reinforcement or crushing of the concrete. This mode of punching failure is more likely in heavily reinforced slabs. Taking into account the shape

factor for square columns ($r_f = 1.15$), the shear punching strength V_{shear} of the connections was:

$$V_{shear} = 1.66\sqrt{f'_c}(c + d)d(100\rho)^{0.25} \quad [\text{N}] \quad (2.35)$$

in [mm] and [MPa].

2.3.3.5 Yamada et al. (1992)

Yamada et al. reported that their control specimen (6.6'×6.6'×7.9") failed in punching shear at the ultimate load that was only 92% of that estimated by ACI 318 Code. The properties of the control specimen were as follows:

- (i) no shear reinforcement
- (ii) 1.23% slab top reinforcement (#4 bars, $f_y = 116$ ksi)
- (iii) 0.62% slab bottom reinforcement (#4 bars, $f_y = 116$ ksi)

2.3.3.6 Strip model (Alexander and Simmonds 1992)

The strip model (also known as bond model) was developed at the University of Alberta, Edmonton, Canada (Alexander and Simmonds 1992, Alexander 1994, Afhami et al. 1998, Alexander 1999, Ospina et al. 2001). The strip model for punching was first developed by Alexander and Simmonds (1992) to determine the punching capacity of slabs with bonded orthogonal reinforcement. Alexander (1999) indicated that the strip model was valuable for assessment of existing structures, but might not be the best approach for design.

Figure 2.7 shows an idealization of an interior flat-plate slab-column connection according to the strip model. An interior connection is defined by four radial strips, extending from the column parallel to the slab reinforcement to a point of zero shear. The model assumes that the slab transfers the load to the radial strips, which in turn transfer the load to the column. Each radial strip is

loaded on its side faces by the adjacent quadrants of two-way slab. The amount of load transferred by the radial strips depends on their flexural capacity.

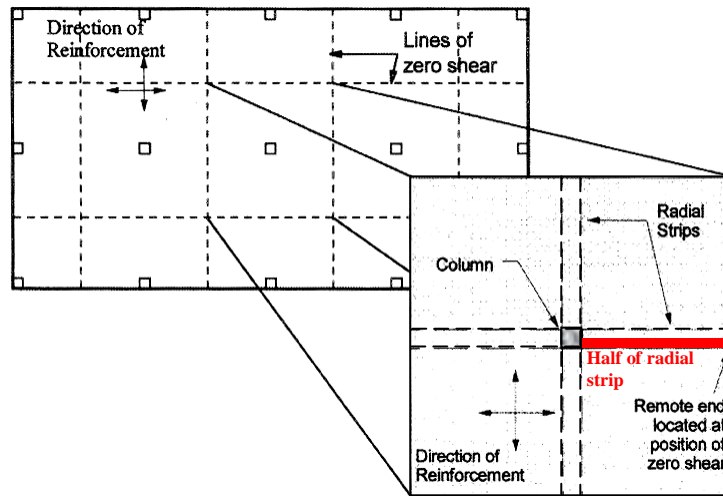


Figure 2.7 Geometry of radial strips (Alexander 1999)

A free body diagram of one-half of a radial strip is shown in Figure 2.8. The strip is loaded on its side face by a combination of plate bending moments m_n , torsional moments m_t , and shear force v . The strip is supported by a vertical reaction P_s at the column supported end and bending moments M_{neg} and M_{pos} at the column and remote ends of the strips, respectively.

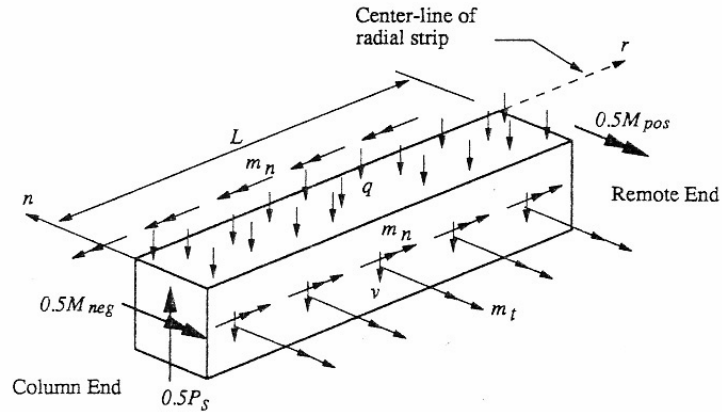


Figure 2.8 FBD of one-half radial strip (Alexander and Simmonds 1992)

At ultimate load, the free body diagram of a radial strip can be simplified as shown in Figure 2.9. The loading term w is a lower bound estimate of the one-way shear that can be delivered by the adjacent slab quadrant to one side of the strip at ultimate (Using ACI 318-05: $w = 2\sqrt{f'_c}$). The total distributed line load on the strip is $2w$ because the radial strip is loaded on two faces.

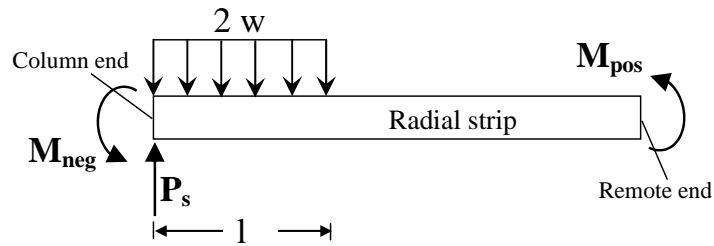


Figure 2.9 Simplified FBD of radial strip

Rotational equilibrium (Eq. (2.36)) indicates that the total flexural strength of the radial strip M_s is the sum of M_{neg} and M_{pos} at the ends of the strip. For slabs with remote ends that are rotationally free (like most interior connection tests in the literature), only M_{neg} needs to be calculated.

$$M_s = M_{neg} + M_{pos} = \frac{2wl^2}{2} \quad (2.36)$$

$$M_{neg} \approx \rho_{neg} \times f_y \times 0.9cd^2 \quad (2.37)$$

$$M_{pos} \approx \rho_{pos} \times f_y \times 0.9cd^2 \quad (2.38)$$

where l is the loaded length of the strip.

Vertical force equilibrium results in:

$$P_s = 2wl \quad \text{or} \quad l = \frac{P_s}{2w} \quad (2.39)$$

Substituting l from Eq. (2.39) into Eq. (2.36) yields the following relation:

$$P_s = 2\sqrt{M_s w} \quad (2.40)$$

Since an interior connection consists of four radial strips, its total punching shear capacity is:

$$P_{s,tot} = 8\sqrt{M_s w} \quad (2.41)$$

Afhami et al. (1998) indicated that the above equation assumes that all slab quadrants equally load the radial strips. This assumption gives the maximum estimate of punching capacity according to the strip model. In general, P_s from each radial strip is different. Considering a free body diagram of a quadrant of interior connection with a rectangular column shown in Figure 2.10, Afhami et al. showed that the minimum estimate of punching capacity $P_{s,min}$ occurs when either P_{s1} or P_{s2} has its minimum value. $P_{s,min}$ can be expressed as follows:

$$P_{s,min} = 2 \times c_2 \times w_1 + 4\sqrt{M_{s1} \times w_1 + M_{s2} \times w_2 - \frac{c_1^2 \times w_1^2}{4}} \quad (2.42)$$

where all subscripts 1 and 2 refer to strip #1 and strip #2, respectively.

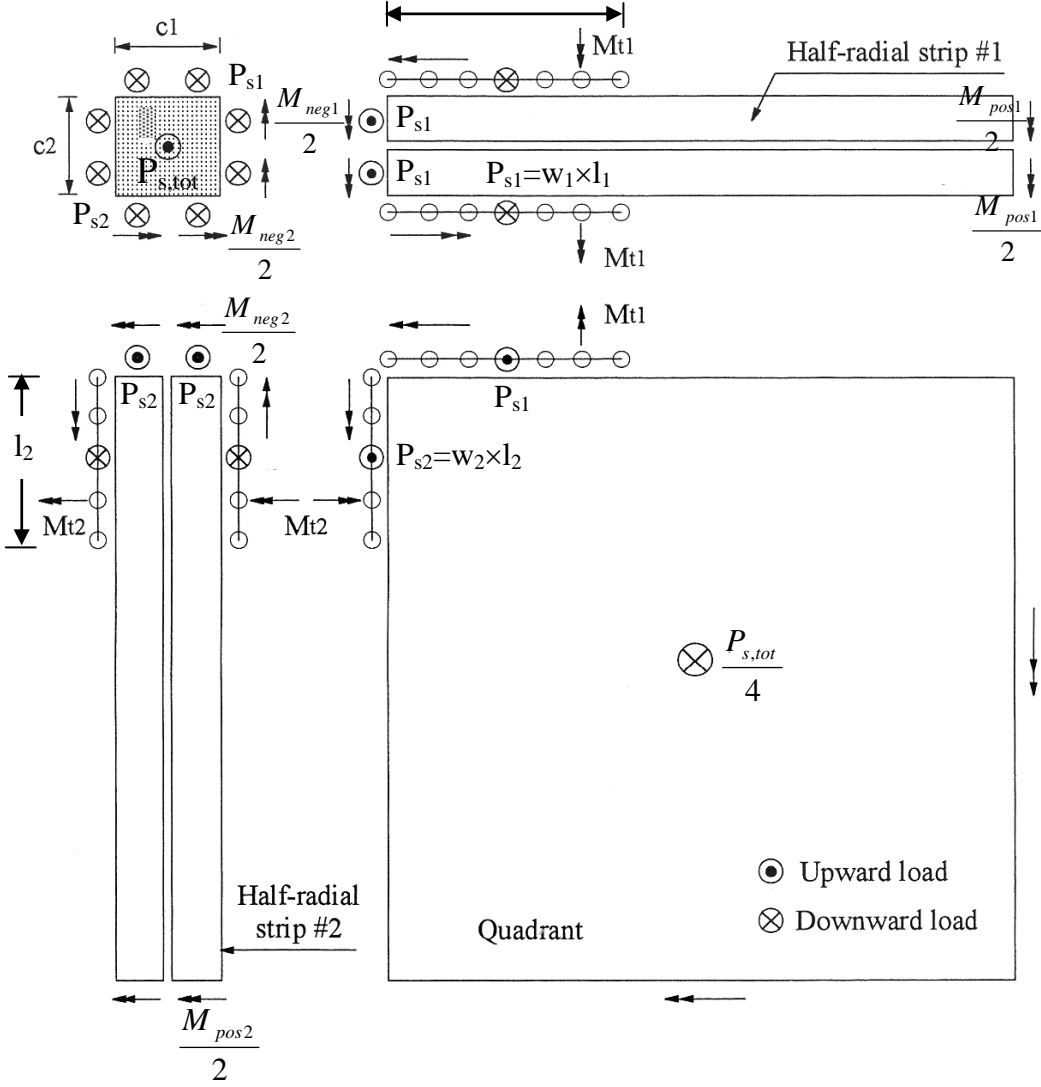


Figure 2.10 FBD of a concentrically loaded interior connection (Afhami et al. 1998)

For an interior connection with a square column ($c_1=c_2=c$) and with a symmetric orthogonal flexural reinforcement ($M_{s1} \cong M_{s2} \cong M_s$ and $w_1 \cong w_2 \cong w$), the actual capacity of the connection P_{actual} can be estimated as follows:

$$P_{s,\min} \leq P_{actual} \leq P_{s,tot}$$

$$2cw + 4\sqrt{2M_s w - \left(\frac{cw}{2}\right)^2} \leq P_{actual} \leq 8\sqrt{M_s w} \quad (2.43)$$

In conclusion, *the strip model assumes that the two-way shear capacity of slab-column connections is a function of both the one-way shear strength and the flexural shear strength of the slab in the vicinity of the column* (Alexander 1994).

2.3.3.7 Gardner (1995, 1996), Gardner and Shao (1996)

Gardner (1995) proposed the following design equation to calculate the two-way shear capacity of slab-column connections:

$$V_u = 0.55\lambda u_o d \left(1 + \sqrt{\frac{250}{h}}\right) \sqrt[3]{\rho f_y f_c'} \sqrt{\frac{h}{u_o}} \quad [\text{N}] \quad (2.44)$$

in [mm] and [MPa], where :

u_o : perimeter of square column of same cross-sectional area

λ : factor to account for different concrete density ($\lambda=1$ for normal density concrete)

ρ : flexural reinforcement ratio within $(c+6d)$ region

Gardner and Shao (1996) conducted a punching shear test on a one-half scale of two-bay-by-two-bay flat plate structure with 0.66% top steel in the interior connection. They found that the interior column failed first (when the edge and corner connections remained relatively intact) at the measured load equal to 83% of the capacity estimated through the use of the ACI Code. Significant cracks, large enough to indicate that the steel had yielded, occurred at the perimeter of all failed connections. They indicated that all failures were combined flexural punching shear failures. They proposed the following equation:

$$V_u = 0.66u_o d \left(1 + \sqrt{\left(\frac{200}{d}\right)} \right) \sqrt[3]{\rho f_y f_c'} \sqrt{\frac{d}{u}} \quad [\text{N}] \quad (2.45)$$

provided that ρ is greater than 0.5% within $(c+6d)$ region.

By extending the work of Shehata and Regan (1989), Gardner (1996) proposed:

$$V_u = 0.62u_o d \left(1 + \sqrt{\left(\frac{200}{d}\right)} \right) \sqrt[3]{\rho f_y f_c'} \sqrt{\frac{d}{u_o}} \quad [\text{N}] \quad (2.46)$$

Gardner et al. (2002) showed that Eq. (2.46) predicted a high probability of punching shear failure in Sampoong Department Store whereas ACI 318 provisions did not. They indicated that the two-way shear strength provisions of ACI 318 were poor for slabs with $\rho < 0.5\%$ and for thick slabs (both of these factors were present in the slabs of Sampoong Department Store).

2.3.3.8 *Sherif and Dilger (1996)*

After studying the effect of different parameters affecting the two-way shear strength of the slab-column connections, Sherif and Dilger (1996) proposed that the two-way shear strength of the connections with a square column is the lesser of the Eqs. (2.47) and (2.48).

$$V_c = 0.7 \sqrt[3]{100\rho f_c'} b_o d \quad [\text{N}] \quad (2.47)$$

$$V_c = 0.7 \left(\frac{6.7d}{b_o} + 0.4 \right) \sqrt[3]{100\rho f_c'} b_o d \quad [\text{N}] \quad (2.48)$$

where b_o is the critical perimeter at $d/2$ away from the column face.

2.4 ACI DESIGN PROVISIONS: FLAT-PLATE SLAB-COLUMN CONNECTIONS

2.4.1 Provisions for two-way shear strength

2.4.1.1 Joint Committee of 1924

In 1924, the ACI code committee (Joint Committee of 1924) recommended that the calculated shear stress v and the allowable shear stress are given in Eqs. (2.49) and (2.50), respectively.

$$v = \frac{V}{bjd} \quad (2.49)$$

$$v = 0.02f_c'(1+n) \leq 0.03f_c' \quad (2.50)$$

where V is the shear force, b is the critical shear perimeter located at a distance of ($t-1.5''$) from the periphery of the loaded area, jd is the distance between the centroid of compression and tension force, t is the slab thickness, f_c' is the concrete compressive strength [psi], and n is the ratio of the flexural reinforcement area crossing directly through the loaded area (column, column capital, etc.) to the total flexural reinforcement area in the slab. The report of 1924 was also adopted by the ACI as standard specifications and only minor changes have been made with respect to shear and diagonal tension in slabs and footings since then.

2.4.1.2 ACI 318-41, ACI 318- 47, ACI 318-51

The three editions of ACI-318 codes from 1941 to 1951 have the same provisions for shear strength. The shear stress v as a measure of diagonal tension is computed using Eq. (2.49) and the allowable v for two-way slabs is:

- $0.03f_c'$ if at least 50% of the total negative flexural reinforcement in the column strip passes through the periphery.
- $0.025f_c'$ if 25% or less of the total negative flexural reinforcement in the column strip passes through the periphery.

The allowable v for footings is $0.03f_c' \leq 85$ psi. As recommended by the Joint Committee of 1924, the critical shear perimeter is located at a distance of $(t-1.5")$ from the periphery of the loaded area.

2.4.1.3 ACI 318-56

ACI 318-56 introduced the maximum limit of 100 psi and 85 psi for the allowable v as follows:

- $0.03f_c' \leq 100$ psi if at least 50% of the total negative flexural reinforcement in the column strip passes through the periphery.
- $0.025f_c' \leq 85$ psi if 25% or less of the total negative flexural reinforcement in the column strip passes through the periphery.

The critical shear perimeter is located at a distance d away from the loaded area.

2.4.1.4 ACI 318-63

The provisions of ACI 318-63 were developed on the basis of the recommendations by ACI-ASCE Committee 426 (formerly 326), Shear and Diagonal Tension. The major philosophy of these provisions was to produce members for which ultimate strength would be governed by flexure rather than shear, so that members would have a ductile character.

Significant changes to shear provisions introduced in ACI 318-63 were:

1. ACI 318-63 was the first edition of the ACI 318 codes that contained an ultimate strength design criteria for shear. ACI 318-63 prescribed the use both load factors and capacity reduction factors ϕ .

2. Diagonal tension for concrete was stated as a function of $\sqrt{f_c'}$.

ACI-ASCE Committee 326 recommended that v was a function of $\sqrt{f_c'}$ and the ratio of column size to effective slab depth c/d . However, the committee pointed out that the variable of c/d could also be taken into account by using a critical perimeter $d/2$ away from the loaded area. For simplicity, especially for irregular column shapes and slabs with openings near the column, ACI 318-63 adopted the following approach: v was independent of c/d and equal to $4\sqrt{f_c'}$.

3. The critical shear perimeter was located at $d/2$ away from the loaded area. Commentary of ACI 318-63 indicated that while the true pyramidal failure surface was at 45 degrees to the neutral axis, the stresses on this surface were complex (containing both shear and bending forces). For simplicity, a vertical section on which the tangential component was caused only by shear was selected. Such a section was located at a distance of $d/2$ from the loaded area.
4. The factor j was eliminated.
5. Long and narrow slabs or footings, acting as a one-way beam and a two-way member, respectively, were differentiated.

ACI 318-63 stated that the nominal ultimate shear strength v_u in slabs and footings is:

$$v_u = \frac{V_u}{b_o d} \quad (2.51)$$

where V_u is the total factored shear force, b_o is the critical shear perimeter located at $d/2$ away from the loaded area. Without shear reinforcement:

$$v_u \leq 4\phi\sqrt{f_c'} \quad (2.52)$$

where ϕ is the capacity reduction factor (= 0.85 for shear).

The ACI 318 provisions for basic two-way shear strength of slab (Eqs. (2.51) and (2.52)) have not changed since 1963, except in 2002, when ϕ -factor was reduced to 0.75.

2.4.2 ACI design provisions for two-way shear strength: Observations of Alexander and Hawkins (2005)

Alexander and Hawkins (2005) indicated that the basic two-way shear strength of ACI provision ($V_c = 4\sqrt{f'_c}b_o d$) is based on Moe's work (1961). Even though the ACI provision does not contain a term to account for flexural reinforcement, it is derived from an equation that accounts for flexural reinforcement (V_{flex} in Eq. (2.17)).

Figure 2.11 shows the ultimate load capacity of slab-column connections as a function of flexural capacity. Moe (1961) developed his design equation by setting $V=1.1 V_{flex}$ (represented by the dashed straight line in Figure 2.11). Point A, where the $V=V_{flex}$, marks a change in the load-deformation behavior of the connection. To the left of A, flexure governs and the slabs will develop significant deflections and extensive cracking before punching shear failures occur. To the right of A, shear governs and there may be little warning before the punching shear failures occur. The philosophy of ACI provisions is to ensure that the design is to the left of point A so that flexural failure mode governs. This philosophy implies that the slab has some ductility.

In Figure 2.11, O-C-A-B is the behavior envelope and O-C-D is the design envelope. Alexander and Hawkins (2005) emphasized that the ACI 318 provisions were never intended as a means to predict the test results. Rather, they were intended to be a means of preventing punching shear failure prior to the development of full flexural strength. They further commented that the quality of

the code equation as a design tool is not supposed to be measured by ratios of test to predicted results. In this case, the usefulness of the code as a design tool depends on how close point C is to point A. Alexander and Hawkins' (2005) opinions about the intent of the code are in agreement with Sozen (2006) who indicated that the function of the code is simply to produce a safe and serviceable structure and not to determine response.

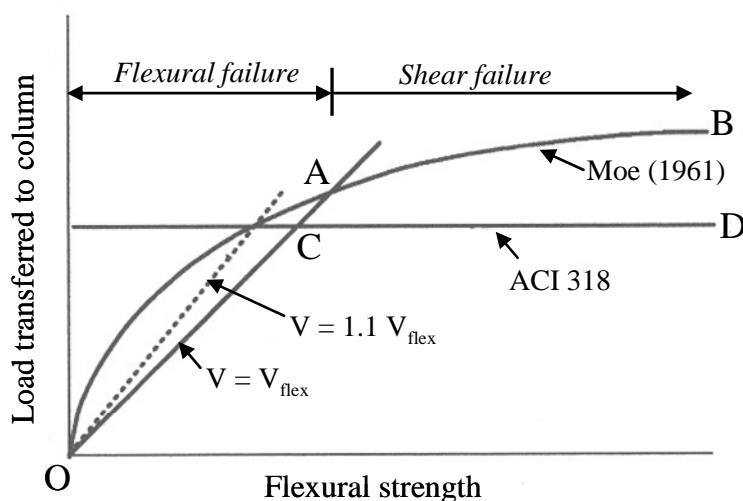


Figure 2.11 Ultimate capacity of slab-column connection (Alexander and Hawkins 2005)

2.4.3 Provisions related to unbalanced moment transfer under gravity loads

2.4.3.1 Calculation of unbalanced moment

Under gravity loads, unbalanced moment M_{unb} can be developed in interior connections due to pattern loading and/or unequal span lengths. This M_{unb} must be transferred from the slab to the columns. If the slab is too thin or insufficiently reinforced near the column, it can fail by a combination of flexure and punching shear around the column.

Two different assumptions for the placement of gravity loads (pattern loading) are shown in Figure 2.12. The most conservative assumption in calculating M_{unb} due to pattern loading is that one side has factored dead load w_d only, while the other side has factored dead and live loads ($w_d + w_l$). ACI 318 is not this conservative. Section 13.6.9 of ACI 318-05 (which originated in ACI 318-77) assumes that one side has w_d only, while the other side has ($w_d+0.5w_l$).

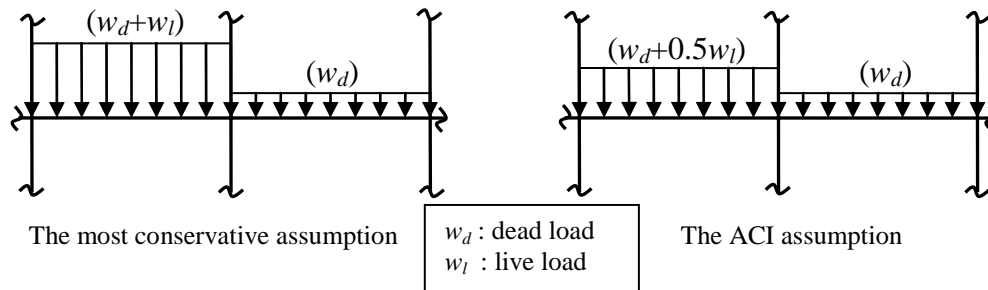


Figure 2.12 Different assumptions for pattern loading

It was assumed that M_{unb} transferred to the columns depends on the relative flexural stiffness of the equivalent column to that of slab (ACI 318-77). ACI 318-83 simplified the formula by assuming that 7/8 of the total M_{unb} is transferred to the column. For interior connections with equal spans on both sides, M_{unb} is

$$M_{unb} = 0.07l_2l_n^2(0.5w_l) \quad (2.53)$$

where l_n is the clear span length in the direction of M_{unb} and l_2 is the clear span length in the direction perpendicular to l_n . This provision remained unchanged up to ACI 318-05.

2.4.3.2 Concentration of reinforcement

It is assumed that M_{unb} is transferred by flexure and eccentric shear. In order to resist the flexural component of M_{unb} , ACI Code indicates that a

concentration of reinforcement around the connection can be used. The development of ACI provisions for concentration of reinforcement in the vicinity of columns can be summarized as follows:

ACI 318-63 article 2102(g) indicated that concentration of reinforcement over the column head by placing additional reinforcement or spacing the rebars closely within $(c+3h)$ could be used to resist the moment of the section. By stating that the “ M_{unb} transfer shall be investigated by a rational analysis”, the code did not provide specific guidance in calculating M_{unb} . The commentary stated that extensive tests reported by ACI-ASCE Committee 426 (previously known as ACI-ASCE Committee 326) showed that the concentration of reinforcement over the column head had no advantage in shear strength.

ACI 318-71 section 13.2.4 stated that the region where the flexural reinforcement is effective in resisting M_{unb} is within $(c+h)$ instead of within $(c+3h)$ in ACI 318-63. In addition, it stated, “... *Concentration of reinforcement over the column head by closer spacing or additional reinforcement “may” be used to resist the moment on this section.*” ACI 318-71 section 11.13.2 specified that for a square column, 40% of the M_{unb} should be considered to be transferred by eccentric shear. The commentary added that 60% of the M_{unb} should be considered to be transferred by flexure.

ACI 318-74 supplement explicitly added the requirement in section 13.2.4 that for a square column, 60% of the M_{unb} should be considered to be transferred by flexure ($\gamma_f = 0.6$). This provision also indicated that the flexural reinforcement within $(c+3h)$ region was effective to resist part of unbalanced moment, just as it was stated in ACI 318-63.

ACI 318-89 section 13.3.3.3 emphasized the need for concentrating reinforcement within $(c+3h)$ to carry 60% of M_{unb} by altering the word “*may*” to “*shall*”. Section 13.3.3.3 reads: “*Concentration of reinforcement over the column*

by closer spacing or additional reinforcement “shall” be used to resist moment on the effective slab width defined in 13.3.3.2” ACI 318-89 specified that the total M_{umb} should be considered to be transferred by eccentric shear and by flexural reinforcement within the $(c+3h)$ region.

ACI 318-95 section 13.5.3.3 permitted designers to increase the value of γ_f up to 25% provided that the factored shear does not exceed 40% of the shear capacity and the reinforcement ratio within $(c+3h)$ required to resist $\gamma_f M_{umb}$ does not exceed $0.375 \rho_b$. The commentary of ACI 318-95 also added that under moment reversal type of loading, both top and bottom reinforcements should be concentrated within $(c+3h)$ region and a ratio of top to bottom reinforcement of about 2 has been observed to be appropriate. The provisions of ACI 318-95 remain unchanged up to ACI 318-05.

2.4.4 Seismic provisions for flat-plate structures

ACI 318-83 is the first edition of ACI 318 codes that has seismic provisions for flat-plate structures in moderate seismic region. Section A.9.6.2 of ACI 318-83 indicated that 60% of factored unbalanced moment involving seismic loads shall be resisted by flexural reinforcement within $(c+3h)$ region. In order to resist the moment, concentration of reinforcement by closer spacing or additional reinforcement “may” be used. These provisions have not changed since 1983, except in 1989, the word “may” was changed to “shall” as discussed in the previous section (Section 2.4.3.2).

2.5 DIFFERENT BUILDING CODES PROVISIONS FOR TWO-WAY SHEAR STRENGTH OF INTERIOR SLAB-COLUMN CONNECTIONS

The basic two-way shear provisions of several major building codes for interior slab-column connections without shear reinforcement under concentric load (i.e. without moment transfer) is summarized in this section. Only square columns and normal density concrete are considered.

Without shear reinforcement, the nominal two-way shear strength of reinforced concrete members V_n is equal to concrete contribution V_c . All code recommendations on punching use the nominal shear stresses calculated by dividing the shear force by an area equal to the product of the length of a critical perimeter and the effective depth of the slab. Various design codes differ in regard to the distance between the column face and the perimeter, and in the expressions used to define the limiting value of the stress, the effect of flexural reinforcement, and the size effect. Reviews of codes are given in Hallgren (1996), Bari (2000), Fib (2001), Albrecht (2002), Salna et al. (2004), Gardner (2005), Mitchell et al. (2005), Dilger et al. (2005), Hegger et al. (2005), and Pisanty (2005).

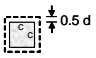
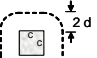
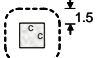
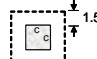
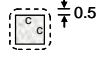
Different building code provisions for V_c are summarized in Table 2.2. A special provision to account for a reduction in nominal shear strength due to different increasing ratios of critical shear perimeter to effective depth is not included. To make the comparison easier, a consistent set of symbols is used for all provisions and the equations are given in SI units (mm and MPa).

In general, V_c can be expressed as follows:

$$V_c = v_c \times \xi \times \kappa_\rho \times b_o \times d \quad (2.54)$$

where v_c is the nominal shear strength, ξ is the size effect factor, κ_ρ is the longitudinal flexural reinforcement factor, b_o is the critical shear perimeter, and d is the effective depth.

Table 2.2 Code provisions for basic two-way shear strength

Building Codes	General equation: $V_c = v_c \times \xi \times \kappa_\rho \times b_o \times d$			
	v_c	ξ	κ_ρ	b_o
	Shear stress	Size effect	Reinforcement ratio	Critical shear perimeter
ACI 318-05	$0.33\sqrt{f_c'}$			 $b_o = 4(c + d)$
CSA A 23.3-04	$0.38\sqrt{f_c'}$	For $d > 300$ mm : $\frac{1300}{1000 + d}$		
AS 3600-1994	$0.34\sqrt{f_c'}$			
IS : 456	$0.25\sqrt{f_{ck,cube}}$			
Eurocode 2-2003 & CEB-FIP MC 90	$0.18(f_{ck})^{1/3}$	$\left(1 + \sqrt{\frac{200}{d}}\right) \leq 2.0$	$(100\rho)^{1/3}$ $\rho \leq 0.02$	 $b_o = 4(c + \pi d)$
DIN 1045-1 (2001)	$0.14(f_{ck})^{1/3}$			 $b_o = 4c + 3\pi d$
BS 8110-97	For $f_{ck,cube} > 25$ MPa : $0.79\left(\frac{f_{ck,cube}}{25}\right)^{1/3}$ For $f_{ck,cube} \leq 40$ MPa	$\left(\frac{400}{d}\right)^{1/4}$	$(100\rho)^{1/3}$ $\rho \leq 0.03$	 $b_o = 4(c + 3d)$
JSCE (1986)	$0.188\left\{1 + \frac{1}{\left(1 + \frac{c}{d}\right)}\right\}\sqrt{f_c'}$	$\left(\frac{1000}{d}\right)^{1/4} \leq 1.5$	$(100\rho)^{1/3} \leq 1.5$	 $b_o = 4c + \pi d$

f_c' : Specified concrete cylinder compressive strength
 f_{ck} : Characteristic concrete cylinder compressive strength
 $f_{cube} \approx 1.25 f_c'$

d : Average depth of slab reinforcement
 c : Column dimension

The European Codes use a characteristic strength f_{ck} instead of a specified concrete strength f_c' . Gardner (2005) reported that f_{ck} can be related to f_c' as follows:

$$f_{ck} = f_c' - 1.60 \text{ MPa} \quad (2.55)$$

2.5.1 American Concrete Institute Code (ACI 318-05)

In US customary units, V_c of an interior slab-column connection with a square column is the lesser of Eqs. (2.56) and (2.57).

$$V_c = \left(40 \times \frac{d}{b_o} + 2 \right) \times \sqrt{f_c'} \times b_o \times d \quad (2.56)$$

$$V_c = 4 \times \sqrt{f_c'} \times b_o \times d \quad (2.57)$$

The critical shear perimeter is located at a distance of $d/2$ away from the column face. The basic form of the Australian Code AS 3600-1994, Indian Code (IS : 456), and Bangladesh National Building Code (BNBC) 1993 provisions are very similar to the ACI 318-05 provisions.

2.5.2 Canadian Standard (CSA-A 23.3-04)

CSA-A 23.3-04 provisions for two-way shear are slightly different than the ACI 318-05 provisions in that the CSA-A 23.3-04 provisions include a size effect factor ξ for slabs having an average depth of reinforcement greater than 12 inches (300 mm).

McHarg et al. (2000) indicated that while CSA A23.3-94 used the same nominal shear stress at failure as the ACI 318-95 (which is the same as ACI 318-05), it further required that a minimum amount of the top flexural reinforcement be concentrated in the $(c+3h)$ region.

2.5.3 Building code provisions: Comparison

As shown in Table 2.2, not all code provisions account for ρ as a factor affecting two-way shear strength. In order to compare the sensitivity of two-way shear strength to the change in ρ according to different code provisions, a prototype structure without shear reinforcement and with a 24-inch square column, 9-inch slab thickness, 7-in effective depth, 4000-psi specified concrete cylinder strength was analyzed. Figure 2.13 shows the estimated two-way shear strength of the interior connection in the prototype structure as a function of ρ .

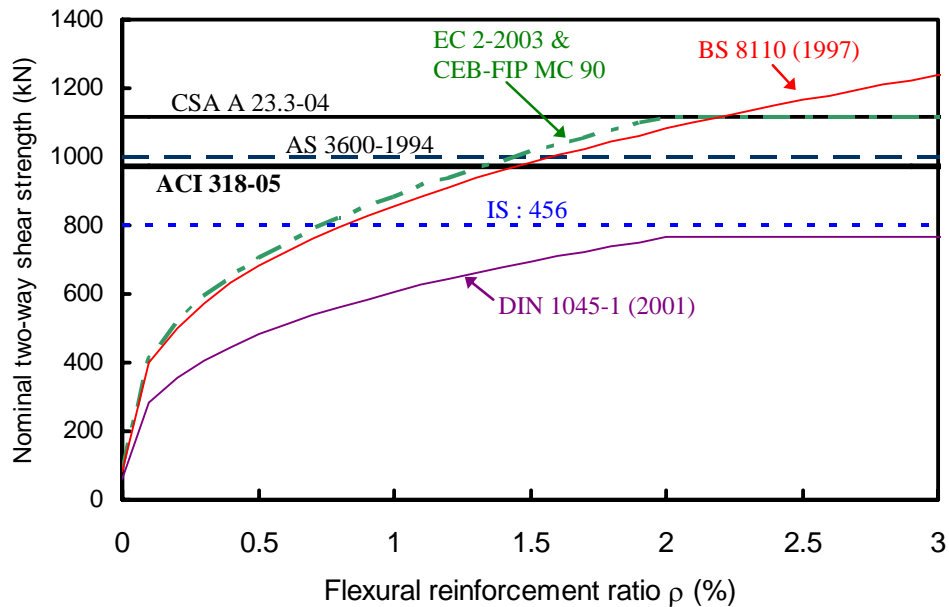


Figure 2.13 Two-way shear strength according to different building code provisions

Figure 2.13 shows that there is a significant variation in the predicted nominal two-way shear strength V_c , especially for $\rho < 1\%$, which is common in many flat-plate structures. DIN 1045-1 (2001) provides the lowest values of V_c for any ρ value. From all code provisions that do not account for ρ , ACI 318-05 results in values of V_c that are about the average of the maximum V_c (from CSA

A23.3-04) and the minimum V_c (from IS:456). For all practical ranges of ρ values in flat-plate structures ($< 2\%$), EC 2-2003, CEB-FIP MC 90, and BS 8110 (1997) predict about the same V_c . For ρ values between 1.3% and 1.5%, the use of ACI 318-05 provisions result in about the same V_c as that estimated using EC 2-2003, CEB-FIP MC 90, and BS 8110 (1997) codes.

2.6 EFFECT OF FLEXURAL REINFORCEMENT ON PUNCHING SHEAR

2.6.1 Flexural reinforcement ratio

There have been conflicting opinions on whether the flexural reinforcement ratio ρ has an effect on the two-way shear strength of slab-column connections V_c . Marzouk and Hussein (1991), Gardner and Shao (1996), and Sherif and Dilger (1996) concluded from their test results that V_c is a function of ρ . Vanderbilt (1972) showed that doubling ρ from 1% to 2% resulted in only a modest increase in V_c . However, Elstner and Hognestad (1956) and Moe (1961) indicated that increasing ρ near the column did not increase V_c . The concentration of reinforcement resulted in $\rho=7\%$ and 6.3% (Elstner and Hognestad 1956) and $\rho = 1.5\%$, 2.3%, and 3.5% (Moe 1961). Whitney (1957) and Alexander and Simmonds (1992) pointed out that these earlier investigations did not show the benefits of increasing ρ by concentrating the flexural steel because the specimens failed due to bond failure of closely spaced bars.

Regan (1981) indicated that ρ may affect punching resistance in several ways:

- (i) An increase of ρ should increase the depth of the compression zone and thus the area of uncracked concrete available to support shear forces. It should also reduce the crack width, thus improving the transfer of forces by aggregate interlock, and increase dowel action.

- (ii) An increase of ρ should enhance the restraint available in the plane of the slab, and therefore increase the two-way shear strength. However, Hawkins and Mitchell (1979) indicated that the available restraint (due to membrane action) around the connection can diminish if flexural reinforcement yields. And therefore, the nominal ultimate shear strength of connections transferring shear decreases as the extent of yielding in the slab flexural reinforcement increases.

Yitzhaki (1966) indicated that the relative amount of ρ with respect to the balanced reinforcement ratio ρ_{bal} (defined as the ρ to make the punching shear strength equal to the flexural strength) can affect mode of failure. When $\rho < \rho_{bal}$, slabs would fail in flexure and increasing ρ is very effective to increase punching resistance. When $\rho > \rho_{bal}$, slabs would fail in punching. In this case, punching resistance was insensitive to ρ and increasing ρ to increase punching resistance would be uneconomical. Gardner (1995) also indicated that while increasing ρ increases the punching resistance, the behavior of the connection becomes more brittle.

2.6.2 Concentration of reinforcement towards the column or loaded area

ACI-ASCE Committee 426 (1974) believed that concentration of reinforcement towards the column or loaded area does not improve the shear strength. However, the committee encouraged the concentration of reinforcement in the column region because it enhances the flexural behavior of the slab under service loads.

Regan (1981) reported that for practical arrangements of bars, Moe's tests (1961) and the CIRIA (Concrete Industry Research and Information Association) results showed decreases of strength by roughly 6% with increasing concentration, compared with those for slabs with uniform steel. Regan and

Braestrup (1985) concluded that concentrating the reinforcement is not beneficial. In extreme cases, the results showed that it can even be harmful, because excessive concentration leaves large radial sectors almost unreinforced.

Rankin and Long (1987) indicated that the local increase of moment capacity due to concentration of reinforcement is offset by the reduction of slab ductility. McHarg et al. (2000) indicated that the concentration of the top mat of flexural reinforcement results in a higher punching shear resistance, higher post-cracking stiffness, a more uniform distribution of strains in the top bars, and smaller cracks at all levels of loading compared with companion specimens with a uniform distribution of top reinforcement.

McHarg et al. (2000) and Salna et al. (2004) also indicated that the concentration of the flexural reinforcing bars near the column increased the size of the shear failure surface. With $\rho=1\%$, the failure surface was at an angle of approximately 45° from the horizontal. With $\rho=2\%$, the failure surface was at an angle of approximately 30° from the horizontal.

2.6.3 Compression steel

ACI-ASCE Committee 426 (1974) reported that compression reinforcement had a negligible effect on the ultimate strength, provided ϕ_o $\left(= \frac{V_{shear}}{V_{flex}} \right)$ was significantly less than unity. However, as ϕ_o approached unity, an increase in the compression reinforcement ratio increased the ultimate capacity because the tensile in-plane force capacity of the slab is increased. Summarizing others' test results, Regan (1981) indicated that the punching shear strength was not significantly influenced by the amount of compression flexural reinforcement. He reported that with the ratios of compression steel varied from 0.3 to 1.0 times

the ratios of tension steel, the maximum increase of punching resistance was only 12%.

2.7 RESIDUAL CAPACITY AFTER PUNCHING SHEAR FAILURE

Criswell (1970, 1974) indicated that some resistance of the connection remains after punching failure because of “*the doweling or suspension action of the tensile reinforcement crossing the failure surface.*” A resistance of 20 to 30% of the failure load remained after the punching failure of the isolated slab-column specimens.

Hawkins and Mitchell (1979) recommended that unless a tensile membrane is deliberately provided, the post-punching shear capacity should be taken as the shearing yield strength of all the bottom reinforcement passing through the column V_d as follows:

$$V_d = 0.5nA_s' f_y \quad (2.58)$$

where n , A_s' and f_y are the number, the area, and the yield stress of bottom reinforcement passing through the column (for all sides).

Regan (1981) and Regan and Braestrup (1985) indicated that once punching had occurred, top flexural reinforcement that were not restrained by shear reinforcement made only a very limited contribution to resistance because their cover was readily torn away. Bottom flexural reinforcement, being much more deeply embedded could not be pulled out in the same way and as such provided resistance initially by dowel action and then at larger deformations by catenary action. Regan (1981) proposed the Rasmussen's (1963) equation as a basis to determine the amount of bottom steel that should pass from a slab into a column for post-punching resistance as follows:

$$V_d = 1.2nd_b^2 \sqrt{f_y f_{c,cube}} \quad (2.59)$$

where n and d_b is the number and the diameter, respectively, of bottom reinforcement passing through the column faces and fully anchored on either side. Any continuous bottom bars are counted twice. Regan (1981) also indicated that Eq. (2.59) was not intended to represent an accurate assessment of strength. It is believed that the intent was to conservatively estimate V_d using a relatively simple formula.

Even though Regan (1981) indicated that top flexural reinforcement was not very effective, he reported that in CIRIA tests of interior slab-column connections that had only tension flexural steel, residual capacity after punching shear failure varied between 25% and 50% of the ultimate capacity. The high values being for cases where the bars were very heavily concentrated near the column.

Pan and Moehle (1992) reported that even though the top slab reinforcement was less reliable and less efficient than the bottom slab reinforcement (due to “tearing out” of top steel and loss of top concrete cover), the top slab reinforcement was also capable of resisting gravity load following initial punching.

Having observed the test results of slab-column connections without bottom slab reinforcement, Hallgren (1996) indicated that after punching failure, the residual load capacity of the slabs without shear reinforcement was due to dowel and membrane effect of the top slab rebars. However, if the rebars intersecting the shear crack yielded, then the dowel force reduced considerably.

2.8 FIBER REINFORCED POLYMERS (FRP)

The use of FRP as a strengthening material has become more popular. Bakis et al. (2002) reported, “... *The number of applications involving FRP as strengthening and repair materials worldwide has grown from just a few 10 years ago to several thousand nowadays...*” Nanni (2003) stated, “... *On the application side, FRP materials have been used in some multi-million dollar projects for strengthening parking garages, multi-purpose convention centers, office buildings, and silos...*”

FRP is defined as a polymer (plastic) matrix that is reinforced with fibers or other reinforcing materials to provide a discernable reinforcing function in one or more directions. Three common fibers used in FRP are carbon fibers, glass fibers, and aramid fibers (Teng et al. 2002). Depending on the fibers used, FRP are classified into three types: Carbon-Fiber-Reinforced Polymer (CFRP), Glass-Fiber-Reinforced Polymer (GFRP), and Aramid-Fiber-Reinforced Polymer (AFRP). Figure 2.14 shows the ranges of stress-strain curves for the three types of FRP in comparison with steel. Compared with other types of FRP, CFRP offers the highest stiffness and strength, but exhibits the most brittle behavior.

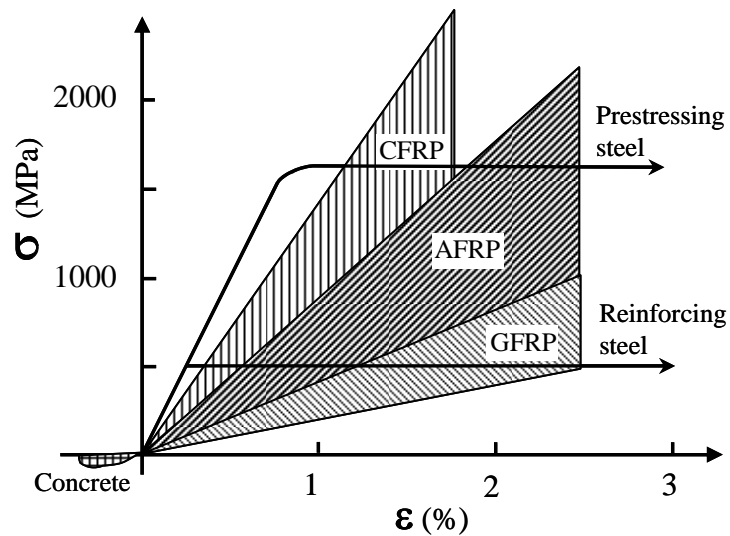


Figure 2.14 Generic characteristics of FRP
(http://www.shef.ac.uk/~ccc/frp/what_is_frp.htm)

2.8.1 Characteristics of FRP used for structural rehabilitation

Some advantageous characteristics of FRP are as follows:

- Corrosion resistance (Fib. 2001b)
- High strength and stiffness per unit weight (Liao et al. 1998, Concrete Society 2000, Karbhari 2001, Fib. 2001b)
- Good fatigue performance (Liao et al. 1998, Triantafillou 1998)
- Excellent creep/relaxation performance (Triantafillou 1998)
- Low thermal expansion (Liao et al. 1998)
- Having adequate weather-proofing properties with regard to tensile strength and bond to concrete, as well as being quite durable to freezing and thawing (Yagi et al. 1997).
- Relatively easy to apply

The installation of FRP can be less labor-intensive and less equipment-intensive than the installation of steel or concrete for structural

rehabilitation (Sheikh 2002), and these attributes make FRP extremely attractive for use in rehabilitation of existing structures, especially in cases where dead weight, space, or time restrictions exist (Karbhari 2001).

- Relatively easy to blend in with the existing architectural features of existing structures and easy to conform to any shape.

Several disadvantageous characteristics of FRP fabrics can be summarized as follows:

- Brittle
Neale (2000) indicated that appreciable strength obtained by bonding FRP to reinforced concrete members is generally accompanied by a loss of ductility or reduction of deflection at failure.
- Relatively expensive (Triantafillou 1998).
- Prone to high-temperature degradation and flammable (Fib. 2001b).
Kodur et al. (2004) indicated that most FRPs suffer degradation of mechanical properties at temperatures that are only slightly higher than ambient temperatures.
- Having incompatible thermal expansion coefficients with concrete (Fib. 2001b)
- Easily damaged by ultraviolet rays if it is exposed to direct sunlight (De Rose 1997)
- Silica-based glass composites may deteriorate in an alkaline environment such as concrete (Concrete Society 2000).

Properties, behavior, and durability of FRPs are summarized in Liao et al. (1998), ACI Committee 440 (2002), Karbhari et al. (2003), and Harries et al. (2003).

2.8.2 Structural performance of FRP under elevated temperatures

The potential impact of fire on structures that are externally reinforced with FRP can be more severe in confined spaces (such as buildings) as opposed to open spaces (such as parking garages or bridges). Even though most fibers are not easily burnt, resins contain large amounts of carbon and hydrogen that are flammable. Therefore, the external application of FRP requires special coatings to meet fire standards (De Rose 1997). A fire-resistant epoxy coating is currently available to achieve a UL (Underwriters Laboratories, Inc.) Class 1 rating in a 3-hour flame and smoke spread test of ASTM E84 (Fyfe Co. LLC 2000). Kodur et al. (2004) showed that under fire tests according to ASTM E119, concrete members externally reinforced with FRP that was fire-proofed with 1.5-inch of fire-resistant epoxy coating could exhibit 4-hour fire endurance.

During fire resistance tests on composite laminates (Davies et al. 2004), internal pressure due to vaporization of chemically bonded water within the resin overcame the tensile strength of the matrix and tore the laminate at about 200°C. In order to maintain a safety factor in case of fire, Bakis et al. (2002) recommended that the degree of strengthening (ultimate capacity of the strengthened element divided by that of unstrengthened element) should be limited.

2.8.3 FRP sheets versus steel plate

Strengthening of reinforced concrete members using externally epoxy-bonded steel plates was commonly used. Even though the technique was relatively simple, cost-effective, and efficient, it has several disadvantages such as prone to corrosion, heavy weight, undesirable stiffness increase, and obstruction of occupancy (Triantafillou 1998).

With the use of FRP, some of the disadvantages of using steel plates can be overcome. FRP sheets can easily conform to the shape of the elements and can also be used in areas with limited access, where traditional techniques could be difficult to implement. FRP sheet is relatively thin so that it does not change the useable space in the building and may not have adverse effects on aesthetics.

Although FRP sheets cost more than steel plates, they are generally easier to install. Easier installation reduces requirements for labor and heavy equipment. In the long run, FRP sheets may also be more durable than steel plates. This may increase the economic life of FRP sheets and reduce the maintenance costs (De Rose 1997). Therefore, when installation and life cycle costs are included in cost comparison, rehabilitation using FRP sheets can be competitive with that using steel plates. Retrofitting by FRP sheets has been shown to be less expensive than that by steel plates, especially if handling is a dominant cost factor (Meier 1997, Liao et al. 1998).

2.8.4 Debonding of FRP

One of the common modes of failure in FRP strengthened structural members is the debonding of FRP from concrete surface (Bonacci and Maalej 2001). Debonding initiates at a crack and then propagates towards the nearer end (Teng et al. 2003). In order to delay debonding and to prevent propagation of the debonding, several solutions have been proposed:

- Limit the FRP strain

Triantafillou (1998) suggested that the FRP strain be limited to the minimum of the following:

1. 5-6 times of the yield strain of internal flexural reinforcement
2. 0.8%
3. one-half of the ultimate tensile strain of the FRP

ACI Committee 440 (2002) introduced expressions for a bond coefficient κ_m and recommended that the FRP strain was limited to κ_m times the ultimate rupture strain.

For $nE_f t_f \leq 1,000,000$:

$$\kappa_m = \frac{1}{60\varepsilon_{fu}} \left(1 - \frac{nE_f t_f}{2,000,000} \right) \leq 0.90 \quad (2.60)$$

For $nE_f t_f > 1,000,000$:

$$\kappa_m = \frac{1}{60\varepsilon_{fu}} \left(\frac{500,000}{nE_f t_f} \right) \leq 0.90 \quad (2.61)$$

where n is the number of plies of FRP reinforcement, E_f is the tensile modulus of elasticity [psi], t_f is the nominal thickness of one ply of the FRP reinforcement [in], and ε_{fu} is the design rupture strain.

Arya et al. (2002) indicated that limiting the FRP strain to 0.008 when the load is uniformly distributed, or to 0.006 if a combined high shear and moment is present, can prevent debonding failure.

Bakis et al. (2002) recommended that for flexural strengthening, the tensile strain in the FRP should be limited to about 0.008 to suppress the delamination of FRP at the termination point. For shear strengthening, in order to prevent considerable opening of diagonal cracks and maintain aggregate interlock, Bakis et al. (2002) suggested that the FRP strain should be limited to 0.004-0.005.

However, Oller et al. (2001) reported that the recommended strain limits of 0.006 to 0.008 were unconservative and that none of FRP strains reached 0.005 at failure of their beams strengthened with FRP.

- Provide bonding beyond the required anchorage length

Concrete Society (2000) recommended that where the FRP is curtailed in the span, a minimum anchorage length of 500 mm should be provided.

Chen and Teng (2001) explained that the anchorage strength cannot always increase with an increase in the bond length, and that the ultimate tensile strength of strengthening materials may never be reached, however long the bond length is.

Binici (2003) found that in order to develop forces at magnitude that are about half of the uniaxial tensile strength of CFRP, a minimum anchorage length of about 12 inches is required for one layer of a CFRP strip bonded to concrete.

- Use mechanical anchors

Khalifa et al. (1999) proposed the use of *U-anchors* (Figure 2.15) by embedding a bent portion of the end (or near the end) of the FRP reinforcement into the concrete. Burr (2004) reported that the *CFRP anchor* connection provided shear and tensile capacity by embedding the FRP into the substrate and bonding with epoxy (Figure 2.16).

Khalifa et al. (1999) and Burr (2004) reported that FRP anchors outperformed conventional steel anchors in anchoring CFRP fabrics. Conventional steel anchors create stress concentrations and discontinuity of the FRP at drilling location resulting in reduced strength. Steel anchors are also prone to galvanic corrosion due to steel-carbon fiber contact. The advantages of using FRP anchors are that they are fully compatible with the FRP fabrics and can be securely bonded to the FRP in a way that steel bolts cannot without additional steel side plates or other hardware.

cantilever slabs. The anchors consisted of the protruding fibers, which were bent and spread out on the GFRP strips, and the anchor bolt, which was inserted into the drilled hole. Even though in some of the slabs, partial debonding had occurred before the FRP rupture took place, all strengthened slabs failed by tensile rupture of the FRP.

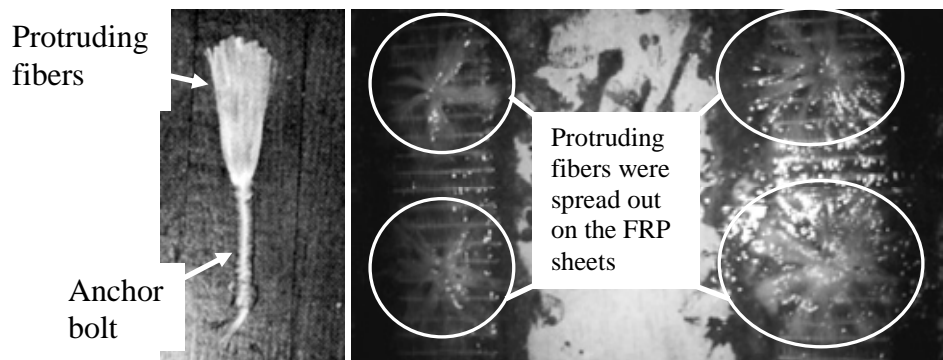


Figure 2.17 Fiber anchors (Teng et al. 2000)

Ibell et al. (2003) found that the use of *GFRP anchor spikes* (which looked similar to the fiber anchors) prevented premature delamination by resisting the transverse tensile stress.

Mostafa (2005) studied the effectiveness of comb-shape *NEFMAC anchors* (Figure 2.18), which was extracted from NEFMAC grid. The comb teeth were inserted into drilled-holes and the comb spine was bonded to the FRP sheets. The anchors were effective in delaying delamination. After initiation of delamination, the well-anchored FRP sheets were still be able to carry loads.

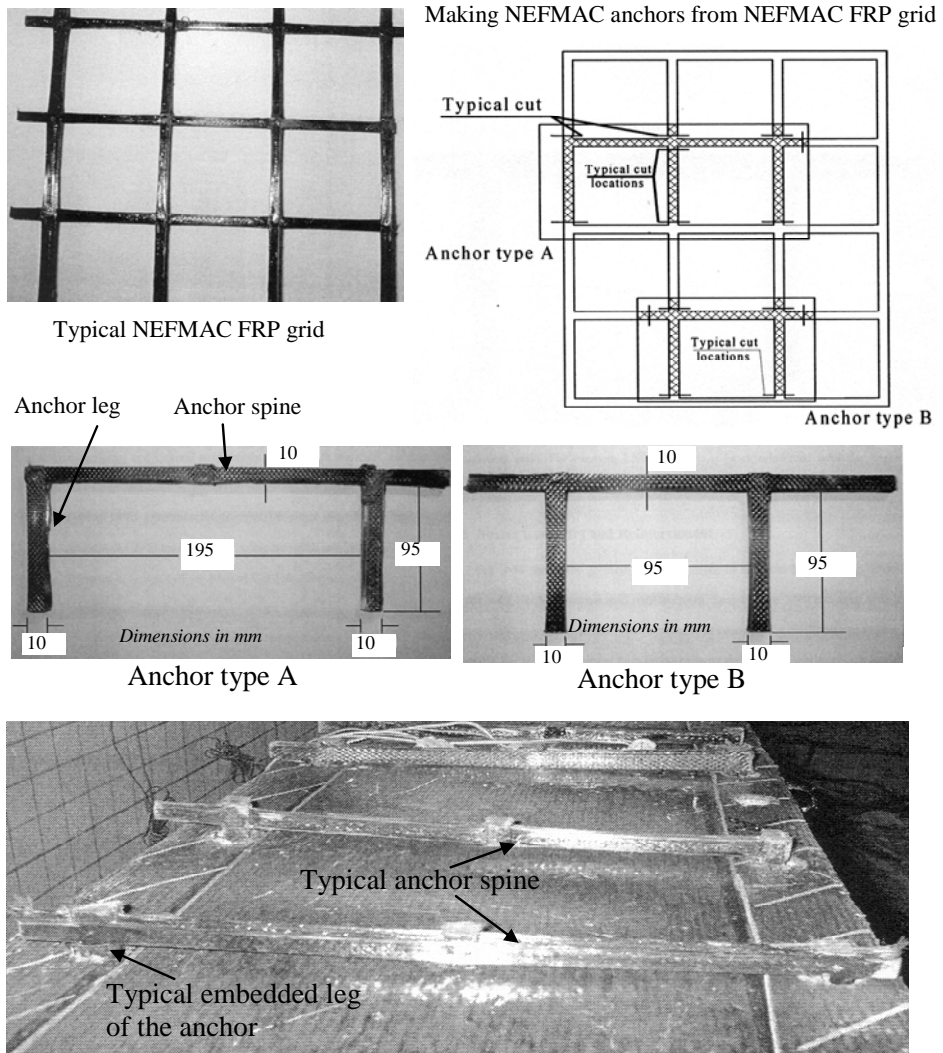


Figure 2.18 NEFMAC anchors (Mostafa 2005)

2.9 PREVIOUS RESEARCH ON STRENGTHENING AND REPAIR OF SLAB-COLUMN CONNECTIONS FOR TWO-WAY SHEAR

Previous research into the strengthening and repair of slab-column connections for two-way shear is summarized in this section. Herein, strengthening and repair refer to relatively undamaged connections and to damaged connections (including failed connections), respectively.

2.9.1 Strengthening methods

2.9.1.1 Adding steel bars, steel rods, and shear bolts

Hassanzadeh and Sundqvist (1998) showed that the insertion of steel bars into drilled holes around the column-slab connection could increase the punching failure load about 55% in comparison with an unstrengthened control slab. They also indicated that the shear reinforcement configurations, shown in Figure 2.19, were at least as effective as ordinary shear reinforcement.

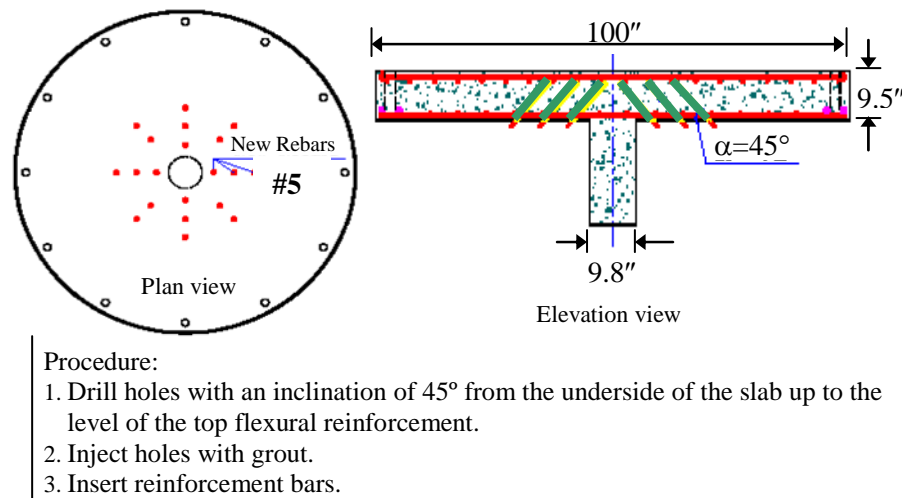


Figure 2.19 Installation of reinforcing bars (Hassanzadeh and Sundqvist 1998)

El-Salakawy et al. (2003) showed that the shear reinforcement could be made of steel rods or shear bolts, shown in Figure 2.20. Installing the steel rods and shear bolts, which were anchored at both ends of the slab surfaces, could increase the strength and ductility of the connection and change the failure mode from punching to flexure.

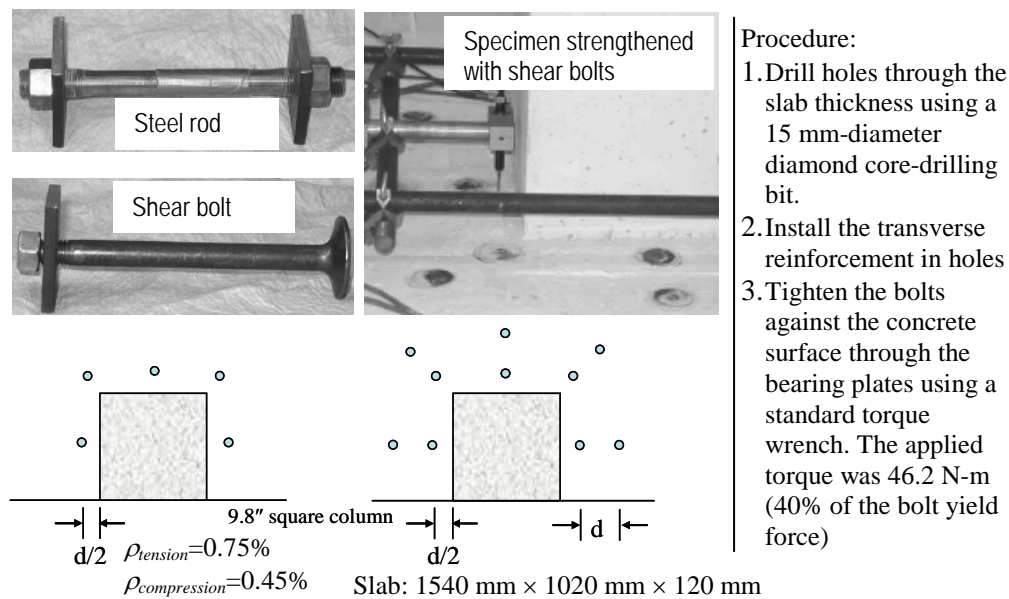
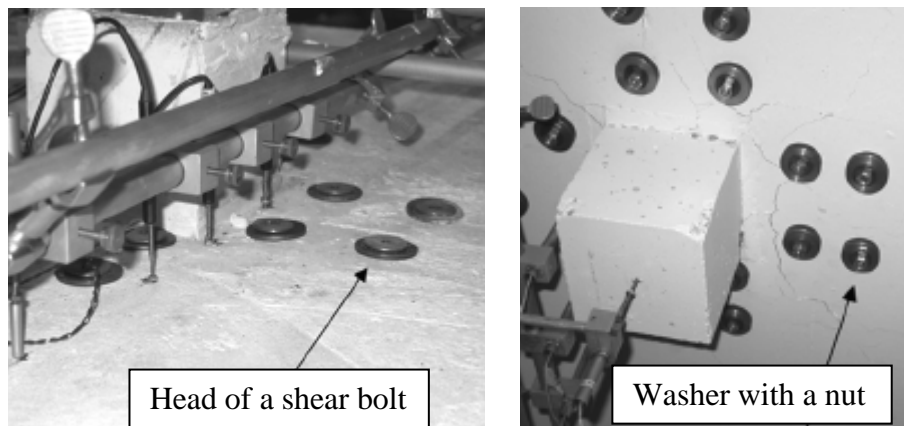


Figure 2.20 Shear reinforcement using steel rods and shear bolts (El-Salakawy et al. 2003)

Comparing test results of El-Salakawy et al. (2003) with those of El-Salakawy et al. (2000), Polak (2005) indicated that the existing connections strengthened with shear bolts had almost the same strength and showed very similar load-deflection characteristics to new connections with shear studs. Two rows of shear bolts gave enough strength and ductility in the connection as compared with six rows of shear studs used in companion specimens.

Adetifa and Polak (2005) studied the use of shear bolts for strengthening interior connections (Figure 2.21). The bolts were 9.5-mm in diameter with 30 mm heads and the washers were 44-mm in diameter and 10 mm thick. Polak (2005) indicated that the bolt heads could be embedded in the slab to prevent intrusion of the bolts into useable space. As in El-Salakawy et al. (2003), the first row was placed at approximately $d/2$ from the column face and subsequent rows were spaced at approximately d .



Slab: 1800 mm × 1800 mm × 120 mm
 $d = 90$ mm
 $\rho_{tension} = 1.2\%$; $\rho_{compression} = 0.55\%$
 Column: 150 mm × 150 mm

Procedure:

1. Drill the holes using 16 mm diamond coring bits
2. Insert shear bolts
3. Torque the bolts to 10% of their yield strength

Figure 2.21 Strengthening using shear bolts (Adetifa and Polak 2005)

Adetifa and Polak's specimens were designed to ensure their punching failure, before the application of the shear bolts. Figure 2.22 shows that the presence of shear bolts increased the ultimate capacity and the deformation capacity of the connection. The deformation capacity of the connection also increased with the number of peripheral rows of shear bolts. In all strengthened connections, the punching cone formed outside the shear reinforced zone. The connection strengthened with two rows of bolts failed in a mixed punching/flexural mode, whereas connections reinforced with three or more rows of bolts failed in flexure.

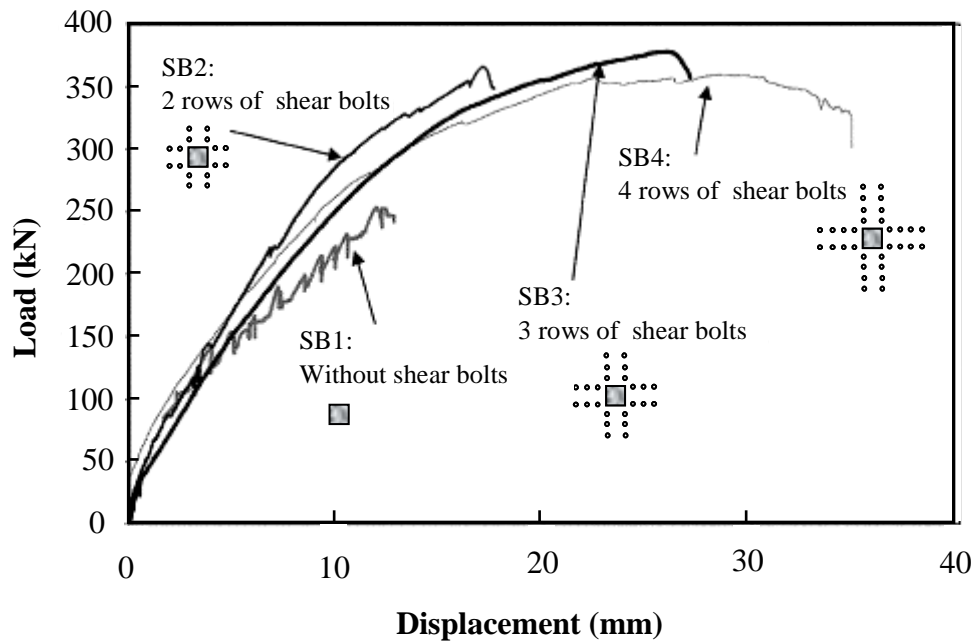


Figure 2.22 Effectiveness of shear bolts (Adetifa and Polak 2005)

2.9.1.2 Steel jacketing

Martinez et al. (1994) strengthened post-tensioned slab-column connections to improve their seismic behavior by installing two steel plates at the top and the bottom of the slab (Figure 2.23). The connections were post-tensioned with two strands in each direction that was continuous through the column. The specimens were strengthened by using 6-mm steel plates (extending about $6d$ away from the column face), which were bolted together with 24 $\frac{1}{4}$ -inch bolts. Just before bolting the plates, epoxy was placed at the top and bottom surfaces of the slab to provide a more uniform bearing and shear transfer surface. The plate dimensions were selected to limit the nominal shear stress due to gravity loads at the critical shear perimeter $d/2$ away from the plate edges to $2\sqrt{f'_c}$ psi. The plate

thickness and the bolt spacing were determined to avoid plate buckling, provide reasonable uniformity, and avoid punching of the bolts through the plate.

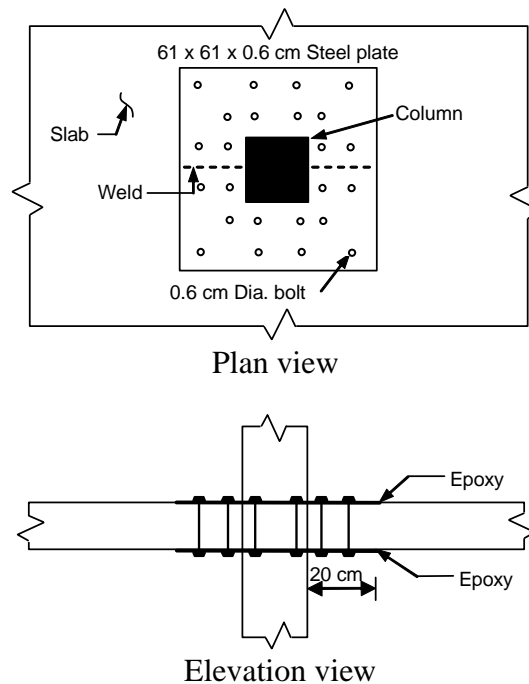


Figure 2.23 Details of steel jacking (Martinez et al. 1994)

Figure 2.24 shows the load-deformation plots of both the original and strengthened specimens. The connection repairs using epoxy and column capitals are discussed in Sections 2.9.2.6 and 2.9.2.7, respectively. The strengthened specimens with steel jackets had stiffness, strength, and deformability superior to the original connection and similar to those exhibited by the connection repaired using column capitals.

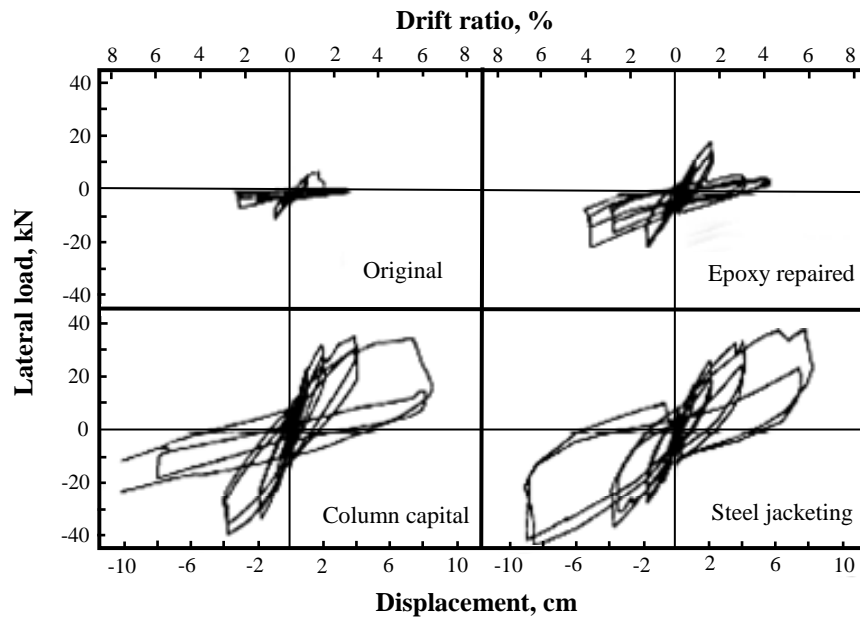


Figure 2.24 Test results of Martinez et al. (1994)

2.9.1.3 Externally installed CFRP stirrups

Binici (2003) studied the use of a tightly knit array of externally installed CFRP stirrups for improving the two-way shear strength and the residual capacity of slab-column connections by engaging more flexural reinforcement into the punching cone. Since the anchorage of CFRP stirrups played an important role in enhancing the punching shear strength, Binici (2003) used an external CFRP stirrup installation technique that involved providing multiple anchorage paths for most of the discrete vertical CFRP stirrup locations.

Binici conducted two test series: Phase I: Monotonic concentric load tests and Phase II: Monotonic eccentric load tests. The proposed upgrade method proved to be successful in strengthening the slab-column connections subjected to pure shear, and combined shear and unbalanced moment transfer. More information about his work can be found in Binici and Bayrak (2003, 2005).

2.9.1.3.1 Monotonic concentric load tests

The slab dimensions were 84"×84"×6". In order to apply the concentrated load, a square steel loading plate (12"×12"×4") simulating a column was used (Figure 2.25). The specimen was supported on steel rollers along its four sides at the assumed contraflexure lines (at 0.2×(span length) away from the column centerline in a continuous prototype structure). The corners were free to lift up. In order to make sure that the flexural capacity is significantly greater than the shear capacity for unstrengthened specimens, all slabs were reinforced with a high amount of flexural reinforcement ($\rho=1.76\%$). In this way, the control specimens would fail in punching shear.

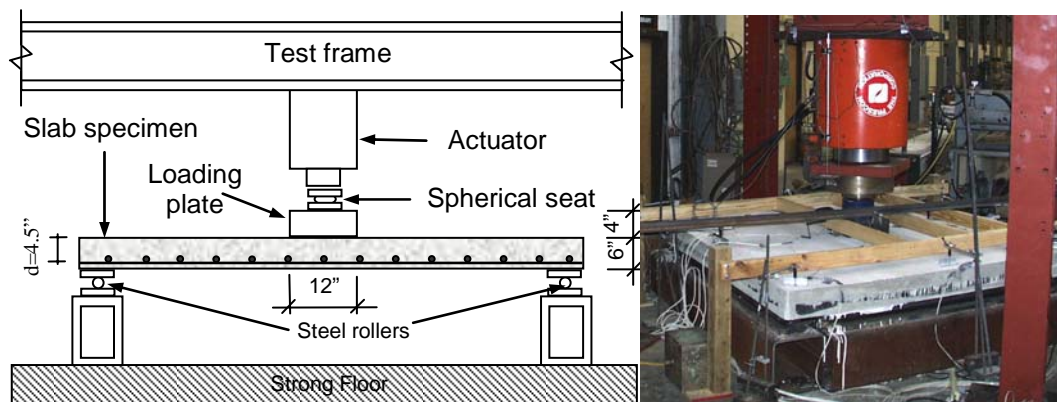


Figure 2.25 Concentric loading test setup (Binici 2003)

Prior to casting strengthened specimens, $\frac{3}{4}$ " diameter PVC pipes were placed to provide vertical holes for CFRP stirrup installation. The pipes were removed after concrete curing. One inch CFRP strips were impregnated with epoxy and weaved through the vertical holes to form continuous closed stirrups in the vertical plane (Figure 2.26). By using closed stirrups, vertical CFRP legs were well anchored on the compressive and tensile faces of the slabs. Since no anchorage failure was observed in the tests, it was concluded that externally installed CFRP stirrups provided sufficient anchorage for the vertical legs.

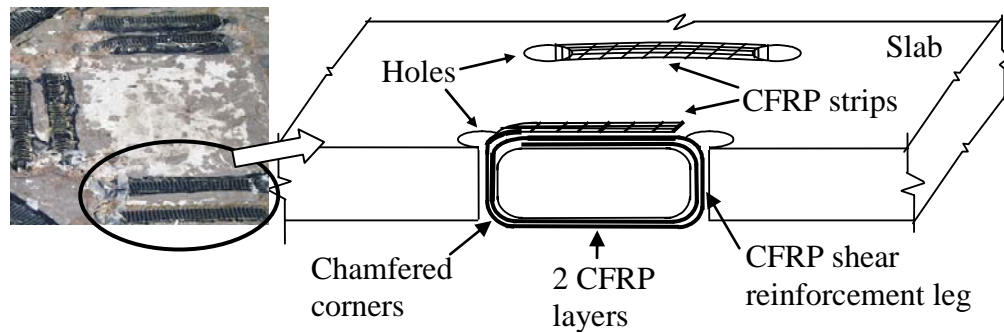


Figure 2.26 CFRP stitching (Binici 2003)

Two stitching patterns were studied. Pattern A specimens (resembling the shear stud and stirrup arrangements used in new construction practice) had shear reinforcement legs arranged in a double cross pattern around the loading area. Pattern B specimens had shear reinforcement placement in a snowflake arrangement extending from the center and corner of the column side. This pattern is typically used in flat plates with circular columns. In both patterns, eight discrete shear reinforcement legs were used for a given shear reinforcement perimeter. The hole locations for patterns A and B are shown in Figure 2.27 and Figure 2.28, respectively. These figures show that the externally installed CFRP stirrups increased the punching shear, deformation, and post-punching capacity of the connection.

Binici also found that the average angle of the punching cone was 30° for Control-1 and ranged approximately from 22° to 35° for the strengthened specimens, with an average of about 28° . This shows that the formation of the inclined crack leading to a punching failure was similar for the properly detailed strengthened specimens as for the control specimen, the only difference being the location of the failure surface.

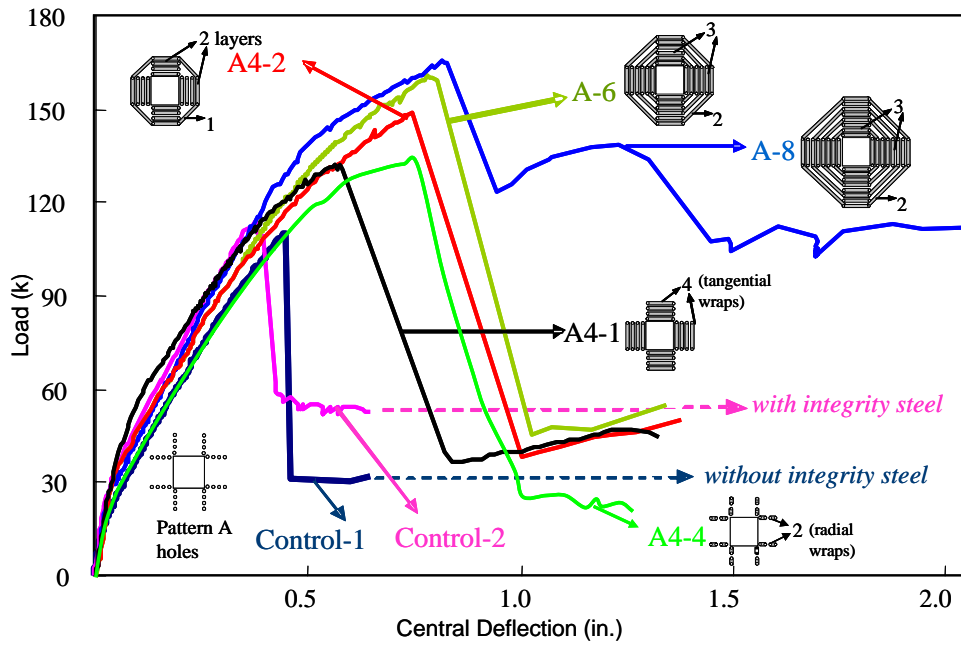


Figure 2.27 Concentric loading test results for pattern A (Binici 2003)

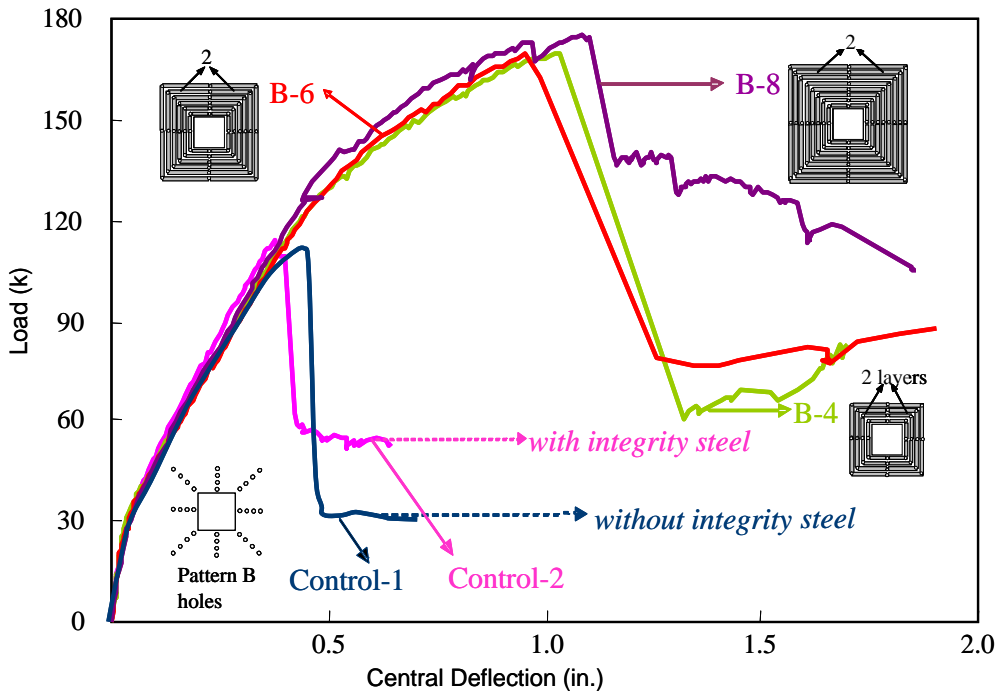


Figure 2.28 Concentric loading test results for pattern B (Binici 2003)

2.9.1.3.2 Monotonic eccentric load tests

Binici (2003) also tested small-scale specimens (40"×40"×3") subjected to monotonic eccentric loads. Longitudinal reinforcement ratios of bottom and top reinforcement were 1.2% and 0.7%, respectively. Patterns A and B with four CFRP perimeters and two CFRP layers per hole were selected as the strengthening patterns.

Figure 2.29 shows the load versus deformation for eccentric load tests. Comparing specimens CE and CC shows that the eccentricity of loading caused 30% decrease in an ultimate capacity compared with that under a concentric loading. Upon strengthening with four CFRP perimeters of patterns A and B, the ultimate load-carrying capacity increased by about 45 and 60%, respectively, compared with specimen CE. More importantly, the strengthened specimens A4E and B4E experienced a more ductile failure.

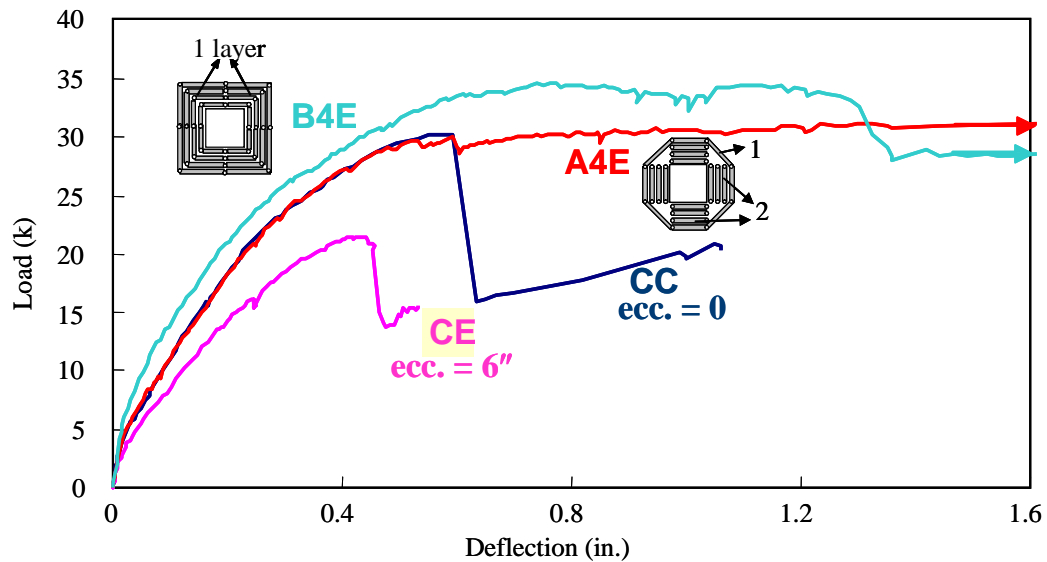


Figure 2.29 Eccentric loading test results (Binici 2003)

2.9.1.3.3 Reversed cyclic load tests

In order to extend Binici's work (2003), Stark (2003) studied the application of externally installed CFRP stirrups for seismic applications. The study showed that the externally installed CFRP stirrups provide an alternative method for upgrading existing flat-plate slab-column connections (that were designed to carry gravity loads only) to improve their seismic performance. The research involved testing four half-scale specimens (9.4'×9.4'×4.5") as follows: Two specimens designed based on ACI 318-63 code were upgraded by externally installed CFRP stirrups and the other two, designed and detailed based on ACI 318-63 and ACI 318-02 codes served as control specimens. Patterns A and B (Binici 2003) with four CFRP perimeters and two CFRP layers per hole were chosen as the strengthening patterns. In order to simplify specimen construction, W10×88 steel columns with 12-in square base plates were used. The steel column section was chosen by matching the stiffness of a typical column in the prototype structure. More information about his work can be found in Stark et al. (2005).

Specimens were tested under a constant gravity load equal to 40% of the concentric punching shear capacity ($1.6\sqrt{f'_c}$ psi) acting on the critical shear perimeter. While the gravity induced shear stresses were maintained, the specimens were tested under lateral displacements that were applied in a reversed cyclic manner. Figure 2.30 shows the test setup. For the test boundary conditions, points on inflection in the slabs and columns were assumed to be located at mid-points. The spreader beam clevises were used to allow the slab specimen to rotate in the direction of lateral loading, while the remaining degrees of freedom were locally restrained.

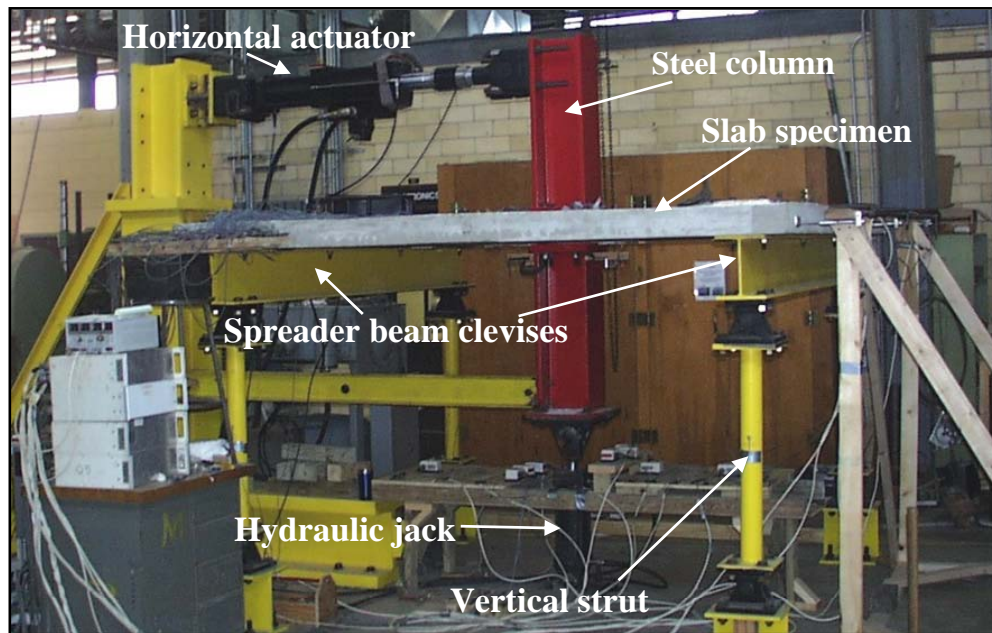


Figure 2.30 Test setup (Stark 2003)

Figure 2.31 shows the lateral load versus inter-story drift backbone curves for the test specimens. Both control specimens C-63 and C-02 failed in punching shear. The poor inelastic behavior displayed by specimens C-63 and C-02 was eliminated in upgraded specimens A4-S and B4-S. Strengthening the region adjacent to the column faces shifted the critical perimeter of the upgraded specimens, which also increased the lateral load capacity. The upgrade method also significantly increased the deformation capacity by eliminating punching shear failures without significantly affecting the stiffness of the connection. Moreover, as the lateral load excursions increased, the stiffness of the upgraded specimens did not degrade rapidly because the CFRP stirrups helped mitigate damage within the connection region. Of the upgraded specimens, specimen A4-S showed the least amount of damage in the connection area (Stark 2003).

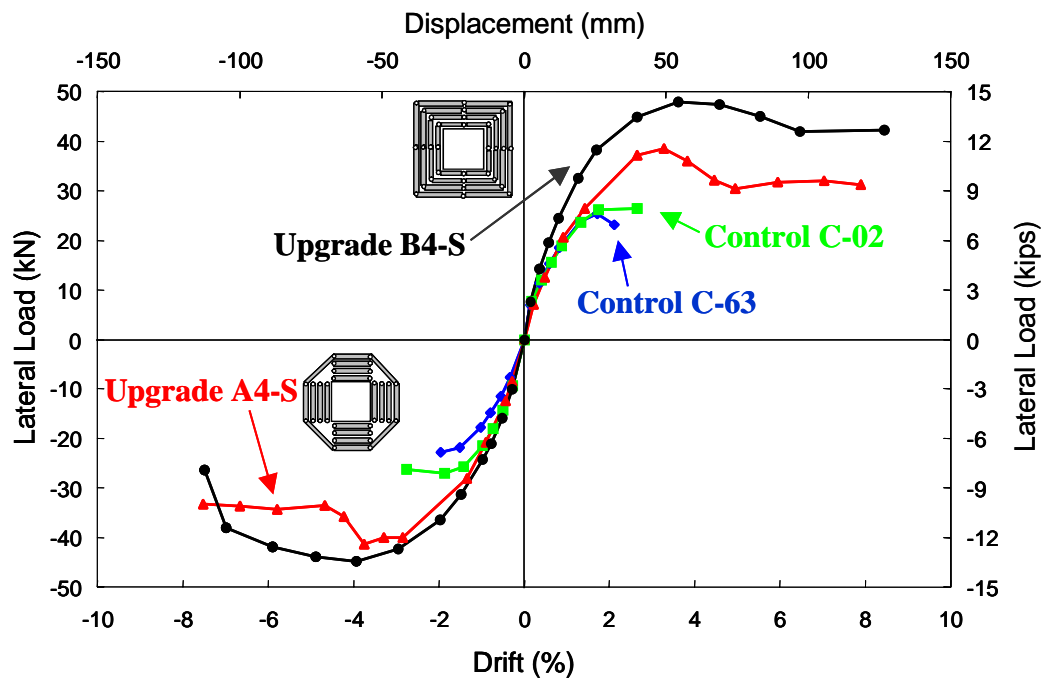
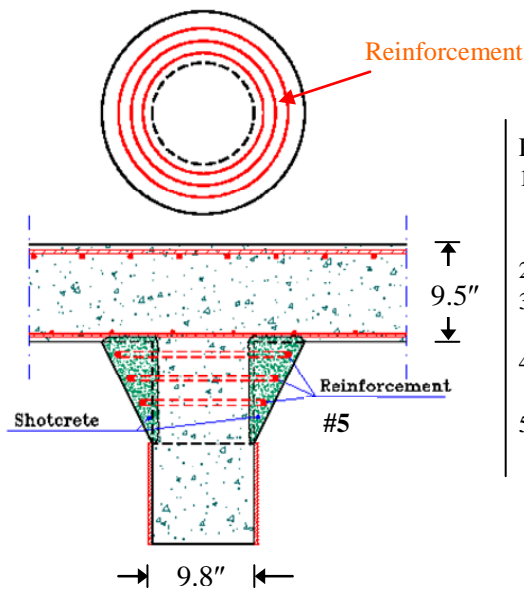


Figure 2.31 Backbone curves (Stark 2003)

2.9.1.4 Increasing column size

Hassanzadeh and Sundqvist (1998) indicated that doubling and tripling column diameter using a column head (Figure 2.32) that was constructed by reinforced shotcrete could increase the punching shear capacity by about 60% and 100%, respectively, with respect to the unstrengthened control slab. The functions of the reinforcement rings were to keep the shotcrete in place during the formation of the column head and to counteract against tensile stresses inside the column head.

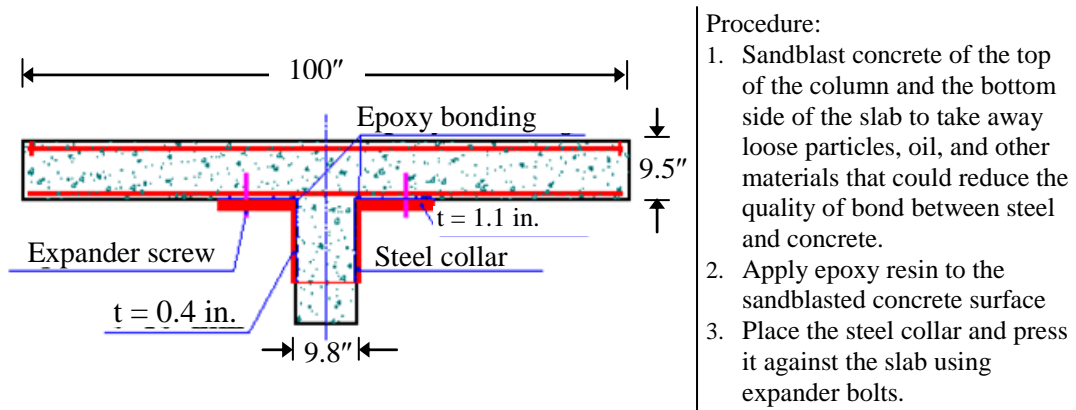


Procedure:

1. Remove the concrete cover of the top of the column and a part of the bottom of the slab using a jackhammer.
2. Sandblast the surface
3. Use several thin layers of $\frac{3}{4}$ to 1 inch dry shotcrete to form the column head.
4. Place three reinforcement rings in the upper part of the column head.
5. Cover the reinforcement rings with concrete cover.

Figure 2.32 Shotcrete column head (Hassanzadeh and Sundqvist 1998)

In addition to shotcrete, column head can be constructed using a steel collar bonded to the slab and to the column (Figure 2.33). Hassanzadeh and Sundqvist demonstrated that this rehabilitation technique could increase the punching load capacity by about 70% with respect to the unstrengthened control slab.



Procedure:

1. Sandblast concrete of the top of the column and the bottom side of the slab to take away loose particles, oil, and other materials that could reduce the quality of bond between steel and concrete.
2. Apply epoxy resin to the sandblasted concrete surface
3. Place the steel collar and press it against the slab using expander bolts.

Figure 2.33 Steel collars (Hassanzadeh and Sundqvist 1998)

Luo and Durrani (1994) developed a connection strengthening scheme using a column capital, which consists of four trapezoidal elements that can be assembled in the field, without drilling neither through the slab nor through the column (Figure 2.34). They tested two retrofitted half-scale interior slab-column connection (INT1 and INT2) with the capital extended $1.4d$ away from the column face under cyclic loading (Figure 2.35). The gravity loads producing the shear stress of $1.74\sqrt{f'_c}$ and $2.02\sqrt{f'_c}$ on the critical shear perimeter of specimens INT1 and INT2, respectively, were maintained during the application of cyclic lateral displacements. The column capital in specimen INT1 was positioned 1 inch below the slab whereas that in INT2 was attached flush with the slab.

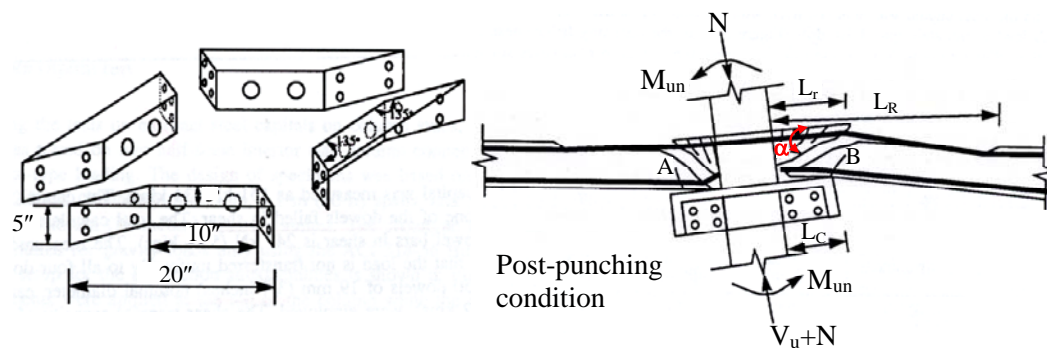
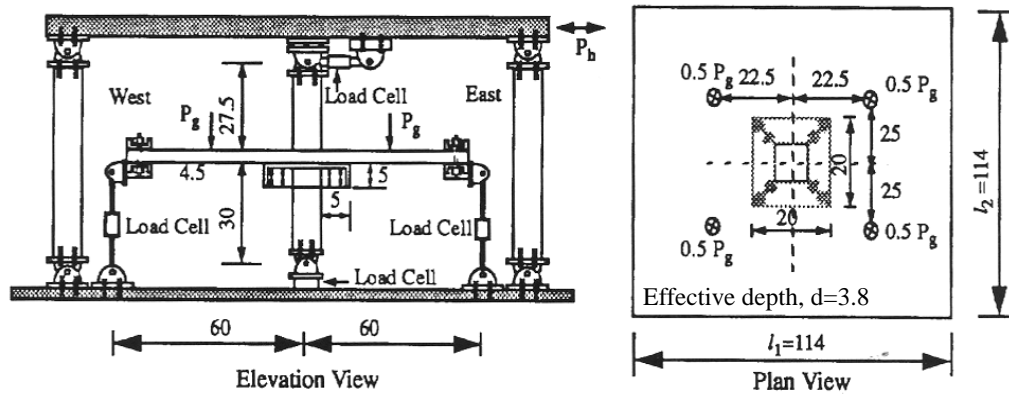
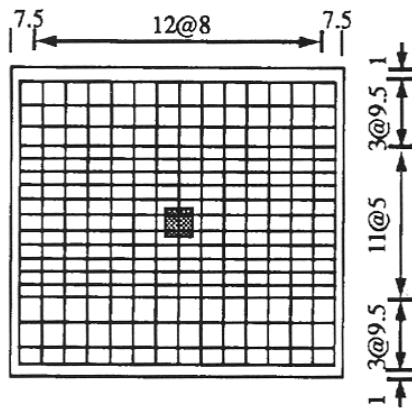


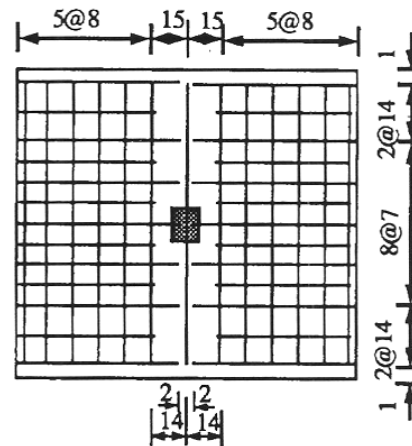
Figure 2.34 Column capital and post punching geometry (Luo and Durrani 1994)



Dimensions in inch



Top flexural reinforcement



Bottom flexural reinforcement

Figure 2.35 Test setup and details of specimens (Luo and Durrani 1994)

When the punching failure occurred in specimen INT1 at 3% drift, the impact of the slab with dead load resulted in a secondary punching of the slab just outside the capital periphery. For specimen INT2, in which the steel capital was attached flush with the slab, the capital was able to safely carry the loads transferred through the slab up to 4.5% drift. Since no dowels were used, the capital in both specimens slipped approximately one inch before engaging firmly with the column. The inclination of the failure surface α (Figure 2.34) was about 22 degrees.

Luo and Durrani (1994) reached the following conclusions:

- (i) The column capital should extend a distance of at least $3d$ from the column face to avoid a secondary shear failure of the slab (based on the observed shear crack inclination of 22°).
- (ii) Since the presence of a column capital may cause yielding of the rebars at the edge the capital, the maximum length of the capital should be limited to a value so that at least the development length of the slab top bars is available beyond the capital edge.
- (iii) As a minimum, two dowels should be used on each column face for a well distributed transfer of gravity load.
- (iv) The column capital should be attached flush with the bottom surface of the slab.
- (v) No mechanical connection is required between the slab and the column capital.

2.9.1.5 Applying FRP sheets or strips

Erki and Heffernan (1995) found that applying external FRP sheets on the tension surface of the slab ($3.3' \times 3.3' \times 2''$; $\rho = 1.8\%$ and 2%) increased the flexural stiffness of the slabs, delayed flexural cracking, and thereby increased the punching shear capacity. They also found that the effect of FRP sheets on the stiffness could be controlled by changing the angle between the fibers and the internal steel reinforcement. At maximum load, FRP sheets debonded from the slab surface because the differential vertical displacement of punching cone pried the sheets off the tension surface of the slab.

Chen and Li (2000, 2005) showed that the presence of GFRP laminates on the tension surface of the slab ($3.3' \times 3.3' \times 3.9''$; $\rho = 0.56\%$ and 1.23%)

substantially increased the punching shear capacity of slab-column connections and was more effective for the slabs with lower concrete compressive strengths and steel ratios. They also indicated that the presence of GFRP laminates may change the flexural punching failure into brittle punching shear failure for lightly reinforced slabs. Figure 2.36 shows the test results for two different steel ratios. Control slab with 0.56% ratio failed in flexure. The presence of GFRP resulted in a substantial reduction of the steel strain. Right after punching shear failure, no bond failure between GFRP and concrete surface was observed except at the location along the perimeter of the truncated cone. When the cone was pushed further, a continued sound of delamination of GFRP was heard. In most slabs, GFRP laminates did not rupture and only developed less than 40% of their full strength.

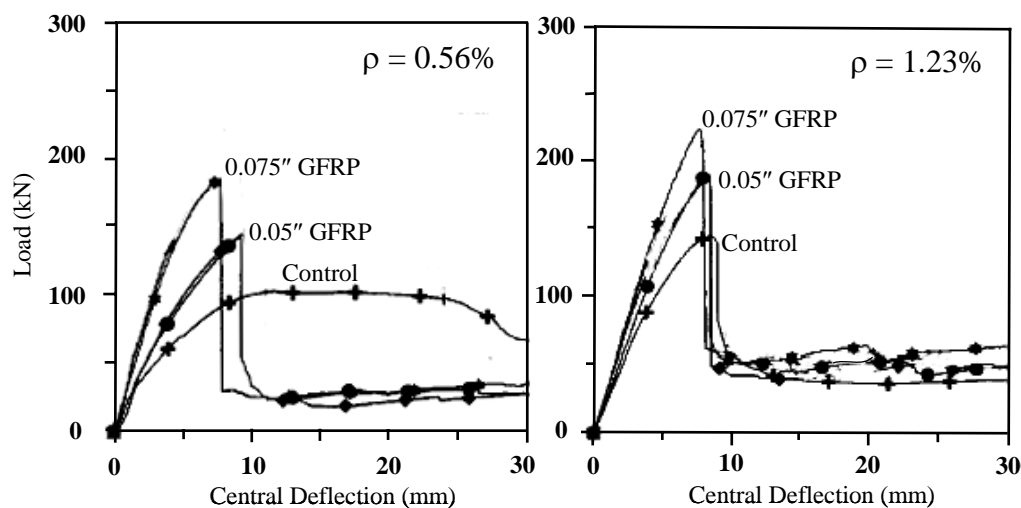


Figure 2.36 Effect of GFRP on ultimate capacity (Chen and Li 2000)

Tan (2000) found that for the slabs (900mm×900mm×35mm) bonded bi-directionally with FRP reinforcement on the tension surface, the punching shear strength increased with the increase in the quantity of the FRP reinforcement. At failure, the FRP reinforcement experienced strains of about 20% of the ultimate

strain capacity and delaminated from the slab at failure. For the same amount of FRP, the slabs bonded with CFRP sheets exhibited the highest punching shear strength, followed by those bonded with GFRP fabrics, and lastly those bonded with discrete CFRP plates. Bonding the slabs uni-directionally with FRP reinforcement did not lead to significant increase in punching shear capacity.

Limam et al. (2003) showed that the two-way shear strength of slabs could be increased by bonding the CFRP strips to the tensile face (Figure 2.37). The strips (Figure 2.37) were spaced at 6 inches. Significant increase in two-way shear strength was accompanied by significant reduction of deformation capacity. The failure mode of the strengthened slab was debonding of the CFRP strips.

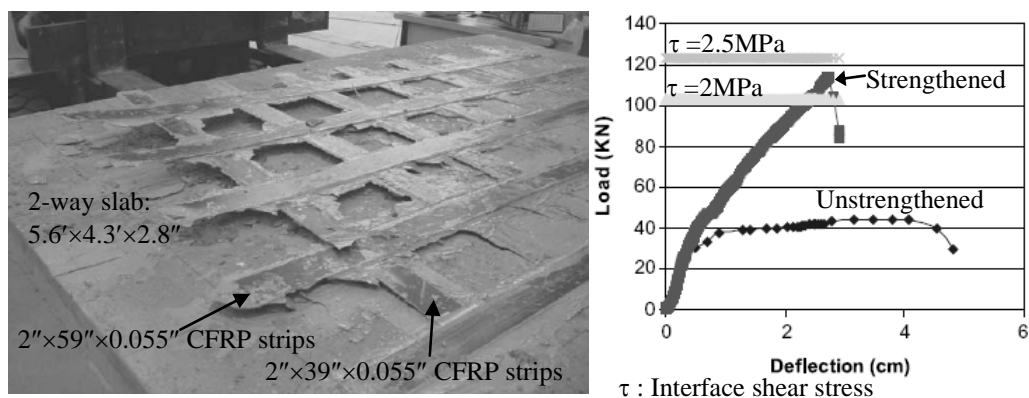


Figure 2.37 Debonding failure of CFRP strengthened slab (Limam et al. 2003)

Harajli and Soudki (2003) showed that applying the CFRP sheets to the tension face of the connection (Figure 2.38), could increase the shear capacity by about 17 to 45%. The corresponding increases in shear resistance tended to level off as the area of CFRP increased. The CFRP sheets bonded to the tension side of the slabs did not change the location of punching shear failure surface significantly, as shown in Figure 2.38. In most specimens, CFRP sheets delaminated at failure. The calculated stress in the CFRP sheets at the maximum load varied between 22% and 69% of the ultimate tensile strength of the fibers.

Using more than one layer of CFRP led to premature bond failure. CFRP increased the shear strength of the connection by restricting the growth of the tensile cracks and increasing the flexural strength of the connections. Harajli and Soudki concluded that the increase in flexural strength as a result of using CFRP may change the failure mode from flexural mode to punching shear mode, thereby reducing the ductility of failure.

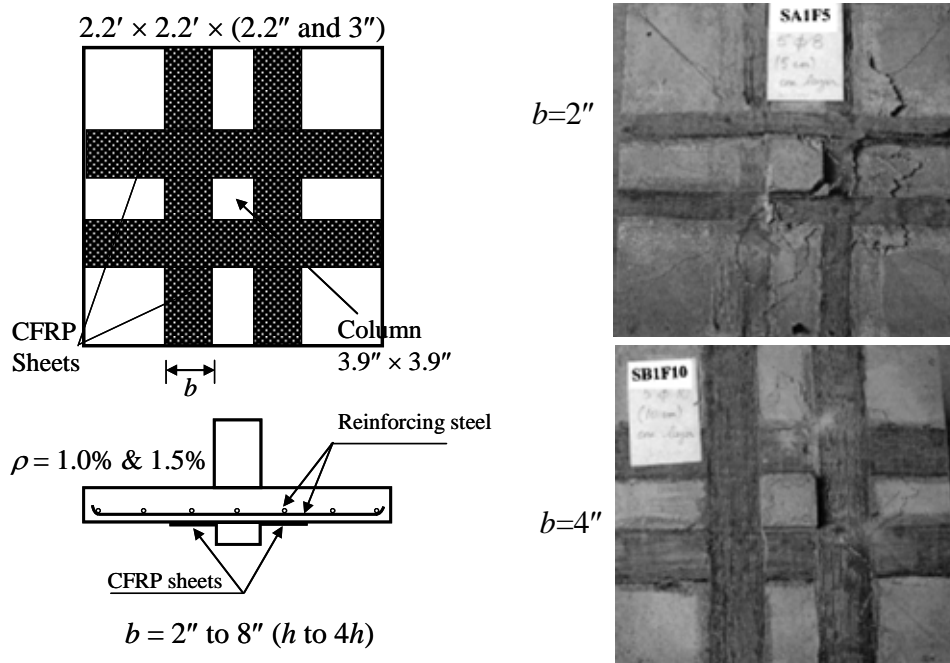


Figure 2.38 CFRP sheet layout and failure surface (Harajli and Soudki 2003)

Casadei et al. (2003) showed that three plies of CFRP laminates applied to the tension face along each side of a slab opening (Figure 2.39) were effective in increasing both overall capacity and stiffness. The capacity of strengthened slab with an opening was higher than the original slab without an opening. They also found that anchoring the CFRP laminates prevented the premature debonding of the laminate. Figure 2.39 shows the anchor, which consisted of four grooves (1-in deep and 0.25-in wide each) to house the carbon tape used to anchor the first ply

of the laminate. Failure of the strengthened specimen was caused by debonding of the laminate from the concrete substrate, followed by a pull-off of the anchoring system at the end of one laminate, with a considerable amount of concrete substrate. The maximum CFRP strain was only 50% of its ultimate strain.

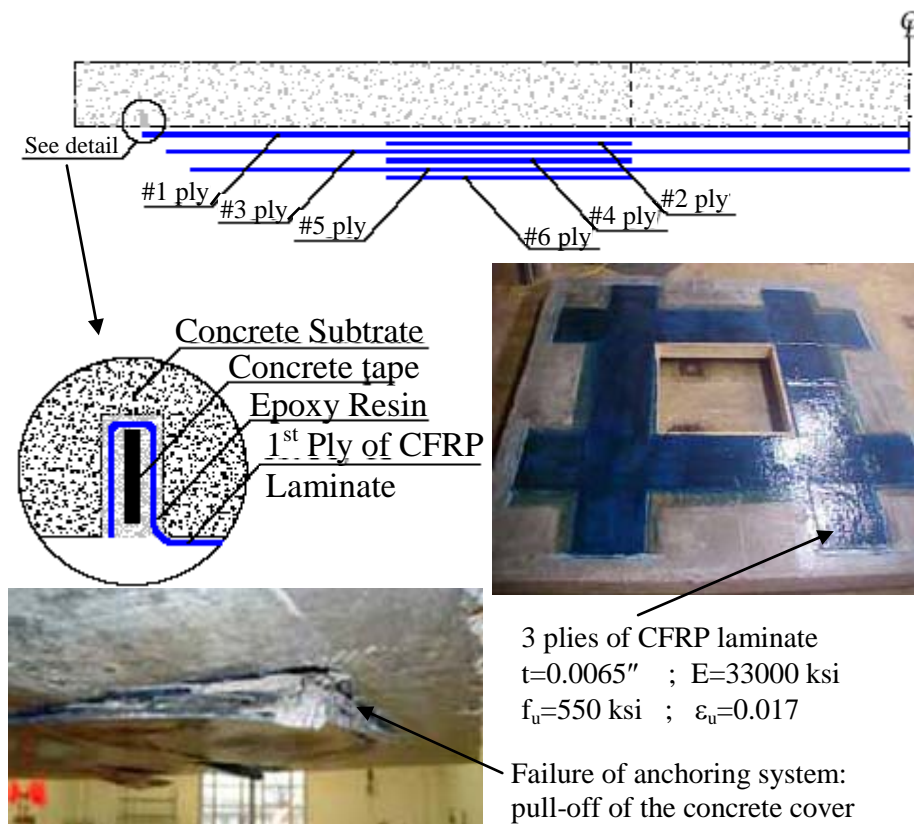


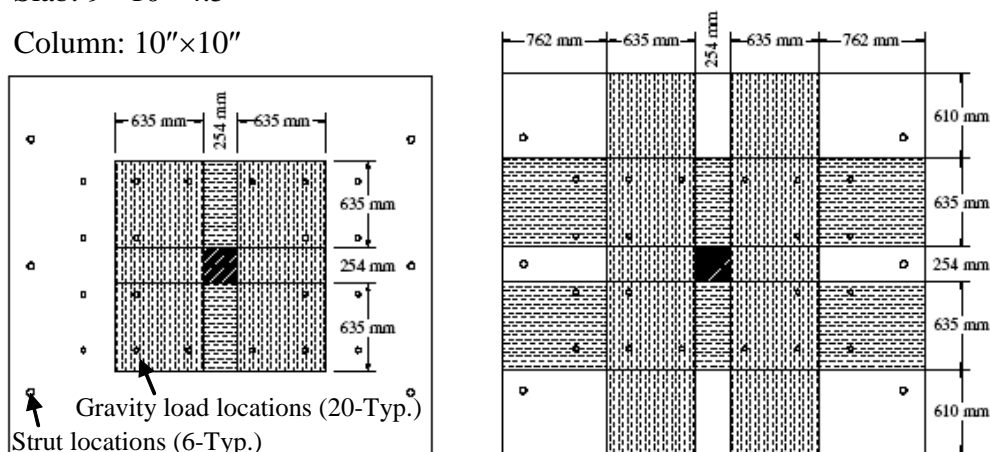
Figure 2.39 CFRP sheets applied around the slab opening (Casadei et al. 2003)

Johnson and Robertson (2004) tested the CFRP-sheet-strengthened slab-column connections (Figure 2.40) designed in accordance with the ACI 318-63 provisions and had no shear reinforcement. The connections were tested under reversed cyclic lateral displacements. Specimen ND2R experienced premature flexural failure around the location where CFRP sheets and slab top reinforcement were terminated. With continuous CFRP sheets in specimen ND3R, the premature

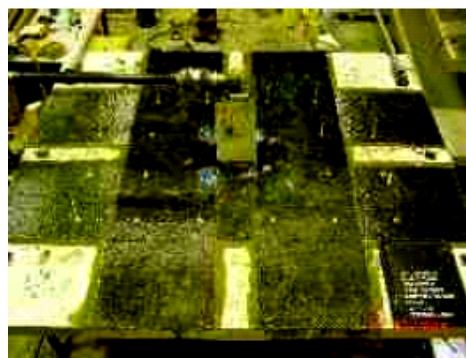
flexural failure was prevented but the connection failed in punching shear. As a general observation, strengthening using CFRP sheets applied to the top surface of the slab increased both the lateral load capacity and the stiffness, but reduced both the ductility and the lateral drift capacity.

Slab: 9'×10'×4.5"

Column: 10"×10"



Specimen ND2R



Specimen ND3R

Figure 2.40 Seismic strengthening using CFRP sheets (Johnson and Robertson 2004)

Johnson and Robertson (2004) also conducted concentric punching shear tests on the connections strengthened with 48 $\frac{1}{4}$ -inch diameter CFRP shear studs (Figure 2.41). The stud spacing was 3" ($d/1.7$) on center, with the first studs

located at 1.5" ($d/3.3$) from the column face. Figure 2.41 shows that the installation of CFRP shear studs only slightly increased the punching shear capacity. However, the use of the studs increased the deformation capacity significantly, which suggests that the CFRP studs could be effective for seismic retrofit of connections.

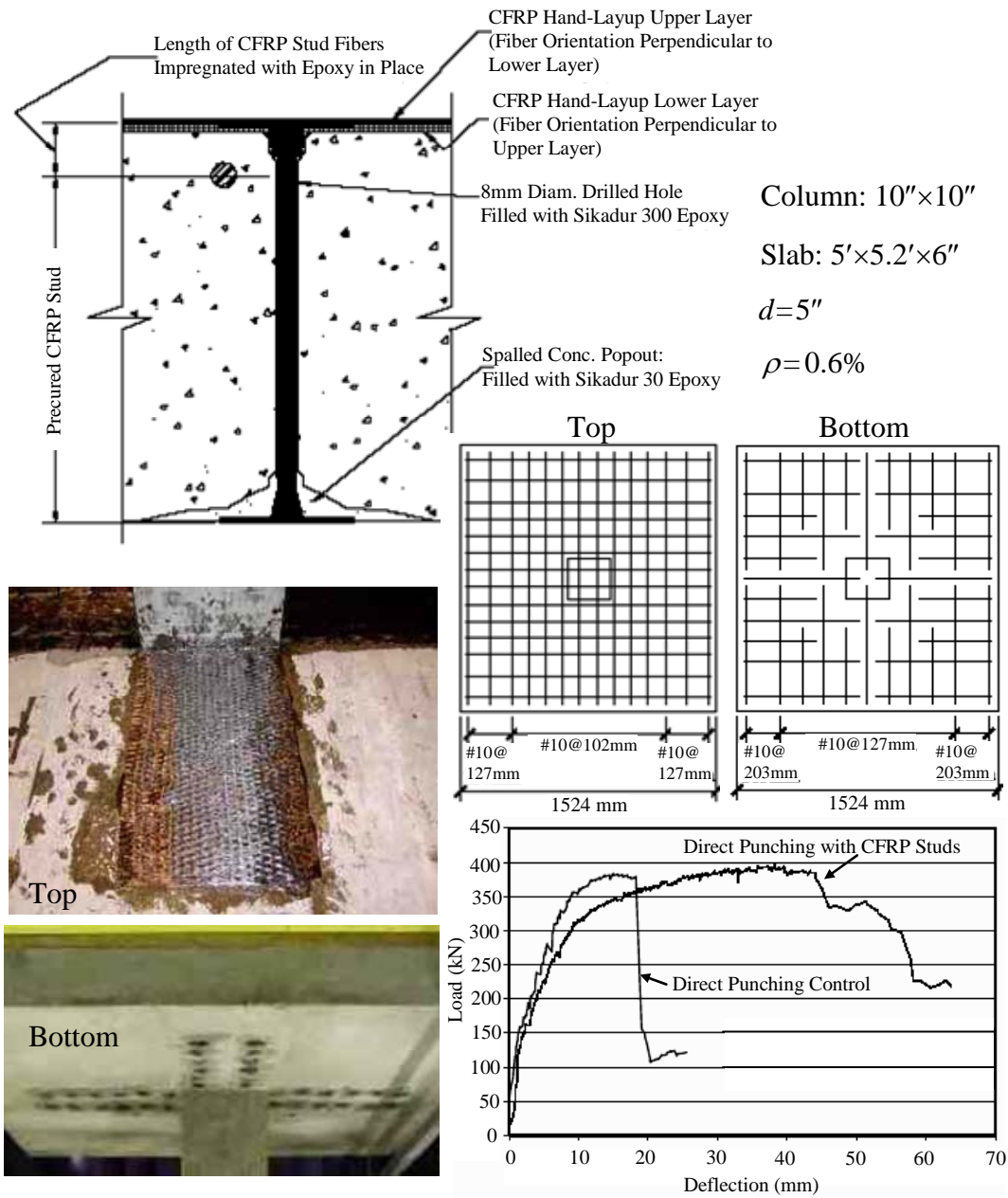


Figure 2.41 CFRP shear studs (Johnson and Robertson 2004)

El-Salakawy et al. (2004) tested slab-column edge connections (1540mm×1020mm×120mm ; $\rho=0.75\%$) strengthened using externally bonded

FRP sheets on the tension slab surfaces around the column (Figure 2.42). Extra FRP sheets were glued on top of the L-shaped strips at the free edge of the slab to improve the anchorage of FRP strips. The specimens were subjected to vertical loads and unbalanced moments. Even though the presence of CFRP sheets did not change the mode of failure and the failure surface location, CFRP sheets increased the flexural stiffness of the slabs, delayed the opening of flexural cracks, and hence, increased the punching shear capacity (between 2% and 23% increase).

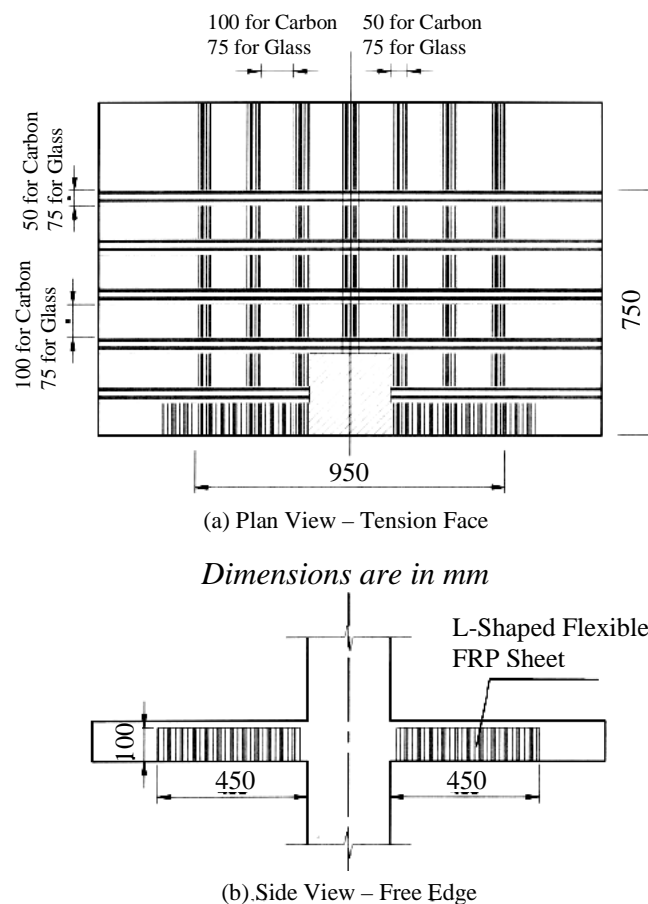


Figure 2.42 Strengthening of edge connection with FRP sheets (El-Salakawy et al. 2004)

El-Salakawy et al. (2004) also combined the FRP sheets with steel bolts to strengthen edge connections (Figure 2.43). The presence of the shear bolts increased the ductility of the connections and changed the failure mode from punching to flexure. The combination of CFRP sheets and steel bolts increased the ultimate strength between 23% and 30% (as opposed to between 2% and 23% for the strengthening with CFRP sheets only).

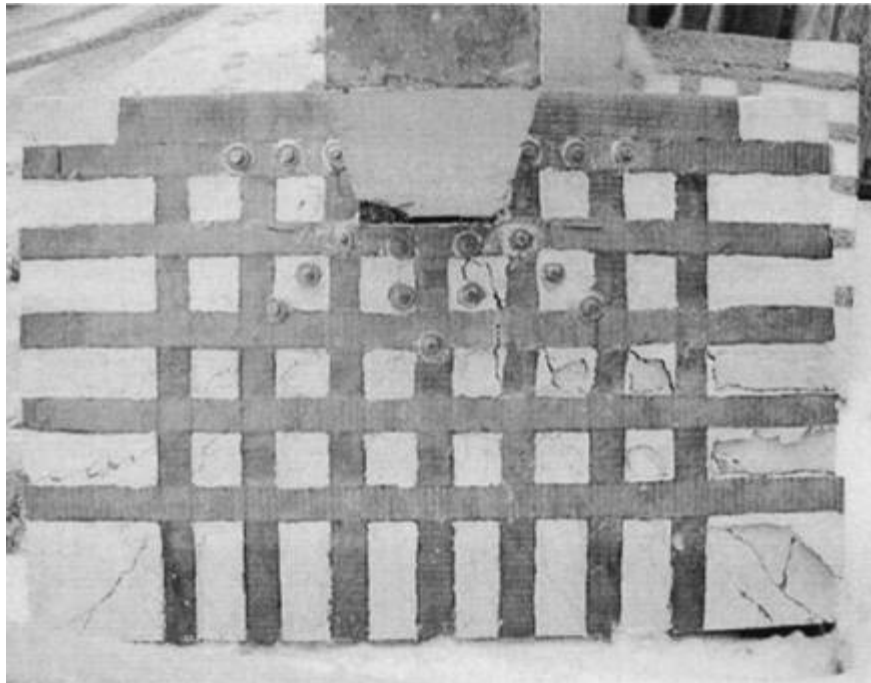


Figure 2.43 Combination of FRP sheets and steel bolts (El-Salakawy et al. 2004)

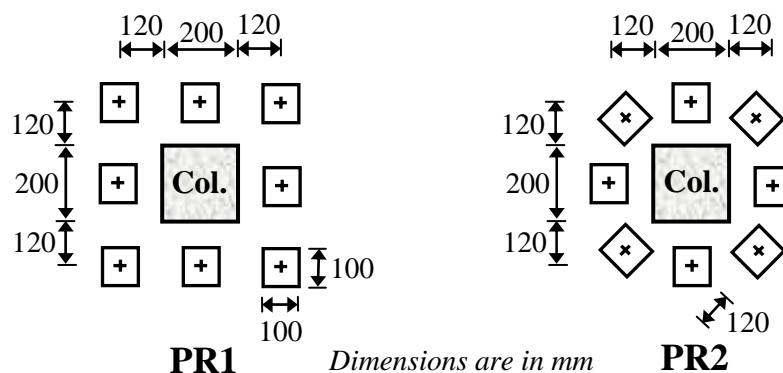
2.9.2 Repair methods

2.9.2.1 Insertion of steel bolts

Ramos et al. (2000) reported on the efficiency of inserting steel bolts that were prestressed against the slab surface (Figure 2.44) to repair the damaged connections that had been loaded up to 70% of the failure load. The damaged

connections were completely unloaded before they were repaired. Holes were drilled through the slab before the steel bolts were inserted.

The forces in the bolts during the tests were approximately inversely proportional to the distance from the column face. Since the corner bolts in PR2 were placed closer to the column than those in PR1, the force distribution among the eight bolts in PR2 was more uniform. The failure loads of the PR1 and PR2 were 51% and 55% higher, respectively, than the estimated ultimate capacity of the unstrengthened specimen using ACI 318-95. The failure surfaces of PR1 and PR2 were inside and outside the strengthened zone, respectively.



Slab: 2000 mm × 2000 mm × 100 mm

Effective depth: 80 mm

Column : 200 mm × 200 mm

Prestressing force: 5.0 kN in PR1 and 15 kN in PR2

Steel bolts were cut from a 12.7 mm threaded bar

Figure 2.44 Steel bolts configurations (Ramos et al. 2000)

2.9.2.2 Steel jacketing

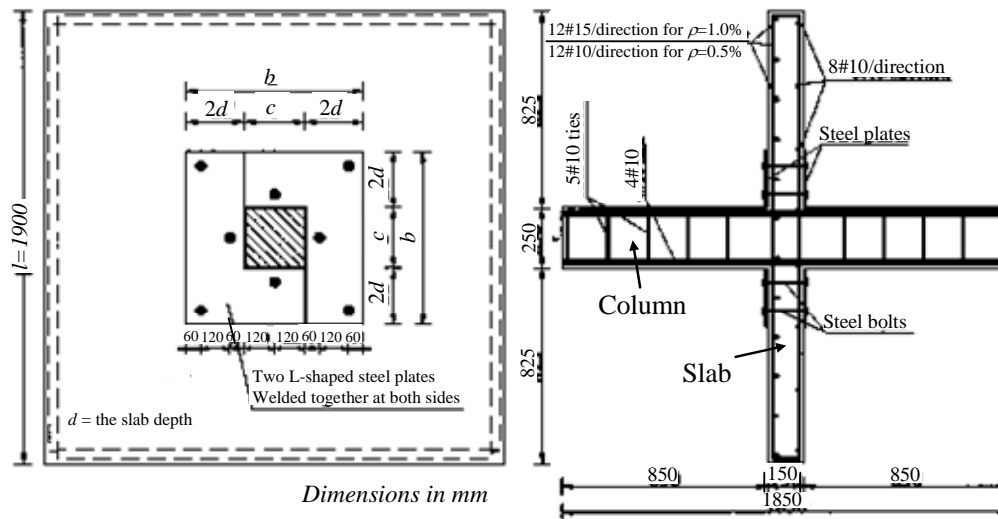
Ebead (2002) and Ebead and Marzouk (2002) developed a rehabilitation technique that was composed of the integration of steel plates and steel bolts (Figure 2.45) to repair specimens that had been concentrically loaded up to 50% of the failure load of the control specimen. 6-mm ASTM A 36 steel plates and 19-

mm diameter ASTM A 325 steel bolts were used. Both steel plates and bolts worked as a unit to confine concrete around the connection, which was sandwiched between the steel plates, and to enhance the performance of the connection against excessive flexural and shear stresses. The confined zone between the steel plates acted like a new drop panel of equivalent concrete depth equals $2n$ times the steel plate thickness, where n is the modular ratio between steel and concrete (Ebead and Marzouk 2002).

During rehabilitation, the load was completely released in order to represent a completely shored structure. The effectiveness of the strengthening technique was evaluated under monotonic concentric and eccentric loadings, and under reversed cyclic loads. The repair method was effective to increase the strength, stiffness, and ductility for all loading cases.

Table 2.3 summarizes the percent increase (with respect to the control specimen) in ultimate capacities of the strengthened specimens. The initial stiffness of the strengthened specimens was 72% higher than the initial stiffness of the control specimen under monotonic concentric and eccentric loadings. Under reversed cyclic loads, the maximum drift capacity of the strengthened specimen was 76% higher than that of the control specimen and the failure occurred in the column.

Ebead and Marzouk recommended the following: (i) steel plates should surround the column to a minimum distance of twice the slab depth measured from the column face, (ii) the minimum plate thickness should be 6 mm (for rust protection), (iii) the minimum number of bolts should be equal to eight. Figure 2.45 shows all of the aforementioned details graphically.



- Procedure:
1. Drill holes in slab using a rotary hammer drill
 2. Roughen the slab surface using a vibrating hammer.
 3. Remove the dust and fine materials with a vacuum cleaner.
 4. Clean steel plates, epoxy, and then bond to the concrete surfaces on both sides.
 5. Immerse the steel bolts in the epoxy resin, insert into the holes, and subject them to a torque of 441 kN.mm using a calibrated torque wrench.

Figure 2.45 Repair using steel jacketing (Ebead and Marzouk 2002)

Table 2.3 Percent increase in ultimate capacities of the strengthened specimens

Loading case	Reinforcement ratio	% increase in ultimate capacities
Monotonic concentric	0.5%	36.5%
	1.0%	54.0%
Monotonic eccentric	0.5%	257%
	1.0%	88.0%
Reversed cyclic	0.5%	15.0%
	1.0%	15.0%

2.9.2.3 Substitution of the damaged concrete (concrete patching)

Pan and Moehle (1992) repaired a previously failed connection using epoxy and grout to replace damaged concrete. Before it was repaired, the original connection had failed in punching shear due to biaxial cyclic lateral loads. The repair procedure was as follows: (i) Remove the damaged concrete in the connection region using a cold chisel and hammer, (ii) Clean the exposed surface of the broken concrete using a high pressure air hose, (iii) Apply a coat of epoxy, and (iv) Pack nonferrous nonshrink grout into the connection. Under biaxial cyclic lateral displacements, even though the repaired connection exhibited a significant reduction in original strength and stiffness, it was still capable of sustaining the gravity loads up to the drifts equal to those imposed on the original connection.

Ramos et al. (2000) indicated that replacing the damaged concrete with the new concrete without a bonding agent could restore the original strength. Their original control specimen (1800mm×1800mm×100mm) was concentrically loaded until failure before the damaged concrete was replaced. The repair procedure was as follows: (i) Remove the damaged concrete, (ii) Roughen and clean the old concrete surface, (iii) Bring the surface to a saturated-dry condition, and (iv) Pour the new concrete. Punching failure of the repaired specimen occurred through the old concrete and not through the bonding surface of the two concretes.

Ospina et al. (2001) concluded that concrete patching is feasible for repairing concrete slabs (13.8'×13.8'×6") that have experienced punching failures. The damaged concrete was crushed with a jack hammer and removed by hand. The old concrete surface was soaked with water before placing the new concrete and no special bonding agent was used. Repaired connections were tested one week after concrete-patching. Two different concrete patch outlines shown in

Figure 2.46 were investigated. The new concrete in ER3-CP2 occupied a larger area and had more vertical interface between the old and new concrete to improve the properties of the cold joint. At the slab bottom surface, the concrete patch in ER3-CP2 extended several times further than that in ER1-CP1.

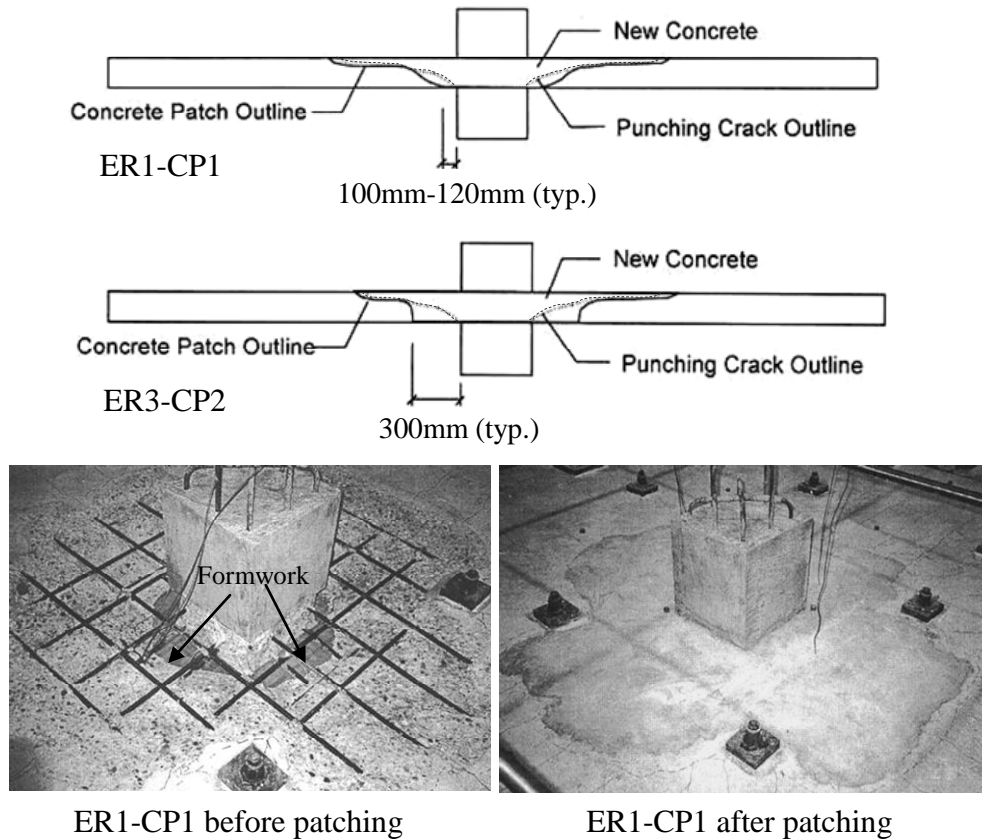


Figure 2.46 Details of concrete patching (Ospina et al. 2001)

The ultimate capacities of ER1-CP1 and ER3-CP2 were 71% and 106%, respectively, of their corresponding original capacities. Specimen ER1-CP1 failed between the old and new concrete, whereas in ER3-CP2, the new punching crack formed in the old concrete. Therefore, Ospina et al. concluded that the concrete patch might restore or even increase the ultimate capacity of the original connection if the patch extended at least 200 mm ($1.75d$) beyond the column face

at the slab bottom surface and an almost vertical junction with the old concrete was provided.

2.9.2.4 Substitution of the damaged concrete and installation of the steel beams

Ramos et al. (2000) showed that the installation of the steel beams that acted as a column head, shown in Figure 2.47, after the substitution of the damaged concrete were effective to repair and strengthen the connection. Before the repair, the specimen was eccentrically loaded up to failure. Since the theoretical punching resistance of the strengthened specimen considering the critical shear perimeter outside the steel column head was higher than the flexural resistance, the repaired specimen failed in a flexural mode. During testing, slipping was observed between the slab bottom surface and the steel beams.

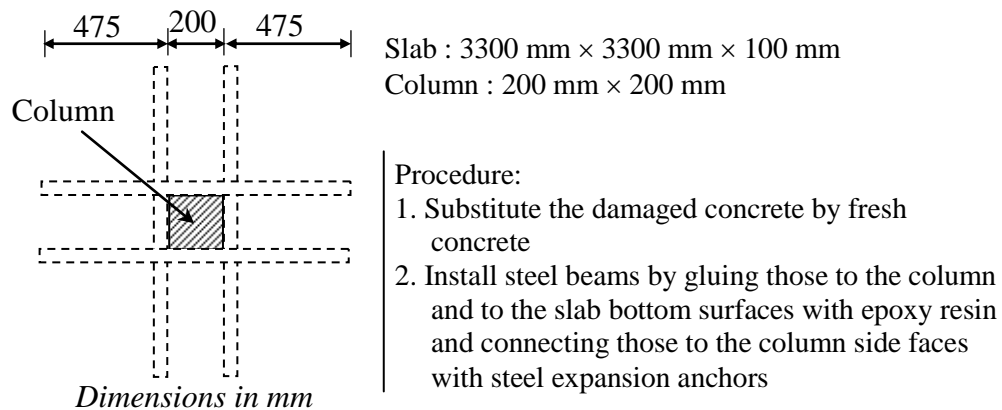


Figure 2.47 Steel beam as a column head (Ramos et al. 2000)

2.9.2.5 Substitution of the damaged concrete, injection of epoxy, and steel jacketing

Farhey et al. (1995) showed that the repair technique shown in Figure 2.48 was effective to restore and even increase strength, stiffness, and the ductility of an earthquake-damaged connection, provided that the slab-column connection remained intact. The original specimens were loaded cyclically up to failure. Then, they were repaired, and re-loaded cyclically until a second failure. The repair technique resulted in about 2 times higher strength and about 4 times higher stiffness in comparison to those of the specimens prior to repair. The suggested high-pressure-injection repair technique produced about three times higher strength and double the stiffness than without it.

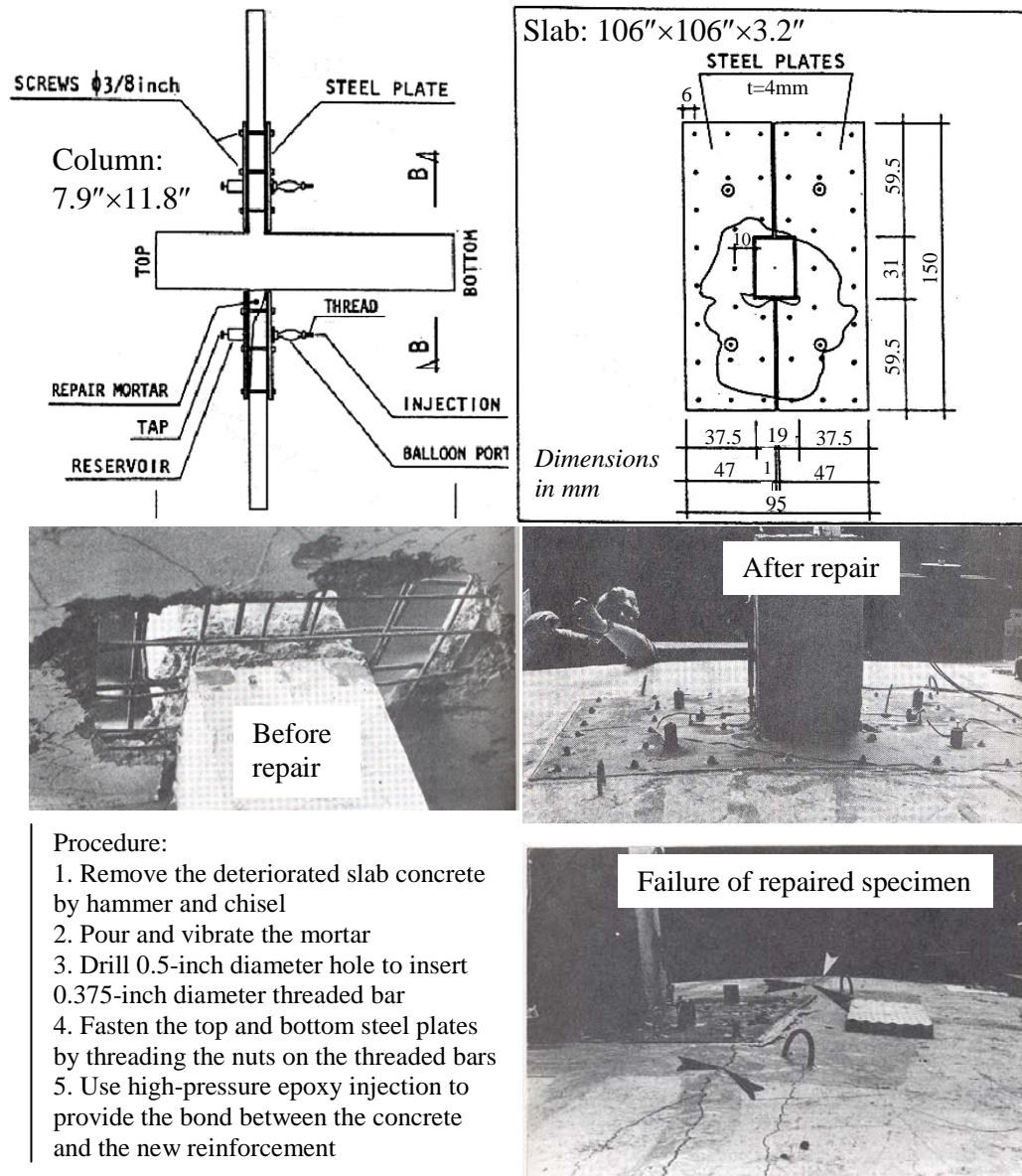


Figure 2.48 Seismic repair using steel jacketing (Farhey et al. 1995)

2.9.2.6 Epoxy repair

Iglesias (1986) and Martin (1986) reported that the epoxy injection was one of the most commonly used methods for repairing earthquake-damaged structural elements after the 1985 Mexico City Earthquake. The equipment used varied from grease guns to high pressure injection machines. Elnashai (1997) indicated that epoxy injection was the most widely used repair method for minor to medium size cracks. When properly performed, epoxy injection can restore the continuity of cracked concrete. However, Cowell et al. (1980) suggested that other means of strengthening and stiffening, in addition to epoxy repair, must be considered if a high level of strength and/or stiffness is required.

Martinez et al. (1994) showed that the post-tensioned slab-column connections repaired with high strength epoxy grout had stiffness and strength exceeding that of the original connection (Figure 2.24). However, the deformation capacity and failure mode of the specimens were not improved. The connections failed in punching shear after completion of the 1.6% drift cycle. The specimen was repaired after initial simulated biaxial earthquake loading. The repair procedure was as follows: (i) Remove all damaged concrete, (ii) Place and compact epoxy mixed with pea-gravel, (iii) Seal all cracks except for openings at 5-cm spacing for an epoxy injection port, (iv) Inject the epoxy under pressure to each visible crack through one opening until it flowed to the next, and (v) Seal the epoxy injection port.

2.9.2.7 Increasing column size

Installing steel column capitals at flat-plate slab column connections (Figure 2.49) was one of the most commonly used techniques for strengthening structural elements after the 1985 Mexico City Earthquake (Iglesias 1986).

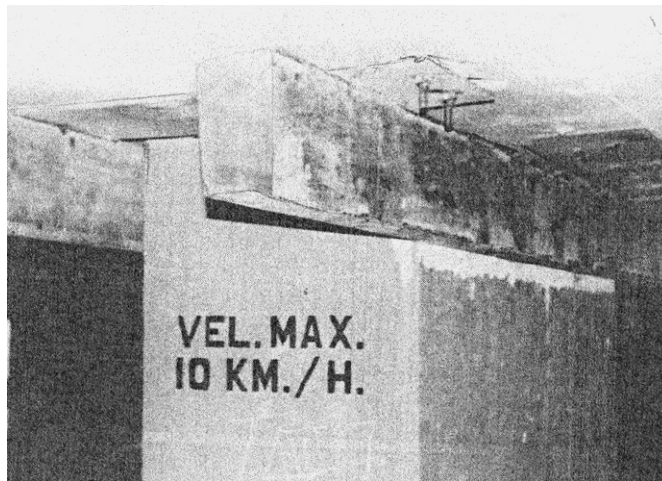


***Figure 2.49 Installation of steel collars after 1985 Mexico City Earthquake
(Iglesias 1986)***

Martinez et al. (1994) indicated that the connection repaired by adding a column capital (Figure 2.50) showed significant increase in stiffness, strength, and ductility in comparison with the original connection (Figure 2.24). The repaired connection failed by punching around the perimeter of the capital at 6.4% drift. Before the repair, the specimen was subjected to biaxial cyclic displacements and was restored to its original position. The repair began with removing damaged concrete in the connection area. The column capital was reinforced with GR-60, US#4 reinforcing bars and twelve 0.5-in diameter A36 steel J-bolts. The diameter of the capital was selected so that under the expected vertical loading, the nominal shear stress at the critical shear perimeter $d/2$ away from the capital edge was less than $2\sqrt{f_c}$ psi.

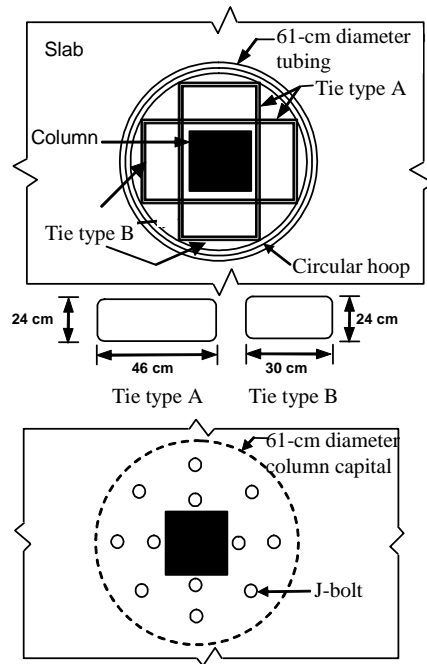
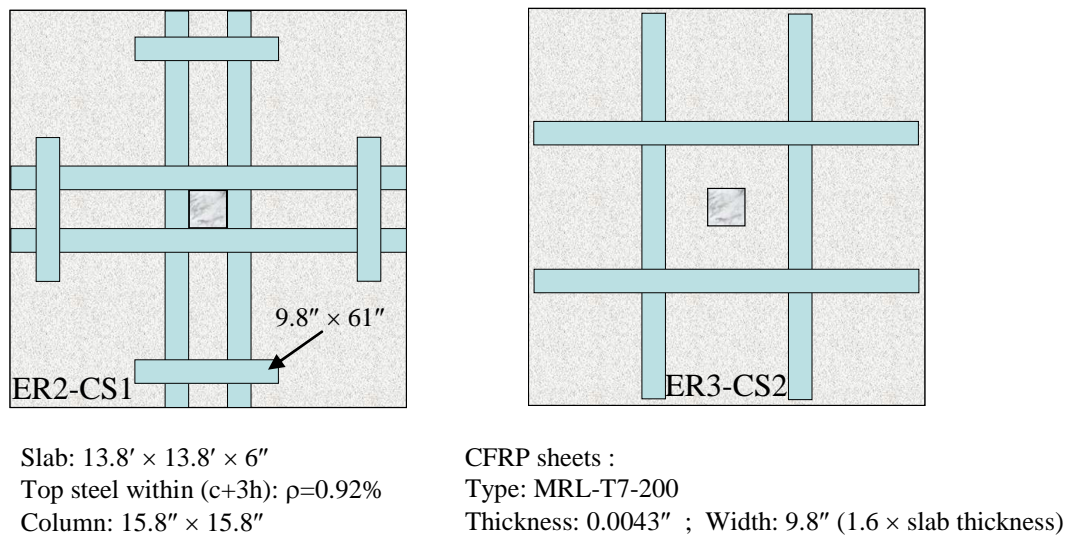


Figure 2.50 Details of column capital (Martinez et al. 1994)

2.9.2.8 Applying FRP

Ospina et al. (2001) examined the effect of bonding CFRP sheets in cruciform patterns on the top surface of two-way concrete slabs to repair the slabs that had been loaded up to 75% of their estimated punching capacity (Figure 2.51). The slabs were unloaded completely before they were strengthened. Each strip consisted of two layers of CFRP sheets. The original connections were designed so that the flexural reinforcement yielded shortly before punching.



Procedure:

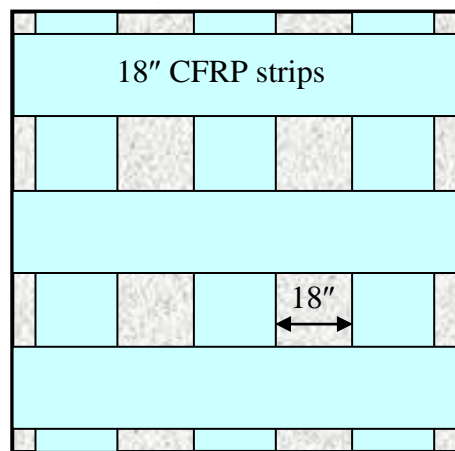
1. Grind the slab surface where the CFRP sheets are to be applied and finish with a putty
2. Apply a primer coat on the slab on the slab and leave to cure for one day
3. Impregnate the CFRP sheets and place them on the slab
4. Roll the CFRP sheets to remove air bubbles underneath the sheets

Figure 2.51 Details of CFRP sheets application

All strips in specimen ER2-CS1 were folded over the chamfered slab edges and anchored with 9.8"×61" single layer of CFRP strips (Figure 2.51). In specimen ER3-CS2, the sheets were terminated near the slab edge and had no additional anchors. Surprisingly, the ultimate capacities of repaired specimens ER2-CS1 and ER3-CS2 were only 95% and 87%, respectively, of the capacities of their corresponding original specimens. In addition, the repaired specimens displayed reduced deformation capacities. At the ultimate load, the maximum CFRP strains were only 12% to 17% of the rupture strain. The CFRP sheets' strain profiles in ER2-CS1 were steeper than those in ER3-SC2 because of the higher slab curvatures around the column.

Mosallam and Mosalam (2003) investigated the ultimate capacity of two-way slabs repaired with CFRP strips (Figure 2.52). Before the repair, the slabs

were loaded up to 85% of their ultimate capacity. The ultimate capacity of the repaired slabs was approximately 198% higher than that of the control slab and the failure was preceded by relatively large deformations (more than 1/45 of the clear span length). The maximum strain in CFRP strips at ultimate load was 0.0078 (65% of the rupture strain). The common failure mode was a localized compression failure of the concrete with some localized debonding near the ultimate.



Slab: 104" × 104" × 3"
 $\rho = 0.43\%$

CFRP strips:
 "FiberBond" FRP composite
 wet/hand lay-up system
 Thickness: 0.023"
 $f_u = 180.7$ ksi
 $\epsilon_u = 0.012$

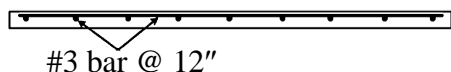


Figure 2.52 Repair using CFRP strips (Mosallam and Mosalam 2003)

Ebead (2002) and Ebead and Marzouk (2004) evaluated the use of CFRP strips (Figure 2.53) for flexural strengthening of two-way slabs that had been loaded up to 50% of their ultimate capacities. Prior to repair, the applied loads were completely removed to simulate a state of shoring in actual structures. Additional transverse layers of CFRP strips were bonded at the end of main CFRP strips to improve the end anchorage.

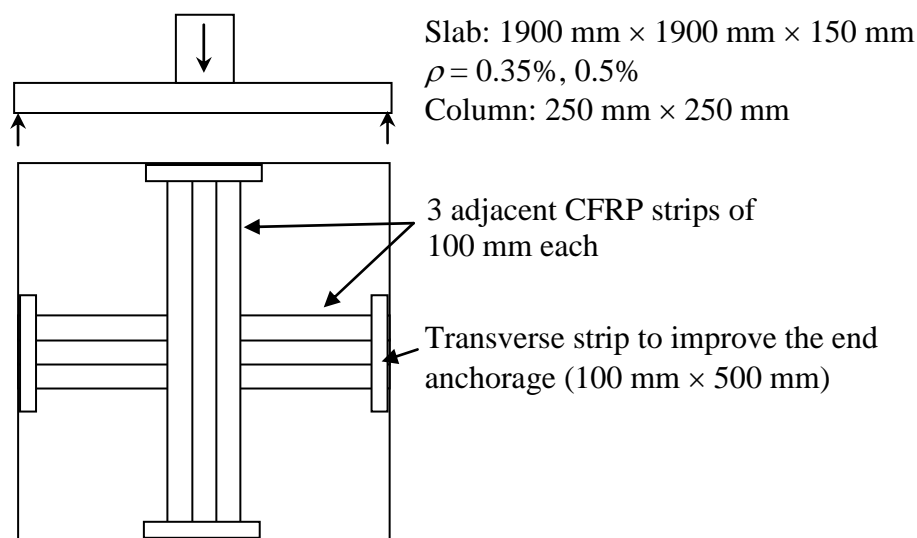


Figure 2.53 Flexural strengthening using CFRP strips (Ebead and Marzouk 2004)

Figure 2.54 shows the load-deformation curves and the failure surface of the strengthened specimen with 0.5% steel. The control specimen with 0.5% steel failed in flexure. The application of CFRP sheets on the tension surface of the slab increased the ultimate capacity and stiffness. However, it also caused a reduction in ductility. The strengthened specimens failed soon after debonding of CFRP strips occurred. Even though the additional transverse layers of CFRP strips at the end of main CFRP strips was effective for preventing a premature bond failure, no CFRP rupture was observed. Ebead and Marzouk (2004)

indicated that the efficiency of CFRP sheets to strengthen the connections was highly dependent on the ability to prevent early delamination.

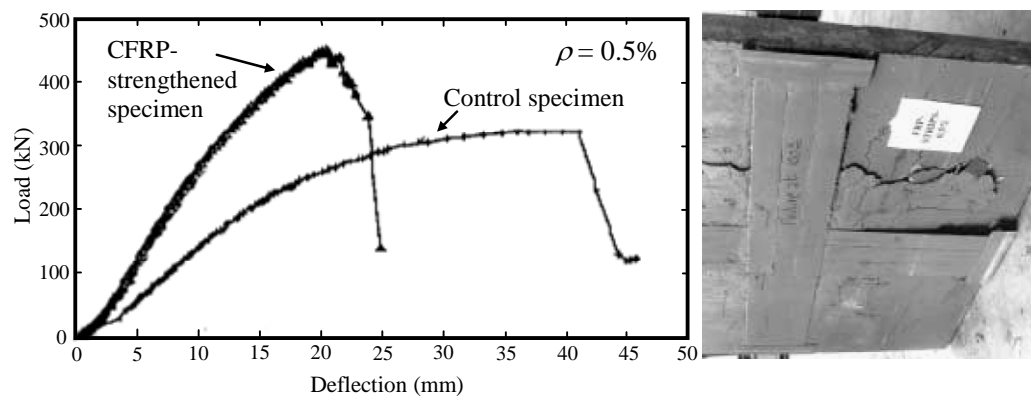


Figure 2.54 Load-deformation response and failure surface of the CFRP-strengthened specimen (Ebead and Marzouk 2004)

Ebead (2002) and Ebead and Marzouk (2004) also combined the use of CFRP strips on both sides of the slab and steel bolts (Figure 2.55) to repair the connections that had been loaded up to 50% of its ultimate capacity. The strengthening material was extended around the column to a distance of twice the slab depth. This repair method was very similar to steel jacketing discussed in section 2.9.2.2 (Ebead and Marzouk 2002), except that the steel plates were replaced by CFRP strips.

The ultimate capacity of the strengthened connection was only 9% higher than that of the unstrengthened connection. In addition, the connection failed in a brittle punching shear mode. When steel plates were used for the same repair technique, the ultimate capacity of the connection increased by about 30% to 50% and the brittle punching shear failure was changed to a more ductile flexural failure.

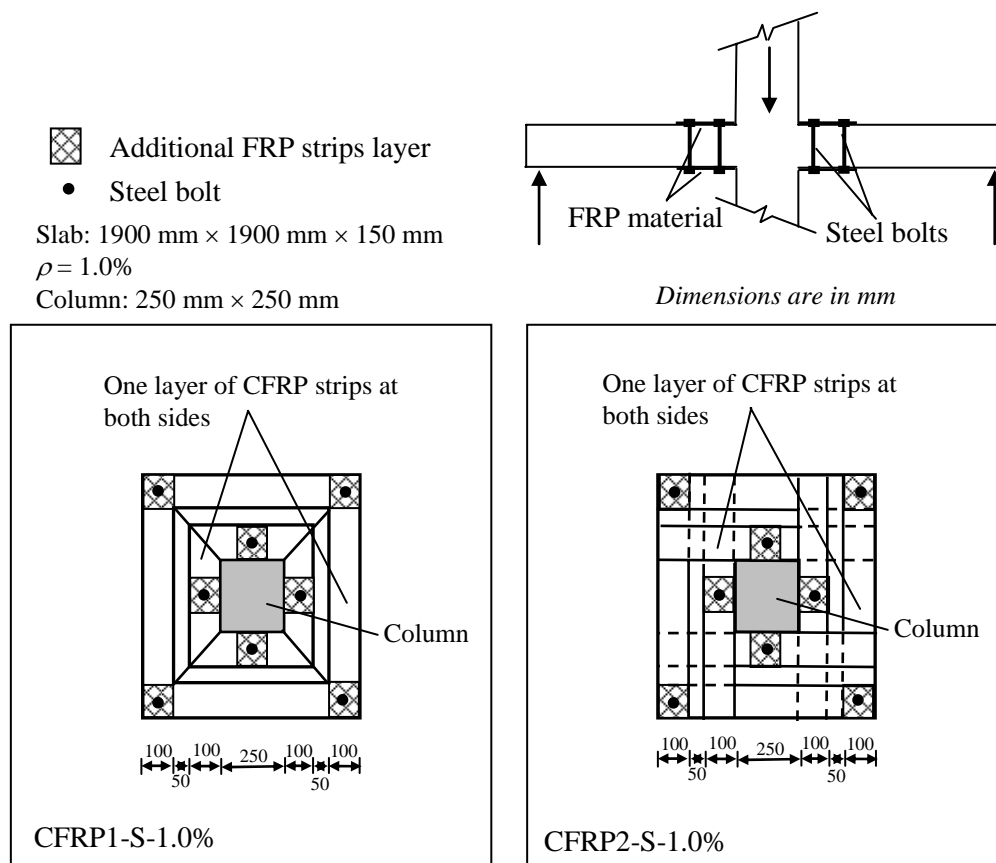
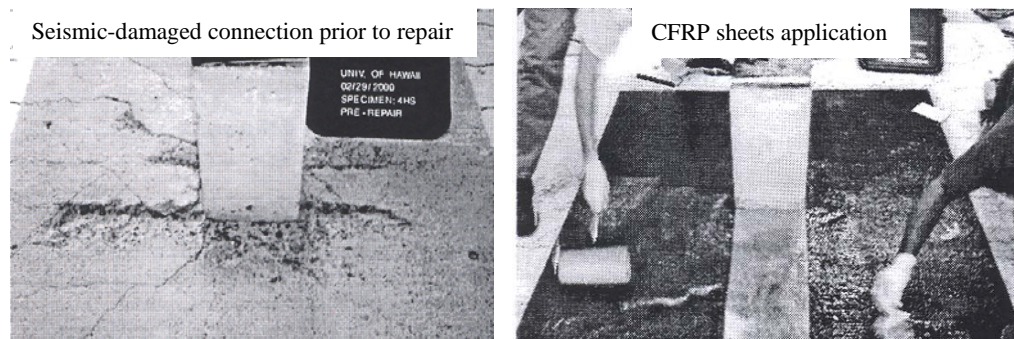


Figure 2.55 Connection repaired by a combination of CFRP and steel bolts (Ebead 2002)

Robertson and Johnson (2001, 2004) studied repair of earthquake-damaged connections that had shear reinforcement using gravity-feed epoxy and CFRP. Before the repair, the slab-column connections were subjected to simulated seismic displacements up to 8% drift. All specimens were subjected to reversed cyclic lateral loads while supporting gravity loads equivalent to dead load plus 30% of the live load. It was found that the epoxy-only repair was able to restore the peak lateral strength but was not able to recover the initial stiffness. Repaired with both epoxy and CFRP application on the top slab surface (Figure 2.56), both initial stiffness and ultimate lateral load capacity of the original

specimen were restored. Debonding of CFRP around the connection was observed at drift levels larger than 5%. It was also concluded that the application of CFRP fabric to the bottom surface of the slab in the connection region did not improve the connection performance over repair with epoxy and CFRP on the top surface only. Robertson and Johnson indicated that without shear reinforcement, the higher lateral loads may have lead to punching shear failure and it was not known from the study whether the CFRP aided in resisting punching shear failure.



Slab: 3000 mm × 3000 mm × 115 mm ; Column: 250 mm × 250 mm

Procedure:

1. Roughen the slab surface with a needle gun to produce a roughness amplitude of 5 mm over the repair area
2. Remove badly cracked and weak concrete around the connection to expose sound concrete
3. Pond the top surface in the area to be repaired with a super-low viscosity epoxy resin
4. Fill any voids in the bottom surface due to spalling using a Hi-Mod Gel.
5. Fill the damaged area on the top surface using a low viscosity epoxy binder mixed with clean silica sand.
6. Apply two-layers of 600-mm wide by 1500-mm long CFRP sheets (the first layer is in the lateral loading direction and the second layer is in the perpendicular direction)

***Figure 2.56 Earthquake-damaged connection and application of CFRP sheets
(Robertson and Johnson 2001)***

2.10 SUMMARY

2.10.1 Behavior of connection, previous research, recommendations, and code provisions on two-way shear strength

As part of the literature review on two-way shear strength presented in this chapter, a total of 31 building codes (and commentaries) and 64 research projects summarized in technical papers, reports, theses, and dissertations were examined. Based on this examination, the following observations can be made:

1. Slab-column connections almost always fail in punching shear (the column together with a portion of the slab pushes through the slab). Punching shear failure may occur before or after the formation of a complete yield line mechanism. For connections of normal proportions and with typical amounts of flexural reinforcement, an extensive flexural yielding will be observed at lower loads than the punching shear load.
2. Flexural and shear strength are interrelated. However, conflicting opinions have been reported on the sensitivity of the two-way shear strength of slab-column connections to the amount of flexural reinforcement near the column.
3. Design recommendations are almost exclusively empirical and were derived by examining experimental results, which were very sensitive to test setups and specimen details. Since test setup, specimens, and reinforcement details varied among research projects, there are considerable divergences among the proposed design recommendations. As a result, there are also significant variations among code provisions. Even for the codes that account for the influence of flexural reinforcement on the two-way shear strength, the influence of flexural reinforcement is accounted for in different ways.
4. Most research related to the development of ACI provisions were conducted on relatively small (7'×7' or smaller) footings supported on a bed of steel springs

simulating soil pressure and slabs supported around their perimeter. Several researchers indicated that the two-way shear strength was sensitive to the size of connection (Regan 1981, Bazant and Cao 1987, Menetrey 1995, 1996). For this reason, the test results from the small-scale specimens may not represent the behavior of actual slab-column connections. In addition, while they represent the soil pressure underneath a footing realistically, it is questionable whether the test results of footings supported on a bed of steel springs can represent the two-way shear strength of slab-column connections.

5. The simple expression that gives the basic two-way shear strength in the current ACI provisions ($V_c = 4\sqrt{f_c'}b_o d$) has not changed since 1963 and had been developed from a relatively complex empirical equation proposed by Moe (1961). It should be noted that Moe's empirical equation was based on a statistical analysis of 106 footing test results from Richart (1948) and 34 slab test results from Eltsner and Hognestad's (1956) and Moe's own tests (1961) that were believed to have failed in shear.

6. The code expression was developed based on the assumption of $\phi_o = \frac{V_{shear}}{V_{flex}} = 1$

(balanced condition: shear strength = flexural strength). The ACI code provisions are intended to prevent brittle shear failure by forcing the formation of a complete yield-line mechanism preceding the shear failure.

7. While some researchers believe that ($V_c = 4\sqrt{f_c'}b_o d$) is conservative, many researchers showed that the use of this expression results in over-predictions of the two-way shear strength of slabs in tests conducted on interior connections and multi-panel flat-plate structures.

8. Many tests results (Guralnick and LaFraugh 1963, Criswell 1970, 1974, Hawkins and Mitchell 1979, Yamada et al. 1992, Gardner and Shao 1996)

indicate that the measured shear stress at failure for lightly-reinforced slabs supported on square columns could be less than $4\sqrt{f_c'}$ if the slabs develop large deflections prior to punching shear failure.

9. Based on the development of ACI provisions, it may be expected that the concentration of reinforcement around the connection in flat-plate structures became a standard practice in 1980s, when the code provisions emphasized the need for concentrating the reinforcement and started to contain the seismic provisions for slab-column connections.

10. There are different opinions about what provides residual capacity after punching shear failure.

Observations made on the research reported in the literature that are summarized in this chapter raise the following questions related to the main objectives of this research:

- What are the most common details of interior slab-column connections in typical flat-plate structures built in the mid 1900s?
- Since the ACI 318 code provisions did not emphasize the need of concentrating reinforcement before 1989 and did not have seismic provisions for flat-plate structures before 1983, it is expected that the concentration of reinforcement within the $(c+3h)$ region was not a common practice before 1980s. Therefore, the connections in typical flat-plate structures built in the mid 20th century are lightly-reinforced. What deficiencies related to two-way shear strength do those connections have? What will be the failure mode? Will the shear failure precede a complete yield-line mechanism or vice versa? Can existing code provisions and/or design recommendations be used to evaluate the capacity of existing connections?

- If flexural and shear strength are interrelated, will the two-way shear strength be sensitive to the concentration of flexural reinforcement (which increases the flexural strength) within the range that is commonly used in practice?

2.10.2 Rehabilitation

Based on the examination of 67 research projects summarized in technical papers, reports, theses, and dissertations, the following observations can be made:

1. Several alternatives to increase the two-way shear resistance of existing slab-column connections without shear reinforcement are:

- Adding external shear reinforcement (steel bars, steel rods, shear bolts, CFRP stirrups, and CFRP shear studs)
- Increasing perimeter of the critical section (reinforced shotcrete column heads and steel collars)
- Increasing the depth of the slab (steel jacketing)
- Adding external flexural reinforcement (CFRP sheets application on the tension surface of the slab)

Some researchers also combined several of those alternatives (steel plates and steel bolts, CFRP sheets and steel bolts)

2. To the best of the author's knowledge, no research has been done on repairing connections with a certain level of seismic damage and no repair has been done on the connections under service loads. Most research on repair were conducted on connections that had been loaded to failure by monotonic eccentric or reversed cyclic loads or significant monotonic concentric loads. After failure, the connections were completely unloaded and repaired.

3. The use of FRP for structural rehabilitation offers many advantages compared with the use of conventional materials, such as steel and concrete. Externally bonded CFRP reinforcement was determined to be the most cost-effective, the least disruptive, and virtually unnoticeable once the installation was complete by many researchers.
4. Two FRP rehabilitation techniques that have been studied are external installation of CFRP stirrups and external installation of CFRP fabrics on tension face of the slab.
5. External installation of CFRP stirrups increased the two-way shear, deformation, and post-punching capacities of connections. CFRP stirrups also improved the seismic performance of connections that were designed to carry gravity loads only by increasing deformation capacity without significantly increasing the stiffness and preventing punching shear failures.
6. Unlike CFRP stirrups, there have been conflicting opinions on whether the application of CFRP sheets can increase the two-way shear strength of the slab. Bonding uni-directional FRP reinforcement to the tension side of the slabs did not increase punching shear resistance. Not all applications of CFRP sheets were successful. In many cases, CFRP sheets delaminated very early, making them inefficient as a strengthening material.
7. Research on rehabilitation using CFRP sheets was mostly conducted on relatively small specimens.
8. Repair of damaged connections typically involved substitution of the damaged concrete and epoxy injection.

Observations made on the research reported in the literature that are summarized in this chapter raise the following questions related to the main objectives of this research:

- Repairing failed connections is not believed to be realistic because connection failure in actual flat-plate structures may cause progressive collapse that would leave no structure to be repaired. What can be done to repair connections with a certain degree of seismic damage? Does the damaged concrete need to be replaced? Can repair be performed on connections under service loads to mimic the repair in flat-plate structures that are unshored?
- Since epoxy injection is relatively expensive and in many cases can cause additional damage due to the injection pressure, will repair without epoxy injection still be successful?
- Will collars that extend shorter than $3d$ away from the column face still be able to prevent shear failure of the slab under reversed cyclic displacements? Will the details of slab flexural reinforcement affect the seismic-performance of the retrofitted connections with collars? What is the performance of collars that transfer the load to the column through friction (without the use of dowels)?
- Research on external installation of CFRP stirrups has been conducted on the connections that were designed to be structurally weaker in shear than in flexure. These slabs were undamaged and had unrealistically high flexural reinforcement ratios (larger than 1.5%). Will the technique work for lightly-reinforced connections, which is typical in flat-plate structures built in the mid 1900s? Will it work for repairing the earthquake-damaged connections? How does the technique work if in actual structures, holes need to be drilled?
- If flexural and shear strengths are interrelated, can applying CFRP sheets on the tension surface of the slab (flexural strengthening) increase the two-

way shear strength of the slab? Does the technique work for repairing earthquake-damaged connections?

- Due to the high cost of CFRP, more optimal utilization of CFRP strength is important. Can CFRP sheets be anchored to prevent early delamination so that their ultimate strength can be exploited?

All questions listed in this section are addressed in the experimental research conducted as part of this study. This work is summarized in the subsequent chapters.

CHAPTER 3

Experimental Program

3.1 GENERAL

In order to achieve the objectives listed in Section 1.4 and to address the issues discussed in Section 2.10, an experimental study was conducted. Seven two-thirds scale interior slab-column connections were constructed and ten different tests were performed on those seven specimens. The details of the experimental program are presented in this chapter. This chapter is organized as follows: Detailed descriptions of the prototype structure and test specimens are presented in Section 3.2. Specimen notation and description of all tests conducted in this study are presented in Section 3.3. Specimen construction is described in Section 3.4. Material properties of concrete, steel reinforcing bars, CFRP, and epoxy used in this study are reported in Section 3.5. Details of test setups for both simulated seismic tests and punching shear tests are presented in Section 3.6. Test instrumentation is described in Section 3.7. Test procedure is discussed in Section 3.8.

Since this study focuses on the rehabilitation of connections in flat-plate structures built in the mid 20th century, the specimens represent typical slab-column connections in such structures. As discussed in Chapters 1 and 2, the flat plate structures built in the mid 20th century were commonly used as office or apartment buildings, and the general characteristics of slab-column connections in such structures are as follows:

- No shear reinforcement

- Lack of concentration of the slab top flexural reinforcement near the column
- Low flexural reinforcement ratio in the column strip

3.2 DESIGN OF TEST SPECIMENS

3.2.1 Prototype structure

The prototype structure used in this study consisted of a flat-plate floor system, acting as the main gravity load carrying system, combined with shear walls and exterior moment-resistant frames, which were designed to resist lateral loads. The prototype structure had office occupancy, with a live load of 50 psf and a partition load of 20 psf. The prototype structure had uniform 21-ft span lengths, and 9-inch thick slab supported on 24-inch square columns. No shear reinforcement was used in the slab. Designing the prototype structure using direct design method of ACI 318-1971 resulted in 0.41% of slab top reinforcement in the column strip and 0.22% of slab reinforcement elsewhere (based on the minimum flexural reinforcement requirements).

Table 3.1 includes a comparison of the minimum requirements for the prototype structure if it would have been designed using the empirical method of ACI 318-1963 and using the direct design method of ACI 318-1971 and ACI 318-05 Codes. The minimum length requirements of the slab reinforcement for an interior connection (*V* through *Z*, shown in Figure 3.1) are also presented in Table 3.1.

If the prototype structure was designed using ACI 318-1963, it would have had 0.36% of slab top reinforcement in the column strip, which is less than that designed using ACI 318-1971 (0.41%). This difference stems from the combination of load factors and the total static moment, M_o , calculations. As a

result, M_o calculated using ACI 318-1963 is only 87% of that calculated using ACI 318-1971. Compared with ACI 318-1971, ACI 318-2005 has smaller load factors but a similar expression for M_o . Therefore, the prototype structure designed using ACI 318-2005 would have a comparable amount of flexural reinforcement than that designed using ACI 318-1971 (0.39% of slab top reinforcement in the column strip in this case).

Table 3.1 Prototype structure designed using different ACI codes

Prototype structure properties		Empirical method of ACI 318-1963	Direct design method of ACI 318-1971	Direct design method of ACI 318-2005	
Factored loads (psf)		289	271	239	
M_o (k.ft)		222	256	227	
Minimum slab thickness (inch)		8.1	7.0	7.6	
Concrete cover (inch)		0.75			
$A_{s, \text{column strip}}$ for 9" slab (inch ²)		3.4	3.9	3.7	
% steel in column strip		0.36%	0.41%	0.39%	
% steel within (c+3h)				0.10%* (0.42%)**	
Minimum length requirement of slab reinforcement (Fig. 3.1)	V (inch)	75.6	68.4		
	W (inch)	63	45.6		
	X (inch)	63	50.2		
	Y (inch)	3	2	continuous	
	Z (inch)	37.8			50%: pass 6 in. from col. face Remainder: 34.2

* Assuming $\gamma_f=0.6$ and M_{umb} was calculated using Eq.(13-7) of ACI 318-05

** Assuming $\gamma_f=1.0$ and M_{umb} was calculated by assuming one side has w_d only, while the other side has (w_d+w_l)

$A_{s, \text{column strip}}$: Required area of steel in the column strip

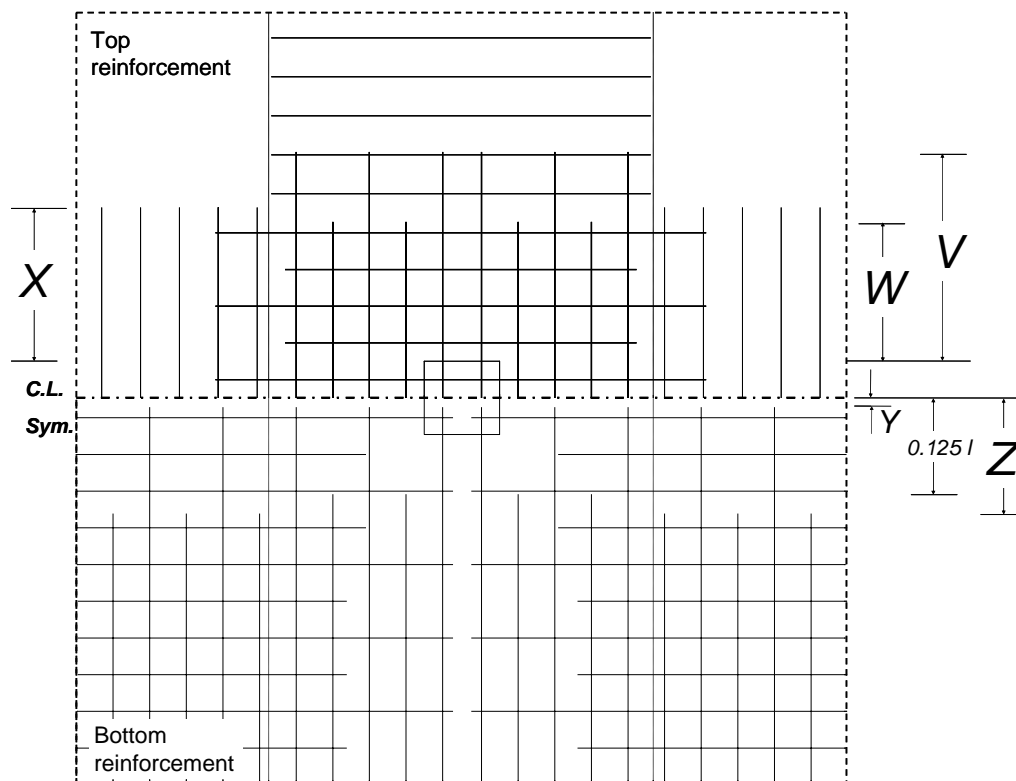


Figure 3.1 Notation for minimum length requirement of slab reinforcement

The concentration of reinforcement within the $(c+3h)$ region was not considered in the design of the prototype structure based on both ACI 318-1963 and ACI 318-1971 because neither of the codes emphasized the need for concentration of reinforcement (as discussed in Section 2.4.3.2). Therefore the percentage of steel, ρ , in column strip and that within $(c+3h)$ region are the same. Unlike ACI 318-1963 and ACI 318-1971, ACI 318-05 emphasizes the need for concentration of reinforcement to resist part of the total unbalanced moment transferred by flexure $\gamma_f M_{unb}$. A concentration of reinforcement based on two extreme assumptions in calculating unbalanced moment transfer was considered in the design of the prototype structure using ACI 318-2005. Assuming that $\gamma_f = 0.6$ and M_{unb} was calculated using Eq. (13-7) of ACI 318-05 (Eq. (2.53) in

Chapter 2 is the simplified version of Eq. (13-7) of ACI 318-05), the required ρ within $(c+3h)$ region was 0.10%. Since this ρ is less than the required ρ for the column strip, concentration of reinforcement is not required. Using a more conservative assumption ($\gamma_f=1.0$ and M_{umb} was calculated by assuming one side has w_d only, while the other side has (w_d+w_l)) resulted in a slightly higher ρ within $(c+3h)$ region, which was 0.42%. It can be concluded that for the gravity load design resulting from the use of any edition of ACI Code since 1963 would have about the same flexural reinforcement ratio. For an office building, typical reinforcement ratio within the column strip is roughly 0.5%. However, the flat-plate structures built after 1980s may have a concentration of reinforcement within $(c+3h)$ region because of the following reasons: (i) All editions of ACI Code since 1989 emphasize the need for concentration of reinforcement (ii) M_{umb} is higher than that considered in this section because the slab-column connections are typically assumed to carry some of the lateral loads as well (Dovich and Wight 1996). Practicing structural engineers were contacted during the course of this research study. These engineers suggested that the typical flexural reinforcement within $(c+3h)$ region of interior slab-column connections in modern flat-plate structures can be about 1.0%.

3.2.2 Test specimens

Test specimens represent a two-third-scale model of an interior flat-plate slab-column connection in the prototype structure that was designed using ACI 318-1971. The test specimens were 14-ft square and had 6-inch thick slabs supported on 16-inch square columns. Slab-column connection specimens (Figures 3.2, 3.3, and 3.4) with 0.5% and 1.0% flexural reinforcement ratios within $(c+3h)$ region were tested during the experimental program. Structural drawings of several flat-plate structures located in western US were examined.

These drawings show that slab-column connections in typical flat-plate structures built in the mid 20th century have roughly about 0.5% top steel in the column strip and lacks of a concentration of flexural reinforcement. As stated earlier, typical connections built using current building code may have about 1.0% steel within $(c+3h)$ region. Therefore, in order to compare the performance of the typical slab-column connections built several decades ago with the behavior of those built recently, the connections with 0.5% and 1.0% top steel within the $(c+3h)$ region were tested.

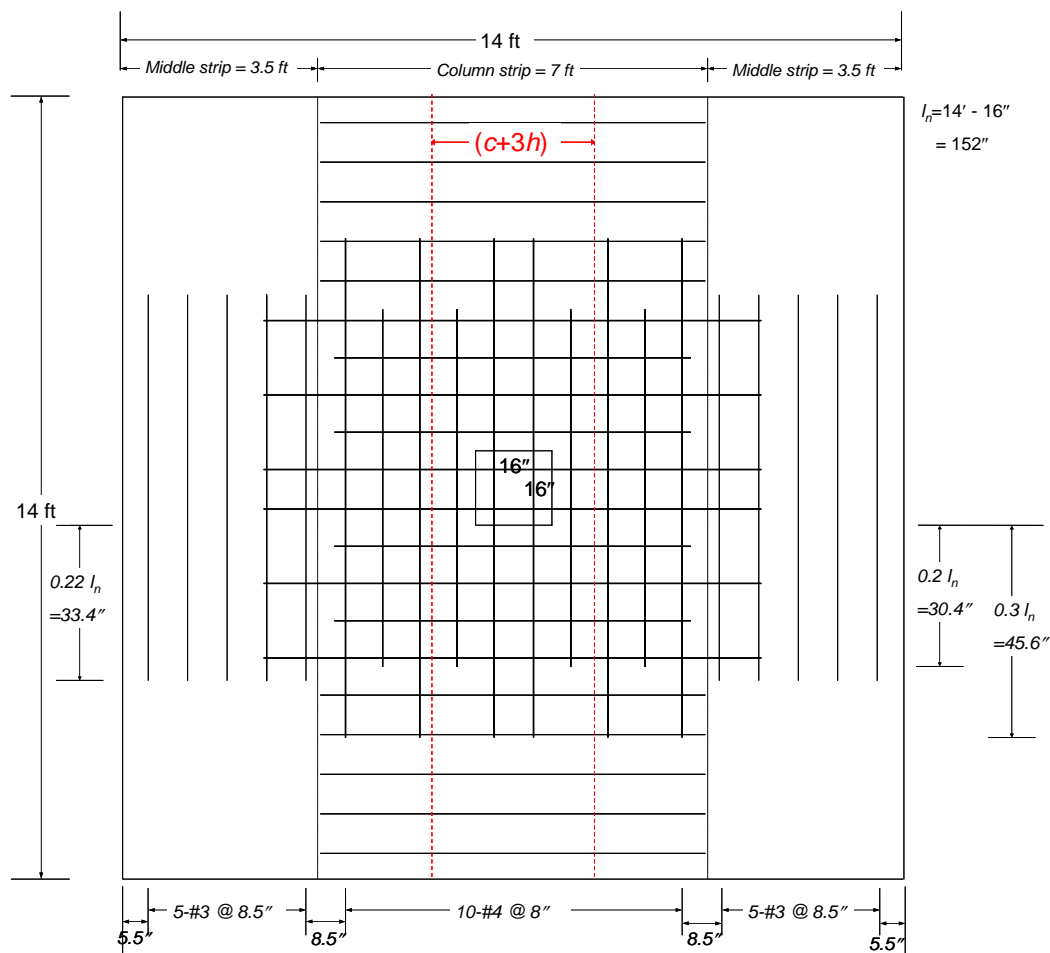


Figure 3.2 Top mat of 0.5% flexural reinforcement within $(c+3h)$

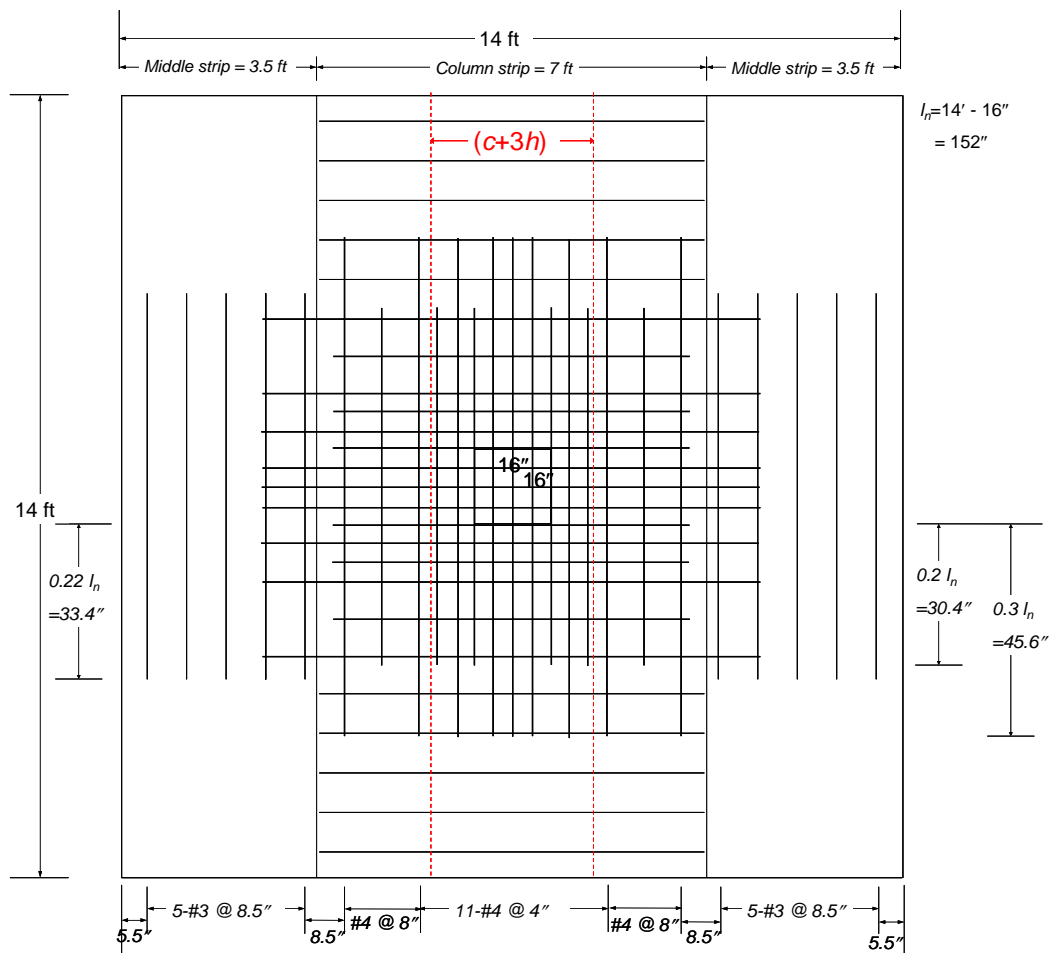


Figure 3.3 Top mat of 1.0% flexural reinforcement within $(c+3h)$

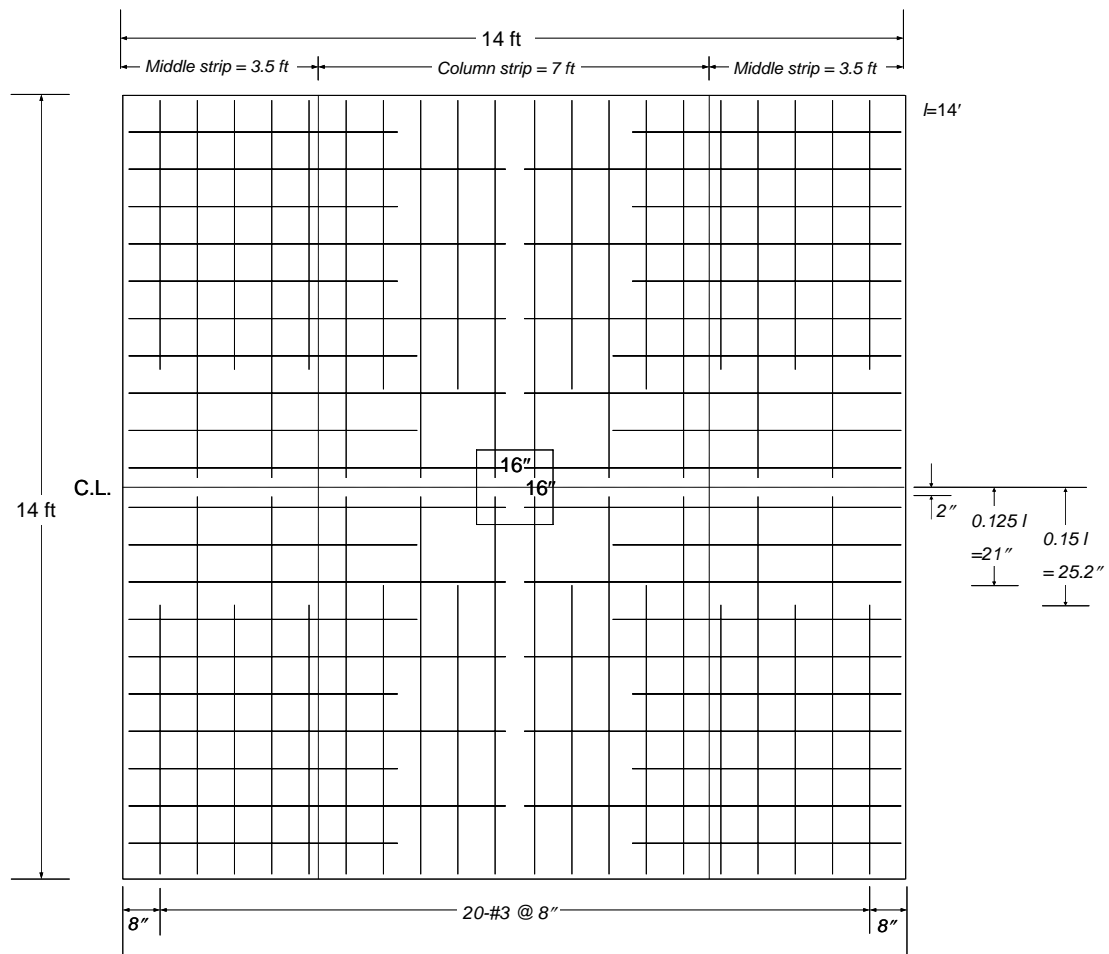


Figure 3.4 Bottom mat of flexural reinforcement

Figures 3.2 and 3.3 show the top mat of flexural reinforcement used in the test specimens with 0.5% and 1.0% steel within $(c+3h)$ region, respectively. Figure 3.4 shows the bottom mat of flexural reinforcement, which was the same for all specimens. Bottom flexural reinforcement was terminated at 1 inch from the slab edge. Top and bottom longitudinal reinforcements were symmetrically placed in perpendicular directions and satisfied the minimum length requirements of section 13.5.6 of ACI 318-1971.

Grade 60 deformed reinforcing bars satisfying ASTM A 706-06 were used. The top reinforcement consisted of US #4 and US #3 bars within the column strip and the middle strip, respectively. The required minimum extended length of top reinforcement from the column face varied from $0.2 l_n$ to $0.3 l_n$, where l_n is the clear span length. US #3 bars were used as bottom reinforcement. Half of the slab bottom reinforcement was stopped at $0.125 l_n$ from the face of the column, and the remaining bars were extended up to 2 inches from the column centerline. The top and bottom reinforcement in the lateral loading direction had a clear cover of 0.5 inches. The average depth of slab reinforcement d was 5 inches.

Columns were reinforced with more steel (5%) and closer stirrup spacing ($s = 6''$ o.c.) than typical columns in order to eliminate the effect of column flexibility (due to cracking) on the connection behavior under simulated seismic loads and to avoid column failure in the strengthened specimens. The use of much stronger columns was consistent with previous experimental research involving lateral loading. Morrison et al. (1983) reported that the columns were much stronger than the slab, negligibly contributing to the lateral displacement of the system. Islam and Park (1976), Pan and Moehle (1988), and Robertson et al. (2002) also indicated that the columns remained essentially elastic during simulated seismic tests.

3.3 TEST SPECIMENS AND PARAMETERS

Seven specimens were constructed and ten different tests (Table 3.2) were performed on those seven specimens. The rehabilitated specimens (strengthening and/or repair) are shaded in Table 3.2. Figure 3.5 shows the notation used for specimen names, which consists of alphanumeric characters and numbers. The alphanumeric characters indicate the sequence of loading and types of

rehabilitation. The numbers designate the percentage of top flexural reinforcement within the $(c+3h)$ region.

Table 3.2 Test program

	Specimen	Test program	% slab top steel within $(c+3h)$
Same specimen	G0.5	Punching shear loading only (to failure)	0.5
	RcG0.5	Strengthening of G0.5 with steel collars, then punching shear loading only (to failure)	0.5
Same specimen	G1.0	Punching shear loading only (to failure)	1.0
	RcG1.0	Strengthening of G1.0 with steel collars, then punching shear loading only (to failure)	1.0
	L0.5	Lateral loading to failure	0.5
	LG0.5	Lateral loading to 1.25% drift, then punched	0.5
	LRstG0.5	Lateral loading to 1.25% drift, rehabilitated by external CFRP stirrups, then punched	0.5
	LRshG0.5	Lateral loading to 1.25% drift, rehabilitated by CFRP sheet, then punched	0.5
Same specimen	LG1.0	Lateral loading to 1.25% drift, then punched	1.0
	RcL1.0	Strengthening of LG1.0 with steel collars, then lateral loading to failure	1.0

Alphanumeric characters

L: Reversed cyclic Lateral loading (simulated seismic loads)
G: Gravity loading up to failure (concentric punching shear loads)
R: Rehabilitation:
 c: using steel collars
 st: using externally installed CFRP stirrups
 sh: using CFRP sheets

Number

0.5: 0.5% slab top steel within $(c+3h)$ region
1.0: 1.0% slab top steel within $(c+3h)$ region

Figure 3.5 Specimen notation

For lateral loading, three fully-reversed displacement cycles were applied at each lateral drift level (Figure 3.6). The lateral displacement protocol used was obtained by modifying the protocol recommended by ACI ITG/T1.1-01 (2001). The column axial load was controlled so that the shear force on the critical shear perimeter was maintained at $1\sqrt{f'_c} b_o d$, which represents dead load plus 25% of live load on the prototype structure. Since the drift capacity of the connections is very sensitive to the level of gravity load (Pan and Moehle 1992, Durrani et al. 1995, Hueste and Wight 1999), applying a realistic level of gravity shear during a simulated seismic test is very important to produce realistic results that will be closer to the behavior of the prototype structure. It is believed that during an earthquake, flat-plate structures typically support the dead load plus a fraction (25% in this case) of live load.

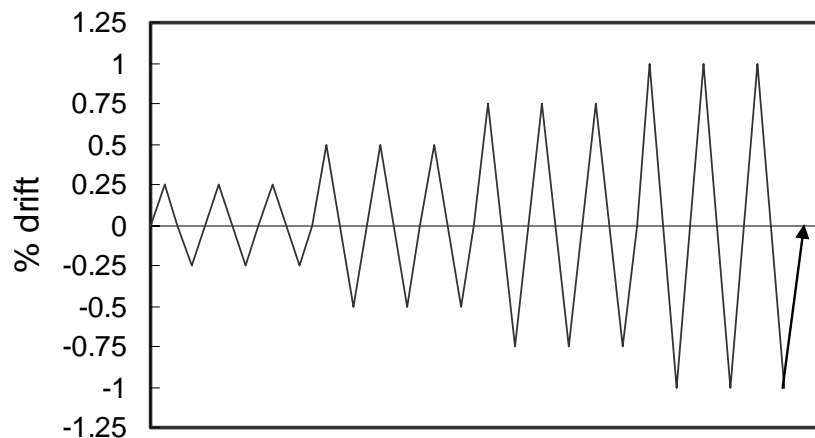


Figure 3.6 Typical displacement protocol

Specimens G0.5 and G1.0 served as control specimens to provide information on the two-way shear strength of undamaged and unstrengthened specimens. After punching shear failure of G0.5 and G1.0, the specimens were unloaded completely, the steel collars were then clamped to the column

underneath the slab, and epoxy was poured to fill cracks around the connection and to restore continuity. The specimens G0.5, G1.0 were renamed as RcG0.5, RcG1.0, respectively, and were tested under gradually increasing gravity loads up to failure to study the effect of steel collars on the two-way shear capacity.

Specimen L0.5 was subjected to reversed cyclic lateral displacements up to failure. Specimen L0.5 served as a control specimen to provide information on lateral load and drift capacities, which were used as bases to determine the required lateral drift, causing a certain seismic damage, for the other specimens.

Based on the results of the test conducted on specimen L0.5, specimens LG0.5, LRstG0.5, LRshG0.5, and LG1.0 were first subjected to gradually increasing reversed cyclic lateral displacements up to 1.25% drift to produce a significant amount of cracking, and then subjected to concentric punching shear loading up to failure. Specimens LG0.5 and LG1.0 were tested to study the two-way shear strength of connections damaged during seismic events. At the end of the lateral loading, specimens LRstG0.5 and LRshG0.5 were rehabilitated using externally installed CFRP stirrups and externally installed CFRP sheets, respectively. Specimens LRstG0.5 and LRshG0.5 were tested to evaluate the efficiency of different rehabilitation methods in improving the two-way shear strength of connections damaged during strong ground motions. Since the amount of CFRP sheets applied to specimen LRshG0.5 was designed and adjusted to produce the same flexural capacity as a connection with 1.0% top steel, the performance of LRshG0.5 could be compared to G1.0.

Similarly to specimen LG0.5, specimen LG1.0 was subjected to reversed cyclic lateral displacements up to 1.25% and then was subjected to concentric punching shear loading up to failure. After punching failure, specimen LG1.0 was unloaded completely. Cracks around the connection were then filled with epoxy and the steel collars were installed. The specimen LG1.0 was then renamed as

RcL1.0 and subjected to reversed cyclic lateral displacements up to failure in order to study the seismic performance of a connection strengthened with steel collars.

3.4 SPECIMEN CONSTRUCTION

Construction of test specimens consisted of the following steps: preparation of the formwork, construction of column reinforcing cage, installation of slab flexural reinforcement, casting the slab and the lower column, casting the top column, and curing.

Formwork (Figure 3.7), was built using $\frac{3}{4}$ -in thick plywood as a slab platform and as part of the column forms. 4×4 stud grade wood was used to support the elevated slab platform. 2×4, 2×6, 2×8 stud grade lumbers were used for bracings, joists, stringers, and sides of slab formwork. Joist and stringer spacings were selected to satisfy the maximum tolerable deflection of $\frac{1}{8}$ inches. A laser level was used to check the level of the slab platform. 1.5-in diameter PVC pipes were used for creating the connection holes for the vertical struts to support the specimen during testing.



Figure 3.7 Formwork

After the formwork was constructed, form oil was sprayed, the column reinforcing cage (Figure 3.8) was placed, and slab flexural reinforcement was then installed. Electrical strain gages were attached to the slab bars before the bars were placed on the formwork. Strain gage placement is further discussed in Section 3.7.1. Slab flexural reinforcement was placed in two mats consisting of bars running in North-South (N-S) and East-West (E-W) directions, tied together in a single mat. Top and bottom bars running in N-S direction (lateral loading direction) were placed in outer layers to give the maximum effective depth in this

direction. 0.5-in plastic chairs were used to provide clear cover for the bottom mat and 4.5-in steel chairs were used to support the top mat. Four lifting inserts were installed at the corners of the slab to provide a support attachment for the cantilever portion of the slab. Figure 3.9 shows the bottom flexural reinforcement that was terminated 6-in away from the column face. Figures 3.10 and 3.11 show the specimens with 0.5% and 1.0% of top flexural reinforcement within the $(c+3h)$ region, respectively, before casting.



Figure 3.8 Column reinforcing cage

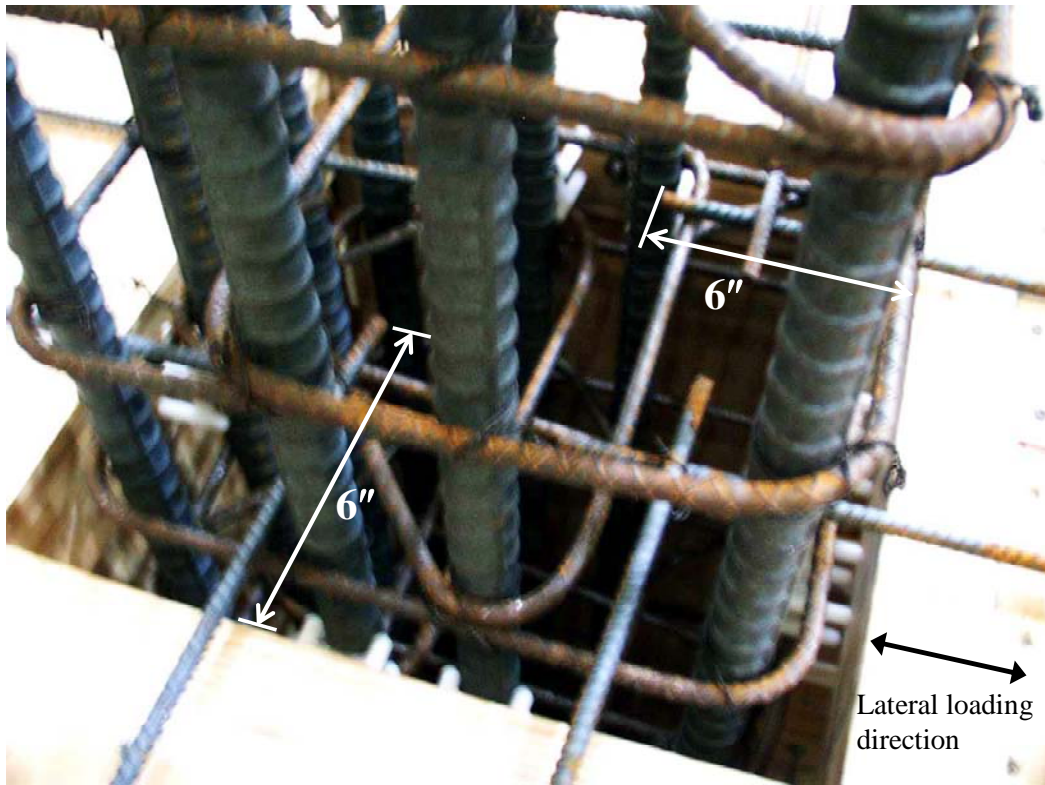


Figure 3.9 Discontinued bottom flexural reinforcement

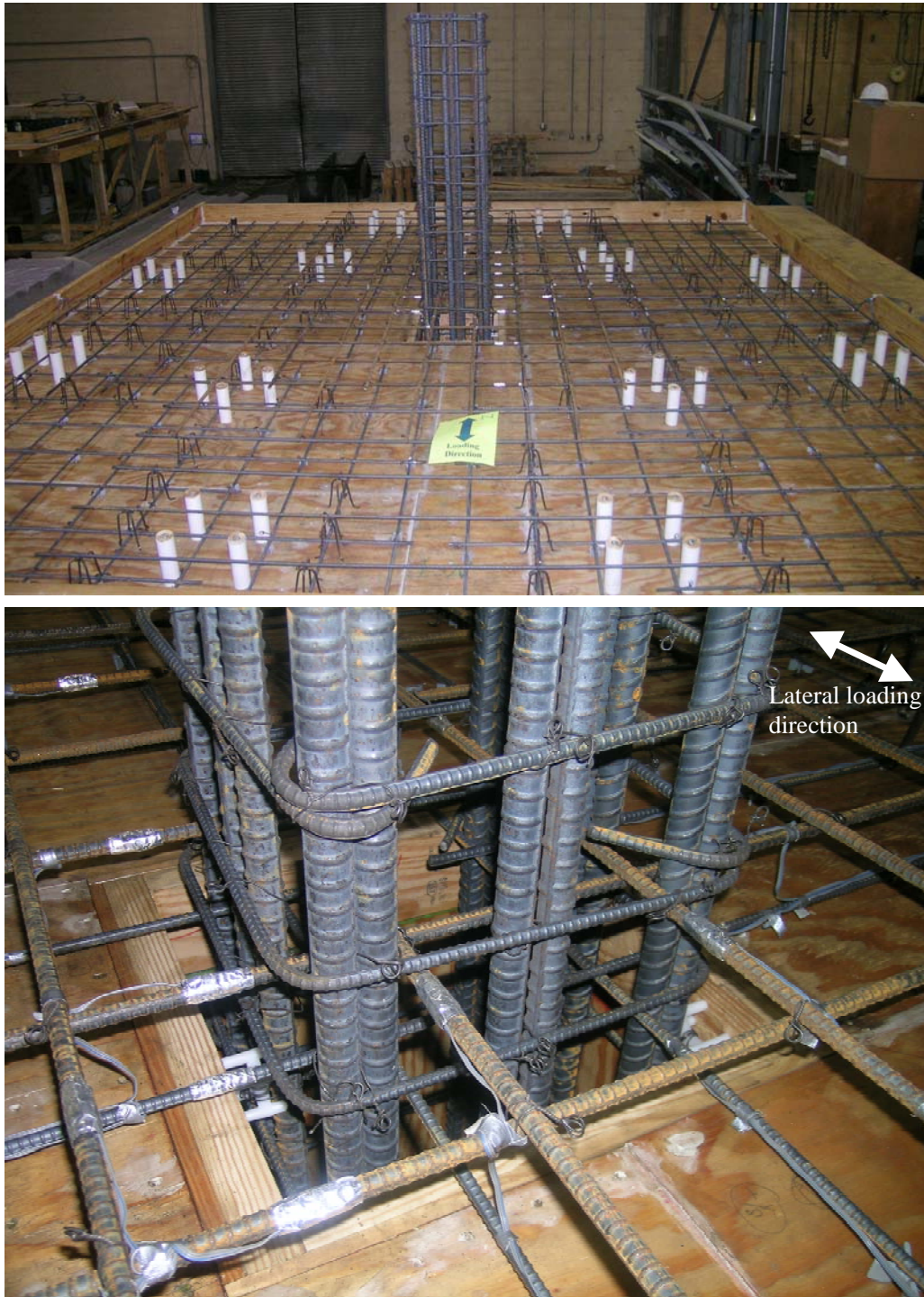


Figure 3.10 Slab reinforcement with 0.5% steel within $(c+3h)$

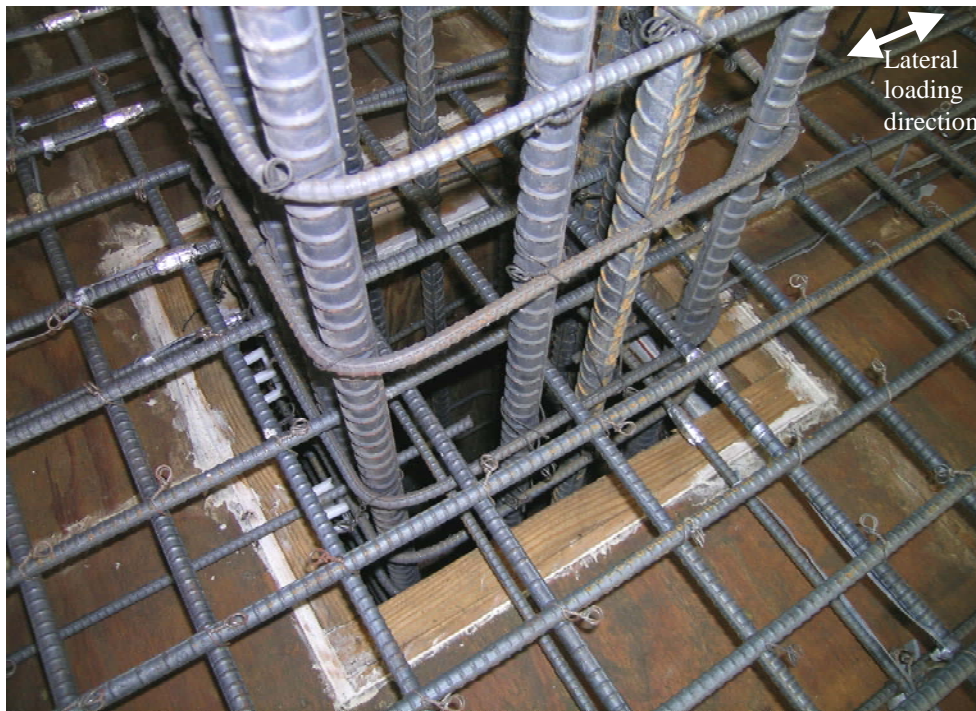
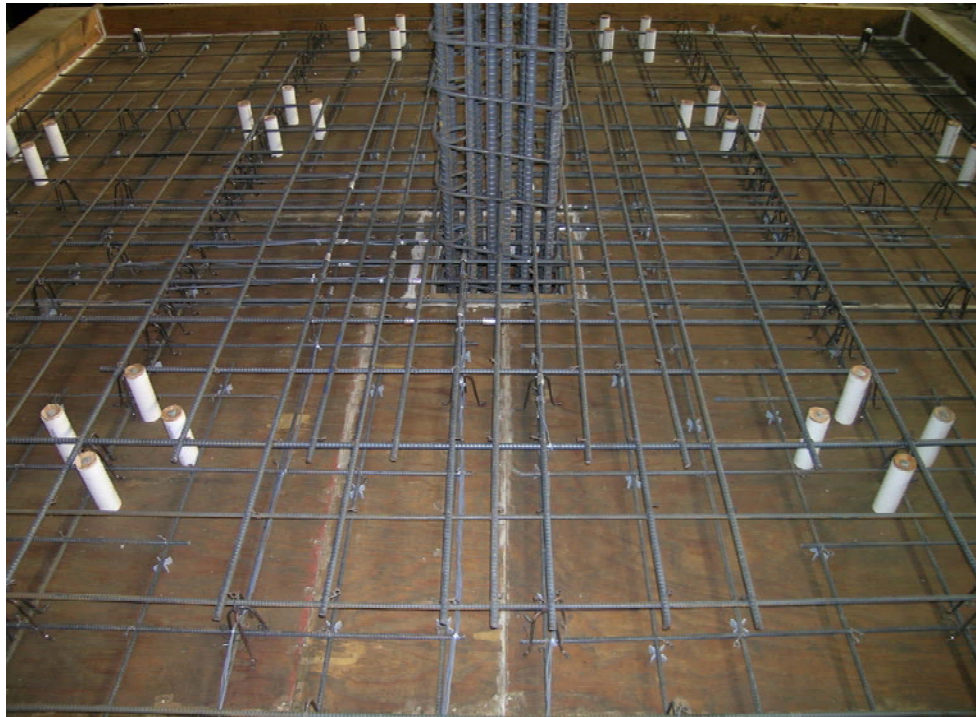


Figure 3.11 Slab reinforcement with 1.0% steel within $(c+3h)$

Ready-mix concrete was used in the specimen construction. Upon arrival, slump was checked according to ASTM C143 procedures. In order to increase the workability of concrete, super plasticizers were used. Concrete was placed using a bucket suspended from an overhead crane and compacted with electric hand vibrators as shown in Figures 3.12 and 3.13. The slab and the lower column stub were cast monolithically. Slab surfaces were finished using hand and bull floats. Figure 3.14 shows the construction joint. Five days after the first cast, the formwork for the upper column was installed and concrete was placed, as shown in Figure 3.15.



Figure 3.12 Concrete placement: slab and lower column



Figure 3.13 Compacting concrete



Figure 3.14 Construction joint at slab-column connection



Figure 3.15 Concrete placement: upper column

For curing, the specimen was covered with wet burlaps and plastic sheets for 7 days to retain moisture. Within those 7 days, water was sprayed every morning and afternoon to ensure moist curing. After the specimen was cured and ready to test, it was lifted from the formwork (Figure 3.16), and was connected to the strong floor and wall. The specimen placement is discussed in Section 3.8.1.

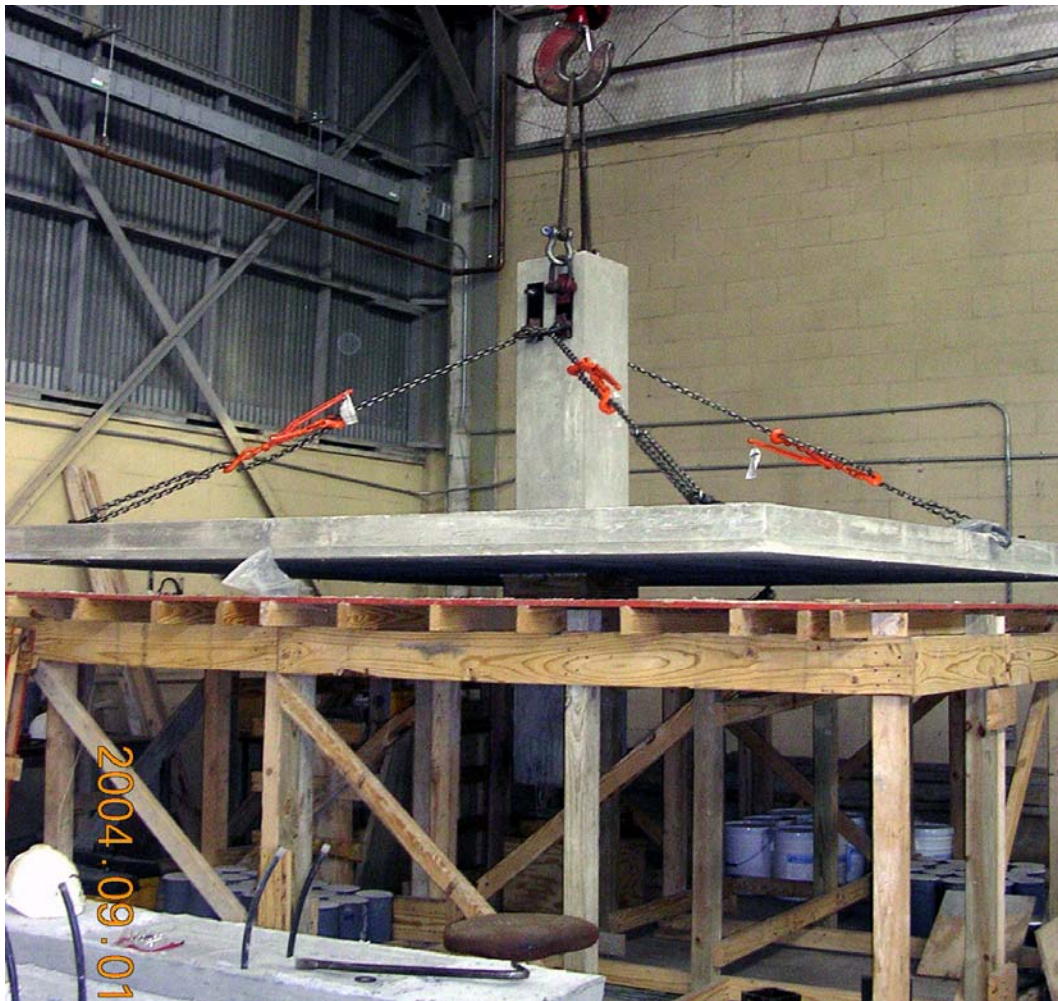


Figure 3.16 Lifting a specimen from the formwork

3.5 MATERIAL PROPERTIES

3.5.1 Concrete

A concrete mixture with $\frac{3}{8}$ -inch maximum aggregate size and a target compressive strength of 4000 psi (used to simulate the design strength of flat-plate structures built in the mid 20th century) was used. Table 3.3 shows concrete cylinder compressive strength, age of specimen at the time of testing, and casting

date for all specimens. The average (three 6×12 cylinders were tested to establish the concrete strength of each test specimen) cylinder compressive strength of all specimens varied between 3700 psi and 4900 psi (Table 3.3).

Table 3.3 Concrete cylinder compressive strength

Specimen	Compressive strength (psi)	Days after casting	Casting
G0.5	4550	53	4 March 2005
RcG0.5	4630	91	
G1.0	4070	64	28 June 2005
RcG1.0	4070	77	
L0.5	3710	104	24 June 2004
LG0.5	4860	84	18 November 2004
LRstG0.5	4930	138	
LRshG0.5	4630	145	4 March 2005
LG1.0	4000	140	28 June 2005
RcL1.0	4000	170	

3.5.2 Steel reinforcing bars

The flexural slab reinforcement was Grade 60 weldable deformed reinforcing bars that satisfy ASTM A 706–06. The ASTM A 706-06 requirements are as follows:

- The minimum ultimate tensile strength is 80 ksi.
- The minimum and maximum yield strength are 60 ksi and 78 ksi, respectively.
- The minimum elongation in 8-in of US#3 and US#4 is 14%

The average mean yield strength obtained from uniaxial tension tests for US#3 and US#4 rebars were 63 and 66 ksi, respectively. The average mean ultimate

strength for US#3 and US#4 rebars were 94 and 96 ksi, respectively. The average strengths were calculated based on repeatable results of three tests per bar size.

3.5.3 CFRP

As one of the strengthening materials, a 0.04-inch thick, unidirectional carbon fiber reinforced polymer (CFRP) with aramid cross fibers (FYFE Co, Tyfo SCH-41S) was used. The carbon fibers were oriented in the 0° direction with aramid fibers at 90°.

The elastic modulus, tensile strength, and ultimate tensile strain of the CFRP laminate based on the ASTM D-3039 test method were 10500 ksi, 127 ksi, and 0.012, respectively (Fyfe Co. LLC 2002). However, CFRP coupon test results reported by Binici (2003) showed significant variations. The comparisons between the manufacturer's reported values and Binici's test results of nine CFRP coupons are summarized in Table 3.4.

Table 3.4 CFRP properties

CFRP properties	Manufacturer's reported values	Coupon test results		
		Range	Average	Standard Deviation
Elastic modulus (ksi)	10500	6682 - 18493	10348	4298
Tensile strength (ksi)	127	96 - 155	116	18
Ultimate tensile strain	0.012	0.007 - 0.017	0.012	0.003

3.5.4 Epoxy

In order to bond CFRP to concrete, Tyfo S epoxy was used. The Tyfo S epoxy is a two-component epoxy matrix material (components A and B). Both components were shipped in 5-gallon containers. The epoxy mix ratio is 100 parts of component A (resin) to 42.0 parts of component B (hardener) by volume or 100 parts of component A and 34.5 parts of component B by weight (Fyfe Co. LLC 2002).

The elastic modulus, tensile strength, and ultimate tensile strain of the epoxy based on ASTM D-638 Type 1 test method were 461 ksi, 10.5 ksi, and 0.05, respectively (Fyfe Co. LLC 2002). The flexural strength and flexural modulus of the epoxy based on ASTM D-790 test method were 17.9 ksi and 452 ksi, respectively (Fyfe Co. LLC 2002).

3.6 TEST SETUP

In order to study the two-way shear capacity of earthquake-damaged connections, two different test setups must be used. The first test setup was designed to simulate seismic loading (combination of reversed cyclic lateral displacements simulating the effects of a ground motion and a constant vertical load simulating the effects of gravity loads acting on the connection during an earthquake). The second test setup is for punching shear tests (monotonically increasing concentric vertical loads). Figure 3.17 shows a schematic of the two test setups (plan and elevation views). Figures 3.18 and 3.19 show perspective views of the test setup for simulated seismic tests and for punching shear tests, respectively.

Since the locations of inflection points during simulated seismic loading are different than those during a punching shear test, the two test setups have different support locations. Assuming that the inflection points are located at the mid-story height, the lateral load was applied at the mid-story height of the upper column and a horizontal strut was connected to the mid-story height of the lower column. The positions of the vertical struts, shown in Figure 3.17, were selected to reflect results of non-linear finite element analyses conducted on the prototype structure subjected to lateral and gravity loads (Tian 2006). During an earthquake, the locations of inflection points in actual structures move as the direction of

seismic waves vary, the ratio of lateral to gravity loads changes, and the internal forces redistribute. However, for all practical purposes in this test program, the inflection points (where the vertical struts were located) were fixed.

Lateral loads were applied in the N-S direction using a horizontal hydraulic actuator attached to the laboratory strong wall and resisted by a horizontal strut attached to the lower column. In order to operate the horizontal actuator in displacement control mode, an MTS 407 controller was used in conjunction with an MTS 290 service manifold. Torsional bracings were installed at both North and South ends of the slab to prevent twisting while lateral displacements were being imposed.

Gravity loads were applied using a hydraulic jack and resisted by vertical struts fixed to the laboratory strong floor. All vertical struts had pin-connections at both ends. Vertical load was maintained manually by using a hand-pump (Power Team model P460) during the application of reversed cyclic lateral displacements. The gravity loads were simulated by applying a concentric upward load on the column instead of placing heavy blocks on the top surface of the slab. This approach was chosen to allow for the observation of the seismic-damage on the slab surface and the evaluation of damage using non-destructive methods (Argudo 2006).

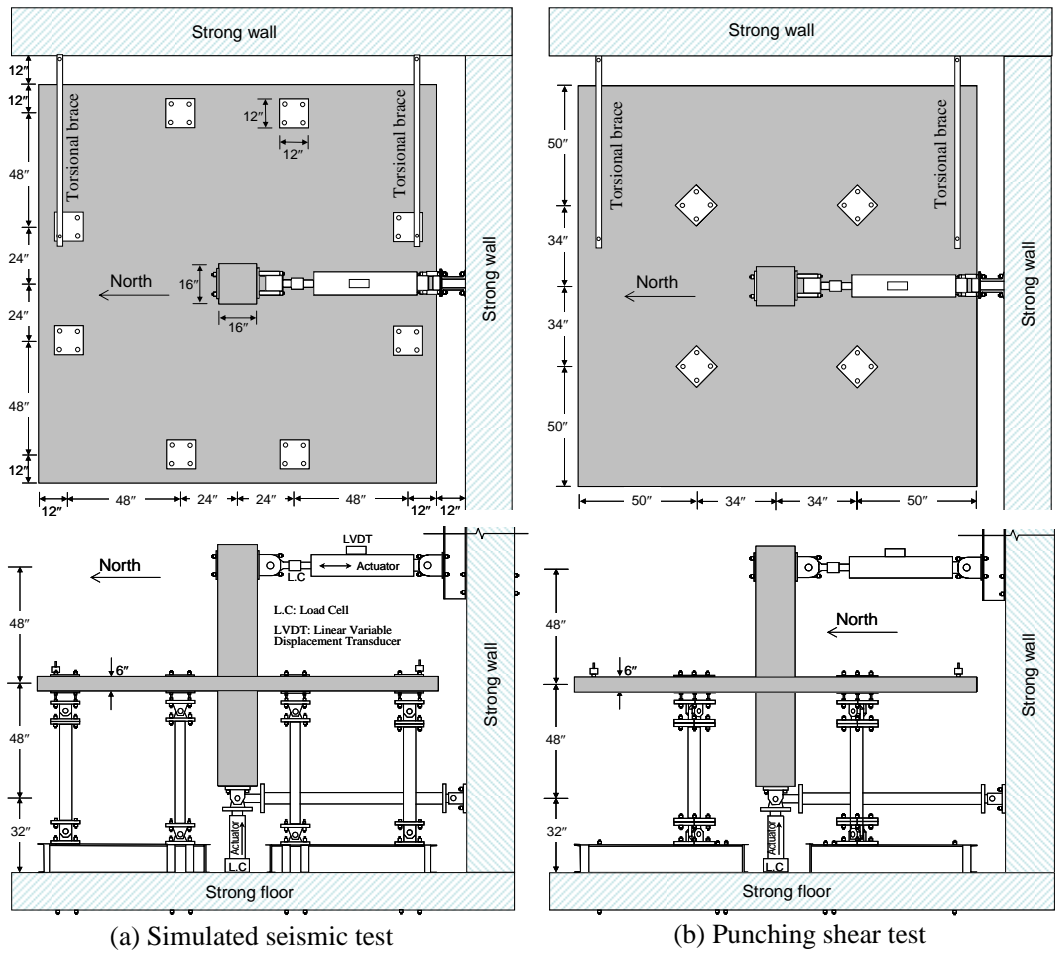


Figure 3.17 Schematic of the test setup

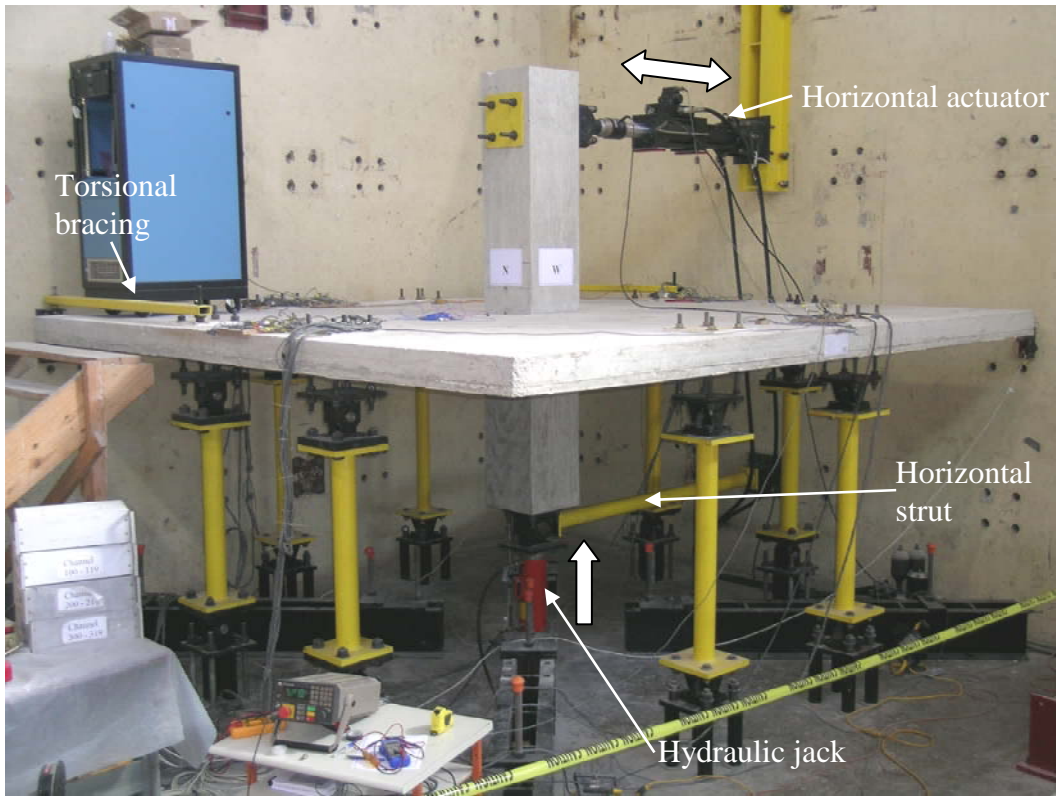


Figure 3.18 Test setup: Simulated seismic test



Figure 3.19 Test setup: Punching shear test

3.7 INSTRUMENTATION

3.7.1 Strain measurements

Electrical resistance strain gages with a nominal resistance of 120 ohms were attached to slab rebars, CFRP stirrups, and CFRP sheets for monitoring strains. Figures 3.20 and 3.21 show typical strain gage locations for simulated seismic tests and punching shear tests, respectively. Strain gages manufactured by the Tokyo Sokki Kenkyujo Company, FLA-5-11-3LT and BFLA-5-11-3LT were used for rebars and CFRP, respectively. Both types of foil strain gages were 1.5-mm wide and 5-mm long. BFLA gages had a special grid pattern in their backing to minimize the reinforcement effect on composite materials.

A pneumatic rotary grinder was used to remove the deformations on rebars at the corresponding strain gage locations. The steel surface was then smoothed using 220 grit silicon-carbide paper and cleaned using Conditioner A and Neutralizer 5A. After the surface dried, strain gages were attached using CN adhesive. In CFRP stirrups and sheets, a smooth surface was obtained by applying PS-2 resin on the surface of FRP. The strain gages were then attached using CN-Y adhesive. Both rebar and CFRP strain gages were water-proofed using M-Coat D and protected using a neoprene rubber sheet and electrical tape. In order to minimize the adverse effects of the gages on the bond between rebars and concrete, grinding of the rebar deformations was minimized and the protection was confined to the immediate vicinity of the gages.

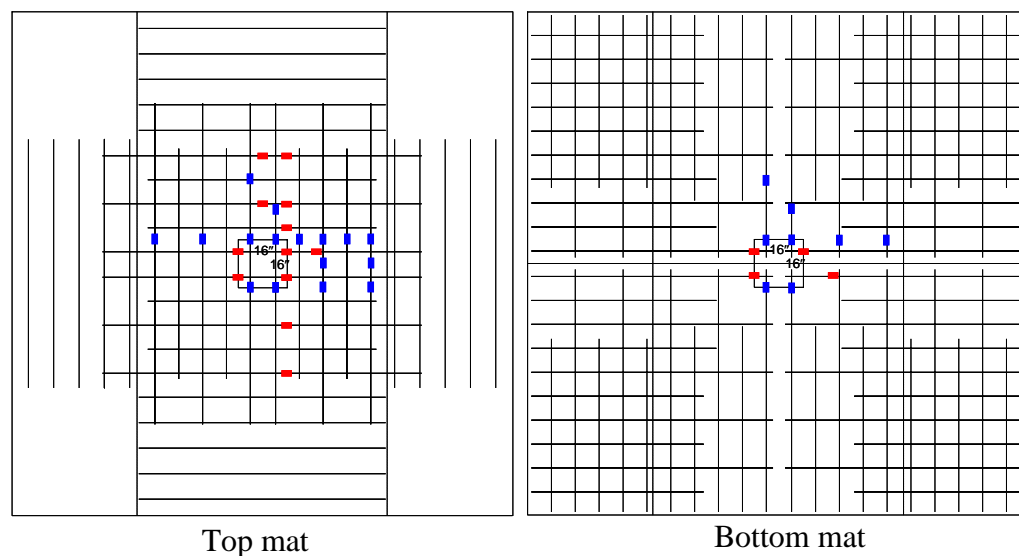


Figure 3.20 Typical strain gage locations used in simulated seismic tests

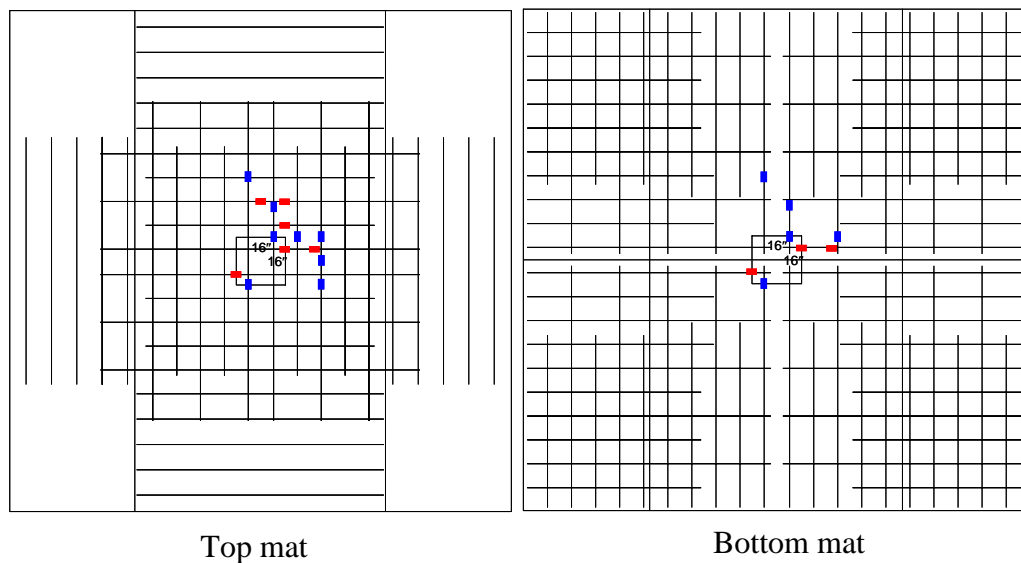


Figure 3.21 Typical strain gage locations used in punching shear tests

3.7.2 Load measurements

Lateral load was measured through a load cell that was integrated into the 55-kip MTS hydraulic actuator (Figure 3.22). Vertical load on the column was measured by a load cell (Interface model 1240, 200-kip capacity) that was placed underneath a 100-ton hydraulic jack (Power Team model RD10013). Pressure transducer on the pump was used as a secondary instrument to monitor the vertical load applied on the column, as shown in Figure 3.22.

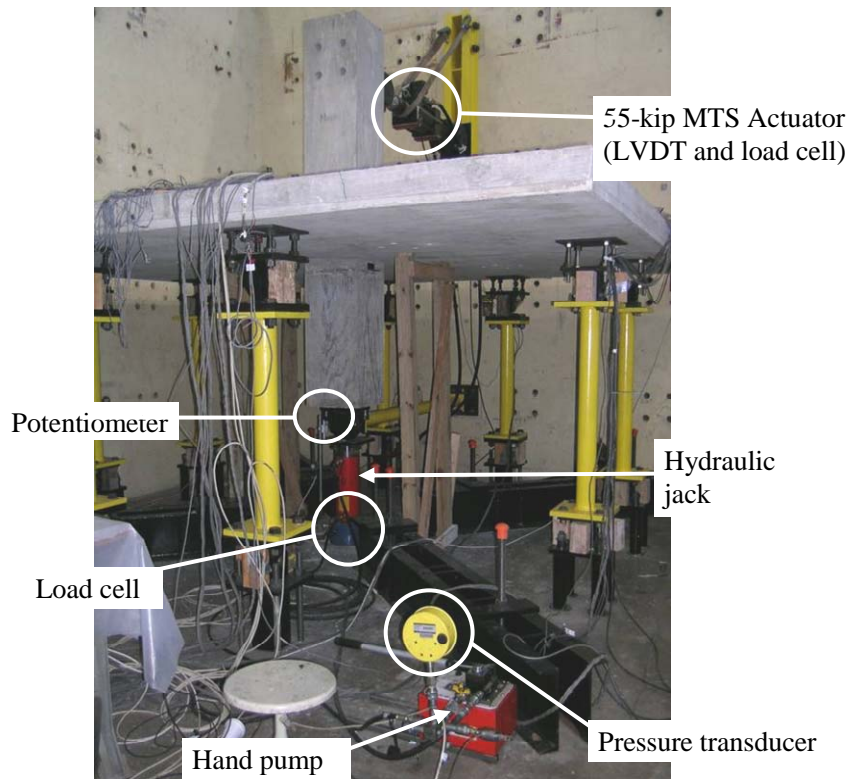


Figure 3.22 Load and displacement measurements

3.7.3 Displacement measurements

Linear variable displacement transducers (LVDT) and linear potentiometers were used to monitor displacements. The displacement of horizontal actuator was monitored by an LVDT integrated within the horizontal actuator. Vertical displacement of the column was measured by a 6-in potentiometer installed underneath the column (Figure 3.22). In the punching shear test performed on the specimen strengthened using steel collars, four 6-in potentiometers were also used to measure vertical displacement of the steel collars at each column face (Figure 3.23).

3.7.4 Data acquisition and monitoring

All instruments were connected into a Hewlett-Packard 75000 scanner and data was recorded using Ferguson Structural Engineering Laboratory's data acquisition software.



Figure 3.23 Linear potentiometers

3.8 TEST PROCEDURE

3.8.1 Specimen installation

Figure 3.24 shows the position of vertical struts used in simulated seismic tests. Prior to specimen installation, all vertical struts were locked into place using wooden blocks. Specimens were moved from the formwork to the testing area using an overhead crane and they were placed on the wood shoring (Figure 3.25). They were then connected to the clevises at the end of the vertical struts and underneath the lower column. The horizontal actuator was connected to the upper column and torsional bracings were attached to the slab. The linear potentiometers were mounted in their proper position underneath the lower column stub, and between the slab and the strong wall in the lateral loading direction.



Figure 3.24 Position of vertical struts: simulated seismic test



Figure 3.25 Installation of a test specimen

The vertical load was then applied to the lower column to produce a shear force on the critical shear perimeter of $1\sqrt{f'_c}b_o d$. The vertical load also counteracted the weights of the column, part of the slab, and part of the horizontal actuator. The total of those weights was calculated to be equal to 2.9 kips and the actual applied vertical load was equal to the load required to produce a shear force of $1\sqrt{f'_c}b_o d$ at the critical perimeter plus 2.9 kips. After the application of vertical load, the shoring and all wooden blocks were removed, the specimen was subjected to reversed cyclic lateral displacements. During the application of lateral displacements, the vertical load on the column was maintained.

For the specimens G0.5 and G1.0, which were not subjected to lateral loading, the vertical struts were positioned for a punching shear test (Figure 3.26), before the specimens were moved to the testing area.



Figure 3.26 Position of vertical struts: punching shear test

3.8.2 Changing boundary conditions

In order to study the two-way shear capacity of the earthquake-damaged connections, the boundary conditions were changed at the end of the application of reversed cyclic lateral displacements. After the lateral load was completely removed, the specimen was shored. Four vertical struts were then moved closer to the column one by one and the other four struts were disconnected from the slab. The specimen was then loaded up to failure under a gradually increasing vertical load underneath the column. During a punching shear test, the horizontal actuator was kept connected to the upper column for stability purposes.

3.8.3 Rehabilitation

In order to study the effectiveness of steel collars in strengthening the connections, specimens RcG0.5 (the same specimen as G0.5) and RcG1.0 (the same specimen as G1.0) were tested. After punching shear failure of specimen G0.5, the vertical load was unloaded completely. The steel collars were clamped to the column, against the bottom surface of the slab, and the specimen G0.5 was renamed as RcG0.5. The specimen was then loaded up to failure under gradually increasing vertical loads underneath the column. The same procedure was repeated after punching shear failure of specimen G1.0.

In order to study the efficiency of different methods in repairing the earthquake-damaged connections, specimens LRstG0.5 and LRshG0.5 were tested. After the specimen was subjected to reversed cyclic lateral displacements up to 1.25% drift, the boundary conditions were changed. In order to mimic the rehabilitation process in a flat-plate building that is unshored, the column axial load producing a shear force of $1\sqrt{f'_c} b_o d$ on the critical shear perimeter was applied and maintained during the rehabilitation process.

In order to study the effectiveness of steel collars in improving the seismic behavior of the connections, specimen RcL1.0 (the same specimen as LG1.0) was tested. After punching shear failure of specimen LG1.0, the vertical load was unloaded completely and the specimen was shored. The boundary conditions were changed for lateral loading. The shoring was then removed and the steel collars were installed (specimen LG1.0 was renamed as RcL1.0). The vertical load was re-applied to the column to produce a shear force of $1\sqrt{f'_c}b_o d$ on the critical shear perimeter. While maintaining the vertical load, the specimen RcL1.0 was then subjected to reversed cyclic lateral displacements up to failure.

All rehabilitation methods involved the use of epoxy to fill cracks, to restore continuity, and to bond the CFRP to concrete. The rehabilitated specimens were tested at least one week after the application of epoxy to allow sufficient time for the curing of epoxy.

3.8.4 Cutting the specimen

At the end of each test, the test specimens were saw cut into three pieces (parts 1, 2, and 3 in Figure 3.27) to observe the location and the angle of failure crack. Figure 3.27 shows the directions of the first and second cuts. The first cut was always in the direction of lateral loading and the second cut was perpendicular to the first cut. Both cuts were made as close to the column face as possible. Typically, the cut was 2.5 inches away from the column face. After removing part 1 (Figure 3.27), the inclined cracks in the lateral loading direction could be observed. After removing part 2, the inclined cracks on the face that was perpendicular to the lateral loading direction could be examined. Figure 3.28 shows the process of making the first cut.

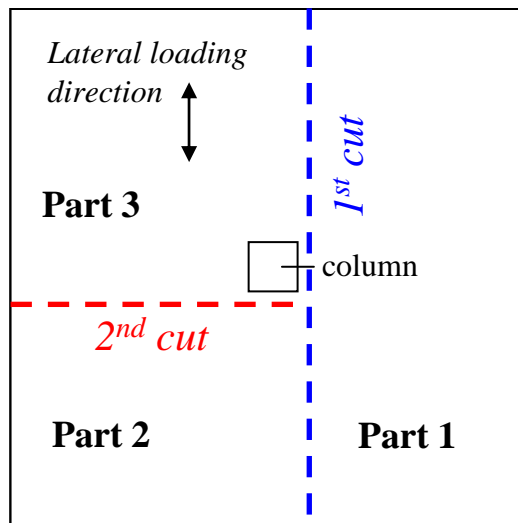


Figure 3.27 Schematic of the cuts



Figure 3.28 Saw cutting the specimen

3.9 SUMMARY

Seven two-third scale interior slab-column connections were tested in this research. Boundary conditions for both simulated seismic loading and punching shear tests were carefully determined to match the internal force distribution in the continuous prototype structures. It is believed that the behavior of the test specimens closely represent the behavior of interior slab-column connections in the prototype structure. Details of slab-column specimens, experimental program, and the test setup are described in Chapter 3. The details of rehabilitation methods and the test results are presented in Chapter 4.

CHAPTER 4

Experimental Results and Discussion

4.1 GENERAL

The results of the experimental program described in Chapter 3 are presented and discussed in Chapter 4. The organization of Chapter 4 is as follows: details of test procedure, behavior of test specimens, failure surfaces, and rehabilitation method for each specimen are presented in Sections 4.2 through 4.9. Results of tests conducted on all specimens are compared in Section 4.10. The comparison between the measured capacities of unstrengthened, undamaged connections and the estimated capacities is also presented in Section 4.10. The effects of flexural reinforcement ratio and seismic damage on the two-way shear strength of slab-column connections, and the effectiveness of different rehabilitation methods are discussed in Section 4.10.

4.2 SPECIMENS G0.5 AND G1.0

Under gradually increasing gravity loads, specimens G0.5 and G1.0 were loaded to failure to evaluate the two-way shear strength of unstrengthened, undamaged connections. Both specimens served as control specimens, with which the two-way shear capacity of earthquake-damaged specimens and rehabilitated specimens were compared.

Figures 4.1 and 4.2 show the top and bottom failure surfaces of specimens G0.5 and G1.0, respectively. The punching cone in both specimens intersected the bottom slab surface right at the slab-column intersection, similar to that observed

in an actual structure (Figure 1.3). The top slab surface of G1.0 exhibited a larger area of delamination than that of G0.5.



Figure 4.1 Failure surface of specimen G0.5

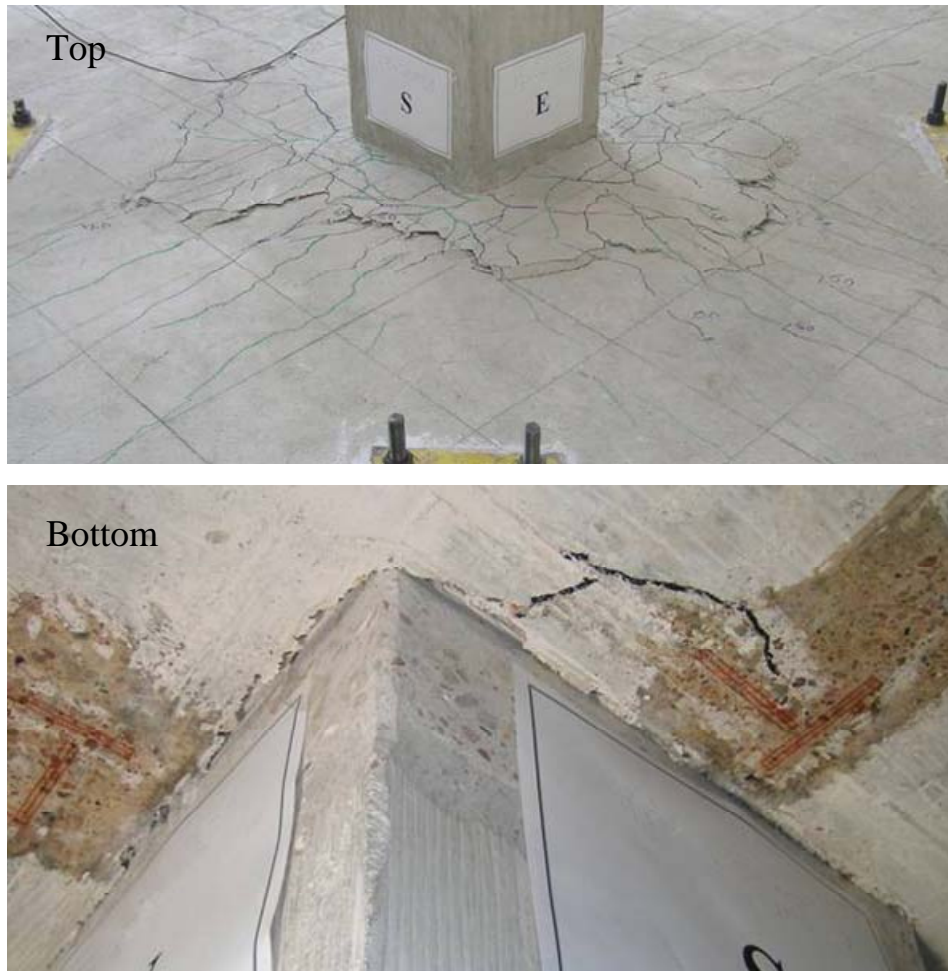


Figure 4.2 Failure surface of specimen G1.0

4.3 SPECIMENS RCG0.5 AND RCG1.0

Specimens RCG0.5 and RCG1.0 were strengthened using collars made from structural steel tubes that were clamped to the column under the slab. After the collars were installed, the specimens were loaded up to failure under gradually increasing concentric gravity loads. Since the collars transferred load to the column through friction that was generated by clamping (without any dowels or other mechanical connectors), the preparation of column surface was important.

Comparing the vertical displacement of the column with those of the collars based on the readings of all potentiometers, which were installed as shown in Figure 3.23, in both specimens RcG0.5 and RcG1.0 indicated that the collars did not slip.

4.3.1 Components of steel collars

Figure 4.3 shows all components for the collars and Figure 4.4 shows the collar after installation. The collar consisted of two 32-in long square tubes ($\square 8 \times 8 \times 3/8$) and two 15.5-in long square tubes ($\square 8 \times 8 \times 3/8$). The 32-in tubes were clamped on the column with four 1-in diameter threaded rods. The 15.5-in tubes were supported on two angles ($L 8 \times 6 \times 3/4$) that were clamped on the column with four 1-in diameter threaded rods (Figure 4.4). The length of shorter tubes (15.5 inches) was 0.5 inches less than the column size (16 inches) to avoid any interference with longer tubes when the longer tubes were clamped. In order to prevent bending of the angles, three 1/2-in thick stiffeners were welded to the angle. In order to prevent local deformations and to get a better clamping force distribution from threaded rods, 3/4-in thick plates were used as washers. Non-shrink grout was used to fill the gap between the steel tubes and the bottom slab surface, and also to obtain a more uniform contact surface.

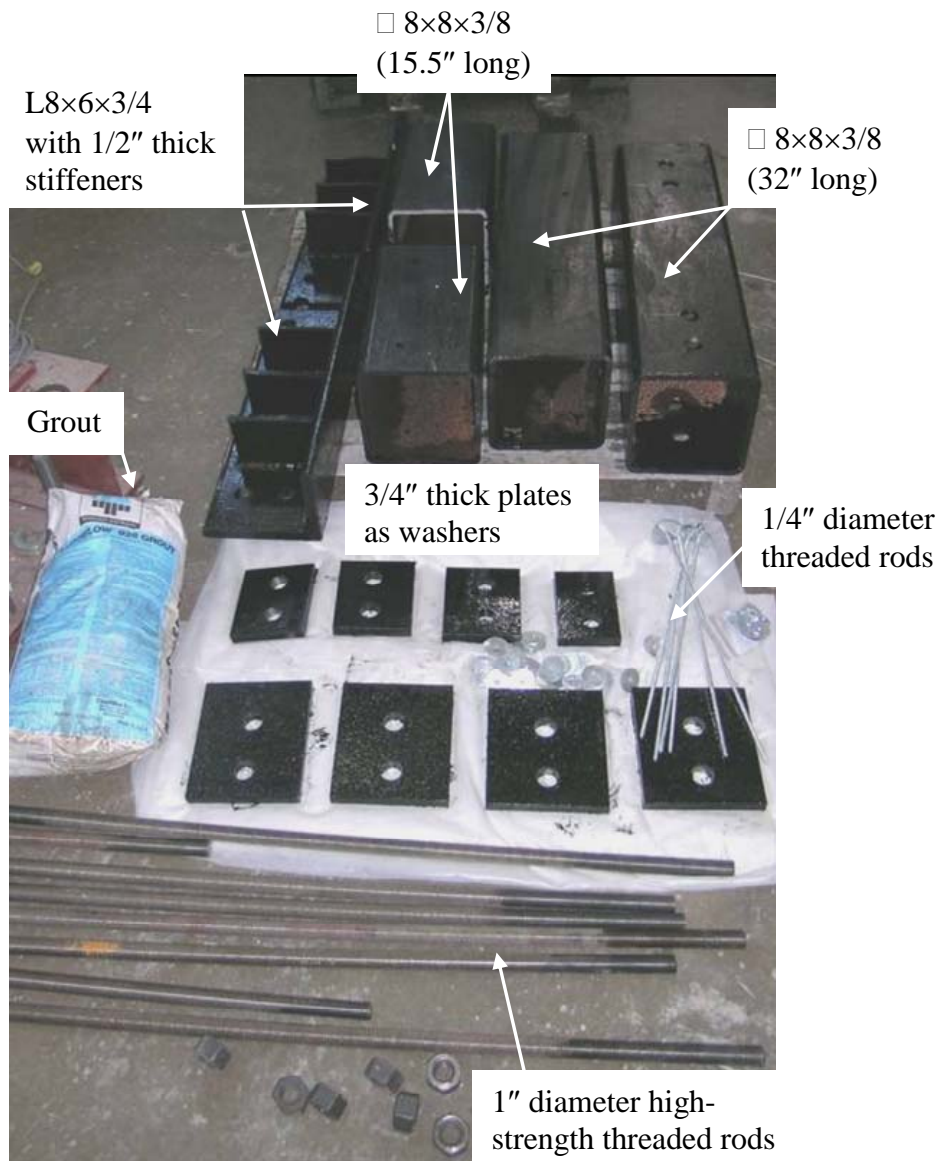


Figure 4.3 Components of the collars



Figure 4.4 Collar after installation

4.3.2 Rehabilitation process

After punching shear failure of specimens G0.5 and G1.0, both specimens were unloaded completely. Then, cracks on the bottom of slab-column intersection were sealed with silicone (Figure 4.5) and the uneven surfaces of the column and the bottom surface of the slab, where the steel collars were installed, were ground to be flat. The column surface where the steel collars were clamped was then roughened using a rotary hammer drill (Hilti TE 55 shown in Figure 4.6). Figure 4.5 shows the concrete surfaces before and after they had been ground and roughened.

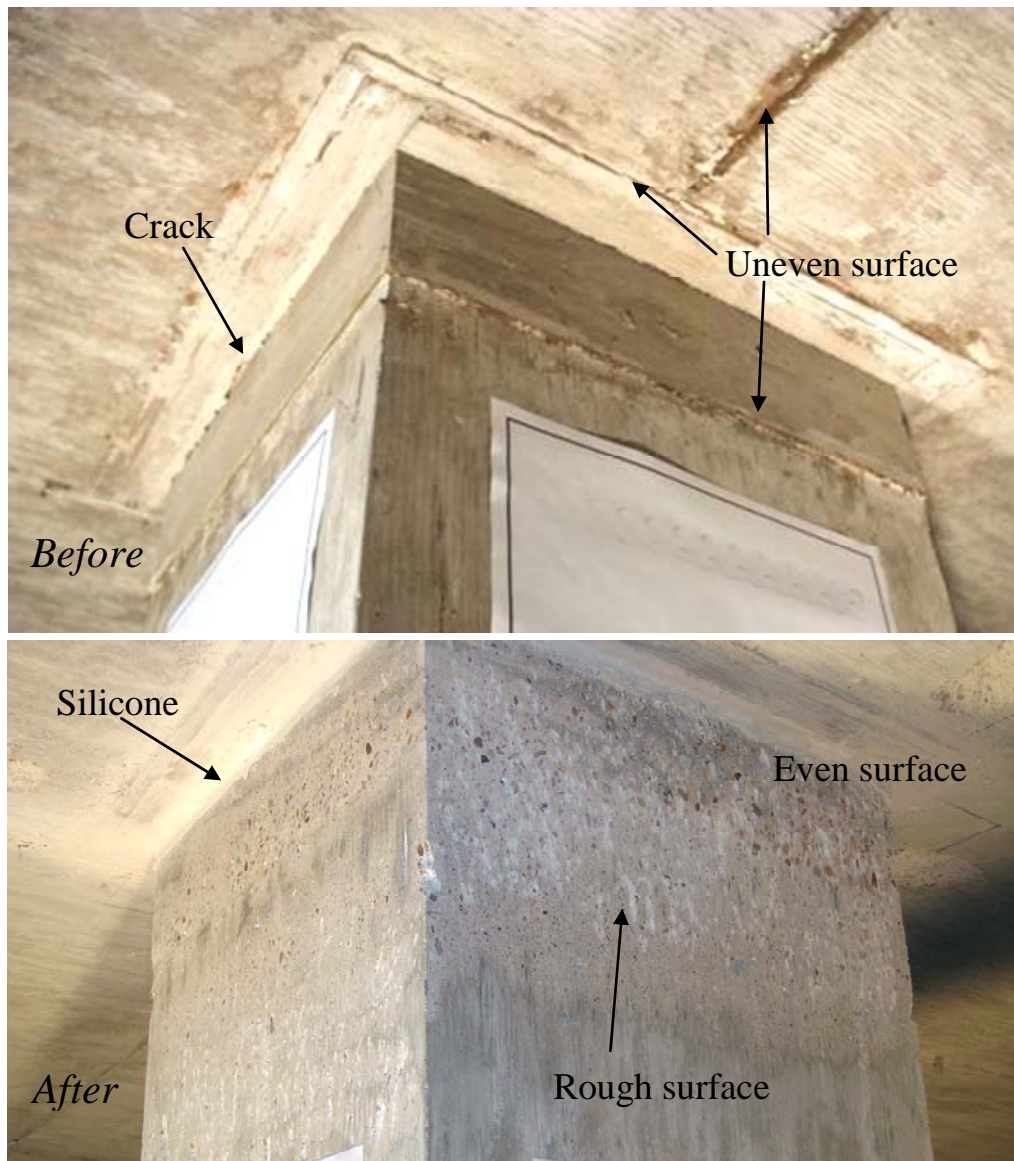


Figure 4.5 Concrete surface before and after preparation



Figure 4.6 Roughening the column surface

Installation of the collars (Figure 4.7) began by (i) hanging the shorter square tubes from the slab with threaded rods, (ii) applying a high consistency grout on the top surface of the tube, (iii) pressing the tube against the slab and against the column, and (iv) tightening the threaded rods from the top to fix the tube in position. After the two shorter tubes were installed (Figure 4.8), the longer tubes were installed in a similar manner. After one of the longer tubes was placed, two high-strength 1-in diameter threaded rods were inserted and the other longer tube was installed (Figure 4.9). After all square tubes were installed, the four high-strength threaded rods connecting the longer tubes were torqued to produce the shear-friction capacity needed. Then the angles supporting the shorter tubes were installed. The installation of the angles (Figure 4.10) involved (i) hanging

both angles by clamping them on the longer tubes and (ii) inserting the high-strength threaded rods and tightening them so that the two angles were fixed in their position. The steel shims and grout were then placed to fill gaps between the angles and the tubes or between the tubes and the slab (Figure 4.11). After installation of the collars was completed, the nuts on the $\frac{1}{4}$ -in threaded rods to hang the steel tubes during installation were loosened so that the rods did not act as shear reinforcement during the test.



Figure 4.7 Installation of the shorter steel tubes



Figure 4.8 After installation of the shorter steel tubes



Figure 4.9 Installation of the longer steel tubes



Figure 4.10 Installation of the angles



Figure 4.11 Gap fillers

Finally, the two-component of Tyfo S epoxy was prepared. 42.0 parts of component B was poured to 100 parts of component A (by volume). Both components were mixed thoroughly for five minutes with 600 RPM mixer (Figure 4.12). When both components were just mixed, the color was clear. After they had been mixed for a while, the color became whitish. Epoxy was then poured to fill cracks of the punching shear cone (due to a previous failure from the punching shear test) from the top surface (Figure 4.13). In room temperature, the epoxy could be poured within 15 minutes after both components had been mixed. Within that period, the epoxy was not viscous and its consistency was not different than that of water. After 15 minutes, the epoxy started to become more viscous and it could not be used to fill cracks.



Both components were just mixed (clear color)



Both components have been mixed for a while (whitish color)

Figure 4.12 Mixing epoxy



Figure 4.13 Pouring epoxy into cracks

4.3.3 Failure surfaces

4.3.3.1 RcG0.5

Figure 4.14 shows a significant vertical deflection after the punching shear failure of specimen RcG0.5. Figure 4.15 shows the punching shear failure surface before and after removal of delaminated concrete. The distance between the failure surface of RcG0.5 and the edges of the collars underneath the slab was about the same as the distance between the failure surface of G0.5 and the column face. Figure 4.16 shows that steel collars were effective in enlarging the critical shear perimeter because the punching cone intersected the bottom slab surface at the edges of steel collars. There was a circular cracking pattern away from the steel collars. Figure 4.17 shows that the angles of diagonal cracks of the punching cone with and without steel collars (RcG0.5 and G0.5) were about the same. Unlike a typical angle of punching cone that varies between 22° and 35° (Binici 2003), the angles of punching cone of RcG0.5 and G0.5 varied between 50° and 83° . These steep angles were quite similar to those of flexural-shear cracks in a beam. Figure 4.17 also shows that the punching cone intersected the top slab surface at the flexural reinforcement locations.



Figure 4.14 Significant vertical deflection at failure of RcG0.5

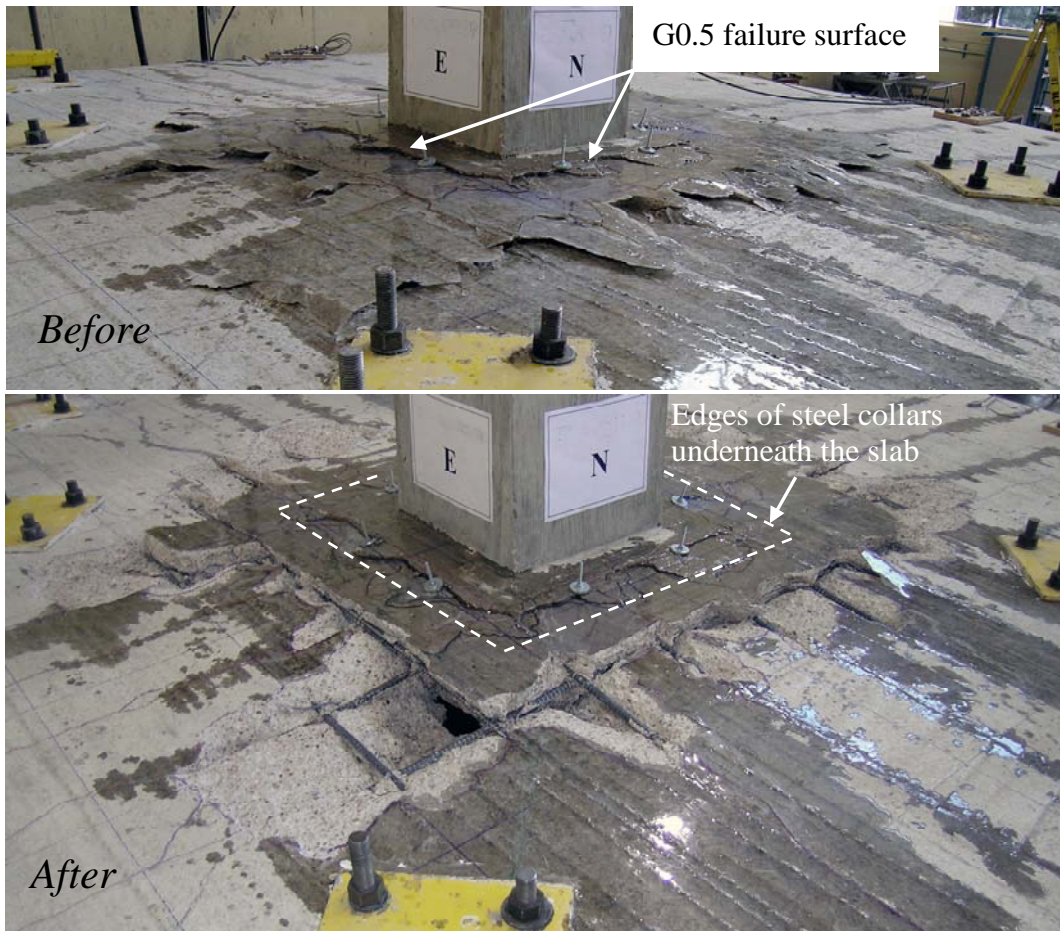


Figure 4.15 Top view of the failure surface of RcG0.5



Figure 4.16 Bottom view of the failure surface of RcG0.5

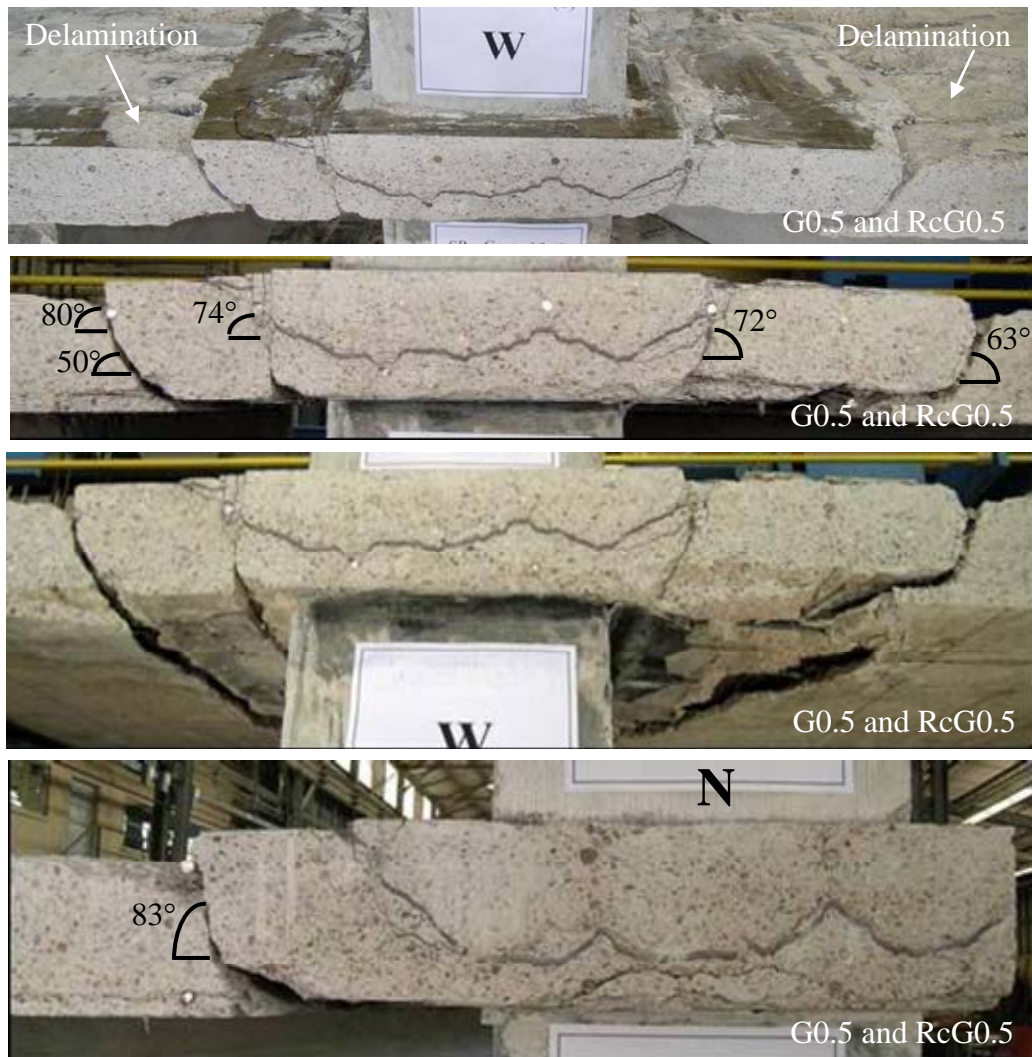


Figure 4.17 Angles of punching cones of G0.5 and RcG0.5

Figure 4.18 shows a close-up picture of the cracks filled with epoxy. The gravity driven (without a special injection method) epoxy filled the cracks effectively, with insignificant amounts of air voids.

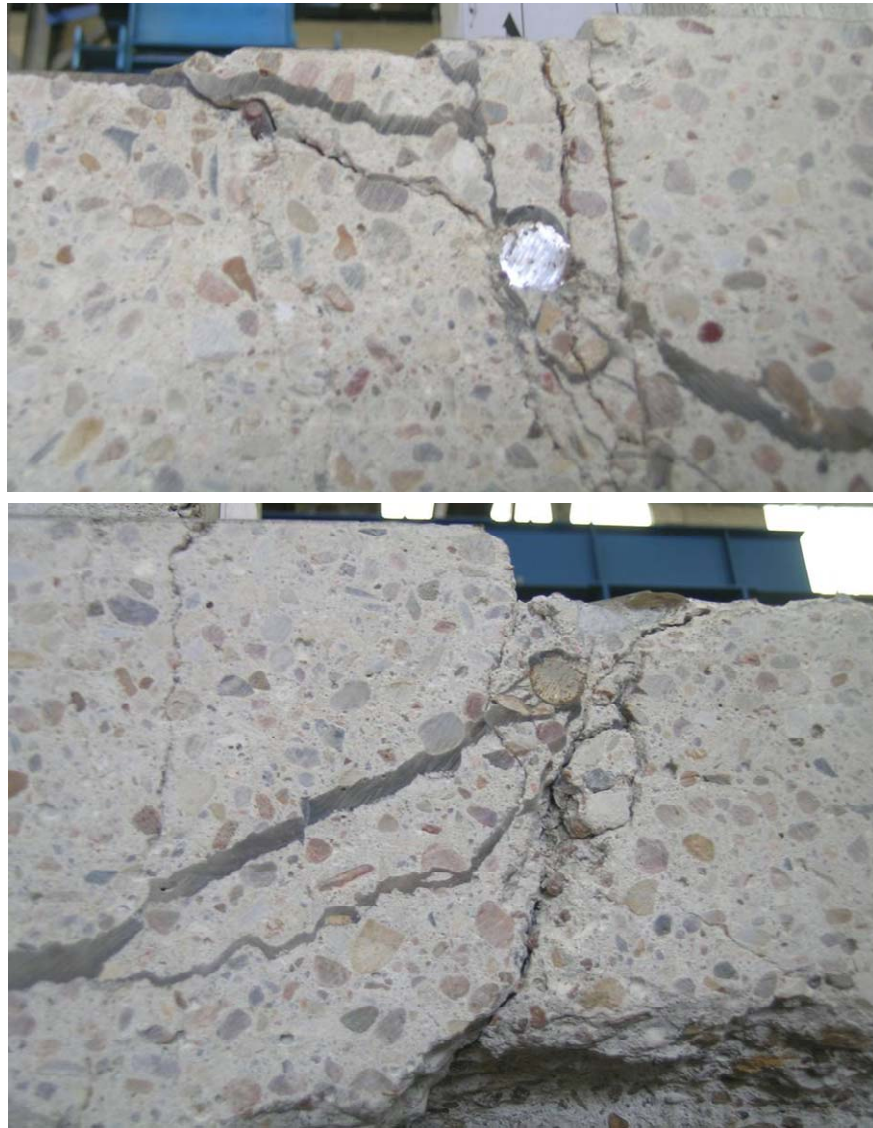


Figure 4.18 Cracks filled with epoxy

4.3.3.2 RcG1.0

Figure 4.19 shows punching shear failure surfaces before and after the removal of delaminated concrete. As in specimen RcG0.5, the steel collars were also effective to enlarge the critical shear perimeter of specimen RcG1.0. When it

was seen from the top slab surface, punching cone of specimen RcG1.0 looked larger than that of RcG0.5 (compare Figure 4.19 with Figure 4.15). Figure 4.20 shows punching shear failure surface on the bottom slab surface. Since the punching cone intersected the bottom slab surface at the same location as that in RcG0.5 (compare Figure 4.20 with Figure 4.16) and the punching cone of RcG1.0 looked larger from the top slab surface than that of RcG0.5, the angle of shear cracks forming the punching cone of specimen RcG1.0 must be smaller than that of RcG0.5. The fact that the punching cone of specimen with the concentration of flexural reinforcement (RcG1.0) was larger than that without the concentration of flexural reinforcement (RcG0.5) was consistent with the findings of McHarg et al. (2000) and Salna et al. (2004). As in specimen RcG0.5, the punching cone intersected the bottom slab surface at the edges of steel collars and there was a circular cracking pattern away from the steel collars.

Figure 4.21 shows that the angles of diagonal cracks of the punching cone with and without the collars (RcG1.0 and G1.0) were about the same, as was the case in RcG0.5. This suggests that the formation of the inclined cracks leading to a punching failure was the same for both the strengthened and the unstrengthened specimens (regardless of the percentage of top flexural reinforcement). The only difference was the location of the failure surface. The collars only shifted the failure surface away from the column and did not change the failure mechanism. Unlike in RcG0.5 and G0.5, the angles of punching cones of RcG1.0 and G1.0 (varied between 22° and 35°) were quite similar to Binici's observation (2003). It should be noted that Binici's specimens had 1.76% flexural reinforcement. These relatively small angles were quite similar to those in a typical punching shear failure.

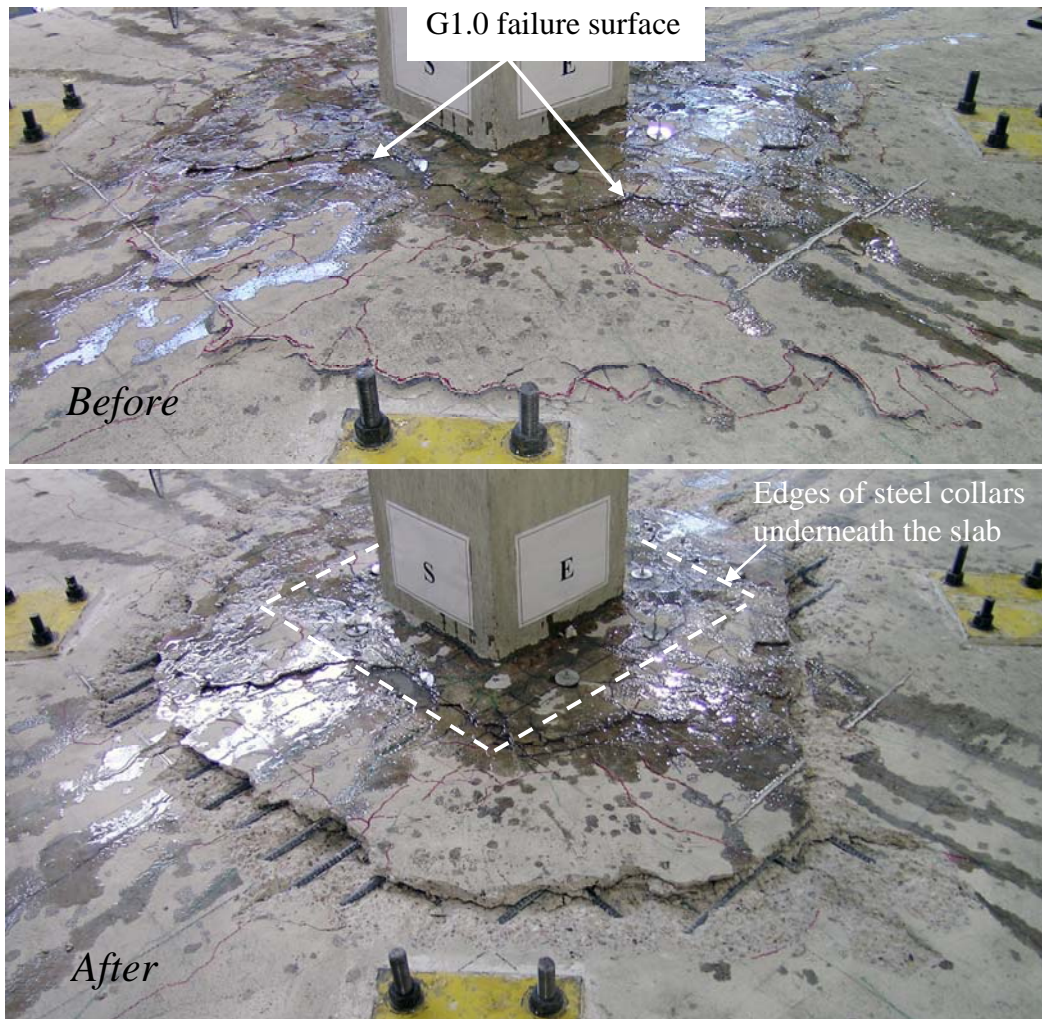


Figure 4.19 Top view of the failure surface of RcG1.0

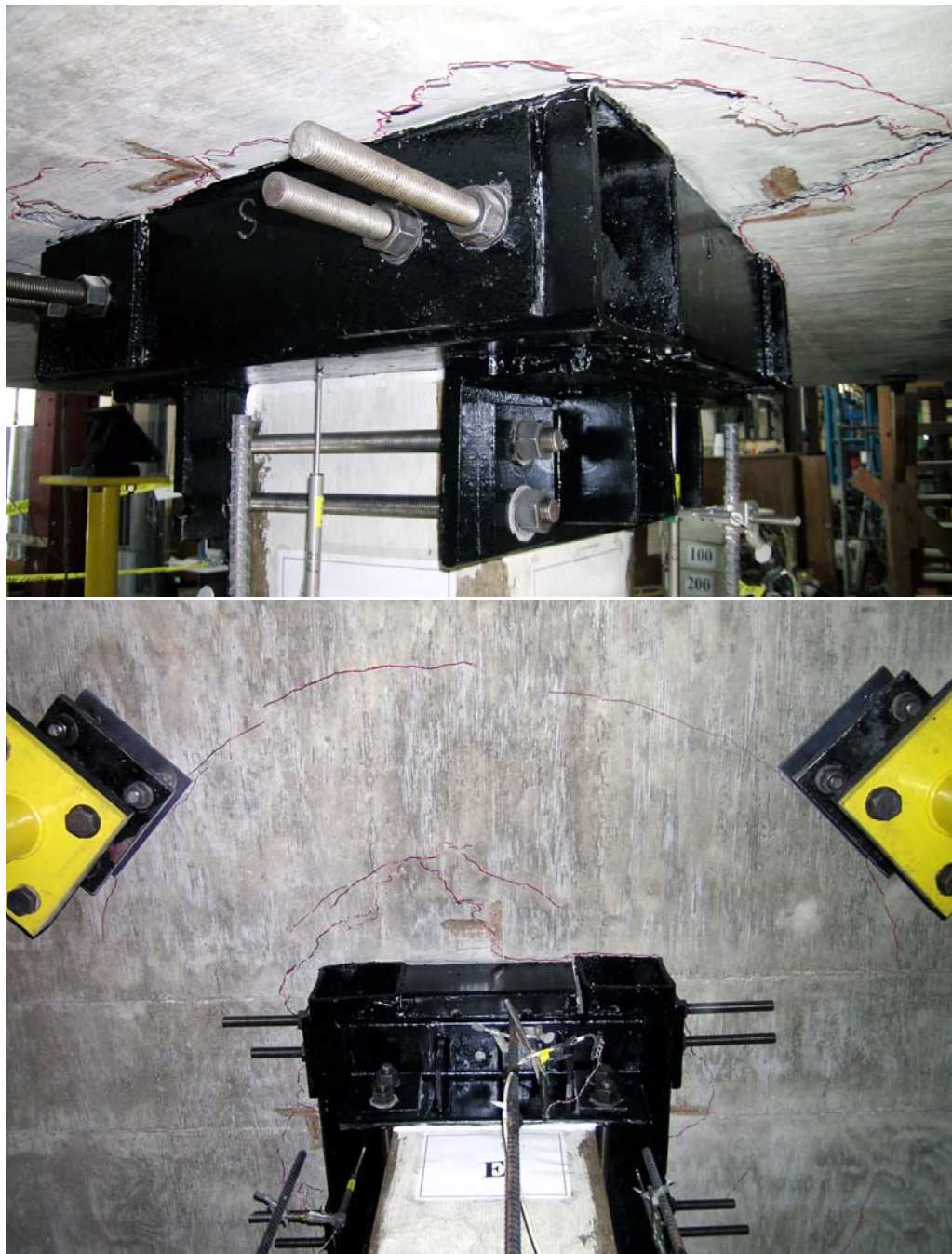


Figure 4.20 Bottom view of the failure surface of RcG1.0

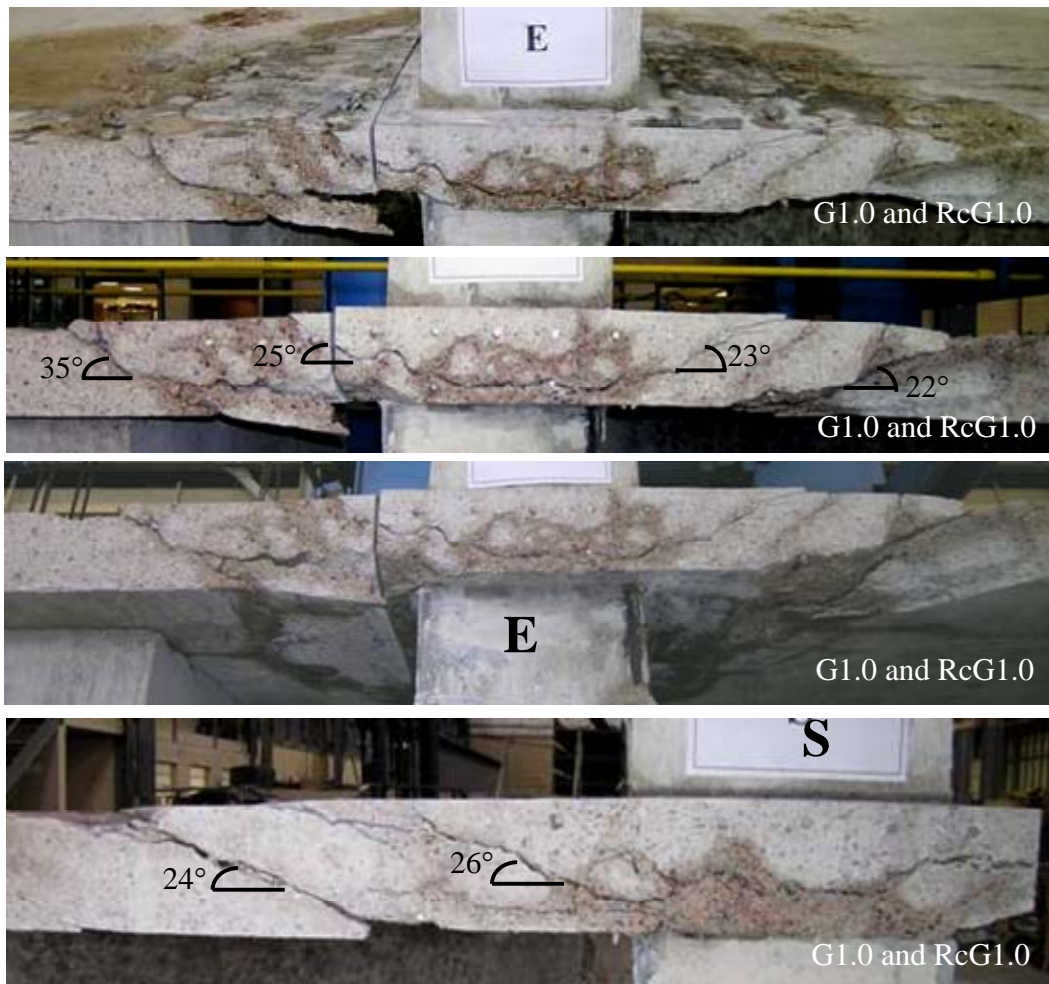


Figure 4.21 Angles of punching cones of G1.0 and RcG1.0

4.4 SPECIMEN L0.5

Before the application of cyclic lateral displacements in the North-South direction, a vertical load of 26.4 kips to produce the shear force of $1\sqrt{f'_c}b_o d$ (representing Dead Load (DL) + 25% Live Load (LL)) on the critical shear perimeter was applied to the column. The 26.4-kip vertical load included an additional 2.9 kips to counteract the weight of the column, part of the slab, and part of the horizontal actuator. While maintaining the vertical load, the specimen

was subjected to lateral displacement excursions shown in Figure 4.22. The lateral load versus drift response of L0.5 is shown in Figure 4.23. Lateral drift is defined as the horizontal displacement of the top of the upper column relative to the bottom of the lower column divided by the total length of 96 inches. The maximum lateral load was reached at 1.5% drift and the specimen failed in punching shear at 2% drift.

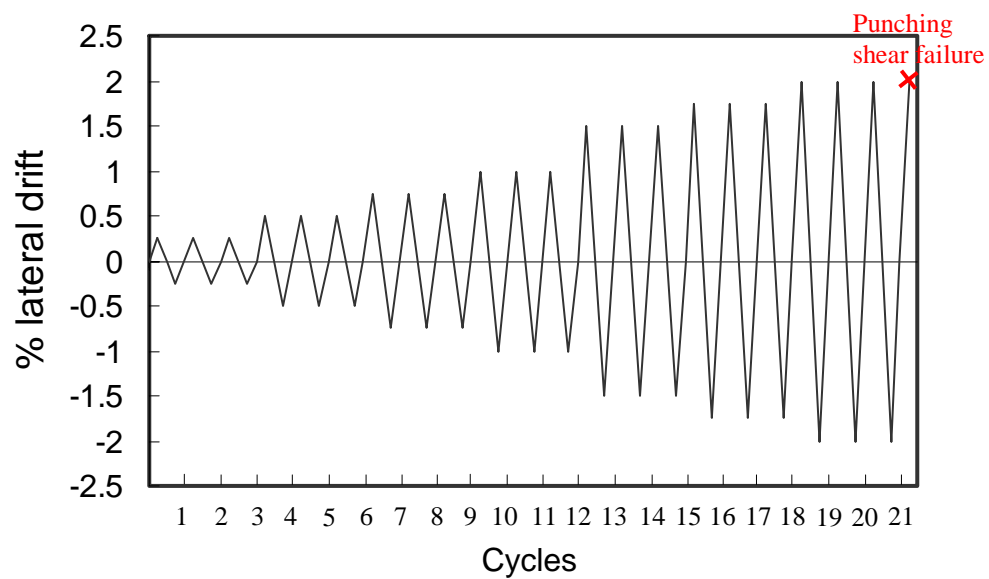


Figure 4.22 Lateral displacement excursions

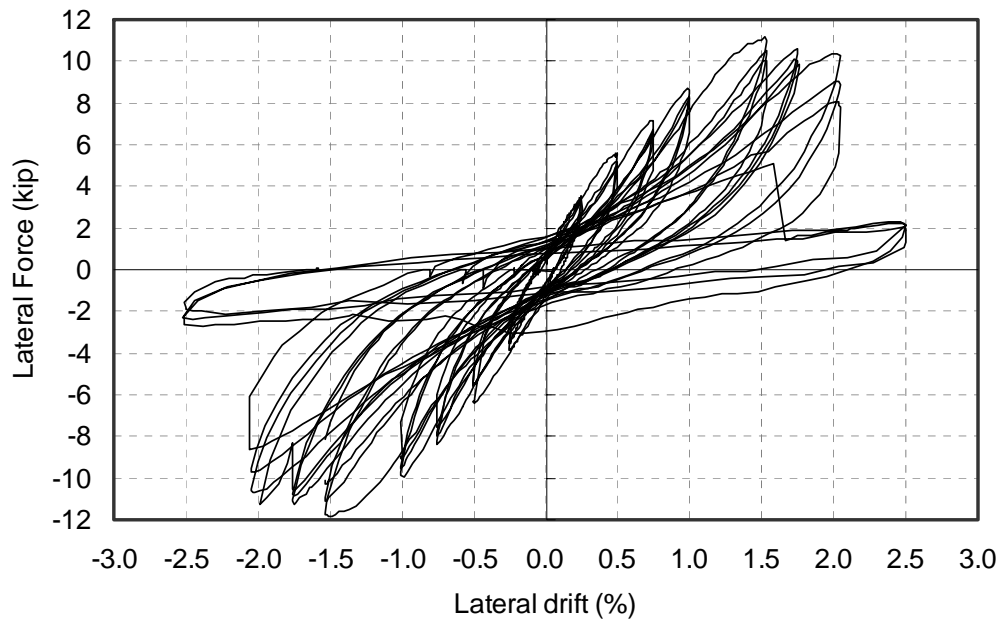


Figure 4.23 Lateral load versus drift response of L0.5

The fact that specimen L0.5 failed at a drift level that was larger than 1.5% was consistent with previous test results and recommendations related to gravity load effects on seismic behavior of flat-plate slab-column connections. Pan and Moehle (1989) indicated that to ensure a drift level of 1.5% prior to failure, the shear force on the critical shear perimeter must be limited to $1.5\sqrt{f'_c}b_o d$. Robertson and Durrani (1992) suggested that the shear force should be limited to $1.4\sqrt{f'_c}b_o d$ to assure a drift level of 1.5% prior to failure. However, the seismic performance of specimen L0.5 was questionable because it failed in punching shear at 2% drift. Megally and Ghali (2000) indicated that in order to satisfy the National Building Code of Canada NBCC95, the slab-column connections must be capable to undergo a drift ratio of at least 2% without the possibility of punching failure.

It is interesting to note that the specimen L0.5 failed in punching shear at 2% lateral drift, right at the limit of Megally and Ghali's (2000) conclusion and provisions of section 21.11.5 of ACI 318-05, which were added in the 2005 code to reduce the likelihood of slab punching shear failure. Megally and Ghali (2000) concluded that the slab-column connections without shear reinforcement can achieve 2% drift without punching failure only if V_u does not exceed $0.3V_c$. Section 21.11.5 of ACI 318-05 indicates that shear reinforcement is not required for slab-column connections if the design story drift ratio does not exceed the larger of 0.5% and $\left[0.035 - 0.05\left(\frac{V_u}{\phi V_c}\right)\right]$, where $\left(\frac{V_u}{\phi V_c}\right)$ is the ratio of the shear force V_u to the nominal shear strength ($V_c = 4\sqrt{f_c}'b_o d$) reduced by $\phi = 0.75$. In specimen L0.5, $\left(\frac{V_u}{\phi V_c}\right)$ was $0.3 \left(= \frac{0.92\sqrt{f_c}'b_o d}{(0.75)4\sqrt{f_c}'b_o d}\right)$. Therefore, the governing design story drift ratio was 2% ($= 0.035 - 0.05(0.3)$). Section 21.11.5 of ACI 318-05 indicates that the shear reinforcement is not required if the design story drift ratio does not exceed 2%. The test result showed that without shear reinforcement, specimen L0.5 failed in punching shear at 2% drift. Even though the test results indicate that specimen L0.5 was able to achieve 2% lateral drift without any shear reinforcement, the fact that failure occurred exactly at the 2% drift limit is of concern in regard to Chapter 21 provisions of ACI 318-05.

The maximum crack width on the top surface at 0.25%, 0.75%, 1.0%, 1.5%, and 2.0% lateral drift were 0.05", 0.07", 0.08", 0.12", and 0.25", respectively. At 0.75% lateral drift, diagonal cracks propagated to the edges of the specimen. Up to 1.0% drift, the cracks closed well when the lateral load was completely removed. At 1.5% drift, development of circular cracks (consisting of flexural and torsional cracks) around the column, which were parts of the

punching cone, was completed and a significant vertical displacement of the punching cone was observed. The first crack on the bottom surface was observed at 0.75% drift. At 2.0% lateral drift, concrete on the bottom surface of the slab started to spall. The crack pattern for each lateral drift level is shown in Appendix A.

The application of a gravity load of 26.4 kips (service loads) prior to the simulated seismic test caused flexural cracks that propagated from the column following the location of the top slab reinforcement. The presence of the cracks under service loads is in agreement with the observations of Stark (2003), Johnson and Robertson (2004), and with the typical cracks observed in flat-plate structures. However, Durrani et al. (1995) indicated that the test slab was uncracked under service gravity loads (DL + 30% LL, where LL = 50 psf and $\rho_{col.strip} = 0.59\%$).

Figures 4.24 and 4.25 show the top and the bottom failure surfaces at the end of the simulated seismic test. Significant torsional cracks and concrete spalling around the connection were observed. The observation of concrete spalling and exposure of reinforcing bars around the column were consistent with the failure surfaces observed in flat-plate structures after strong ground motions (Figures 1.7 and 1.10). Figure 4.26 shows the inclination of failure surface. Unlike a typical punching shear failure surface with the angle of punching cone varies between 22° and 35° (Binici 2003), the angle of punching cone of specimen L05 was very steep near the top surface. This suggests that the punching cone originated from flexural cracks that occurred at the location of reinforcing bars. As the punching shear failure surface propagated to the bottom surface of the slab, it turned toward the slab-column intersection. As those in specimens G0.5 and G1.0, the punching cone intersected the bottom slab surface at the slab-column intersection.

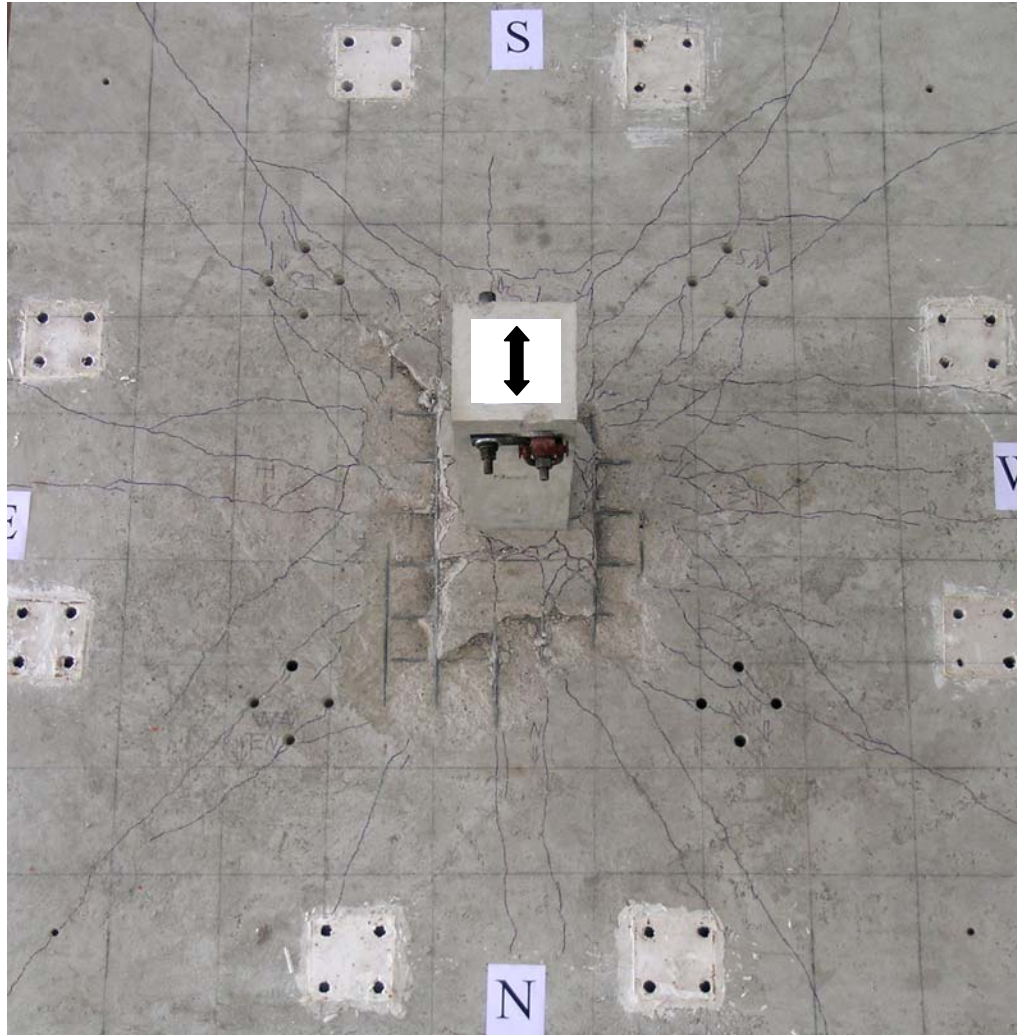


Figure 4.24 Top failure surface of L0.5



Figure 4.25 Bottom failure surface of L0.5

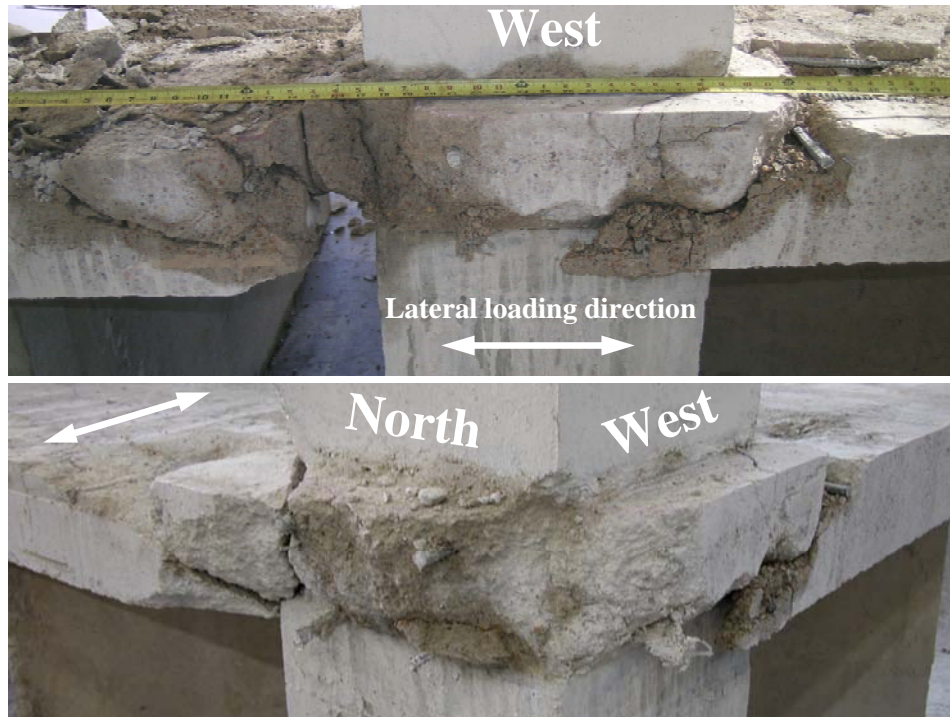


Figure 4.26 Punching cone of L0.5

Test results of and observation of damage in specimen L0.5 indicated that in order to produce considerable damage in connections without initiating failure, the connections could be safely subjected to 1.25% drift. For this reason, specimens LG0.5, LG1.0, LRstG0.5, and LRshG0.5 were loaded cyclically up to 1.25% drift before testing them under gradually increasing gravity loads, or repairing them.

4.5 SPECIMEN LG0.5

After subjected to reversed cyclic lateral displacements up to 1.25% drift, specimen LG0.5 was loaded to failure under gradually increasing gravity loads to study the two-way shear capacity of an earthquake-damaged connection. Figure

4.27 shows the typical damage at 1.25% drift. As can be observed in Figure 4.27, significant flexural and torsional cracks developed around the connection. The maximum crack width after the lateral load had been completely removed was 0.04 inches. The cracks penetrated through the entire slab thickness (water that was poured on the top surface dripped from the bottom surface). Figure 4.28 shows the failure surface after a punching shear test and diagonal cracks of punching cone on the faces that were parallel and perpendicular to the lateral loading direction.

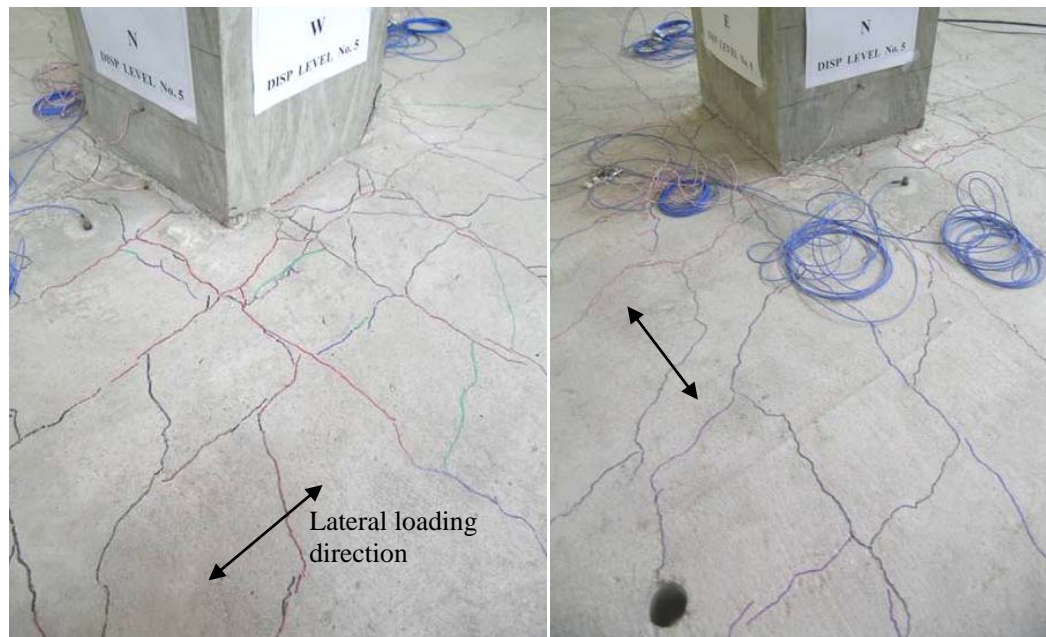


Figure 4.27 Damage in specimen LG0.5 at 1.25% drift

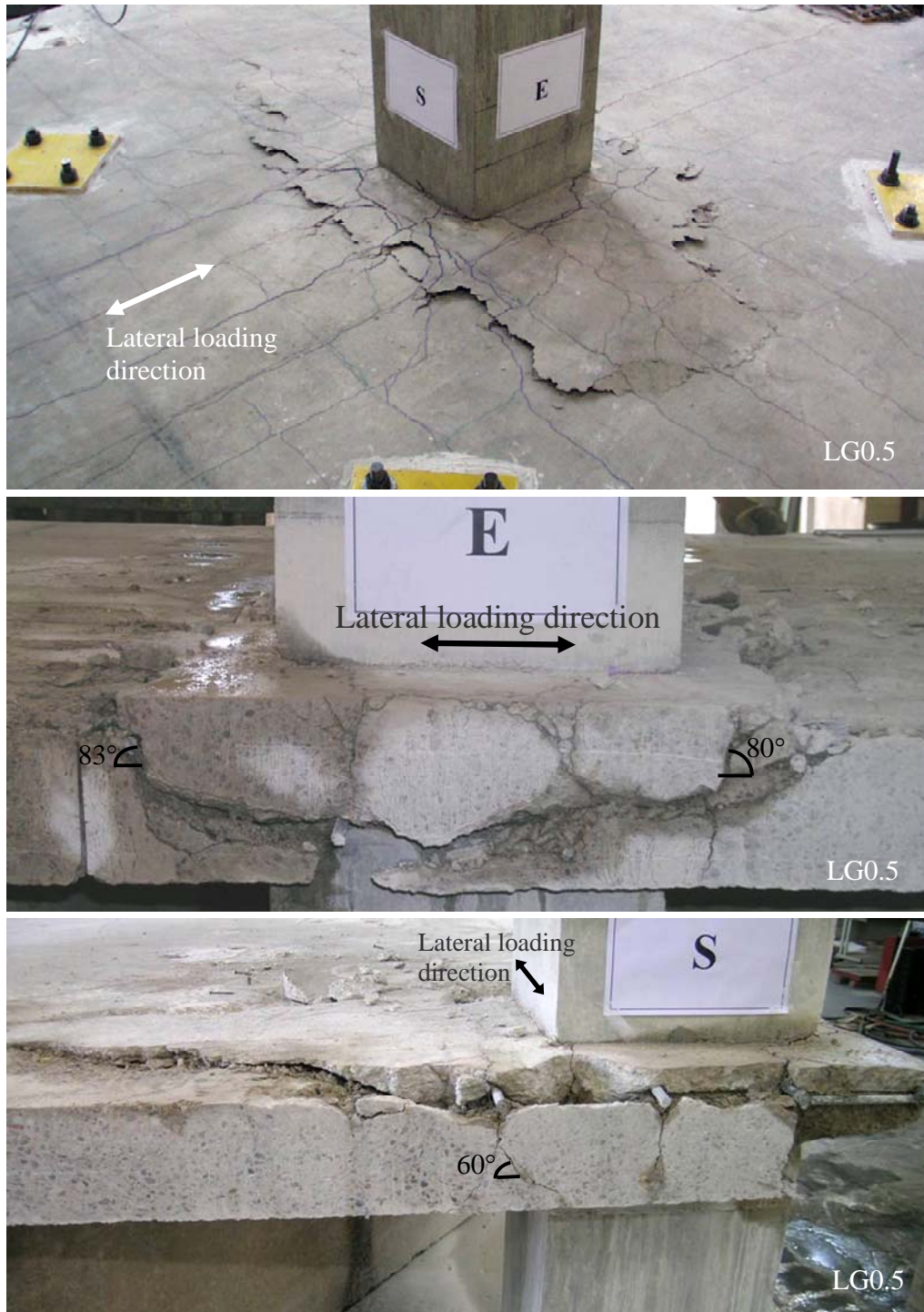


Figure 4.28 Failure surface after punching shear test

4.6 SPECIMEN LRSTG0.5

After (i) the specimen had been subjected to reversed cyclic lateral displacements up to 1.25% drift, (ii) the boundary conditions had been changed for a punching shear test, and (iii) the gravity load to produce a shear force on the critical shear perimeter of $1\sqrt{f'_c} b_o d$ had been applied and maintained, specimen LRstG0.5 was repaired.

4.6.1 Rehabilitation process

Specimen LRstG0.5 was repaired by installing external CFRP stirrups around the column (Figure 4.29). This rehabilitation technique was previously studied by Binici (2003). It is believed that the pattern of CFRP stirrups shown in Figure 4.29 helps to restore the continuity of the discontinuous bottom reinforcement. Stark (2003) also showed that connections strengthened using this pattern of CFRP stirrups experienced smaller damage under reversed cyclic loading compared with connections strengthened using other CFRP stirrup installation patterns.

In this research, the rehabilitation technique that was studied by Binici (2003) was extended in four ways:

- (i) The technique was applied to the connections damaged during simulated seismic loadings.
- (ii) Rehabilitation was performed in a more realistic manner by drilling holes while the slab still carried gravity loads corresponding to service loads.
- (iii) The stirrups were installed to a larger and more realistic specimen (with a monolithic column and more realistic boundary conditions).

(iv) Instead of applying the technique to slabs that were designed specifically to fail in punching shear and had unrealistically high flexural reinforcement ratios (e.g. 1.76%), in this research, the technique was applied to slabs with a low flexural reinforcement ratio (0.5%). This ratio is common in flat-plate structures built in the mid 20th century.

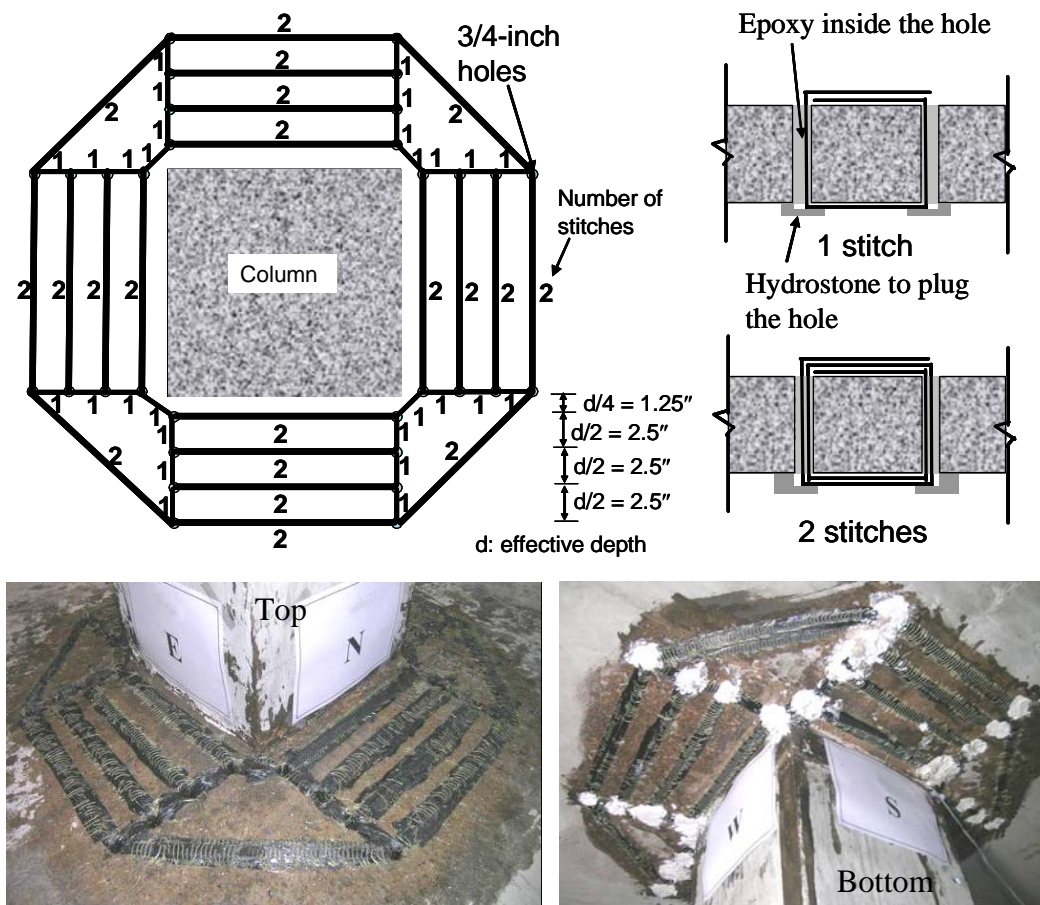


Figure 4.29 Externally installed CFRP stirrups

Figure 4.30 shows the surface preparation, which involved (i) locating the slab reinforcement using non-destructive testing, (ii) drilling 3/4–inch holes, (iii) grinding the slab surface, and (iv) chamfering the edge of the holes to minimize

stress concentrations. Figure 4.31 shows the concrete surface before and after grinding and chamfering. 0.75-inch wide CFRP strips were cut from a stock roll of CFRP fabric. Then, one end of the strip was inserted to a needle made from a rebar tie. The length of the rebar tie needle was about the same as the slab thickness. In order to intercept the shear crack and to prevent the failure inside the CFRP-reinforced zone, the first row of CFRP stirrups were located as close to the column face as possible ($d/4$ away from column face was the practical limit of drilling a hole). The other rows of CFRP stirrups were spaced at about $d/2$. The actual hole locations are discussed in the following section. After impregnated with epoxy and passed through a saturator to remove any excessive epoxy, the CFRP strips were stitched through the holes and wrapped around to form closed stirrups. The CFRP strips were stitched once, 1, or twice, 2, through each hole, as shown in Figure 4.29. CFRP overlaps at the top slab surface complied with the minimum CFRP to CFRP anchorage length of 6 inches, based on the test results reported by Binici (2003). After the completion of CFRP stirrup placement, the bottom of the vertical hole was plugged with hydrostone and the holes were filled with epoxy to avoid leaving any perforations in the slab that can affect its integrity.



Figure 4.30 Surface preparation

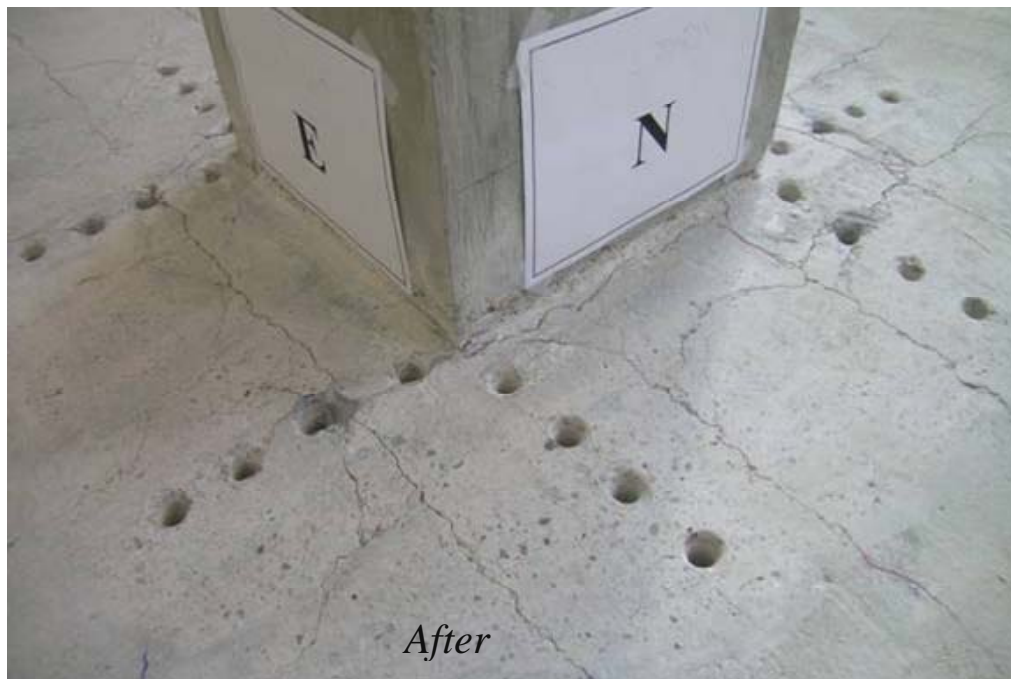
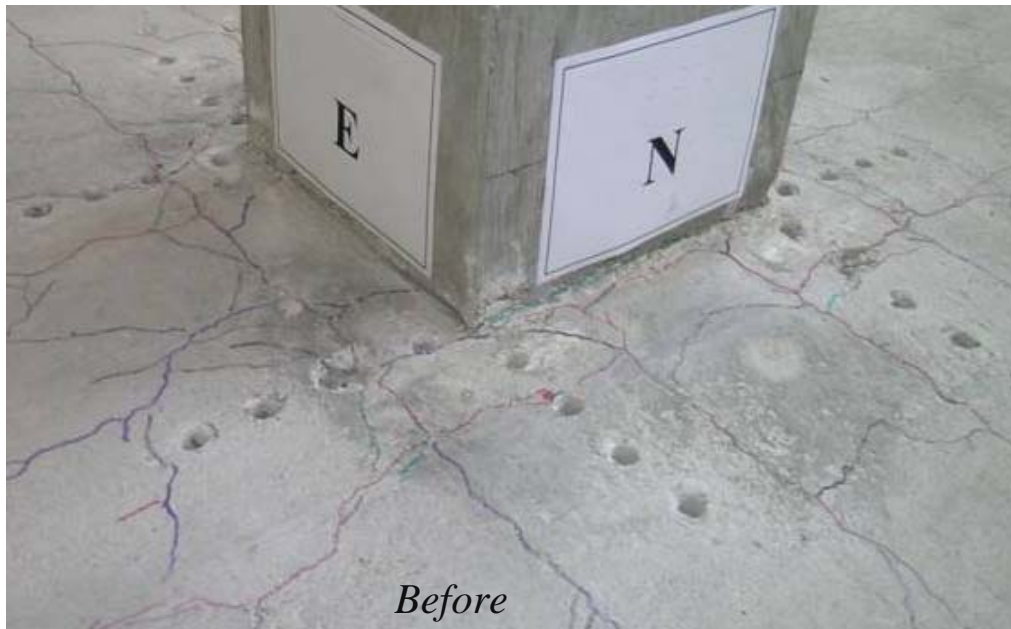


Figure 4.31 Concrete surface before and after grinding and chamfering

4.6.2 Actual hole locations and critical shear perimeter

As shown in Figure 4.29, the first row of CFRP stirrups was intended to be located at $d/4$ away from column face and the spacing of the other rows of CFRP stirrups was intended to be spaced at $d/2$. In order to avoid drilling through rebars, the actual hole locations varied as shown in Figure 4.32. The minimum and maximum actual distances between the first CFRP stirrups and the column face (“a” in Figure 4.32) were 1.5” ($d/4$) and 2” ($d/2.5$), respectively. The minimum and maximum actual spacings of the other rows of CFRP stirrups (“b” in Figure 4.32) were 2.4” ($d/2.1$) and 4.4” ($d/1.1$), respectively. Assuming that the last row of CFRP stirrups was located roughly 10 inches away from the column face and the critical shear perimeter b_o is located at $d/2$ away from the outermost CFRP stirrups, b_o can be calculated as 135 inches ($b_o = 4(16) + 4\{(10 + 5/2)\sqrt{2}\} = 135$). It should be noted this b_o was about the same as that of the specimens rehabilitated with the steel collars, which was 148 inches.

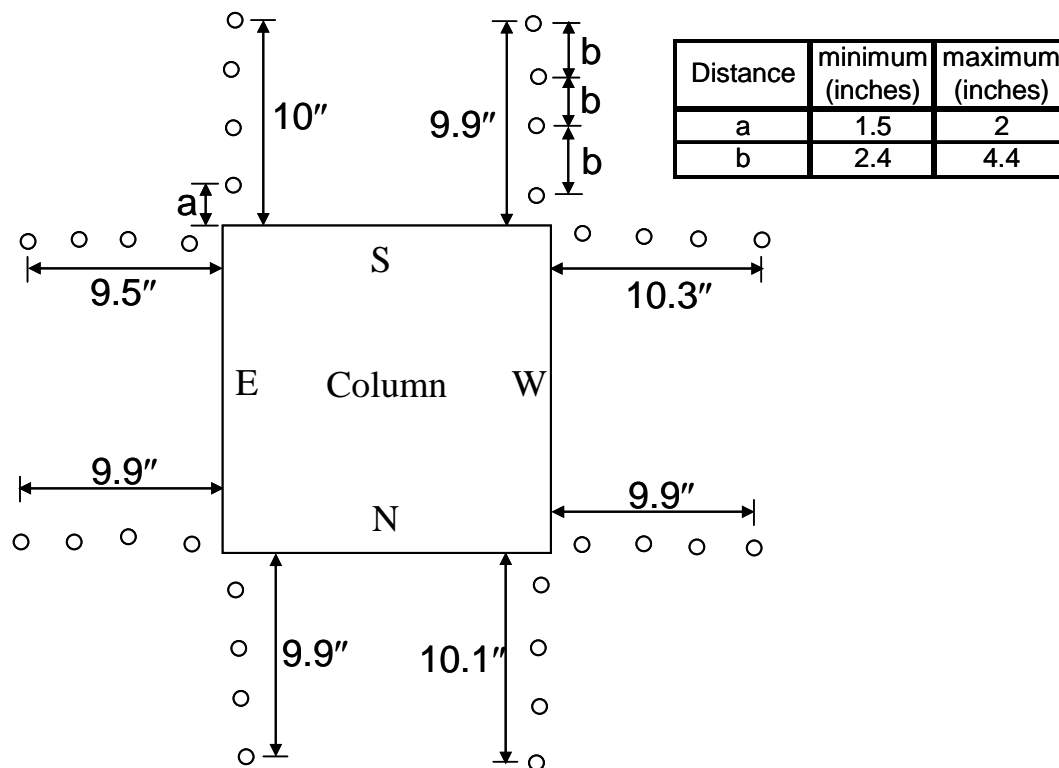


Figure 4.32 Actual hole locations

4.6.3 Failure surface

Figure 4.33 shows that specimen LRstG0.5 exhibited a significant vertical displacement at failure. This indicates that the externally installed CFRP stirrups increased ductility of the connection. Figure 4.34 shows the top and bottom failure surfaces. It can be seen that the tightly knit array of CFRP stirrups was effective in shifting the failure surface away from the shear reinforced zone and thus, increasing the critical shear perimeter. Figure 4.35 shows the failure surface after the specimen LRstG0.5 was saw-cut. Even though there were many flexural cracks within the shear reinforced zone due to the simulated seismic test, the punching cone formed outside the shear reinforced zone. This indicates that the tightly knit array of CFRP stirrups was also effective to restore the continuity of

seismic-damaged region. The angle of the punching cone on the face parallel to the direction of lateral loading was much steeper than that on the face perpendicular to the lateral loading. This indicates that the punching cone on the face parallel to the lateral loading originated from flexural cracks that formed during the simulated seismic test, just as in specimen LG0.5. With the presence of CFRP stirrups, the final punching cone formed away from the column. The angle of the punching cone on the face perpendicular to the lateral loading was 38° , which was somewhat steeper than the average angle observed by Binici (2003). As McHarg et al. (2000) and Salna et al. (2004) pointed out, the increase of the amount of slab flexural reinforcement reduced the angle of the shear cracks forming the punching cone. Specimen LRstG0.5 had only 0.5% of steel and shallower shear cracks as opposed to 1.76% reinforcement ratio and steeper shear cracks seen in Binici's specimens.

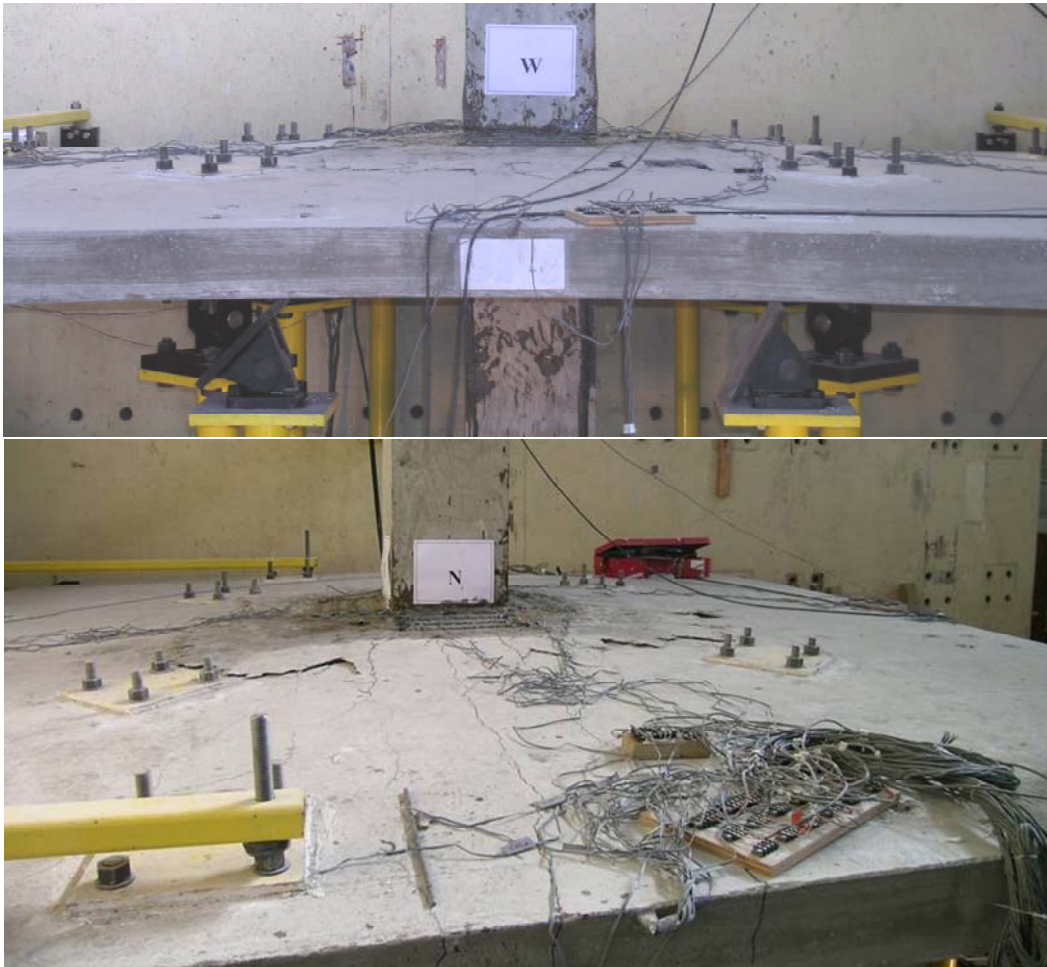


Figure 4.33 Significant vertical displacement at failure of LRstG0.5



Figure 4.34 Failure surfaces of LRstG0.5



Figure 4.35 Failure surface of LRstG0.5

4.7 LRSHG0.5

After (i) the specimen had been subjected to reversed cyclic lateral displacements up to 1.25% drift, (ii) the boundary conditions had been changed for a punching shear test, and (iii) the gravity load to produce a shear force on the critical shear perimeter of $1\sqrt{f'_c} b_o d$ had been applied and maintained, specimen LRstG0.5 was repaired.

4.7.1 Rehabilitation process

Specimen LRshG0.5 was repaired by applying 12-in wide sheets of CFRP around the column, on the tension slab surface to increase the flexural capacity of the slab that had only 0.5% steel within the $(c+3h)$ critical section. The flexural

strengthening was chosen because in slab-column connections with 0.5% reinforcement ratio within $(c+3h)$ region, the flexural failure was more likely to occur over the punching shear failure (Marzouk and Hussein 1991). The test results of specimen G0.5 were also consistent with Marzouk and Hussein's findings. Since 1.0% reinforcement ratio is typical in a modern slab-column connection and the flexural failure is less likely to govern in the connection with 1.0% reinforcement ratio, the amount of CFRP sheets was selected to produce the same flexural capacity within $(c+3h)$ region as that of the connection with 1.0% steel. The sheets were applied in 12-inch wide by 88-inch long strips on all four sides of the column. The 12-inch width was selected for convenience because it was half of the total width of the roll of CFRP sheet. The first layer of CFRP sheets were applied in the direction of lateral loading (North-South direction).

CFRP sheets were applied only on the top slab surface because the application of CFRP fabric on the bottom surface of the slab in the connection region did not improve the connection performance (Robertson and Johnson 2001, 2004). Since Ospina et al. (2001) showed that the strain profile on CFRP sheets that were placed closer to the column was steeper than those further away from the column, it is believed that the closer to the column the CFRP sheets were, the more effective they became. For this reason, the CFRP sheets in specimen LRshG0.5 were placed against the column (similar to those in specimen ER2-CS1 of Ospina et al. 2001).

In addition, anchors were used to anchor CFRP sheets because previous researchers found that the effectiveness of CFRP sheets for strengthening the connection was highly dependent on the ability to prevent early delamination (Ebead and Marzouk 2004). Without any mechanical anchors, CFRP sheets delaminated at failure and became ineffective at low strains (Erki and Heffernan 1995, Chen and Li 2000, Tan 2000, Ospina et al. 2001, Ebead and Marzouk

2004). Casadei et al. (2003) found that anchors prevented premature debonding of the CFRP sheets. Since Casadei et al.'s anchors (which were only 1-in deep) pulled out, deeper anchors ($4\frac{1}{2}$ -in deep, which was roughly equal to the effective depth of the slab) were used in specimen LRshG0.5.

Figure 4.36 shows the surface preparation before CFRP sheet installation, which involved (i) grinding the concrete surface where the CFRP sheets were placed, (ii) drilling four holes ($\frac{3}{4}$ -inch diameter and $4\frac{1}{2}$ -inch deep) at each corner of the column so that CFRP anchors could be inserted, (iii) chamfering the edges of the holes to minimize stress concentrations, and (iv) cleaning the concrete surface. Concrete surface before and after the surface preparation are shown in Figure 4.37. Since the cracks around the column (due to reversed cyclic lateral displacements up to 1.25%) penetrated through the entire slab depth, the bottom surface of the slab was sealed with silicone as shown in Figure 4.38. The rehabilitation was then continued (Figure 4.39) with (v) pouring epoxy into cracks and holes, (vi) coating the concrete surface with the epoxy using a paint roller, (vii) inserting the epoxy-impregnated CFRP sheet into a saturator to remove excessive epoxy, (viii) placing the sheets on the concrete surface and rolling the sheets with a paint roller to avoid any wrinkles and to remove air pockets below the sheets.

After all CFRP sheets had been placed, the CFRP anchors were prepared and installed as shown in Figure 4.40. The total area of all CFRP anchors was equal to the total area of the CFRP sheets to be anchored. It is important to recognize that the CFRP anchors must be installed right after CFRP sheets have been placed (before the epoxy is cured) so that both CFRP anchors and sheets can act as a system. Preparing and installing CFRP anchors involved (i) cutting a small piece of CFRP sheet (in this repair: $3''\times 15''$), (ii) inserting the sheet into a

needle (made of a rebar tie) and spreading the fibers at both ends, (iii) impregnating the anchors in epoxy, (iv) making a hole in the CFRP sheet so that the anchor could be inserted, (v) folding the anchor and inserting it into the hole until the bottom of the hole was reached, (vi) after the needle end touched the bottom of the hole, splaying the protruding end of the anchor over the CFRP sheets, and (vii) applying even pressure in an outward motion where the anchors were installed to remove air voids and to ensure good bond between the anchors and the CFRP sheets. Figure 4.41 shows the top surface of the slab at the completion of CFRP sheet application.



Figure 4.36 Surface preparation before the application of CFRP sheets

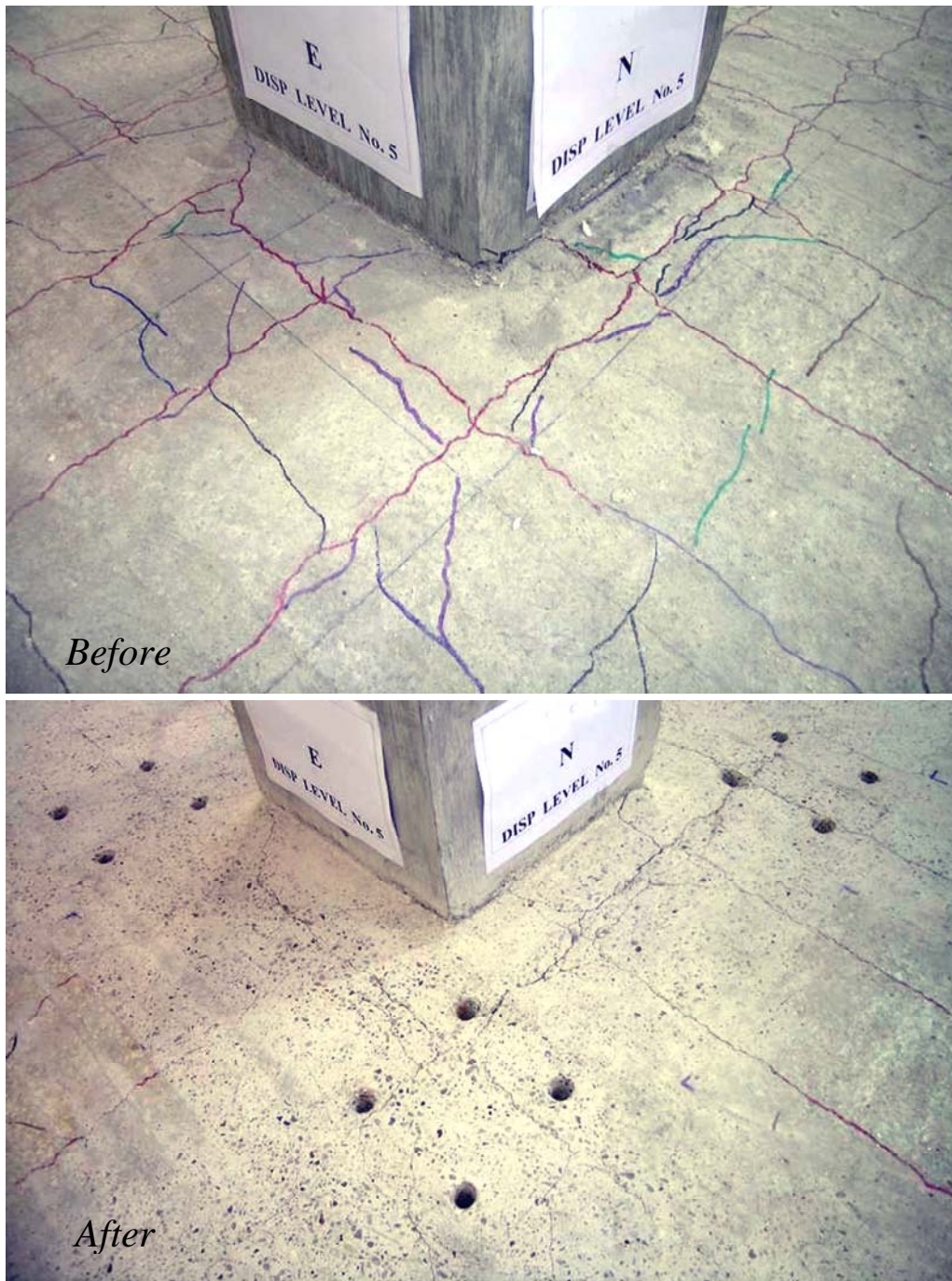


Figure 4.37 Concrete surfaces before and after surface preparation



Figure 4.38 Cracks were sealed with silicone



Figure 4.39 Installation of CFRP sheets

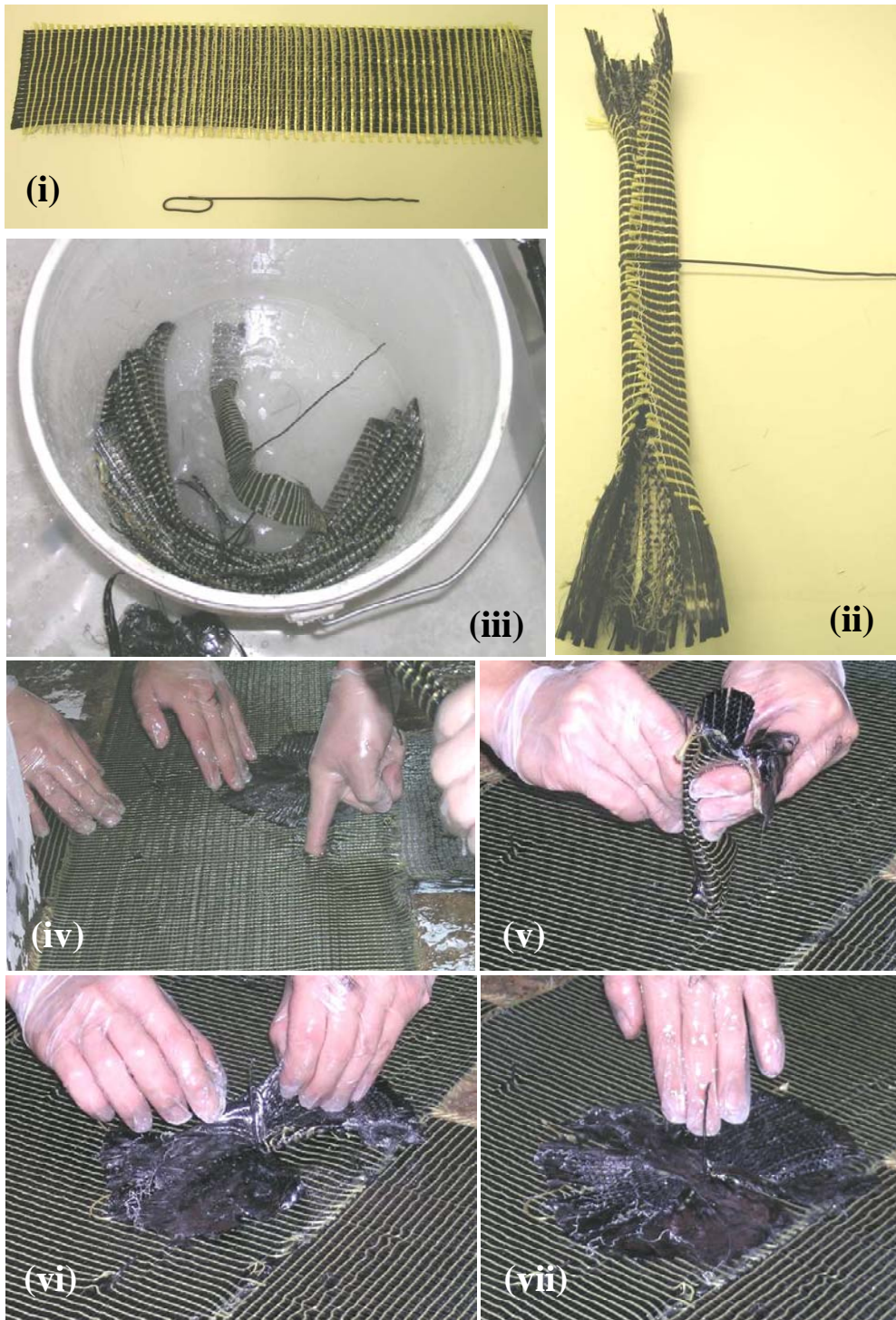


Figure 4.40 Preparation and installation of CFRP anchors



Figure 4.41 After installation of CFRP sheets and CFRP anchors

4.7.2 CFRP strain

Figures 4.42 and 4.43 show the variation of strain along the CFRP sheets installed in the E-W direction and across the width of CFRP sheets installed in the N-S direction, respectively, at different levels of gravity loads V . The solid lines and the dashed lines indicate the strain profile before and after the maximum gravity load V_{max} was reached, respectively.

Figure 4.42 shows that the strain of CFRP sheets in the region beyond the location of the anchors were generally low (less than 0.001) for all levels of gravity loads. This indicates that extending the sheets 36 inches away from the column face was not necessary. The CFRP sheets may be terminated about 12 inches beyond the location of the last anchors. At the maximum load, the strains were generally less than 0.004. Since CFRP sheets ruptured at failure, it is believed that the earthquake-damage caused stress concentration on CFRP sheets. After the maximum load was reached and punching cone formed (punching shear failure occurred), the well-anchored CFRP sheets started to act as tension bands (catenary action) and allowed the slab to carry substantial loads through larger deformations. For this reason, the strain of CFRP sheet in the middle of four anchors increased significantly after punching shear failure. Figure 4.43 shows that the strain was generally uniform across the width of CFRP sheets prior to punching shear failure. This indicates that the 12-in wide sheet was fully effective in resisting the load.

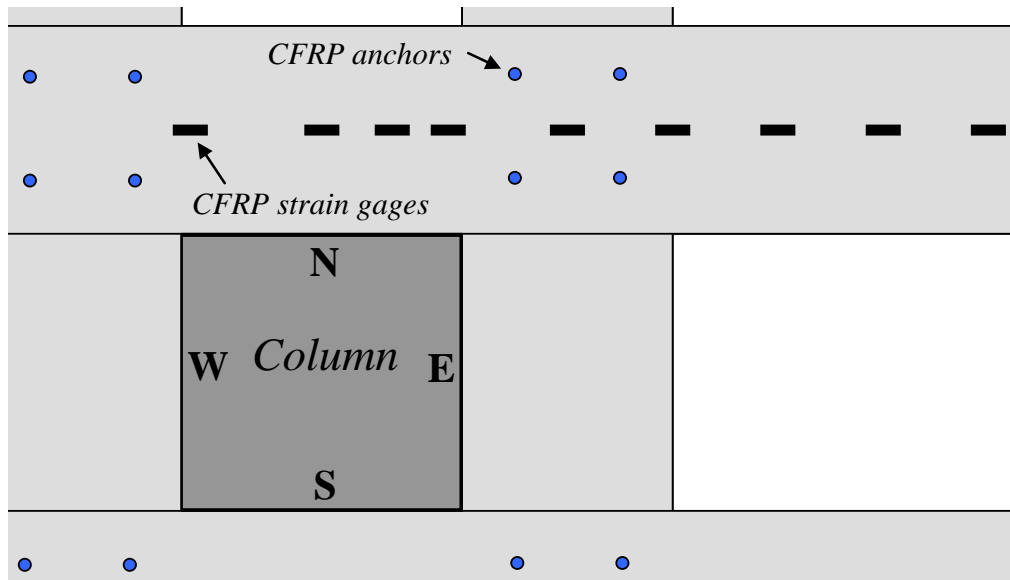
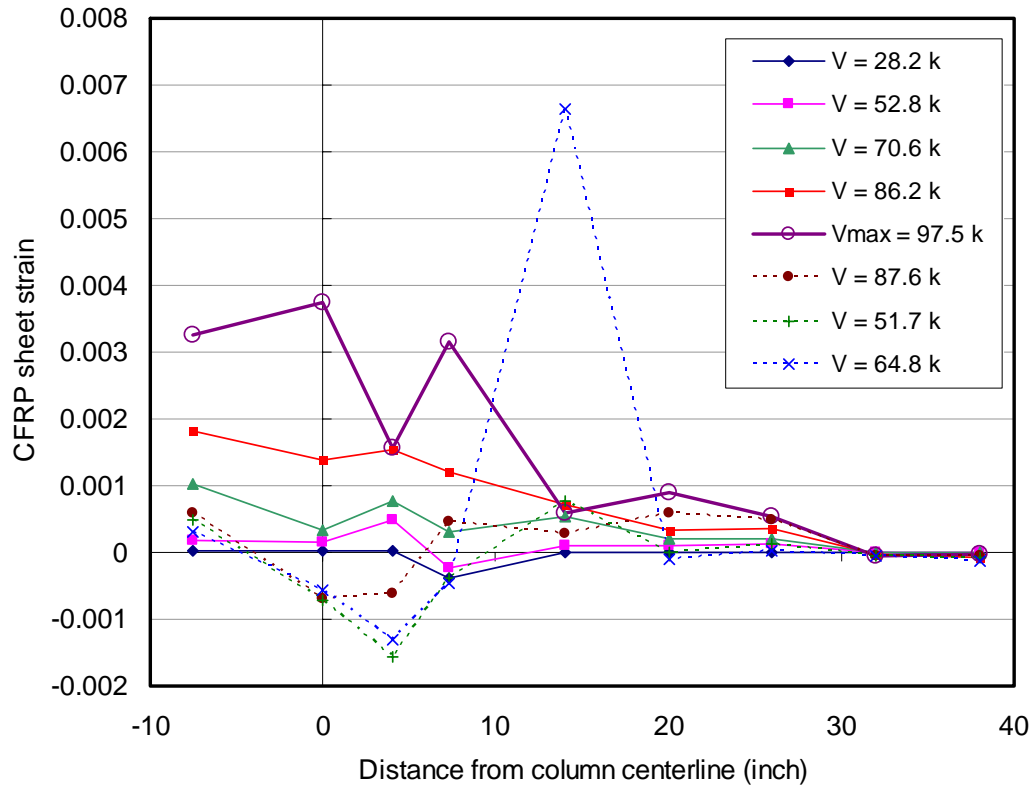


Figure 4.42 CFRP strain profile along the West-East sheet

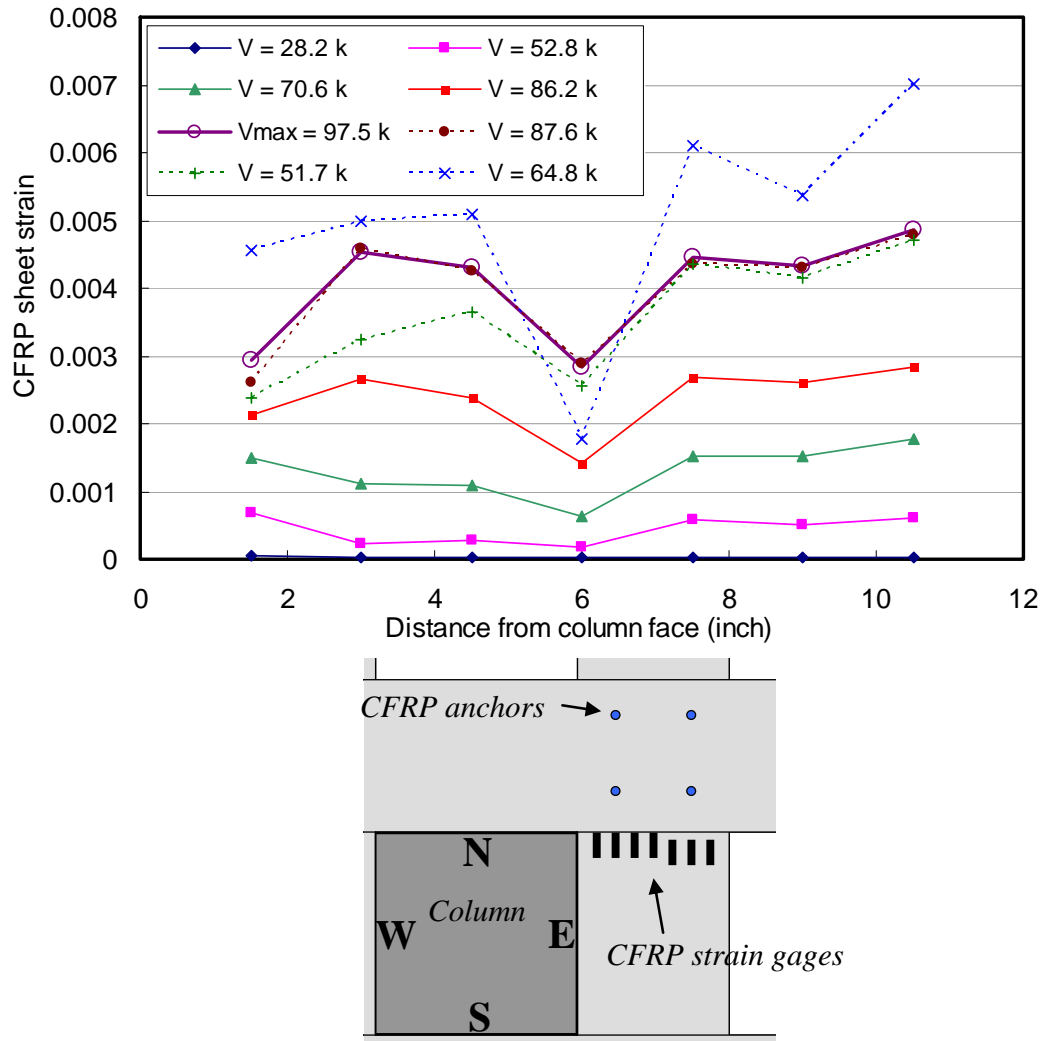


Figure 4.43 CFRP strain profile across the North-South sheet

4.7.3 Failure surface

Figure 4.44 shows the top failure surface. It can be seen that at failure, both CFRP sheets running in E-W direction (installed on the top of the sheets running in N-S direction) ruptured in the middle of column face. The rupture of the CFRP sheets indicated that the rehabilitation method was very effective since

the full capacity of CFRP sheets was utilized and showed the superior performance of CFRP anchors. As previous researchers found, without anchors, CFRP sheets always delaminate at relatively low strains.

Figure 4.45 shows the CFRP anchors at failure. The yellow dashed line in Figure 4.45 illustrates the failure surface underneath the CFRP sheets. As Erki and Heffernan (1995) observed, the differential vertical displacement of punching cone tried to pry the CFRP sheets off the tension slab surface. However, the CFRP anchors prevented delamination of CFRP sheets and permitted the CFRP sheets to act as tension bands, shown in Figure 4.45, and allowed the slab to carry substantial loads after punching shear failure.

Figure 4.46 shows the bottom failure surface. The diagonal shear cracks intersected the bottom slab surface right at the slab-column intersection, indicating that the presence of CFRP sheets did not change the location of failure surface. This observation was consistent with previous findings (Harajli and Soudki 2003).

Figure 4.47 shows the punching cone after slab was saw-cut. Both Figures 4.45 and 4.47 clearly show that at each column corner, one CFRP anchor closest to the column corner moved up with the punching cone, where the other three other anchors were still attached to the rest of the slab. For this reason, the use and positioning of four anchors per column corner was very effective. Punching shear cracks on the South side looked quite similar to a typical punching shear crack, whereas the cracks on the East side looked quite similar to those commonly seen at flexural failures (steep angles). The fact that the punching shear cracks of the specimen LRstG0.5 on the South side (perpendicular to the direction of lateral loading) looked more similar to those of the specimen G1.0 (Figure 4.21) than to those of the specimen G0.5 indicates that adding external CFRP sheets was as effective as adding more reinforcing bars. The cracks on the East side looked

quite similar to those of the specimen LG0.5 (Figure 4.28) supports the opinion that the external CFRP sheets did not change the location of the failure surface. Figure 4.48 shows the anchor after it was removed from the slab. The anchor was relatively undamaged, indicating that it did not act as shear reinforcement (it did not intersect punching shear cracks).



Figure 4.44 Top view of failure surface of LRshG0.5

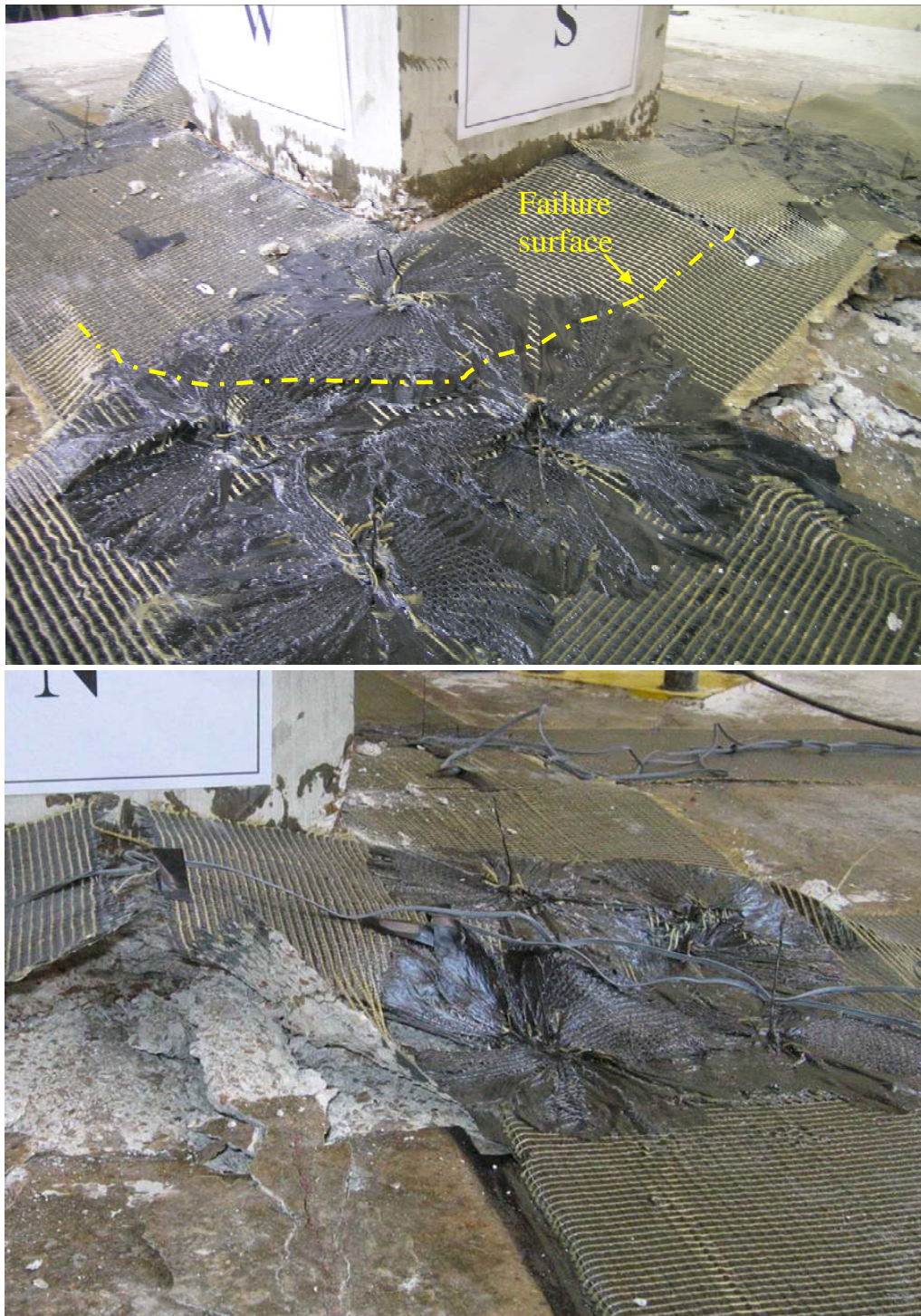


Figure 4.45 Close-up view of CFRP anchors at failure



Figure 4.46 Bottom view of failure surface of LRshG0.5

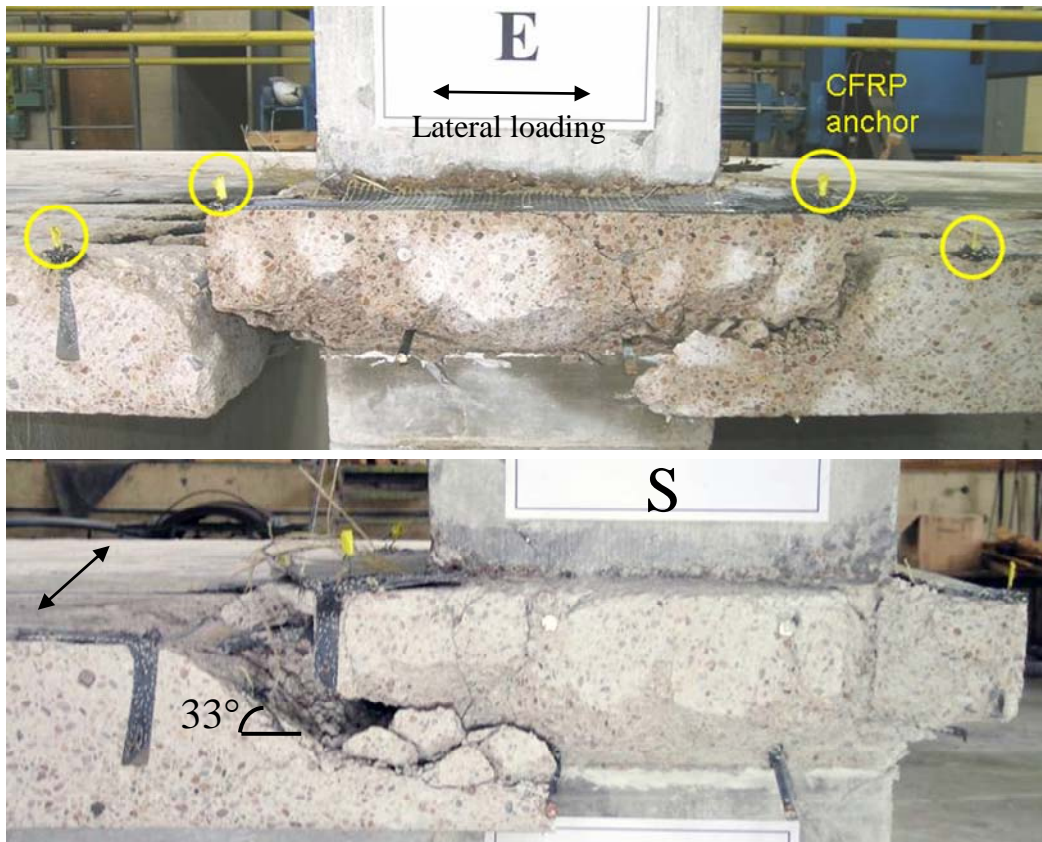


Figure 4.47 Failure surface of LRshG0.5



Figure 4.48 CFRP anchor

4.8 SPECIMEN LG1.0

After being subjected to reversed cyclic lateral displacements up to 1.25% drift, specimen LG1.0 was loaded to failure under gradually increasing gravity loads to study the two-way shear capacity of a connection that had seismic damage. Figure 4.49 shows damage at 1.25% drift. First cracks on the bottom slab surface were observed at 0.5% drift. In simulated seismic tests of specimens with 0.5% flexural reinforcement within the $(c+3h)$ region, the first cracks on the bottom surface were observed at 0.75% drift. An earlier occurrence of cracks on the bottom slab surface of specimen LG1.0 was expected because its bottom mat flexural reinforcement was relatively weaker with respect to the top mat than those of specimens with 0.5% flexural reinforcement within the $(c+3h)$ region. The maximum crack width after the removal of the lateral load corresponding to 1.25% lateral drift was 0.013 inches, only about a quarter of that measured in connections with 0.5% flexural reinforcement within the $(c+3h)$ region. A comparison of Figure 4.49 with Figure 4.27 shows that cracks were better distributed around connection with a larger amount (1.0%) of flexural reinforcement. Figure 4.50 shows the top and bottom failure surfaces after a punching shear test. The punching cone intersected the bottom slab surface right at the slab-column intersection, similar to that observed in specimen LG0.5.

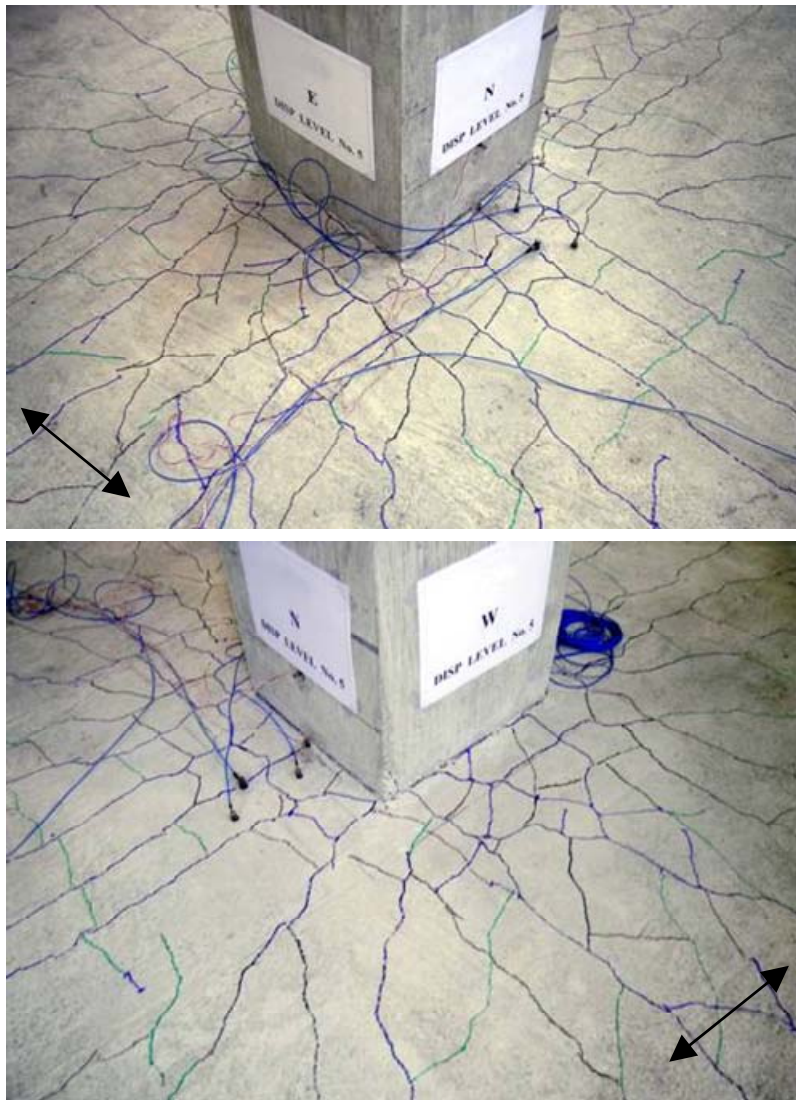


Figure 4.49 Damage in specimen LG1.0 at 1.25% drift

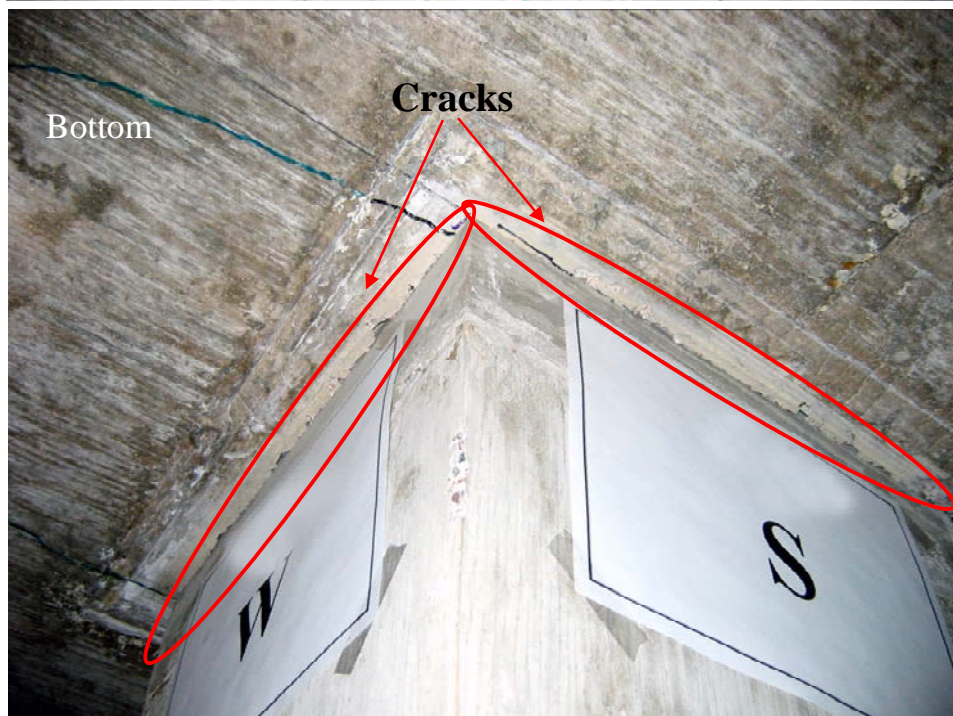
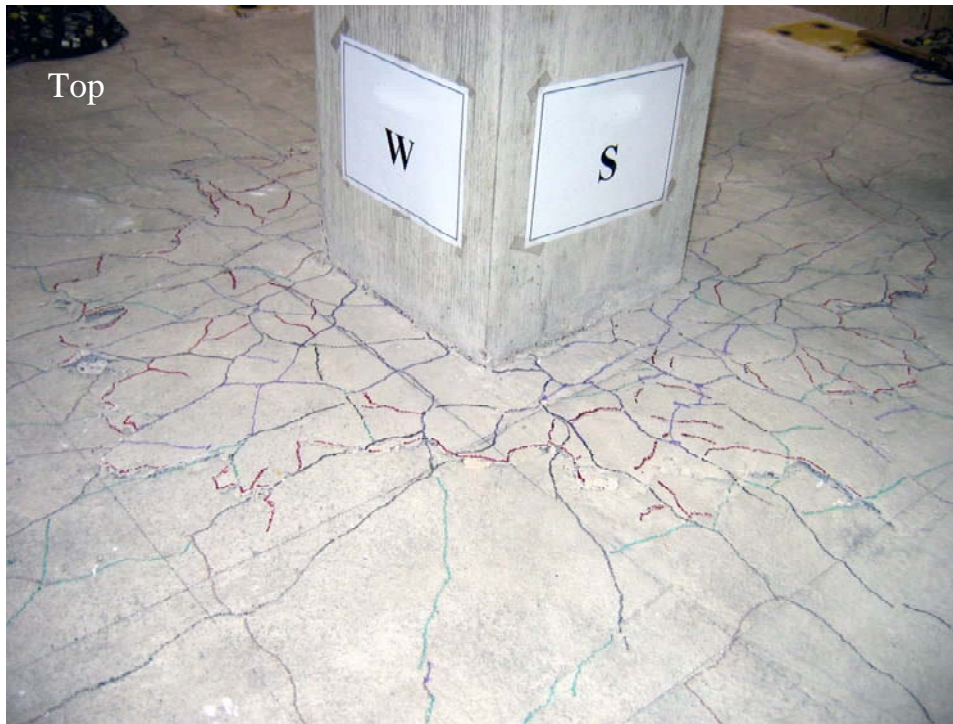


Figure 4.50 Punching shear failure surfaces of LG1.0

4.9 SPECIMEN RCL1.0

Specimen RCL1.0 was fabricated from failed specimen LG1.0. At the end of the punching shear test of specimen LG1.0, the specimen was unloaded completely and the boundary conditions were changed for a simulated seismic test. After the cracks on the junction of slab and lower column were sealed with silicone, the steel collars were installed (using the same technique as described in Section 4.3.2) and the epoxy was poured to fill cracks from the top slab surface (Figure 4.51). The specimen LG1.0 was then renamed as RCL1.0. Figure 4.52 shows the top surface of specimen RCL1.0 after epoxy pouring and Figure 4.53 shows the specimen RCL1.0 just before the test. Specimen RCL1.0 was then subjected to reversed cyclic lateral displacements up to failure.

It should be noted that the steel collars extended $1.6d$ away from the column face, smaller than the recommendations of previous researchers. Wey and Durrani (1992) tested several connections ($c = 10"$, $h = 4.5"$) with different sizes of concrete column capitals ($3.3h$, $2.4h$, and $1.5h$ away from the column face) subjected to reversed cyclic lateral displacements. Assuming that the angle of the punching cone was between 25° and 30° , Wey and Durrani (1992) recommended that the minimum size of column capital was $(c+4h)$ or the column capital should extend at least $2h$ away from the column face to prevent punching shear failure. Luo and Durrani (1994) recommended that the column capital should extend at least $3d$ away from the column face to prevent punching shear failure under reversed cyclic lateral displacements.

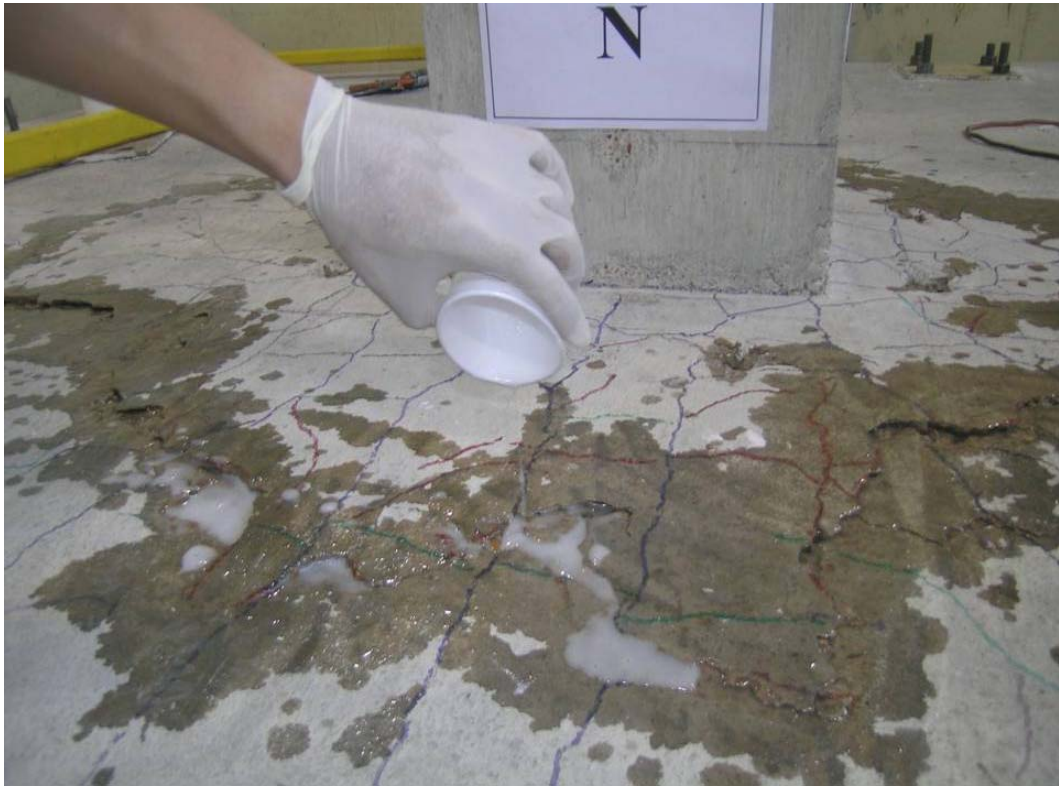


Figure 4.51 Epoxy pouring after punching shear failure of LG1.0



Figure 4.52 After epoxy pouring in RcL1.0



Figure 4.53 RcL1.0 just before the test

4.9.1 Behavior during a simulated seismic test

Figure 4.54 shows the lateral load versus drift response of RcL1.0. Unlike specimen L0.5 that reached its maximum lateral load capacity (about 12 kips) at 1.5% lateral drift, specimen RcL1.0 reached its maximum lateral load (about 18 kips) at 1.5% lateral drift towards the South and 2.0% lateral drift towards the North. The behavior of specimen RcL1.0 was not symmetric because of the previous failure (specimen LG1.0). Before a simulated seismic test was conducted, there was a residual deformation of 0.08% drift toward South (upon the removal of lateral load).

Unlike specimen L0.5 that failed in punching shear at 2.0% drift, specimen RcL1.0 did not experience punching shear failure. The heavily damaged area around the connection (because of a punching shear failure of LG1.0) did not experience more damage under simulated seismic displacements. The failure of specimen RcL1.0 was a one-way flexural-shear failure, through the development of large flexural cracks across the slab at the location where the top flexural reinforcement was terminated (at a distance of $0.3 \times (\text{clear span length}) = 45.6''$ away from the column face), as shown in Figure 4.55. The cracks penetrated through the entire depth of the slab. In Figure 4.54, the one-way flexural-shear failure can be seen from a drop in lateral load. After one-way shear failure occurred, the specimen was able to support a constant lateral load under increasing lateral drift cycles. The flexural cracks acted as plastic hinges and the rotation of the specimen was concentrated in those cracks. As the lateral drift increased, the cracks became larger because there was no top reinforcing bars crossing those cracks. From 2% lateral drift, the specimen was able to resist a constant lateral load of 14 kips. Figure 4.56 shows the large cracks that formed across the specimen and significant concentrated rotations at the crack location at 3.25% lateral drift.

Since the collars were not attached to the slab, there was a gap between the collars and the slab that closed and opened depending on the column inclination during the lateral displacement excursions. Figure 4.57 shows a close-up picture of the collars when the horizontal actuator pushed the top of the upper column to a 3.25% lateral drift towards North. At this drift level, the maximum gap between the collars and the slab was 0.6 inches. Since the specimen still held a constant lateral load of 14 kips at 3.25% drift, it is believed that the collars need not be attached to the slab (i.e. closing and opening of the gap between the collars and the slab did not affect the performance of the connection). Luo and Durrani

(1994) also concluded that no mechanical connection is required between the slab and the steel collars.

Significant torsional cracks on the bottom slab surface were observed at 2.25% drift. At 2.5% drift, concrete on the bottom slab surface started to spall due to the formation of significant torsional cracks.

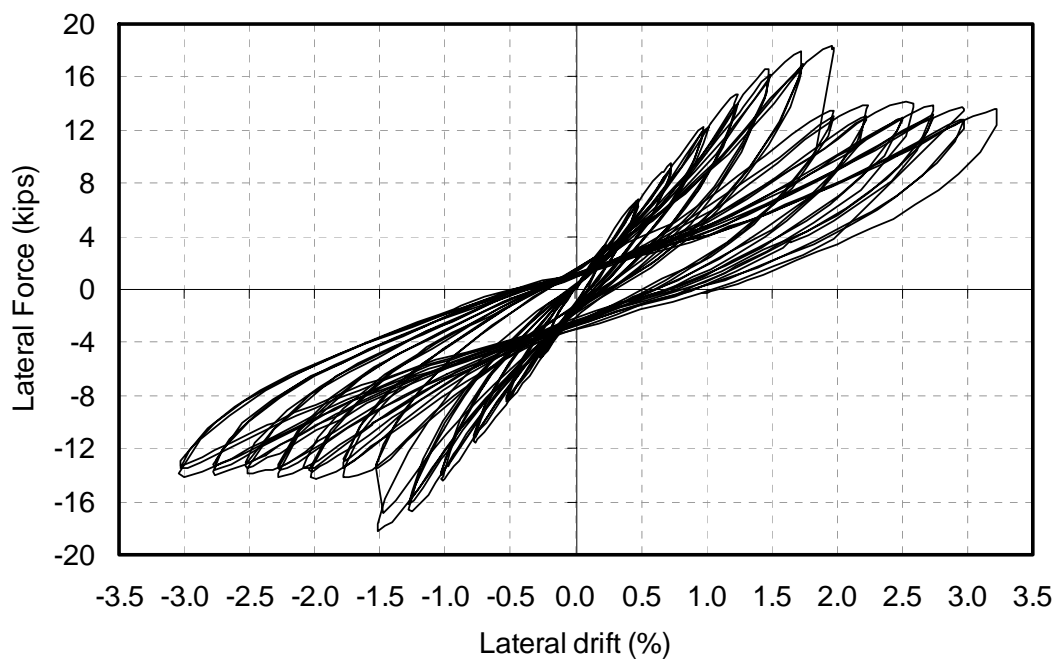


Figure 4.54 Lateral force versus drift of RcL1.0

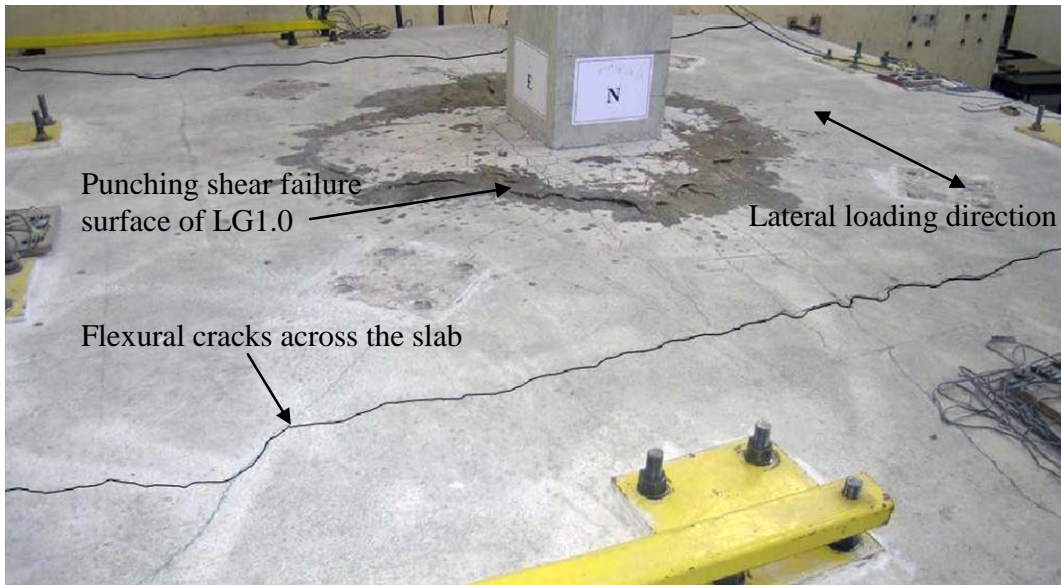


Figure 4.55 One-way shear failure of RcL1.0

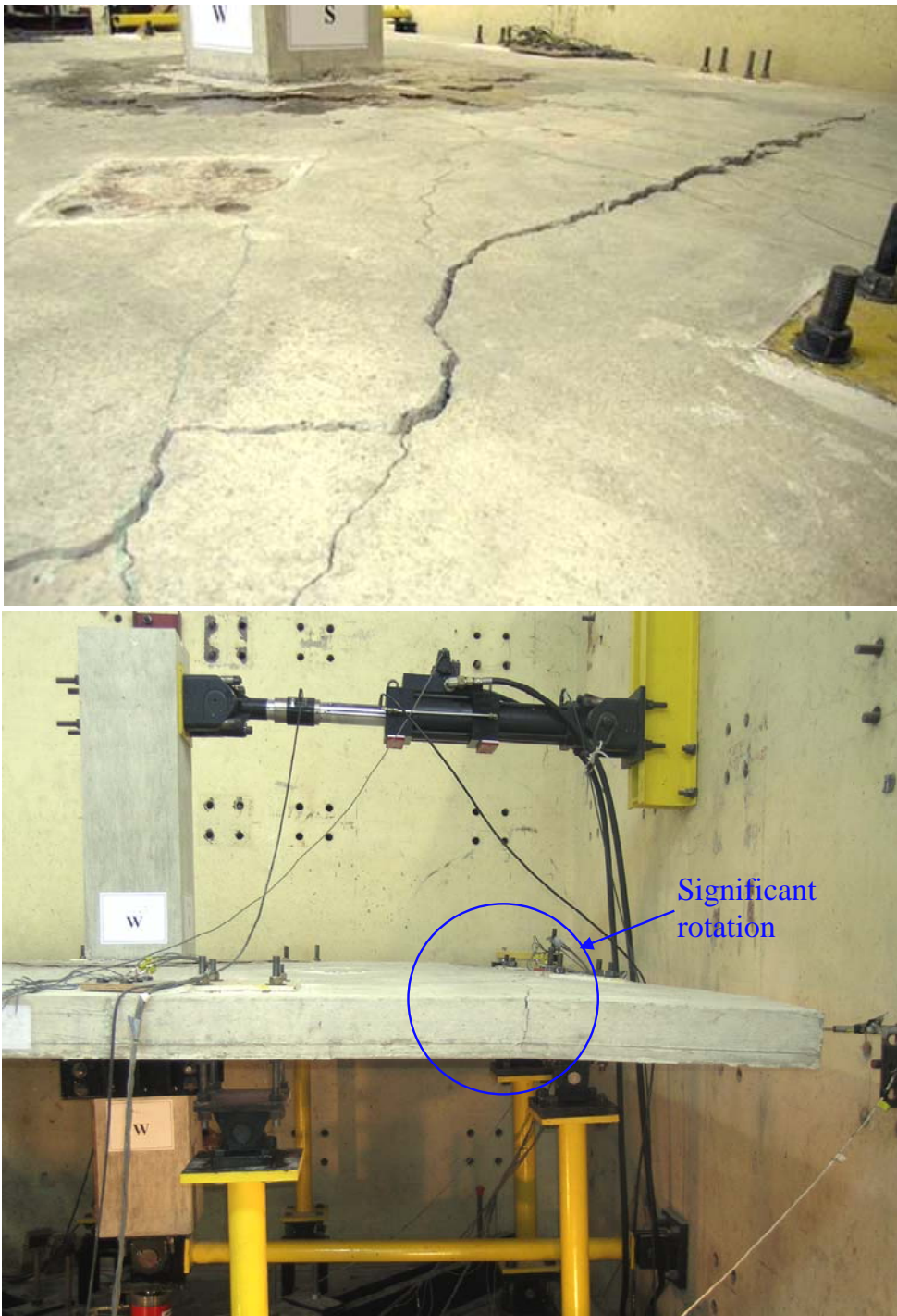


Figure 4.56 Flexural cracks and concentration of rotation at 3.25% drift

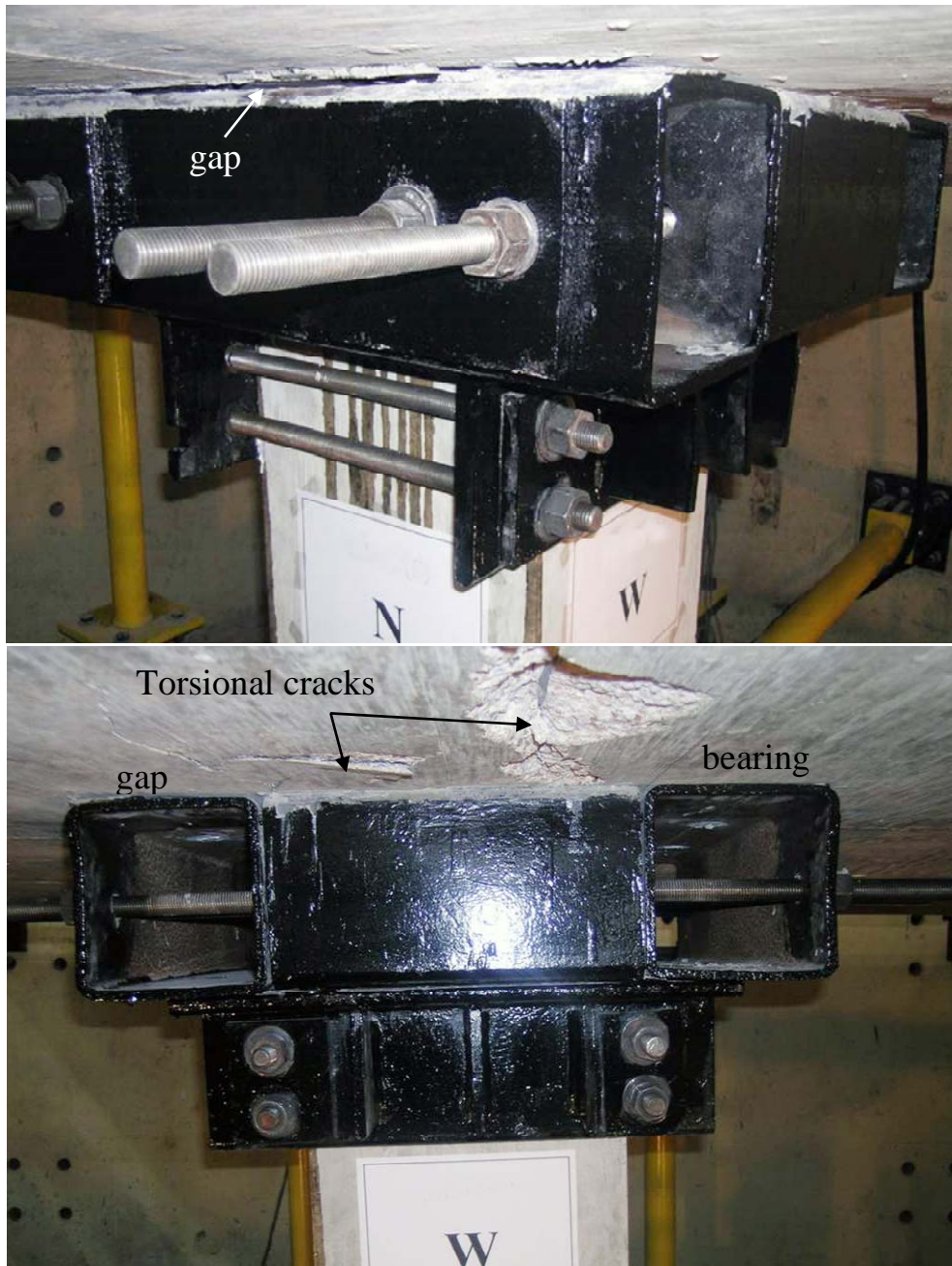


Figure 4.57 Close-up view of the collars at 3.25% drift

4.9.2 Failure surface

Figure 4.58 shows the flexural, torsional cracks, and concrete spalling on the bottom surface at the end of the test, after steel collars had been removed. Unlike in specimen L0.5 (Figure 4.25), the flexural and torsional cracks in specimen RcL1.0 were not limited to the connection region only. The propagation of the flexural and torsional cracks to the edge of specimen indicates that the collars were effective to spread the flexural and torsional action away from the connection so that more slab area contributed to the resistance.

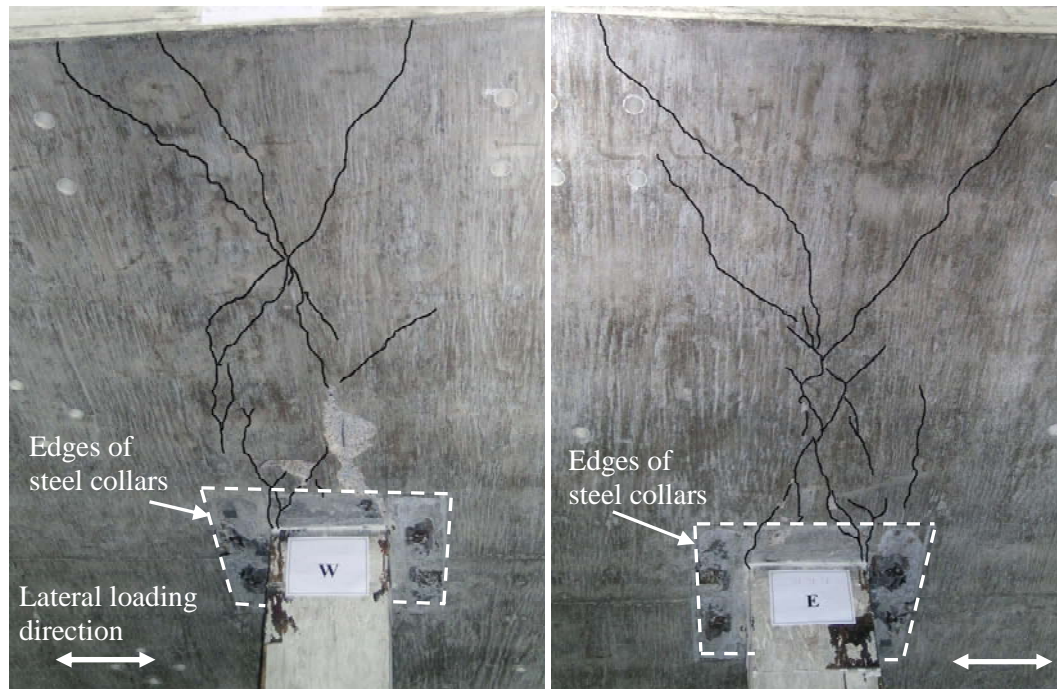


Figure 4.58 Bottom slab surface of RcL1.0 at the end of the test

Figure 4.59 shows the West side of failure surface after the specimen RcL1.0 was saw-cut. Figure 4.59 clearly illustrates that the one-way flexure-shear cracks across the specimen on the North and South sides occurred at the location where the flexural reinforcement was terminated. As typical in one-way flexure-shear failure, the crack angles were very steep (73° and 86°).

Figure 4.59 also shows that the inclined crack of the punching cone in specimen LG1.0 was significantly less steep (38°) than that in specimen LG0.5 (80° and 83° , shown in Figure 4.28). This observation was consistent with previous findings that as the flexural reinforcement ratio increased, the angle of the inclined cracks forming the punching cone became less steep.

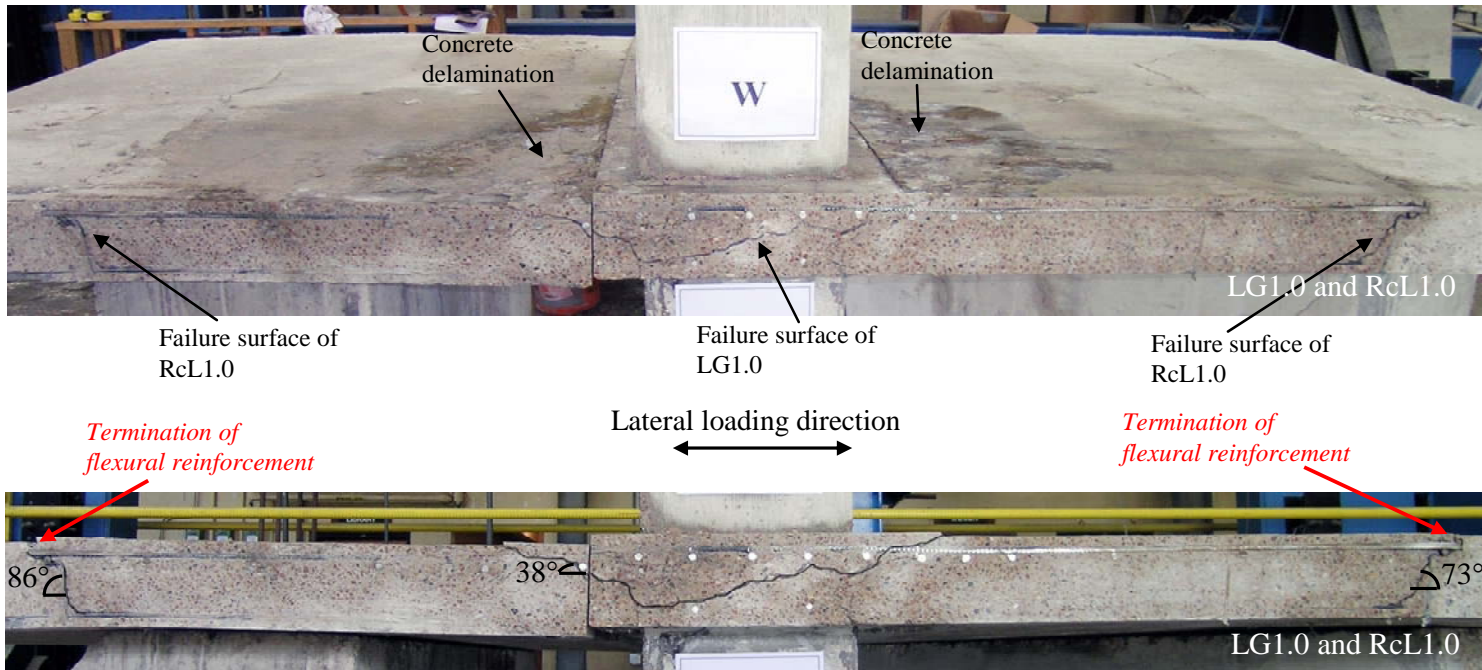


Figure 4.59 Failure surface on the West side of LG1.0 and RcL1.0

Figure 4.60 shows the North side of the failure surface. Unlike in the previous specimens that were strengthened using steel collars (RcG0.5 and RcG1.0), there was only one failure surface in specimen RcL1.0, which was formed at punching shear test of specimen LG1.0. This observation confirmed that punching shear failure did not occur in specimen RcL1.0. The angle of the punching cone of specimen LG1.0 (33°) was significantly less steep than that of specimen LG0.5 (60°). The 33° angle was similar to that in a typical punching shear failure and about the same as that in specimen G1.0 (Figure 4.21). The angle of the punching cone on the North side (perpendicular to the lateral loading direction) of specimen LG1.0 looked similar to that on the South side of specimen LRshG0.5 (Figure 4.35). This supports an earlier observation (Section 4.7.3) that the failure mechanism of both specimens was basically the same and applying CFRP sheets on the tension side was as effective as adding reinforcing bars.

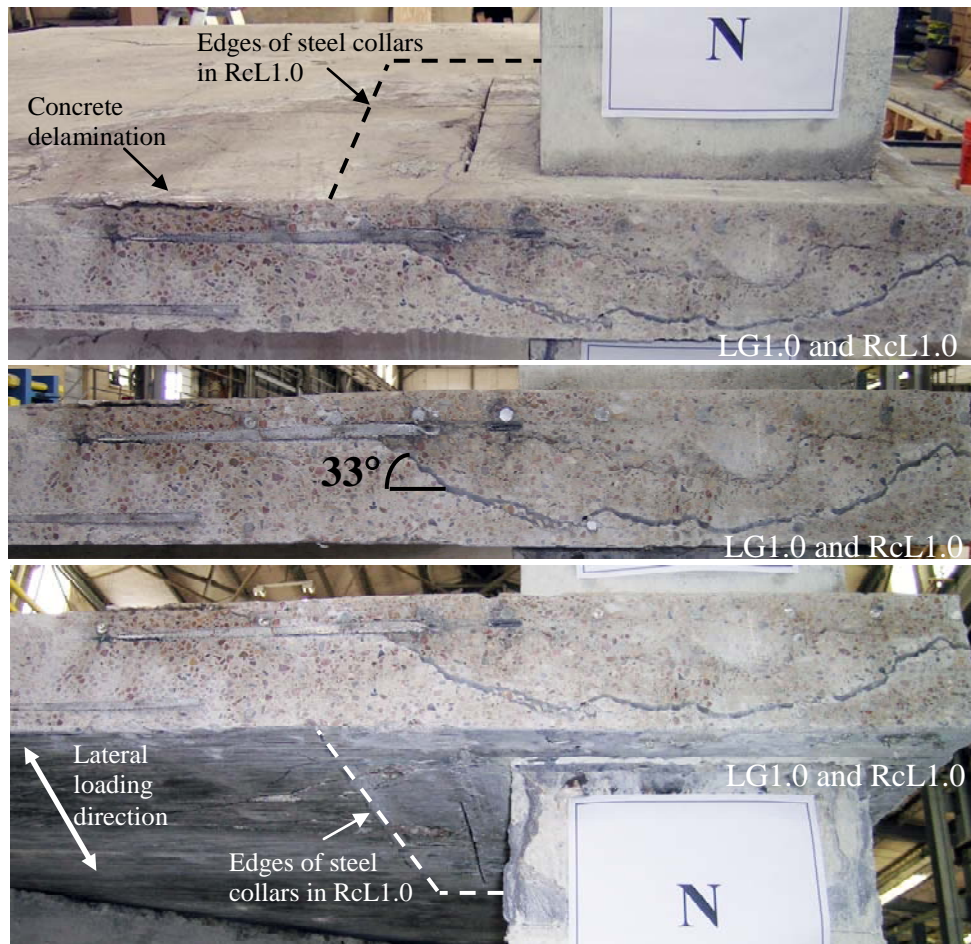


Figure 4.60 Failure surface on the North side of LG1.0 and RcL1.0

4.10 SUMMARY OF TEST RESULTS AND DISCUSSION

4.10.1 Concentric punching shear test

Figure 4.61 shows the gravity load versus vertical displacement (at the column) curves for punching shear tests.

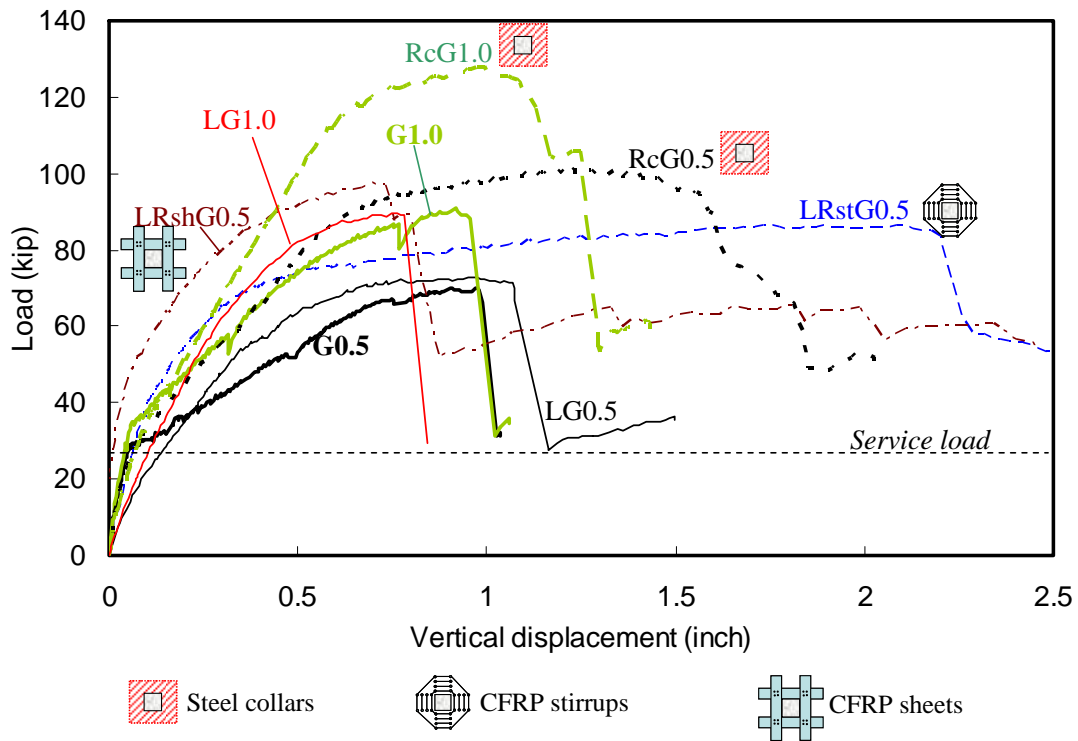


Figure 4.61 Results of the punching shear tests

4.10.1.1 Two-way shear strength

The gravity load capacity and the shear stress at failure calculated at the critical shear perimeter v_c are summarized in Table 4.1. For the connections tested in this study (all specimens except RcG0.5, RcG1.0, and LRstG0.5), Eq. (2.57) governs the design using ACI 318-05. The critical shear perimeters of RcG0.5, RcG1.0, and LRstG0.5, which are at $d/2$ away from the steel collars or from the outermost CFRP stirrup, are larger than those of the other specimens. Thus, Eq. (2.56) governs the design using ACI 318-05 and gives a v_c value of $3.35\sqrt{f'_c}$ for both RcG0.5 and RcG1.0, and $3.48\sqrt{f'_c}$ for LRstG0.5. The v_c (inferred from the load measurements and ACI definition of critical perimeter) of RcG0.5, RcG1.0,

and LRstG0.5 were $2.01\sqrt{f_c'}$, $2.71\sqrt{f_c'}$, and $1.83\sqrt{f_c'}$, respectively. The v_c of RcG0.5, RcG1.0, and LRstG0.5 were only 60%, 81%, and 53% of that estimated using ACI 318-05 (Eq. (2.56)). The results summarized in Table 4.1 indicate that all specimens tested in this study failed at shear stress levels that were lower than $4\sqrt{f_c'}$, the value used in most designs using ACI Code. Punching shear failure was initiated by large flexural cracks that reduced concrete contribution to shear strength.

It should be noted that specimens RcG0.5 and RcG1.0 were fabricated from previously failed specimens G0.5 and G1.0, respectively. In order to restore the continuity of the previously failed specimens, epoxy was poured. Herein, the epoxy was assumed to be equivalent to undamaged concrete. In addition, since the locations of the failure surface in both specimens RcG0.5 and RcG1.0 were different than those in their corresponding specimens G0.5 and G1.0, the test results of specimens RcG0.5 and RcG1.0 were assumed to be unaffected by previous failure.

Table 4.1 Failure loads and stresses

Specimen Name	Punching load, V (kip)	ACI critical shear perimeter, b_o (in)	Failure shear stress at critical perimeter, $v=V/(b_o d)$
G0.5	69.9	84	$2.47 \sqrt{f_c'}$
RcG0.5	101.3	84* / 148**	$3.55 \sqrt{f_c'} / 2.01 \sqrt{f_c'}$
G1.0	90.2	84	$3.37 \sqrt{f_c'}$
RcG1.0	128	84* / 148**	$4.78 \sqrt{f_c'} / 2.71 \sqrt{f_c'}$
LG0.5	72.7	84	$2.48 \sqrt{f_c'}$
LRstG0.5	86.5	84* / 135***	$2.93 \sqrt{f_c'} / 1.83 \sqrt{f_c'}$
LRshG0.5	97.5	84	$3.41 \sqrt{f_c'}$
LG1.0	89.8	84	$3.38 \sqrt{f_c'}$

* $b_o=84"$ was calculated for the critical perimeter $d/2$ away from the column face

** $b_o=148"$ was calculated for the critical perimeter $d/2$ away from the edge of steel collars

*** $b_o=135"$ was calculated for the critical perimeter $d/2$ away from the outermost CFRP stirrup

The estimated two-way shear strengths (through the use of different building codes) of control specimens G0.5 and G1.0 are compared with the measured strengths in Figure 4.62. As can be seen in Figure 4.62, only DIN 1045-1 gave conservative estimates of the two-way shear strength. All building codes that did not consider flexural reinforcement influence on the two-way shear strength (ACI 318-05, CSA-A 23.3-04, AS 3600-1994, and IS-456) estimated that specimen G1.0 had a lower two-way shear strength than specimen G0.5 because specimen G1.0 had somewhat lower concrete strength. As expected, the other building codes that considered the influence of flexural reinforcement (EC2-2003, MC 90, DIN 1045-1, BS 8110-97, and JSCE 1986) estimated that specimen G1.0 had a higher two-way shear strength than specimen G0.5 because specimen G1.0 had a higher percentage of flexural reinforcement. It can clearly be seen that all

building code provisions but DIN 1045-1 overestimated the two-way shear strength of an interior slab-column connection in existing structures.

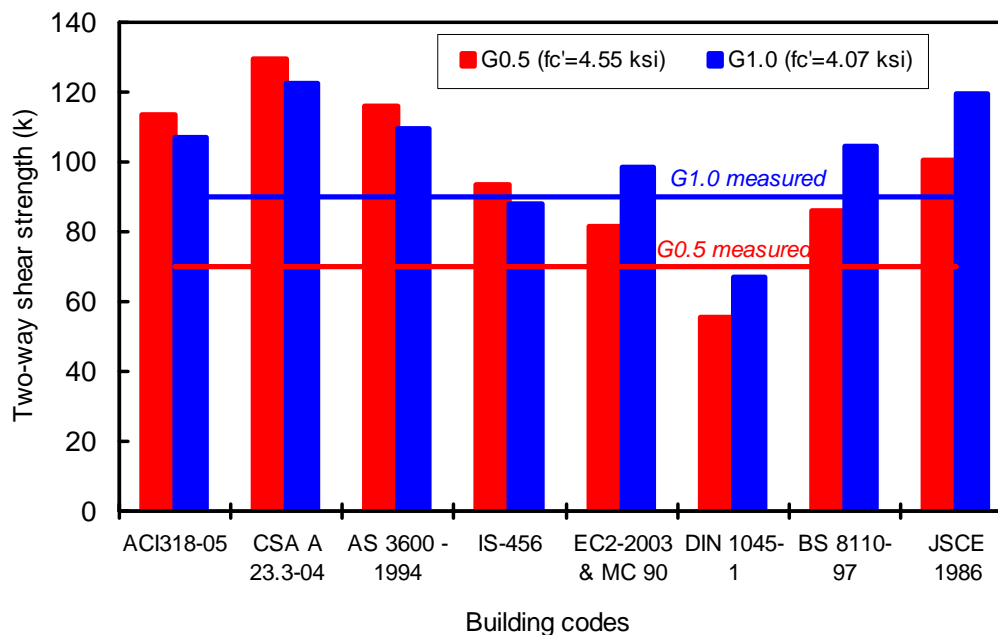


Figure 4.62 Estimated strength from building codes versus measured strength

The estimated two-way shear strengths using several approaches are compared with the measured strength of specimens G0.5 and G1.0 in Figure 4.63. The following observations can be based on an examination of Figure 4.63:

- Since the approaches considered in preparing Figure 4.63 account for the effect of flexural reinforcement on two-way shear strength, specimen G1.0 was expected to have a higher two-way shear strength than specimen G0.5.
- The measured two-way shear strengths of both specimens G0.5 and G1.0 were very close to the estimated strengths using the yield-line theory. Since the ultimate flexural strength is estimated by the yield-line theory, it is believed that the failure of both specimens G0.5 and G1.0 was preceded

by general yielding of reinforcing bars, which caused large flexural cracks. As mentioned before, large flexural cracks reduced concrete contribution to shear strength and caused early punching shear failure. The load versus deformation curves (Figure 4.61) and the strain gage readings (Figure 4.64) support the fact that reinforcing bars yielded before punching shear failure occurred.

It is interesting to note that even though the failure of specimen G0.5 was preceded by general yielding of rebars, the measured strength of specimen G0.5 was only slightly smaller than the estimated strength from the yield-line theory. In general, the actual flexural strength corresponding to general yielding can be considerably above V_{flex} estimated from the yield-line theory because of in-plane forces, membrane action, strain hardening, and edge restraint due to support friction (Criswell 1974). However,

Criswell indicated that the $\left(\frac{V}{V_{flex}}\right)$ values for his slab-column connections,

which displayed yield-line development before failure, were smaller than the values often reported, primarily because of the low restraint offered by the roller supports. In the test setup used in this experimental program, the supports consisted of 4 struts with hinges at the top and bottom of each strut. It is believed that this type of support condition offered a negligible edge restraint, similar to Criswell's specimens that were supported on rollers. Consistent with Criswell observation, the actual failure load for specimen G0.5 was slightly smaller than V_{flex} from the yield-line theory.

- Even though Moe's (1961) equation (Eq. (2.17)) considers flexural strength, it was derived based on a statistical analysis of the results of slab and footing (supported on springs simulating soil pressure) tests that were believed to have failed in shear. Test results of slabs and footings that

were believed to have failed in flexure were excluded from Moe's statistical analysis. Consequently, Moe's equation significantly overestimated the two-way shear strength of lightly-reinforced slab-column connections, those are believed to have failed in flexure. The percent discrepancy was smaller for the slab-column connection with a higher percentage of flexural reinforcement (specimen G1.0). Since the ACI 318 provisions were based on Moe's equation, the fact that ACI 318-05 significantly overestimates the two-way strength of specimens G0.5 and G1.0 is not surprising.

- Relatively simple equations derived by Nolting (1984) and Gardner (1996) (Eqs. (2.28) and (2.46), respectively) estimated the two-way shear strength of specimens G0.5 and G1.0 reasonably well.
- The strip model proposed by Alexander and Simmonds (1992) and Afhami et al. (1998) provided the lower and upper bounds ($P_{s,min}$ (Eq. (2.42)) and $P_{s,tot}$ (Eq. (2.41)), respectively) of the two-way shear strength of specimens G0.5 and G1.0 very well.

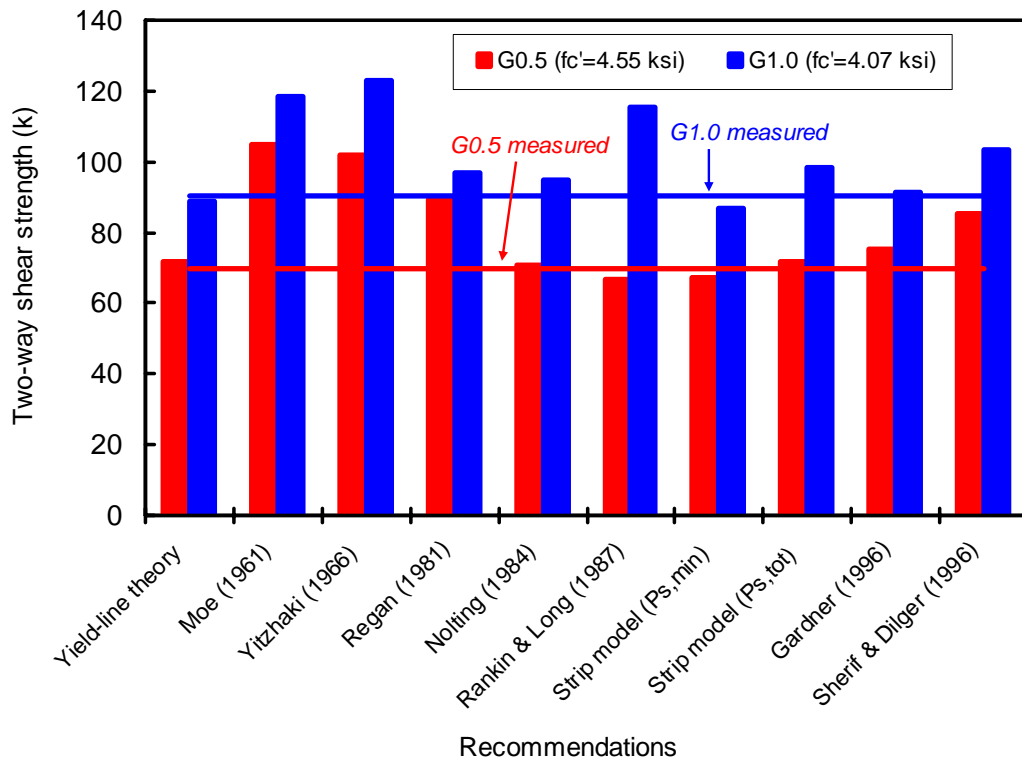


Figure 4.63 Estimated strength from researchers versus measured strength

4.10.1.1.1 Undamaged, unstrengthened specimens (Effect of flexural reinforcement ratio)

At failure, v_c of G0.5 and G1.0 reached $2.47\sqrt{f'_c}$ and $3.37\sqrt{f'_c}$, respectively. The measured strengths were only 63% and 85% of the strength estimated using ACI 318-05 expression (Eq. (2.57)). This observation is consistent with the test results of a 45-ft. square flat-plate structure (Guralnick and LaFraugh 1963). The results of the tests conducted in this experimental study indicate that two-way shear capacity of a connection is sensitive to the amount of flexural reinforcement within $(c+3h)$ region.

Figure 4.64 compares the strains in reinforcing bars running in both North-South and East-West directions at the maximum load V_{max} of both specimens G0.5 and G1.0. At $V = V_{max}$, reinforcing bars within $(c+3h)$ region in both specimens G0.5 and G1.0 yielded. This explains why the two-way shear strengths of both specimens G0.5 and G1.0 were very close to those estimated using the yield-line theory. The fact that flexural yielding preceded punching shear failure of specimens G0.5 and G1.0 was consistent with the observation of failure in actual structures reported in Section 1.1.2 (16-story apartment building in Boston and 5-story apartment building in Cocoa Beach). Figure 4.64 also shows that the reinforcing bars outside the $(c+3h)$ region did not deform as much as those within the $(c+3h)$ region. This indicates that the reinforcing bars outside the $(c+3h)$ region were not as effective as those within the $(c+3h)$ region.

The strains in reinforcing bars of specimen G1.0 at the maximum load of specimen G0.5 ($V = 69.9$ kips) are also shown in Figure 4.64. At the maximum load of specimen G0.5, the rebar strain in specimen G1.0 was generally only half of that in specimen G0.5. This indicates that for a given load level, the rebar strain decreased as the percentage of flexural reinforcement increased. Smaller rebar strains mean smaller crack widths and more aggregate interlock contribution to the shear strength. Therefore, in lightly-reinforced slab-column connections (i.e. with 1% flexural reinforcement or less), increasing the amount of flexural reinforcement within $(c+3h)$ region will result in reductions of rebar strains and improvements of the two-way shear strength.

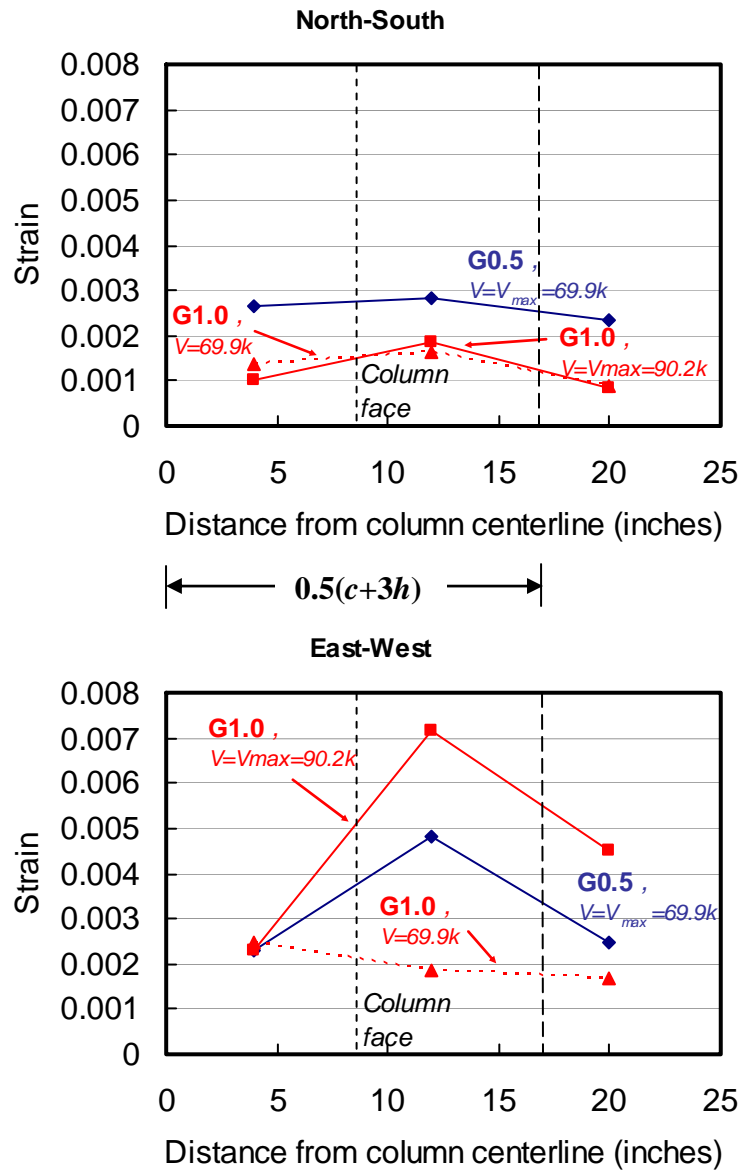


Figure 4.64 Reinforcing bar strains

4.10.1.1.2 Effect of seismic damage

In order to study the effect of seismic damage, the behaviors of specimens LG0.5, LG1.0 can be compared with those of their companion specimens G0.5, G1.0

G1.0 that were undamaged. This comparison shows that the seismic damage in the connection region due to uniaxial reversed cyclic lateral displacements up to 1.25% drift had no noticeable adverse effects on the two-way shear strength (Figure 4.61 and Table 4.1).

4.10.1.1.3 Effectiveness of steel collars

Comparing the behaviors of specimens RcG0.5, RcG1.0 with those of their companion specimens G0.5, G1.0 that were unstrengthened shows that the steel collars increased the two-way shear and deformation capacities of the connection (Figure 4.61 and Table 4.1). The steel collar installation improved the two-way shear and deformation capacities of specimen G0.5 by 45% and 53%, respectively. It also increased the two-way shear and deformation capacities of specimen G1.0 by 42% and 15%, respectively.

Examination of failure surfaces of specimen RcG0.5 (Figures 4.15 through 4.17) and those of specimen RcG1.0 (Figures 4.19 through 4.21) shows that the steel collars were effective in enlarging the critical shear perimeter and hence increasing the two-way shear capacity.

4.10.1.1.4 Effectiveness of externally installed CFRP stirrups

Comparing the behavior of LRstG0.5 with that of LG0.5 shows that the externally installed CFRP stirrups improved the two-way shear strength and deformation capacity of a seismic-damaged connection (Figure 4.61 and Table 4.1). The installation of external CFRP stirrups improved the two-way shear and deformation capacities by 19% and 106%, respectively. A tightly knit array of CFRP stirrups shifted the failure surface away from the column (increased the critical shear perimeter), as shown in Figure 4.34, and hence increased the two-way shear capacity.

Comparing the behavior of LRstG0.5 with that of RcG0.5 shows that even though the new critical shear perimeter outside the shear reinforced zone of both specimens were about the same (135" versus 148"), the two-way shear capacity of LRstG0.5 was 15% smaller than that of RcG0.5 (Figure 4.61 and Table 4.1). This indicates that the externally installed stirrups were less effective than the steel collars in increasing two-way shear capacity because the externally installed stirrups were not as stiff as the steel collars. Hawkins and Mitchell (1979) indicated that the shear strength decreases as the stiffness of the connection decreases. Therefore, since the shear reinforced zone with externally installed stirrups was less stiff, it is expected that the shear strength of LRstG0.5 would be smaller than that of RcG0.5. However, even though the rehabilitation with the externally installed stirrups was not as effective as that with the steel collars for increasing the two-way shear strength, rehabilitation with the externally installed stirrups resulted in 47% higher deformation capacity than that with the steel collars (Figure 4.61).

4.10.1.1.5 Effectiveness of well-anchored CFRP sheets

Comparing the behavior of LRshG0.5 with that of LG0.5 shows that the installation of well-anchored CFRP sheets on the tension side of the slab improved the two-way shear strength of an earthquake-damaged connection. Results summarized in Table 4.1 show that the CFRP installation improved the two-way shear capacity of the connection by 38% (from $2.47\sqrt{f_c'}$ to $3.41\sqrt{f_c'}$). The area of the CFRP sheets was selected to match the flexural capacity of a connection with 1.0% steel within $(c+3h)$ region. Figure 4.61 shows that the ultimate capacity of specimen LRshG0.5 was about the same as that of specimen G1.0, implying that external CFRP sheets were just as effective as the steel reinforcement.

Four CFRP anchors per column corner were very effective in preventing delamination. At failure, the CFRP sheets close to the middle of the column face ruptured, whereas the sheets elsewhere were still attached to the slab (Figure 4.44). The CFRP sheets did not change the location of the failure surface but limited the width of flexural cracks (that occurred due to simulated seismic displacements) so that the area of concrete resisting shear was maintained and the connection was able to carry more load before a punching shear failure occurred.

4.10.1.2 Residual capacity after punching shear failure

Maintaining a high residual capacity after punching shear failure may be very important to limit shedding of the load to adjacent connections once punching shear failure occurs, and thus reducing the risk of a progressive collapse. As discussed in Section 2.7, there are different opinions about what provides residual capacity, V_r , after punching shear failure. Even though most researchers agree that the resistance after punching shear failure is provided by dowel and catenary actions of reinforcing bars crossing the failure surface, V_d , they do not agree on whether the top or the bottom slab reinforcing bars are really effective. Criswell (1970, 1974) indicated that the main resistance was provided by top slab rebars, whereas Hawkins and Mitchell (1979) suggested that only the bottom slab rebars contributed to the dowel resistance. Even though Regan (1981), Regan and Braestrup (1985), Pan and Moehle (1992) acknowledged the contribution of top slab rebars, they indicated that the bottom slab rebars were much more effective in resisting gravity loads following initial punching. Hallgren (1996) suggested that if the rebars intersecting the shear crack yielded, then the dowel force reduced considerably.

The measured residual capacity after punching shear failure, $V_{r,test}$, and the shear force due to dead loads (self-weight and partition loads), $V_{dead\ loads}$, for all specimens are summarized in Table 4.2. Hawkins and Mitchell (1979) recommendation (Eq. (2.58)) gives $V_d = 27.7$ kips for all specimens and Regan (1981) recommendation (Eq. (2.59)) gives $V_d = 25.6$ kips for all specimens. These recommendations produce a conservative, but inaccurate estimation of V_r . Since the bottom slab reinforcing bars next to those passing through the column were terminated at 21" from the column centerline (=13" from the column face), there was no additional bottom reinforcing bars passing through the new critical shear perimeter at the edge of the collars or at the outermost of CFRP stirrups. According to Hawkins and Mitchell and Regan's recommendations, there were only 8 bottom reinforcing bars ($n=8$), which passed through the column, contributed to V_d in all specimens. Even though the specimens rehabilitated with steel collars and externally installed CFRP stirrups had a larger critical shear perimeter, the number of bottom reinforcement contributing to V_d in all specimens was the same.

Table 4.2 Residual capacity after punching shear failure

Specimen	b_o (inch)	$V_{r,test}$ (kip)	$V_{dead\ loads}$ (kip)
G0.5	84	31.4	27.4
RcG0.5	148*	48.9	
G1.0	84	31.1	28.8
RcG1.0	148*	55.1	
LG0.5	84	27.7	26.6
LRstG0.5	135**	57	26.5
LRshG0.5	84	51.7	27.2
LG1.0	84	29.3	29.1

* $b_o=148"$ was calculated for the critical perimeter $d/2$ away from the edge of steel collars

** $b_o=135"$ was calculated for the critical perimeter $d/2$ away from the outermost CFRP stirrup

4.10.1.2.1 Effect of flexural reinforcement ratio on residual capacity

In order to study the effect of flexural reinforcement ratio, $V_{r,test}$ of specimen G0.5 can be compared with that of specimen G1.0. It can be seen from Table 4.2 that $V_{r,test}$ of both specimens G0.5 and G1.0, which had different amount of top rebars but the same amount of bottom rebars, were about the same. If the concrete contribution to V_r is considered negligible, it can be concluded that V_r is insensitive to the tensile flexural reinforcement ratio.

4.10.1.2.2 Effect of seismic damage on residual capacity

In order to study the effect of seismic damage, $V_{r,test}$ of specimens LG0.5, LG1.0 can be compared with those of their companion specimens G0.5, G1.0 that were undamaged. This comparison shows that the seismic damage in the connection region caused a reduction of V_r because of cracks and yielding of the top slab rebars during the simulated seismic tests. This observation supports

Hallgren's (1996) opinion that when the rebars intersecting the shear crack yield, then the dowel force is reduced considerably and hence V_r also reduces.

Specimens LG0.5 and LG1.0 showed 12% and 6% reduction, respectively, compared with their companion specimens G0.5, G1.0 that were undamaged. The reduction was smaller for connections with a higher ρ because at the same drift level, connections with a higher ρ had smaller crack widths and smaller inelastic rebar strains.

4.10.1.2.3 Effectiveness of steel collars on residual capacity

Specimens RcG0.5 and RcG1.0 that were rehabilitated with steel collars exhibited a higher $V_{r,test}$ than their companion specimens G0.5, G1.0 that were unstrengthened. As discussed earlier, the steel collars were effective in enlarging the critical shear perimeter, which means engaging more flexural reinforcement into the punching cone for improved V_r . Thus, the collars were effective in increasing residual capacity after punching shear failure. Since the presence of the collars did not change the number of the bottom slab rebars contributing to V_r , it is believed that the top slab rebars also contributed to V_r , as suggested by Regan (1981), Regan and Braestrup (1985), and Pan and Moehle (1992). Therefore, when the amount of top rebars crossing the punching cone increased, V_r also increased. This observation is interesting because it is inconsistent with the previous observation discussed in Section 4.10.1.2.1. The reason behind this inconsistency is explained in Section 4.10.1.2.6.

4.10.1.2.4 Effectiveness of externally installed CFRP stirrups on residual capacity

Specimen LRstG0.5 that was rehabilitated with externally installed CFRP stirrups exhibited a higher $V_{r,test}$ than its companion specimen G0.5 that was unstrengthened. As discussed earlier, a tightly knit array of CFRP stirrups

increased the critical shear perimeter, which means engaging more flexural reinforcement into the punching cone for improved V_r . Ignoring the difference in concrete strength between the specimens LRstG0.5 and Rc0.5 and assuming that b_o of both specimens were about the same, it can be seen that the tightly knit array of CFRP stirrups was more effective than the steel collars in increasing V_r . The reason for this is that in addition to increasing the critical shear perimeter, the externally installed CFRP stirrups prevented stripping out of the tensile flexural reinforcement (Binici 2003), whereas the steel collars did not.

4.10.1.2.5 Effectiveness of well-anchored CFRP sheets on residual capacity

Specimen LRshG0.5 that was rehabilitated with well-anchored CFRP sheets exhibited a higher $V_{r,test}$ than its companion specimen G0.5 that was unstrengthened. At failure, due to the superior performance of CFRP anchors, most of the CFRP sheets were still attached to the slab. The well-anchored CFRP sheets acted as tension bands and allowed the slab to carry substantial shear force through larger deformations. For this reason, the well-anchored CFRP sheets were effective in increasing V_r .

4.10.1.2.6 Effectiveness of top slab reinforcing bars on residual capacity

Increasing the number of the top slab rebars crossing the punching failure surface could be done in two ways: (i) increasing ρ and (ii) enlarging the critical shear perimeter. For the same rebar spacing, increasing the number of the top slab rebars crossing the punching failure surface by enlarging the critical shear perimeter increased V_r (Section 4.10.1.2.3). However, increasing the number of the top slab rebars crossing the failure surface by increasing ρ (i.e. reducing the rebar spacing) did not increase V_r (Section 4.10.1.2.1). It is believed that the effectiveness of top slab rebars on providing V_r depends on the ability of concrete cover to prevent stripping out of the rebars. Increasing ρ was not effective

because increasing ρ reduced the ability of concrete cover to prevent stripping out of the rebars. When the ability of concrete cover for preventing stripping out of the rebars was enhanced by using a tightly knit array of external CFRP stirrups, V_r increased (Section 4.10.1.2.4). Therefore, it can be concluded that the top slab rebars contributed to providing V_r . However, they were only effective if concrete cover could confine them (prevent stripping out of the rebars).

4.10.2 Simulated seismic tests

4.10.2.1 Effect of flexural reinforcement ratio

In order to study the effect of tensile flexural reinforcement ratio within $(c+3h)$ region on the seismic behavior of slab-column connections, the behavior of specimen LG1.0 can be compared with that of specimen L0.5. As can be seen in Figure 4.65 specimen LG1.0 exhibited a stiffer response than specimen L0.5. In addition, the maximum lateral load capacity of specimen LG1.0 was higher than that of specimen L0.5. Therefore, it can be concluded that increasing the tensile flexural reinforcement ratio within $(c+3h)$ region is effective in increasing the stiffness and the lateral load capacity of slab-column connections. Since the connection with 1.0% flexural reinforcement was not subjected to lateral deformations up to failure, the effect of flexural reinforcement ratio on the lateral drift capacity and type of failure cannot be evaluated based on these tests.

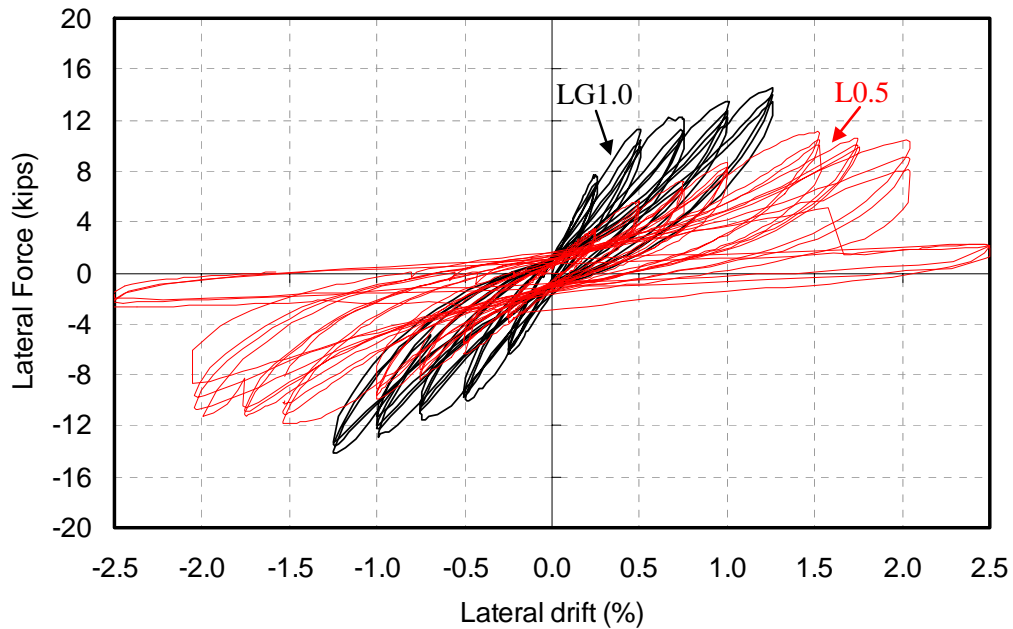


Figure 4.65 Lateral load versus drift of specimens LG1.0 and L0.5

4.10.2.2 Effectiveness of steel collars

Figure 4.66 shows the lateral load versus drift response of specimen LG1.0 up to 1.25% drift (before the punching shear test was conducted) and specimen RcL1.0 up to failure. As seen in Figure 4.66, steel collars increased the lateral load capacity of the connection. Since the connection had failed in punching shear before the steel collars were installed, specimen RcL1.0 was not as stiff as specimen LG1.0. And unlike specimen L0.5 that failed in punching shear at 2.0% drift, specimen RcL1.0 did not experience punching shear failure. Even though the collars used in this study extended only $1.6d$ away from the column face, which was smaller than the recommendations of previous researchers (Wey and Durrani (1992) and Luo and Durrani (1994) recommended

that the column capitals should extend at least $2h$ and $3d$, respectively, away from the column face), the collars were still effective to prevent punching shear failure.

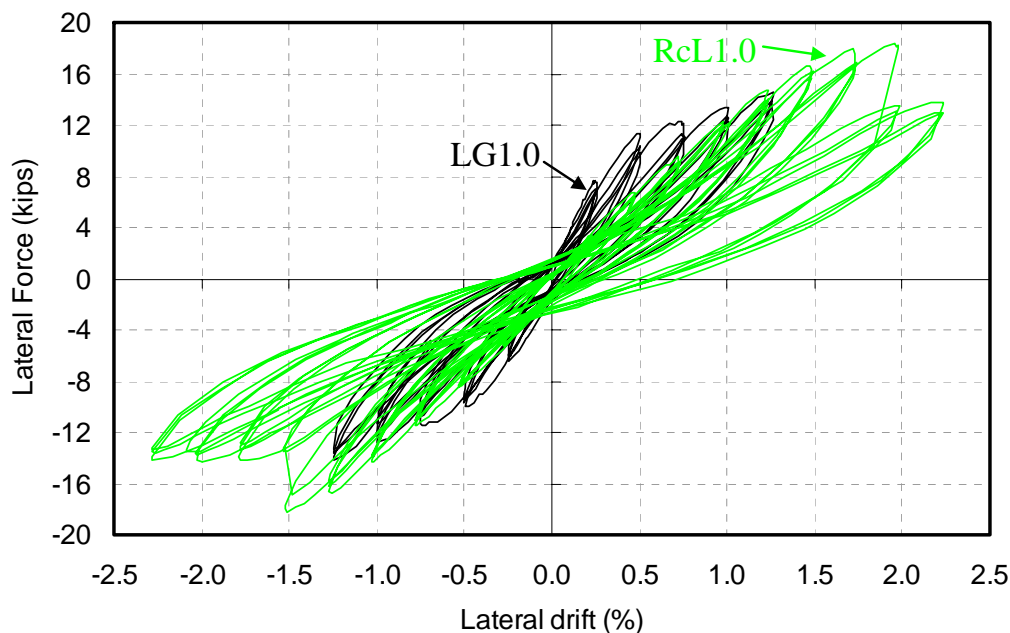


Figure 4.66 Lateral load versus drift of specimens LG1.0 and RcL1.0

Even though the rehabilitated connection exhibited a significant reduction in its original stiffness, it showed an increase in lateral load capacity and it was still capable of sustaining the gravity load and lateral displacements up to 1.5% drift. Pan and Moehle (1992) indicated that a stiffness reduction in repaired connections may not be such a critical factor in cases where, as is commonly practiced, shear walls or ductile moment resisting frames are designed to carry the total lateral forces in flat-plate structures. They also indicated that a 1.5% drift under severe seismic loads is a reasonable upper bound for a properly reinforced concrete buildings. Since RcL1.0 (i) did not experience punching shear failure, (ii) did not exhibit a reduction in lateral load up to 1.5% drift, and (iii) could

maintain the loads in a stable manner up to 3.25% drift (as shown in Figure 4.54), the seismic behavior of RcL1.0 was satisfactory.

Therefore, it can be concluded that the steel collars were effective in improving the seismic behavior of damaged slab-column connections by preventing the punching shear failure and increasing the lateral load capacity. The installation of the collars reduced the maximum shear stress due to gravity loads and moment transfer calculated at the critical section away from the collars so that the maximum shear stress was smaller than the nominal shear strength and the requirements of Section 11.12.6.2 of ACI 318-05 were satisfied.

CHAPTER 5

Evaluation and Rehabilitation Guidelines

5.1 GENERAL

Guidelines for the evaluation and rehabilitation of existing, lightly-reinforced ($\rho \leq 1.0\%$), slab-column connections are presented in Chapter 5. These guidelines are based on the results of the tests conducted in this study and on the synthesis of the literature review conducted as part of this research project. These guidelines are intended to give practicing engineers some insight for evaluating and rehabilitating existing connections. The process for evaluation and rehabilitation of existing slab-column connections and the organization of Chapter 5 are shown in Figure 5.1.

Three alternatives for strengthening and repairing slab-column connections and important design considerations for each alternative are discussed in this chapter. The three alternatives and important design considerations for each alternative are as follows:

1. Installation of friction based steel collars on the column under the slab (Section 5.4)
 - Size of the collars (Section 5.4.2)
 - Stiffness of the collars (Section 5.4.3)
 - Clamping force (Section 5.4.4)
2. Installation of external Carbon Fiber Reinforced Polymers (CFRP) stirrups (Section 5.5)
 - Spacing of stirrups (Section 5.5.2)

- Shear strength inside and outside the CFRP reinforced zone (Section 5.5.3)
3. Application of well-anchored CFRP sheets on the tension side of the slab (Section 5.6)
- Position, amount, and depth of anchors (Section 5.6.2)
 - Length of CFRP sheets (Section 5.6.3)
 - Amount of CFRP sheets (Section 5.6.4)

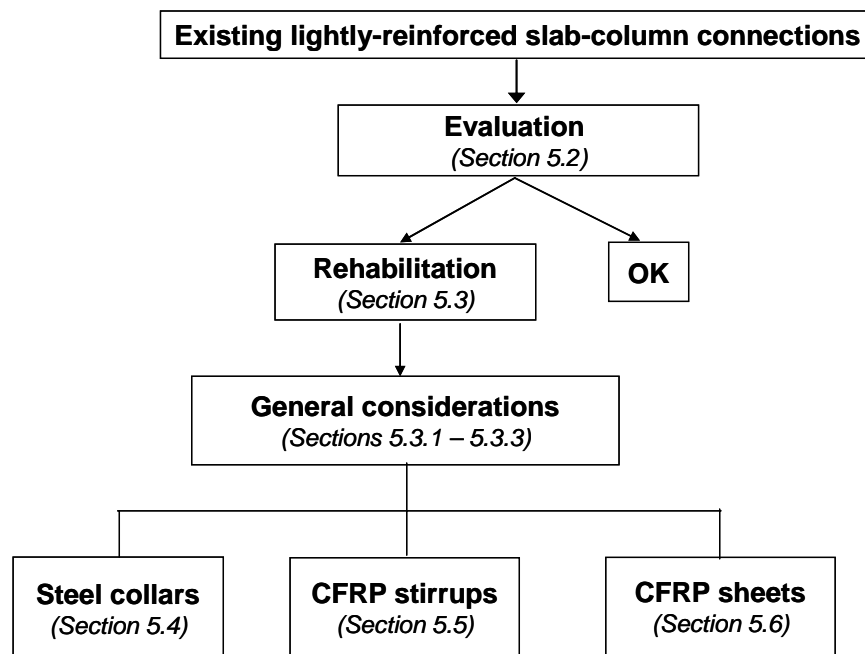


Figure 5.1 Flowchart for evaluation and rehabilitation

5.2 EVALUATION

Prior to selecting an appropriate rehabilitation method, the two-way shear strength of a slab-column connection should be evaluated and the general condition of the existing structure and its connections should be assessed. For

estimating the existing capacity of lightly-reinforced connections, the use of the Euro Code EC 2-2003 (Model Code CEB-FIP MC 90) is recommended. The concrete contribution to two-way shear strength of slab-column connections V_c according to EC 2-2003 (in US customary units) is:

$$V_c = 0.05 \xi \{100 \rho (f_c' - 0.23)\}^{1/3} u d \quad [\text{k}]$$

where: $\xi = \left(1 + \sqrt{\frac{7.9}{d}}\right) \leq 2.0$ (5.1)

in [inch] and [ksi]

where ξ is the size effect factor, ρ is the flexural reinforcement ratio, f_c' is the specified concrete cylinder compressive strength, d is the average depth of slab reinforcement, u is the critical shear perimeter located at $2d$ away from the face of the column (For a square column: $u = 4(c + \pi d)$, where c is the dimension of the square column). The metric equivalent of Eq. (5.1) is shown in Table 2.2.

As discussed in Section 4.10.1, V_c of lightly-reinforced connections is sensitive to ρ . EC 2-2003 (CEB-FIP MC 90) is recommended for estimating the existing capacity of lightly-reinforced connections because it recognizes that V_c is a function of ρ . Binici (2003) showed that the CEB-FIP MC 90 gives a better estimation of two-way shear strength of previous researchers' specimens (Eltner and Hognestad, Moe, Corley and Hawkins, Regan, Broms) than the ACI 318-02 does. In addition, as shown in Figure 4.62, Eq. (5.1) provides reasonable estimates (within 17%) for the capacity of specimens G0.5 and G1.0.

The assessment of the existing connections should cover the examination of:

- Details of slab flexural reinforcement (can be obtained from the as-built drawings and using non-destructive evaluation (NDE))
- Actual concrete strength (can be obtained using NDE)

- Condition of concrete substrate around the connections, such as damage level, residual deformation, the moisture condition of the concrete surface, and out-of-plane variations, which are important for evaluating a feasibility of a rehabilitation using CFRP. (can be obtained by visual inspection and using NDE).
- Actual column dimensions and slab thickness (can be obtained using tape measurements, NDE).
- The space limitations for rehabilitation

5.2.1 Damage level

Figure 5.2 shows damage around the connections of specimens LG0.5 and LG1.0 after they were subjected to uniaxial reversed cyclic lateral displacements up to 1.25% drift. The maximum crack widths in specimens LG0.5 and LG1.0 were 0.04 inches and 0.013 inches, respectively. In both specimens, the cracks penetrated through the entire slab thickness and no loose concrete was found around the connection.

Damaged concrete around connection that is less severe than those shown in Figure 5.2 does not need to be replaced. Based on test results of specimens LG0.5 and LG1.0 (Figure 4.61 and Table 4.1), the two-way shear strength of such damaged connections can be assumed equal to that of the undamaged connections. However, a reduction in the two-way shear strength may be expected if there is loose concrete around the connection and all loose concrete should be removed. More detailed information about damage assessment using NDE can be found in Argudo (2006).

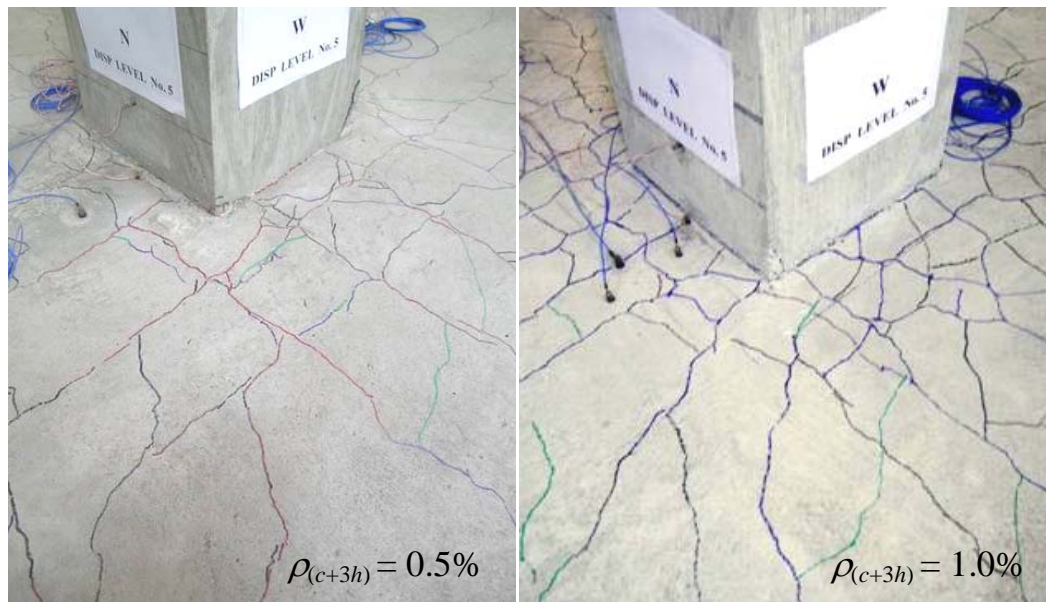


Figure 5.2 Damage after reversed cyclic displacements up to 1.25% drift

5.3 REHABILITATION

If the estimated capacity of the existing slab-column connections is smaller than the required capacity, rehabilitation (for increasing the existing capacity) should be conducted. In order to select the best rehabilitation alternative, the main purpose of the rehabilitation (to improve performance under gravity loads or under seismic loads) needs to be determined and the feasibility of rehabilitation using FRP needs to be evaluated.

5.3.1 General considerations for gravity loads

The relative effectiveness of different rehabilitation methods for improving the performance (two-way shear strength, deformation capacity, and post-punching capacity) of slab-column connection under gravity loads is summarized in Table 5.1. The most effective and the least effective alternatives

are indicated with numbers 1 and 3, respectively. It should be emphasized that each objective does not carry equal weight. All three techniques increased two-way shear capacity of the earthquake-damaged connections and improved the residual capacity after punching shear failure. The installation of the steel collars and the external CFRP stirrups increased the deformation capacity of the connection, whereas the application of CFRP sheets reduced the deformation capacity. For this reason, the application of CFRP sheets is given a (-) for increasing the deformation capacity in Table 5.1.

Table 5.1 Relative effectiveness of different rehabilitation techniques

Objectives	Steel collars	CFRP stirrups	CFRP sheets
Increasing two-way shear capacity of lightly-reinforced connections	2	3	1
Increasing deformation capacity of connections	2	1	(-)
Increasing residual capacity after punching shear failure	3	1	2

5.3.2 General considerations for seismic loads

The use of the steel collars (that extend at least $1.6d$ away from the column face) to repair the earthquake-damaged connections prevented punching shear failures under reversed cyclic lateral displacements and increased lateral load capacity. Luo and Durrani (1994) concluded that the column capital should extend at least $3d$ away from the column face to avoid shear failure of the slab under reversed cyclic lateral displacements. However, test results of Specimen RcL1.0 show that the steel collars that extend $1.6d$ away from the column face could prevent punching shear failure under reversed cyclic lateral displacements.

It should be noted that the use of the steel collars did not restore the original stiffness of the undamaged connections.

In addition to preventing a punching shear failure, it is believed that installing external CFRP stirrups will restore the original stiffness of the undamaged connection because when they were installed on the undamaged connections, Stark (2003, 2005) indicated that the stiffness increased slightly.

The installation of CFRP sheets on the tension surface of the slab increased flexural strength, stiffness, and the lateral load capacity of the connections (Johnson and Robertson 2004). However, it did not prevent punching shear failures of the connections without shear reinforcement, reduced the ductility, and reduced the lateral drift capacity (Johnson and Robertson 2004).

5.3.3 General considerations for rehabilitation using FRP

For any FRP application, ACI Committee 440 (2002) suggested that the maximum localized out-of-straightness variations on concrete surface, including form lines, are $\frac{1}{32}$ inches. All surfaces where FRP is applied should be dry because water in the pores can inhibit resin penetration and reduce mechanical bond. Externally bonded FRP systems should not be applied to concrete substrates containing corroded reinforcing steel because the expansive forces that are associated with the corrosion process can affect the structural integrity of the FRP system.

The installation of FRP system cannot be done in extreme temperatures that are outside of the limits recommended by epoxy manufacturers. Temperatures which are significantly different than the room temperature will also affect the viscosity and the curing time of the epoxy. For an outdoor application, durability must be carefully considered because the durability and long-term performance of FRP systems highly depend on environmental

conditions (such as exposure to sunlight, extreme temperatures, freeze and thaw, and presence of water).

The installation of an FRP wrapping system should be done by skilled workers. Protective clothing that is resistant to epoxy is recommended because skin contact with epoxy may cause skin irritation, such as burns, rashes, and itching. Gloves and respiratory protection are also recommended when cutting and handling CFRP sheets because fibers may become airborne and may cause skin irritation and respiratory complications.

In order to be effective, CFRP stirrups and CFRP sheets must be well-anchored. Closed CFRP stirrups used in this study were superior to CFRP shear studs used in Johnson and Robertson (2004). The 4.5-in deep CFRP anchors used in this study proved to be adequate, whereas 1-in deep carbon tape anchors used by Casadei et al. (2003) were not adequate.

Since the external FRP reinforcement is considered to be essentially nonexistent in the event of fire, the FRP reinforcement is not recommended as a primary dead-load resisting system in order to maintain a proper safety margin in case of fire and to prevent progressive collapse. It is also suggested that the unstrengthened connections should be able to carry at least the self-weight of the slab around it plus the full superimposed dead load acting on the slab. Even though the FRP systems do not intrude with usable space, they require fire-resistant epoxy coating, which can be as thick as 1.5 inches (Kodur et al. 2004). The use of external CFRP stirrups may require fire-proofing on both top and bottom slab surfaces. This may necessitate overhead application of fire proofing material, whereas the use of external CFRP sheets may require fire-proofing only from the top surface.

In general, the external CFRP sheets may not be effective in the connections that have a concentration of slab flexural reinforcement and/or are

reinforced with more than 1% steel. The flexural strength of such connections may be very close to or even higher than their shear strength. Therefore, the use of well-anchored CFRP sheets is only effective for cases in which slab-column connections do not have sufficient flexural reinforcement. Ospina et al. (2001) showed that applying CFRP sheets in cruciform patterns with no anchors on connections reinforced with 0.92% steel was not effective.

5.4 REHABILITATION USING STEEL COLLARS

5.4.1 General

The collars are effective for increasing the two-way shear strength of slab-column connections because they enlarge the critical shear perimeter. The use of steel collars is generally not feasible when there are pipes, HVAC ducts, and slab openings adjacent to columns. Steel collars are not considered to be architecturally pleasing. The installation of steel collars requires work from underneath the slab only.

From a constructability perspective, the installation of steel collars that does not involve dowel or other mechanical connectors (drilling holes in columns) is preferable. Experimental results (Chapter 4) showed that as long as the clamping force was sufficient, the collars that transferred load to the column through friction did not slip and were effective to increase the two-way shear strength. In order to obtain a more uniform contact surface, non-shrink grout can be used to fill the gap between the collars and the bottom slab surface. Important design considerations for friction based steel collars include the size and stiffness of the collars, and the clamping force used to install them.

5.4.2 Size

Martinez et al. (1994) suggested that the size of the collars is selected so that under maximum factored design loads, the nominal shear stress at the critical shear perimeter at $d/2$ away from the edge of the collars is less than $2\sqrt{f_c'}$ psi. As can be seen in Table 4.1, the failure shear stress at the critical perimeter at $d/2$ away from the edge of the collars in specimens RcG0.5 and RcG1.0 are $2\sqrt{f_c'}$ and $2.7\sqrt{f_c'}$, respectively.

In order to prevent punching shear failure under reversed cyclic lateral displacements, the collars should extend at least $2d$ away from the column face and be attached flush with the slab.

5.4.3 Stiffness

In order to be effective, collars should have sufficient stiffness so that they do not deform significantly under loading. Stiffeners and relatively thick plate thickness should be used for the collars to prevent local deformation. Collars should remain elastic under maximum factored design loads. Using a simplified free body diagram shown in Figure 5.3, steel collars can be designed. The design objective is to ensure that the maximum stress at point A is smaller than 50% of the yield stress.

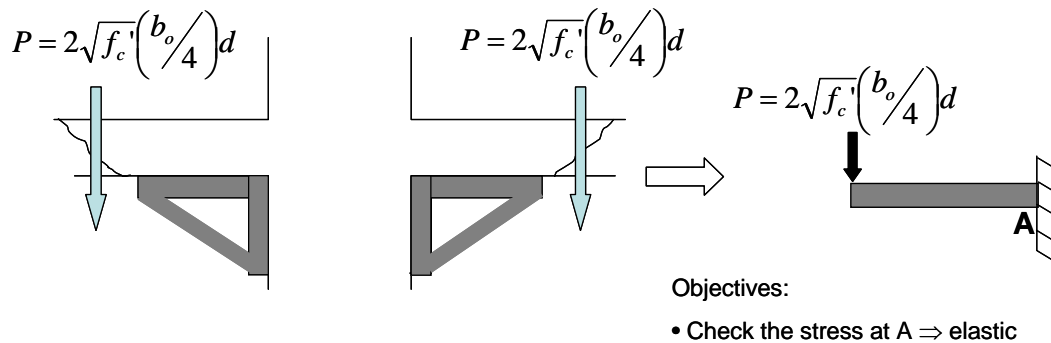


Figure 5.3 Simplified free-body diagram of steel collars

5.4.4 Clamping force

The number and size of threaded rods are determined to produce sufficient clamping force so that collars do not slip. The required total clamping force N is calculated using shear-friction equation as follows:

$$N = \frac{V(\text{F.S.})}{\mu} = nA_{net}f_p \quad (5.2)$$

where V is the total shear force that needs to be transferred to the column, F.S is the factor of safety (F.S=2 is recommended), μ is the coefficient of shear friction between steel and concrete, n is the number of threaded rods, A_{net} is the net area of the threaded rods, and f_p is the prestressing stress of the threaded rods. Since ACI 318-05 recommended that μ for normal weight concrete anchored to structural steel by headed studs or reinforcing bars is 0.7, it is believed that without any dowels, μ can be taken as 0.5. Even though load factors have been used to determine V , the use of F.S. of 2 is recommended in order to account for a non-uniformity of clamping force and a variation in μ .

In order to assure that the design f_p is obtained, a torque-wrench should be used. Since the prestressing stress in a threaded rod decreases as other rods are torqued, it is important to recheck the prestressing stress in all rods after all rods

are torqued. In order to obtain a more uniform contact surface and to improve shear friction, column surface where the collars are attached should be leveled and roughened.

5.5 REHABILITATION USING EXTERNALLY INSTALLED CFRP STIRRUPS

5.5.1 General

The externally installed CFRP stirrups are effective for increasing the two-way shear strength of slab-column connections because they enlarge the critical shear perimeter. Since the shear reinforced zone with the externally installed CFRP stirrups is more flexible than that strengthened with the steel collars, the CFRP stirrups are less effective than the steel collars for increasing the two-way shear strength. However, the rehabilitation with the CFRP stirrups results in a higher deformation capacity than that achieved by using steel collars. Unlike the installation of the steel collars, the installation of CFRP stirrups requires work on both the top and underneath the slab. In addition, externally installed stirrups require fire-proofing on both top and bottom slab surfaces (overhead application of fire proofing material).

Binici (2003) indicated that the use of closed loops was an efficient anchorage method for the vertical legs of CFRP stirrups. Providing multiple anchorage paths for most of the discrete vertical CFRP stirrup locations is important, especially for the outermost stirrups. In the pattern of CFRP stirrups used in specimen LRstG0.5, the alternative anchorage path for the outermost stirrups was along the diagonals. Binici (2003) also reported that the cross-sectional area of diagonal strips should be no less than half the area of primary CFRP stirrups used in the first perimeter. Binici (2003) indicated that in order to develop the strength of the CFRP strips, the minimum anchorage length for CFRP

bonded to CFRP is 6 inches. Therefore, when constructing the stirrups, the CFRP overlaps at the top slab surface must be larger than 6 inches.

5.5.2 Spacing of stirrups

In order to intercept the shear cracks and to prevent the failure inside the CFRP-reinforced zone, the first row of CFRP stirrups should be located as close to the column face as possible. For all practical purposes, the first row of CFRP stirrups can be located at a distance of $d/4$ away from the column face. The other rows of CFRP stirrups should be spaced at about $d/2$.

In order to avoid drilling through rebars, the actual hole locations may vary. In specimen LRstG0.5 (shown in Figure 4.32), the actual distances between the first row of CFRP stirrups and the column face ranged between $d/4$ and $d/2.5$. The actual spacings of the other rows of CFRP stirrups ranged between $d/2.1$ and $d/1.1$. However, these variations did not affect the performance of the rehabilitated specimen. The failure of specimen LRstG0.5 occurred outside the CFRP-reinforced zone.

5.5.3 Strength calculations

There are two failure modes that may occur in a slab-column connection rehabilitated using externally installed CFRP stirrups:

1. Failure inside the CFRP-reinforced zone due to a sudden loss of load carrying capacity as a result of CFRP stirrup failure.
2. Failure outside the CFRP-reinforced zone due to an inclined crack that develops outside the shear reinforced zone.

Therefore, in designing the externally installed CFRP stirrups, the shear strength inside and outside the CFRP-reinforced zone must be checked.

Even though the EC2-2003 (CEB-FIP MC 90) is recommended for evaluating the capacity of existing slab-column connections, the ACI 318-05 is

used as a basis for calculating the two-way shear strength of the connections rehabilitated using externally installed CFRP stirrups. Binici (2003) indicated that ACI 318-02 provisions for two-way shear (which are exactly the same as ACI 318-05) account for a reduction in shear strength as b_o/d (where b_o is the critical shear perimeter and d is the effective depth of the slab) values increase and provide a lower bound for the strength estimations outside the CFRP-reinforced zone. On the other hand, CEB-FIP MC 90 does not account for a reduction in shear strength as b_o/d values increase and overestimates the punching shear capacity outside the CFRP-reinforced zone. Binici (2003) showed that unlike the ACI 318-02, the CEB-FIP MC 90 also incorrectly predicts the location of failure surface of the connections rehabilitated using externally installed CFRP stirrups.

5.5.3.1 Shear strength inside the CFRP-reinforced zone

The shear strength inside the CFRP-reinforced zone can be used to determine the required amount of vertical CFRP material per hole. It is conservative to use the same amount of CFRP stirrups in all holes based on the required amount of CFRP stirrups for the first row (located at $d/4$ away from the column face). Therefore, instead of performing calculations for every CFRP perimeter, it is sufficient to analyze the shear strength at the critical shear perimeter $d/2$ away from the column face.

The *total* shear strength inside the CFRP-reinforced zone $V_{T,i}$ for an interior column can be calculated as follows:

$$V_{T,i} = V_c + V_{CFRP} \leq 8\sqrt{f_c'}b_o d \quad (5.3)$$

$$V_c \text{ is the lesser of : } \begin{cases} V_c = 2\sqrt{f'_c} b_o d \\ V_c = \left(\frac{40 \times d/b_o + 2}{4} \right) \times 2\sqrt{f'_c} b_o d \end{cases} \quad (5.4)$$

$$V_{CFRP} = 0.004 E_{CFRP} A_{CFRP} \quad (5.5)$$

where V_c and V_{CFRP} are the concrete and CFRP contributions, respectively, inside the CFRP-reinforced zone, b_o is the critical shear perimeter calculated at a distance of $d/2$ away from the column face, E_{CFRP} is the elastic modulus of CFRP, and A_{CFRP} is the total cross-sectional area of CFRP per perimeter.

It is recommended that relevant V_c expressions of ACI 318-05 (Eqs. (2.56) and (2.57)) are reduced to those shown in Eq. (5.4) because the shear reinforced zone with externally installed CFRP stirrups is flexible and the shear strength decreases as the stiffness of the connection decreases (Hawkins and Mitchell 1979). Recommended V_c terms expressed in Eq. (5.4) are half of V_c of ACI 318-05 (Eqs. (2.56) and (2.57)). As will be shown in Section 5.5.5, V_c of ACI 318-05 significantly overestimates (190%) the two-way shear capacity of specimen LRstG0.5, whereas the use of the recommended V_c (Eq. (5.4)) results in a slightly conservative estimation (within 5%) of the capacity of specimen LRstG0.5.

In order to prevent concrete crushing inside the CFRP-reinforced zone, Binici (2003) recommended that $V_{T,i}$ should be limited to $8\sqrt{f'_c} b_o d$. In Eq. (5.5), 0.004 is the recommended usable strain in externally installed CFRP stirrups (Binici 2003). Binici indicated that when the CFRP strain is larger than 0.004, the connection is prone to shear failure inside the CFRP-reinforced zone because wide shear cracks reduce concrete contribution to punching shear significantly.

The required area of CFRP per hole, $A_{CFRP/hole}$, and the required number of CFRP legs per hole, n_{leg} , can be calculated as follows:

$$A_{CFRP/hole} = \frac{A_{CFRP}}{n_{hole}} \quad (5.6)$$

$$n_{leg} = \frac{A_{CFRP/hole}}{w_{CFRP} t_{CFRP}} \quad (5.7)$$

where n_{hole} is the number of holes per CFRP perimeter, w_{CFRP} and t_{CFRP} are the width and thickness, respectively, of CFRP strips.

5.5.3.2 Shear strength outside the CFRP-reinforced zone

The shear strength outside the CFRP-reinforced zone governs the required number of CFRP perimeters. Using the ACI 318-05 concept, the shear strength outside the CFRP-reinforced zone is calculated at the critical shear perimeter located at $d/2$ away from the outermost of CFRP stirrups.

The total shear strength outside the CFRP-reinforced zone $V_{T,o}$ is equal to concrete contribution V_c , expressed in Eq. (5.4). For the pattern of CFRP stirrups used in specimen LRstG0.5, b_o for the shear perimeter located at $d/2$ away from the outermost of CFRP stirrups can be calculated as follows:

$$b_o = 4 \left[c + \left\{ \sqrt{2} d (0.5 n_{per} + 0.25) \right\} \right] \quad (5.8)$$

where c is the dimension of the square column, n_{per} is the number of CFRP perimeters.

5.5.4 Proposed rehabilitation design procedure

The proposed rehabilitation design procedure for gravity loads shown in Figure 5.4 can be summarized as follows:

1. Assess the geometric and material properties of the slab-column connection and determine the required strength $V_{required}$.

2. Confirm that $V_{required}$ is less than the maximum capacity of $8\sqrt{f_c}b_o d$. If not, reduce $V_{required}$ by decreasing the gravity loads or load rating the building.
3. Evaluate the existing capacity V_n using the Euro Code EC 2-2003 (CEB-FIP MC 90). For slab-column connections without any shear reinforcement, $V_n = V_c$, where V_c is expressed in Eq. (5.1).
4. If $V_{required} > V_n$, rehabilitate the slab-column connection.
5. Select pattern of externally installed CFRP stirrups and measure the geometric and material properties of CFRP stirrups.
6. Determine the required area of CFRP per hole, $A_{CFRP/hole}$, and the required number of CFRP legs per hole, n_{leg} , by calculating the shear strength inside the CFRP-reinforced zone, at the critical shear perimeter located at $d/2$ away from the column face.
7. Determine the required number of CFRP perimeters n_{per} by calculating the shear strength outside the CFRP-reinforced zone, at the critical shear perimeter locate at $d/2$ away from the outermost stirrups.

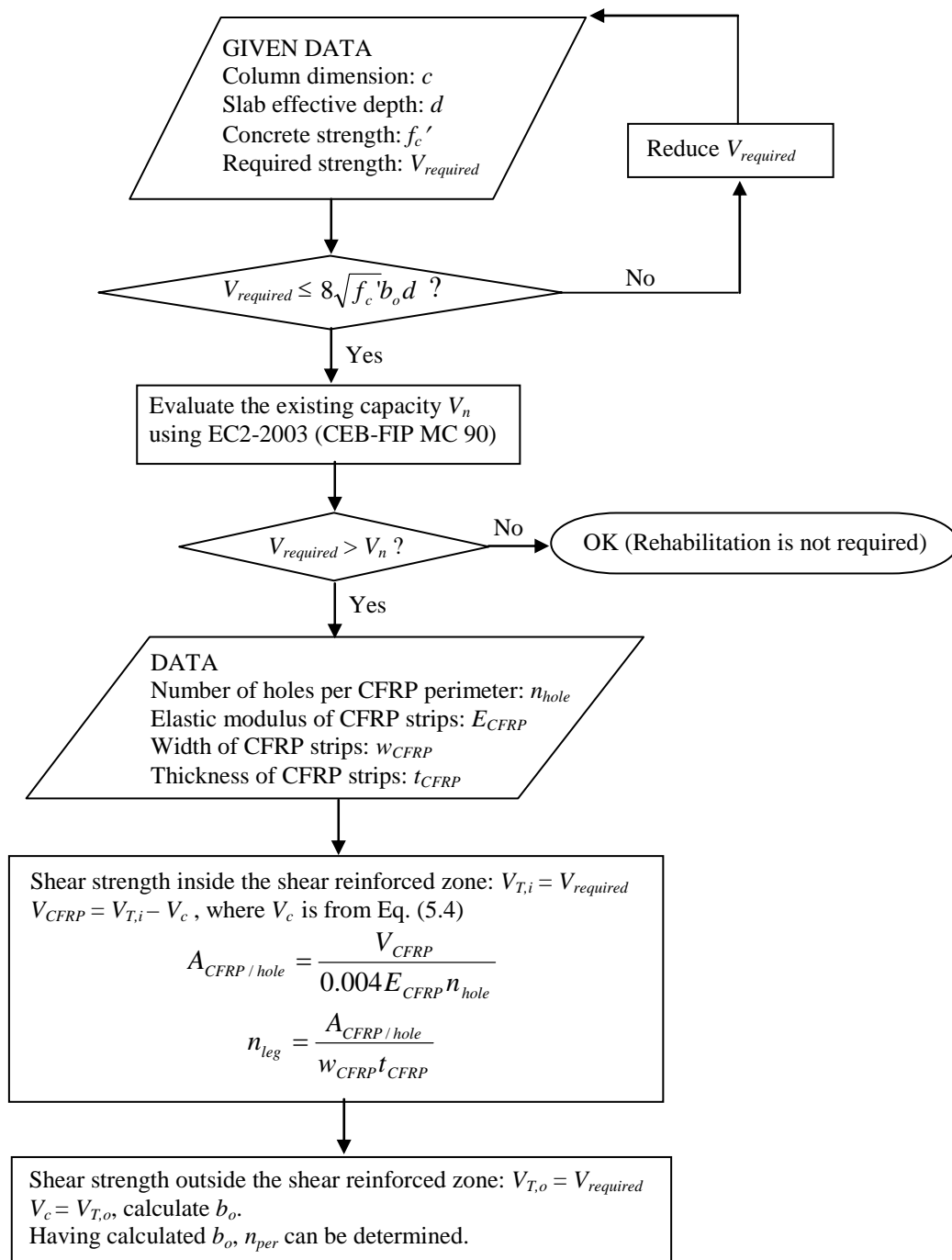


Figure 5.4 Design procedure for rehabilitation using external CFRP stirrups

5.5.5 Example calculations – Specimen LRstG0.5

In order to illustrate the design procedure, the calculated two-way shear capacity of the rehabilitated specimen LRstG0.5 was compared with the failure load. Geometric and material properties of specimen LRstG0.5 and details of rehabilitation are summarized in Table 5.2.

Table 5.2 Geometric and material properties of specimen LRstG0.5

Properties	Values
Column dimension, c	16 in.
Slab effective depth, d	5 in.
Concrete strength, f_c'	4900 psi
Number of holes per CFRP perimeter, n_{hole}	8
Elastic modulus of CFRP strips, E_{CFRP}	10500 ksi
Width of CFRP strips, w_{CFRP}	0.75 in.
Thickness of CFRP strips, t_{CFRP}	0.04in.
Number of CFRP legs per hole, n_{leg}	4
b_o at $d/2$ away from the column face	84 in.
b_o at $d/2$ away from the outermost stirrups (measured)	135 in.

Using the procedure outlined in Section 5.5.3, the calculated shear strengths inside and outside the CFRP-reinforced zone are 99 kip and 83 kip, respectively. Since the calculated strength outside the CFRP-reinforced zone is less than that inside the CFRP-reinforced zone, the failure is expected to occur outside the CFRP-reinforced zone. As shown in Table 4.1, the failure load of specimen LRstG0.5 was 86.5 kip. Figure 4.34 shows that the failure occurred outside the CFRP-reinforced zone. The calculated shear strength and the expected failure surface location are consistent with the experimental results.

As shown in Table 4.1, the calculated failure shear stress at the critical shear perimeter $d/2$ away from the outermost CFRP stirrups of specimen LRstG0.5 is $1.8\sqrt{f_c'}$. Using the V_c of ACI 318-05 (Eq. (2.56)), the estimated

failure shear stress is $3.5\sqrt{f_c'}$, which is roughly twice as large as the measured capacity. Using the recommended V_c (Eq. (5.4)), the estimated failure shear stress is $1.7\sqrt{f_c'}$, which is a reasonable and conservative (within 5%) estimate.

5.6 REHABILITATION USING EXTERNALLY INSTALLED CFRP SHEETS

5.6.1 General

The externally installed CFRP sheets are effective for increasing the two-way shear strength of slab-column connections because they limit the width of flexural cracks so that the area of concrete resisting shear is maintained and the connection can carry more loads before a punching shear failure occurs. Unlike the installation of steel collars and CFRP stirrups, the installation of CFRP sheets does not require overhead work.

CFRP sheets should be applied on the tension surface of the slab. Robertson and Johnson (2001, 2004) indicated that the application of CFRP sheets on the bottom surface of the slab did not improve the performance of the connection. Since bonding the slabs uni-directionally with FRP reinforcement did not lead to significant increases in punching shear capacity (Tan 2000), CFRP sheets should be applied in both orthogonal directions. CFRP sheets should be placed as close to the column as possible because it is believed that the closer to the column the CFRP sheets are, the more effective they become. In order to prevent early delamination, CFRP sheets must be well-anchored.

Important design considerations for externally installed CFRP sheets include (i) designing anchors and (ii) determining the length and the amount of CFRP sheets.

5.6.2 CFRP Anchors

CFRP anchors must be installed right after CFRP sheets have been placed, before the epoxy is cured, so that both CFRP anchors and sheets can act as an integral system.

5.6.2.1 Position

Four CFRP anchors per column corner, shown in Figure 5.5 were very effective in preventing delamination. The first row of CFRP anchors should be located at $d/2$ away from the column face.

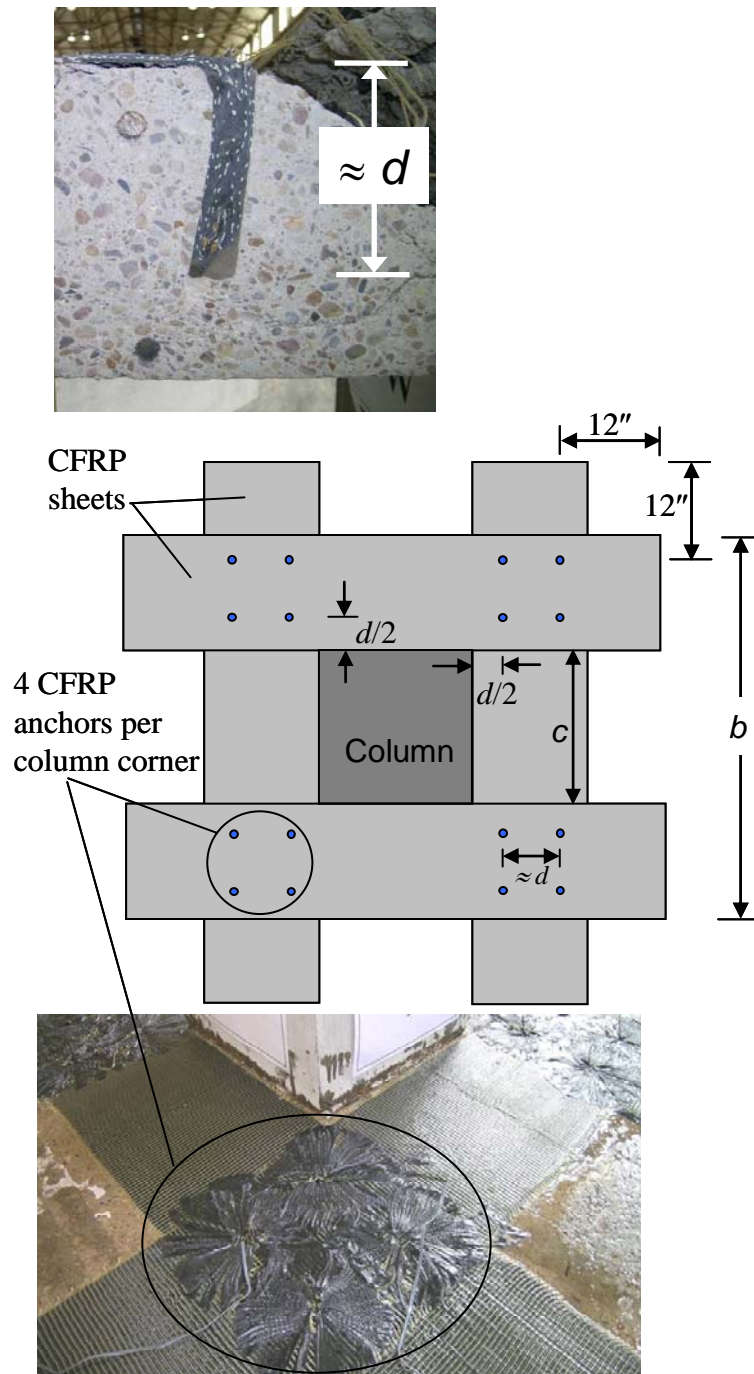


Figure 5.5 Recommended details of CFRP sheets and anchors

5.6.2.2 Cross-sectional area

Since the CFRP anchors provide anchorage for the CFRP sheets in orthogonal directions, the total area of all CFRP anchors should be equal to the $\sqrt{2}$ times the total area of the CFRP sheets to be anchored. However, even though the total area of all CFRP anchors in specimen LRshG0.5 is equal to the total area of the CFRP sheets, no anchor failure was observed.

5.6.2.3 Depth

The depth of the anchor should be roughly equal to the effective depth of the slab (Figure 5.5).

5.6.3 Length of the CFRP sheets

CFRP sheets can be terminated about 12 inches beyond the location of the last anchor (Figure 5.5).

5.6.4 Area of the CFRP sheets

Since the CFRP sheets placed further away from the column are not as effective as those placed adjacent to the column, the width of CFRP sheets on each column side should be kept between $1.5h$ and $2.5h$, where h is the slab thickness. The amount of CFRP sheets is determined by matching the flexural capacity of the connection with the required flexural reinforcement ratio to reach $V_{required}$. The proposed rehabilitation design procedure for determining the required amount of CFRP sheets shown in Figure 5.6 can be summarized as follows:

1. Assess the geometric and material properties of the slab-column connection and determine the required strength $V_{required}$. (For normal-weight concrete with f_c' between 4000 psi and 5000 psi, $\epsilon_c' \approx 0.002$).

2. Evaluate the existing capacity V_n using the Euro Code EC 2-2003 (CEB-FIP MC 90). For slab-column connections without any shear reinforcement, $V_n = V_c$, where V_c is expressed in Eq. (5.1).
3. If $V_{required} > V_n$, rehabilitate the slab-column connection.
4. Using EC2-2003 (CEB-FIP MC 90), find the required flexural reinforcement ratio $\rho_{required}$ to reach $V_{required}$.
5. By selecting the width of CFRP sheets on each side of the column (between $1.5h$ and $2.5h$), the total width of the column plus CFRP sheets on both sides, b , and the total area of CFRP sheets on both sides of the column, A_F , are known ($A_F = w_F \times t_F$, where w_F is the width of the CFRP sheet on each side of the column and t_F is the thickness of the CFRP sheet).
6. Calculate the flexural capacity of the rectangular section that has the width b and the flexural reinforcement ratio $\rho_{required}$ (calculated in step 4), M_o . Figure 5.7 shows the procedure for calculating M_o .
7. Calculate the flexural capacity of the rectangular section that has the width b and the existing flexural reinforcement ratio ρ , rehabilitated with CFRP sheets, M_F . If M_F is significantly less than M_o , increase A_F by increasing the width of CFRP sheets w_F or applying additional CFRP sheets and CFRP anchors. Figure 5.8 shows the procedure for calculating M_F .

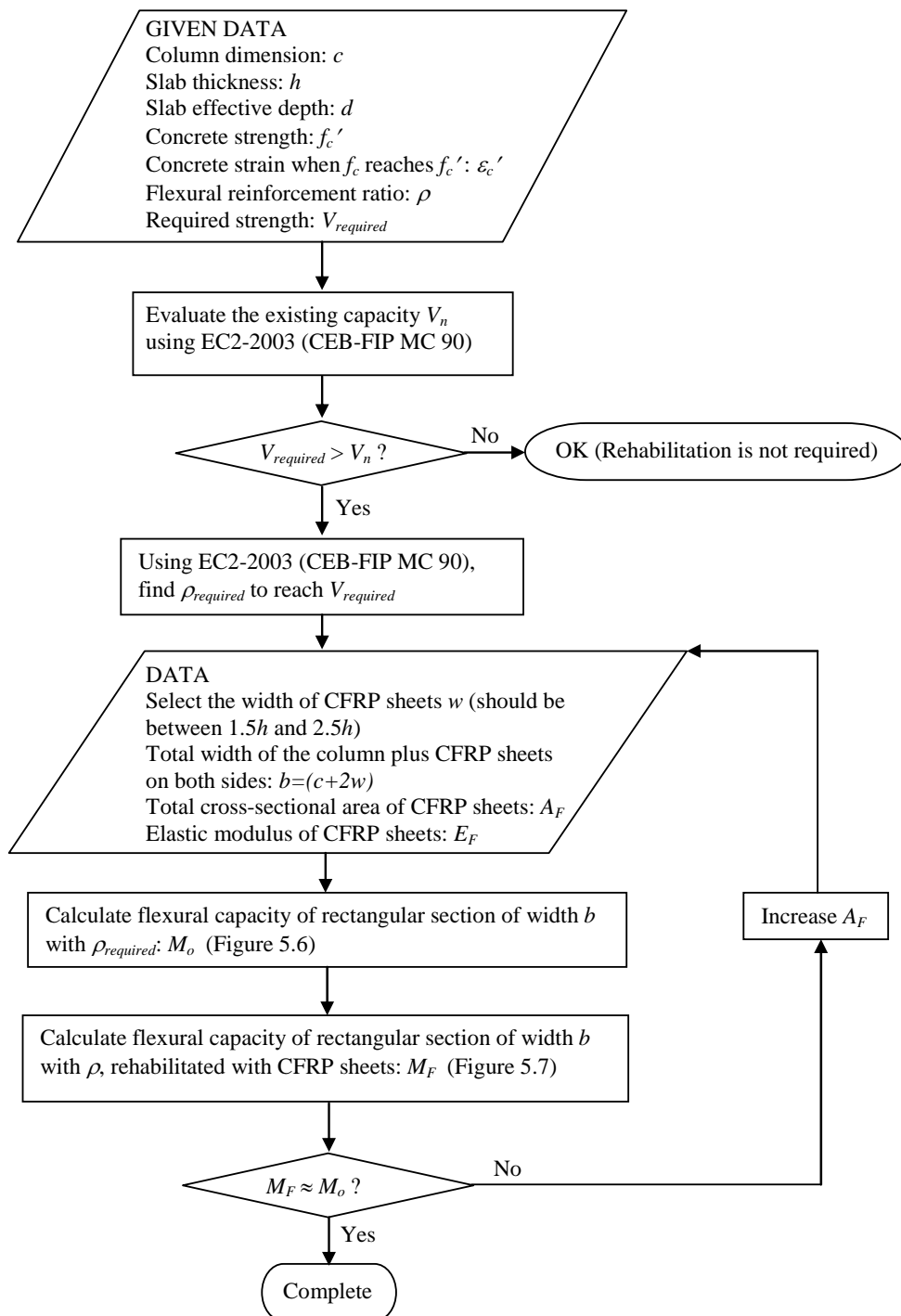
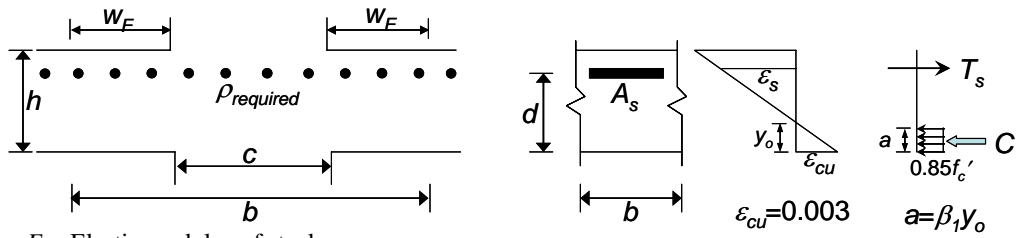


Figure 5.6 Design procedure for rehabilitation using external CFRP sheets



E_s : Elastic modulus of steel

ϵ_y : Yield strain of steel

b should be between $(c+3h)$ and $(c+5h)$, depending on the width of FRP sheets

Ignore compression reinforcement (they are not continuous)

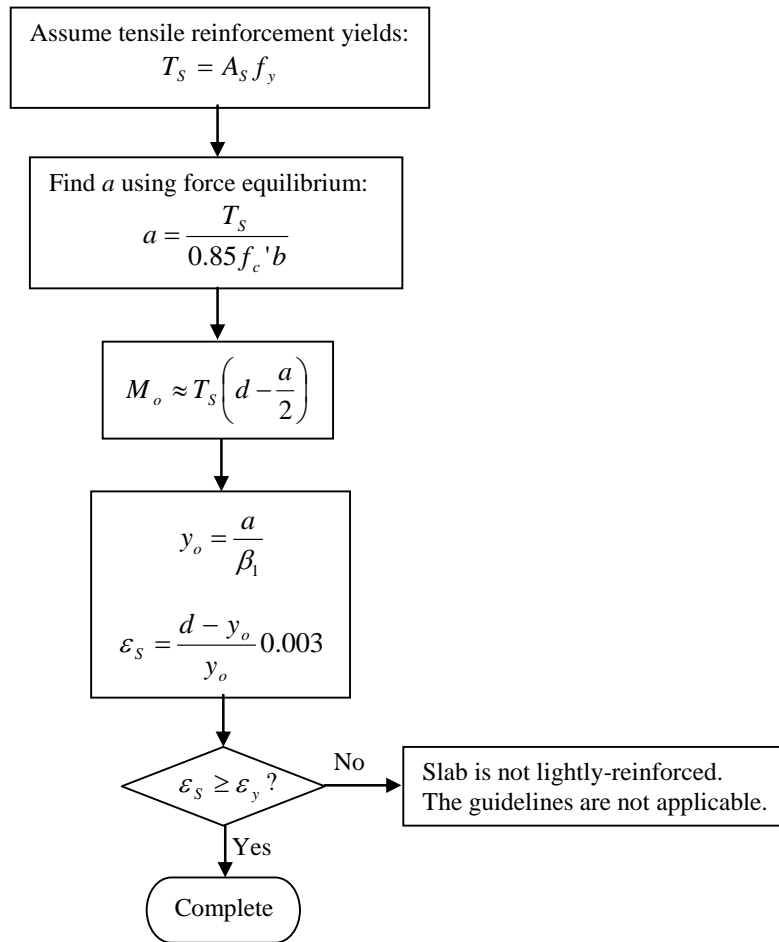
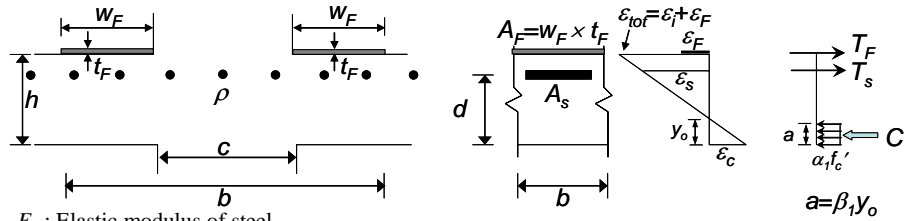


Figure 5.7 Procedure for calculating M_o



E_S : Elastic modulus of steel

E_F : Elastic modulus of CFRP sheets

ϵ_y : Yield strain of steel

α_1, β_1 : Stress block factors

ϵ_i : Strain level in the concrete substrate at the time of CFRP installation

Experimental results show that after subjected to a simulated seismic test up to 1.25% lateral drift, $\epsilon_i \approx 0.006$. Parametric study shows that M_F is insensitive to ϵ_i .

ϵ_F : Effective strain level in the CFRP sheets at ultimate

Recommendation based on Figures 4.42 and 4.43 : $\epsilon_F = 0.004$

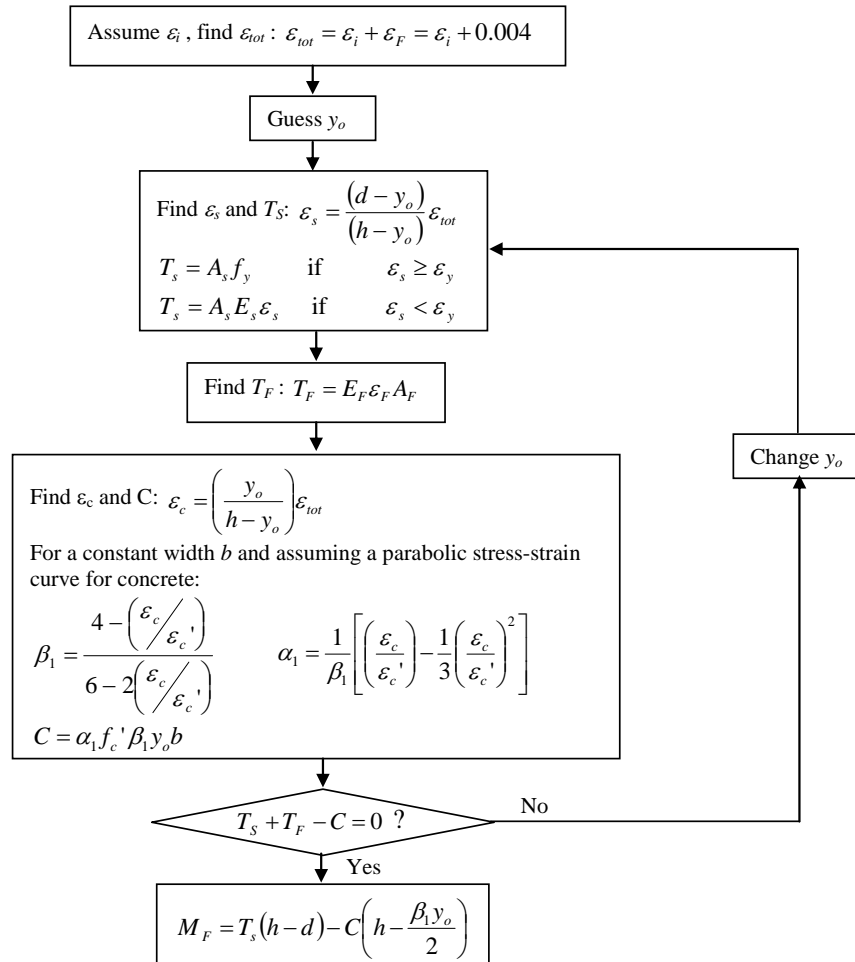


Figure 5.8 Procedure for calculating M_F

5.6.5 Verification using experimental results

The amount of CFRP sheets in specimen LRshG0.5 was selected to produce the same flexural capacity as that of the connection with 1.0% steel (specimen G1.0). In order to verify the design procedure, the two-way shear capacity of the rehabilitated specimen LRshG0.5 was compared with that of specimen G1.0. Geometric and material properties of specimen LRshG0.5 and details of rehabilitation are summarized in Table 5.3.

Table 5.3 Geometric and material properties of specimen LRshG0.5

Properties	Values
Column dimension, c	16 in.
Slab thickness, h	6 in.
Slab effective depth, d	5 in.
Concrete strength, f_c'	4600 psi
Concrete strain when f_c reaches f_c' , ε_c'	0.002
Yield stress of steel, f_y	68 ksi
Flexural reinforcement ratio, ρ	0.5%
Total width of column plus CFRP sheets, b	40 in.
Total cross-sectional area of CFRP sheets, A_F	0.96 in. ²
Elastic modulus of CFRP strips, E_{CFRP}	10500 ksi
Initial concrete strain, ε_i	0.006
Effective strain level in the CFRP sheets at ultimate, ε_f	0.004

The calculated flexural capacity of specimen G1.0 within the width $b=40$ inches ($c+4h$) using the procedure shown in Figure 5.7 is roughly 564 k.in. The calculated flexural capacity of specimen LRshG0.5 within the width $b=40$ inches using the procedure shown in Figure 5.8 is roughly 545 k.in. The failure loads of specimens G1.0 and LRshG0.5 were 90.2 kip and 97.5 kip, respectively. It can be concluded that increasing the flexural capacity of lightly-reinforced connections

by applying CFRP sheets to match that of a connection with a higher percentage of steel give about the same two-way shear strength.

5.7 SUMMARY

Guidelines for evaluation and rehabilitation of lightly-reinforced ($\rho \leq 1.0\%$) slab-column connections are presented in Chapter 5. For evaluating the existing two-way shear capacity, the use of the Euro Code EC 2-2003 (Model Code CEB-FIP MC 90) is recommended.

Important design considerations for each one of the three rehabilitation techniques are discussed. The three rehabilitation techniques and these considerations are:

4. Installation of friction based steel collars on the column under the slab
 - Size of the collars
 - Stiffness of the collars
 - Clamping force
5. Installation of external CFRP stirrups
 - Spacing of stirrups
 - Shear strength inside and outside the CFRP reinforced zone
6. Application of well-anchored CFRP sheets on the tension side of the slab
 - Position, amount, and depth of anchors
 - Length of CFRP sheets
 - Amount of CFRP sheets

CHAPTER 6

Summary and Conclusions

6.1 GENERAL

Results of the experimental study and conclusions based on the experimental results are summarized in this chapter. In addition, the questions that arose after reviewing literature are addressed and recommendations for future research are presented. The organization of Chapter 5 is as follows: Summary of the experimental program is presented in Section 5.2. Conclusions of this experimental study are reported in Section 5.3. Questions listed in Section 2.10 are also addressed in Section 5.3. Several recommendations for future research are discussed in Section 5.4.

6.2 SUMMARY

Flat plate structures require relatively simple formwork, which reduces construction time and cost, and such structures provide more clear space for given story heights. However, the structural system is also prone to brittle shear failure at slab-column connections, which may result in the progressive collapse of a building. For that reason, connections with insufficient two-way shear strength may need to be rehabilitated and rehabilitation can be a cost-effective alternative to replacement.

The focus of this study was on the rehabilitation of slab-column connections in existing structures built in the mid 20th century. The main objectives of this study were to develop efficient strengthening methods for deficient connections that do not satisfy current code requirements and to develop

efficient post-earthquake repair methods for connections that experience seismic-damage. Three alternatives for repairing and strengthening slab-column connections were experimentally evaluated: (i) installation of steel collars on the columns underneath the slab, (ii) installation of external Carbon Fiber Reinforced Polymers (CFRP) stirrups, and (iii) application of well-anchored CFRP sheets on the tension side of the slab. In addition to the two main objectives, an indirect objective of this study was to evaluate the effects of earthquake-damage and flexural reinforcement ratio on two-way shear strength of slab-column connections.

Seven 2/3-scale interior slab-column connections were tested to quantify the effects of low flexural reinforcement ratio, earthquake-damage, and the efficiency of various rehabilitation techniques on the two-way shear strength of connections. In order to study the two-way shear capacity of earthquake-damaged connections, two different test setups were used. The first test setup was designed to simulate seismic loading (combination of reversed cyclic lateral displacements simulating the effects of a ground motion and a constant vertical load simulating the effects of gravity loads acting on the connection during an earthquake). The second test setup is for punching shear tests (monotonically increasing concentric vertical loads). Boundary conditions for both simulated seismic tests and punching shear tests were determined based on non-linear finite element analyses to match the internal force distribution in the prototype structure.

Five specimens represented typical connections in flat-plate structures built in the mid 20th century, which had 0.5% flexural reinforcement ratio in the column strip. Since typical connections in flat-plate structures built recently have a concentration of flexural reinforcement within the $(c+3h)$ region, in order to compare the performance of the typical connections built several decades ago with those built recently and to study the effect of concentration of steel on the

two-way shear strength, two specimens with 1.0% top steel within the $(c+3h)$ region were also tested. In this chapter, typical interior connections in flat-plate structures built in the mid 20th century are referred to as the “older” connections and those built recently are referred to as the “modern” connections.

6.3 CONCLUSIONS

6.3.1 General behavior of connections in older structures

The most common details of the older connections are: (i) no shear reinforcement, (ii) lack of concentration of the slab top flexural reinforcement near the column, and (iii) low flexural reinforcement ratio in the column strip (i.e. $\rho=0.5\%$).

The general behavior of the older connections under concentric gravity loads was studied by analyzing the behavior of specimen G0.5. Since the capacity of specimen G0.5 was very close to that estimated using the yield-line theory, it can be concluded that the capacity of specimen G0.5 was very close to its flexural capacity, which was smaller than its two-way shear capacity. Even though the failure surface of specimen G0.5 looked the same as that in a typical punching shear failure (i.e. the column together with a slab portion pushed through the slab), the failure occurred after widespread yielding of longitudinal reinforcement. Yielding of slab reinforcement resulted in large flexural cracks that reduced concrete contribution to shear strength and caused early punching shear failure.

The behavior of the older connections during strong ground motions was assessed by studying the behavior of specimen L0.5. It can be concluded that the seismic performance of the older connection details was poor. Specimen L0.5 was subjected to reversed cyclic lateral displacements and failed in punching shear at 2% drift. The ACI code provisions (Section 21.11.5 ACI 318-05), which were

added in the 2005 code to reduce the likelihood of slab punching shear failure, indicate that shear reinforcement for the interior connections with $\left(\frac{V_u}{\phi V_c} = 0.3\right)$ (where $\left(\frac{V_u}{\phi V_c}\right)$ is the ratio of the shear force V_u to the nominal shear strength ($V_c = 4\sqrt{f_c'}b_o d$) reduced by $\phi = 0.75$) is not required when the design story drift ratio is 2% or less. However, the results of this experimental study indicate that without shear reinforcement, specimen L0.5 failed in punching shear at 2% drift.

6.3.2 Effect of flexural reinforcement ratio

In order to study the effect of flexural reinforcement ratio on the performance of connections behavior under concentric gravity loads, the behavior of specimen G0.5 can be compared with that of specimen G1.0. Both specimens were identical in all aspects but the amount of slab top reinforcement ratio ρ within the $(c+3h)$ region. Since the capacity of specimen G1.0 was 30% higher than that of specimen G0.5, it can be concluded that the two-way shear capacity was sensitive to ρ within the $(c+3h)$ region. In lightly-reinforced slab-column connections (i.e. $\rho = 0.5\%$), increasing ρ within the $(c+3h)$ region resulted in a reduction in rebar strains (means a reduction in flexural-crack widths and an enhancement of aggregate interlock contribution to the shear strength) and an improvement of the two-way shear strength.

The effect of ρ within the $(c+3h)$ region on the seismic behavior of slab-column connections can be studied by comparing the behavior of specimen LG1.0 with that of specimen L0.5. From this comparison, it can be concluded that

increasing ρ within the $(c+3h)$ region was effective in increasing the stiffness and the lateral load capacity of the slab-column connections.

6.3.3 Estimation of the capacity of existing connections

The results of this study show that the capacity of the older connections (specimen G0.5) was significantly overestimated (between 17% and 87%) by the American Concrete Institute ACI 318-05, Canadian Standards CSA A.23.3-04, Australian Standards AS 3600-1994, Indian Standards IS-456, Euro Code EC2-2003, Model Code MC-90, British Standards BS 8110-97, and JSCE (Japan Society of Civil Engineers) 1986. Since the two-way shear capacity was sensitive to ρ , the degree of the overestimation was larger for the code provisions that did not explicitly consider ρ as a parameter affecting the two-way shear strength (ACI 318-05, CSA A.23.3-04, AS 3600-1994, and IS-456). Unlike the other building codes, *Deutsches Institut für Normung* DIN 1045-1 provided a 20% conservative estimate of the capacity for the older connections. It is interesting to note that the capacity of the modern connections (specimen G1.0) was also overestimated (between 9% and 36%) by ACI 318-05, CSA A.23.3-04, AS 3600-1994, EC2-2003, MC-90, BS 8110-97, and JSCE 1986.

The capacity of specimens G0.5 and G1.0 could be estimated by the yield-line theory very well (within 3%). The two-way shear strength of specimens G0.5 and G1.0 could be estimated by the relatively simple equations derived by Nolting (1984) and Gardner (1996) reasonably well (within 8%). And the lower and upper bounds of the capacities of both specimens G0.5 and G1.0 could be provided by the strip model (Alexander and Simmonds 1992 and Afhami et al. 1998).

It can be concluded that, since existing connections are lightly-reinforced ($\rho \leq 1.0\%$), most code provisions cannot be used for estimating the two-way shear

capacity of these connections. For evaluating the two-way shear capacity of existing connections, calculating the flexural strength using the yield-line theory is recommended.

6.3.4 Effect of seismic damage

The effect of seismic damage was studied by comparing the behaviors of specimens LG0.5, LG1.0 with those of their companion specimens G0.5, G1.0 that were undamaged. This comparison shows that seismic damage in the connection region due to uniaxial reversed cyclic lateral displacements up to 1.25% lateral drift had no noticeable adverse effects on the two-way shear strength of lightly-reinforced connections tested in this study.

6.3.5 Residual capacity after punching shear failure

It can be concluded that the top slab rebars were not always effective for providing V_r . In some cases increasing the number of top slab rebars crossing the punching cone by enlarging the critical shear perimeter increased the residual capacity after punching shear failure, V_r . However, in other cases, increasing the number of top slab rebars crossing the punching cone by increasing ρ (reducing the spacing of rebars) was not effective for increasing V_r . Since the top slab rebars were not always effective for providing V_r , they should not be relied on.

When the rebars intersecting the shear crack yielded, V_r also reduced. For this reason, large cracks and yielding of reinforcement crossing those cracks due to seismic-damage in the connection region reduced V_r . This reduction was smaller for connections with a higher ρ because at the same drift level,

connections with a higher ρ had smaller crack widths and smaller inelastic reinforcing bar strains.

6.3.6 Rehabilitation

All three rehabilitation techniques studied during the course of this research could be used to repair lightly-reinforced earthquake-damaged connections. As part of the rehabilitation techniques studied herein, removal and replacement of the damaged concrete was not necessary. Gravity-feed epoxy was used to fill cracks instead of using epoxy injection. Rehabilitation could also be performed on connections under service loads, without shoring.

6.3.6.1 Installation of steel collars on the column under the slab

The collars made from structural steel tubes that were clamped to the column under the slab were effective in enlarging the critical shear perimeter and hence increasing the two-way shear capacity. Enlargement of the failure surface also increased the number of reinforcing bars crossing the shear cracks and hence increased V_r .

The steel collars that extended $1.6d$ away from the column face were also effective in improving the seismic behavior of damaged slab-column connections by preventing punching shear failure and increasing lateral load capacity. It is believed that the use of dowels or shear keys was not necessary and as such the collars were not attached to the slab. Under simulated seismic displacements, the rehabilitated connection (specimen RcL1.0) failed in one-way shear. Flexure-shear cracks initiated the development of large flexural cracks across the slab at the location where the slab top rebars were terminated. It can be concluded that the reinforcement detailing affected the seismic-performance of the connections repaired with steel collars.

6.3.6.2 Installation of external CFRP stirrups

A tightly knit array of CFRP stirrups increased the critical shear perimeter and therefore increased the two-way shear strength of connections. Even though the rehabilitation with the externally installed CFRP stirrups was less effective than that with the steel collars for increasing the two-way shear strength, the rehabilitation with the CFRP stirrups resulted in a higher deformation capacity than that with the collars.

Enlargement of the failure surface increased the number of reinforcing bars contributing to the resistance following punching shear failure and hence increased V_r . Since the tightly knit array of CFRP stirrups also prevented stripping out of the tensile flexural reinforcement, CFRP stirrups were more effective than the steel collars in increasing V_r .

6.3.6.3 Application of well-anchored CFRP sheets

The well-anchored CFRP sheets were as effective as the steel reinforcement for increasing the flexural strength. Since the two-way shear capacity of lightly-reinforced connections increased as the flexural strength (or flexural reinforcement ratio) increased, the application of well-anchored CFRP sheets on the tension side of the slab improved the two-way shear strength of lightly-reinforced connections. The CFRP sheets did not change the location of the failure surface but limited the width of the flexural cracks so that the area of concrete resisting shear was maintained and the connection was able to carry more load before a punching shear failure occurred.

The test conducted on specimen LRshG0.5 clearly showed that CFRP sheets could be anchored, early delamination could be prevented, and as a result the ultimate strength of CFRP sheets could be exploited. Four CFRP anchors per column corner were very effective in preventing delamination due to prying

action when the column pushed through the slab. At failure, CFRP sheets close to the middle of the column face ruptured, whereas the sheets elsewhere were still attached to the slab. After punching shear failure occurred, the well-anchored CFRP sheets acted as tension bands, allowed the slab to carry a substantial shear force (53% of V_{max}) through larger deformations, and thus increased V_r .

6.4 RECOMMENDATIONS FOR FUTURE RESEARCH

The following recommendations can be made based on the comprehensive literature review and the findings of the study:

1. Pan and Moehle (1992) indicated that the results of biaxial tests showed significant reductions in strength, drift capacity, ductility, and stiffness compared with the results of equivalent uniaxial tests. In addition, the specimens repaired using concrete patching and subjected to biaxial cyclic lateral displacements showed significant reduction in original strength and stiffness. In this research, the seismic-damage in the connection region due to uniaxial cyclic lateral displacements up to 1.25% drift had no noticeable adverse effects on the two-way shear strength of lightly-reinforced connections. Research should be conducted to determine the effects of seismic-damage due to biaxial cyclic lateral displacements on the two-way shear strength.
2. Research needs to be conducted on the effectiveness of steel collars, fire-proofed CFRP stirrups and CFRP sheets subjected to elevated temperatures. Evaluation of the loss in clamping force of the steel collars due to elevated temperatures is necessary.
3. The installation of external CFRP stirrups was the most efficient method to increase the deformation capacity and the residual capacity after punching shear failure. However, the installation of external CFRP

stirrups was the least efficient method to increase the two-way shear capacity of the connections. Even though the installation of external CFRP sheets was the most efficient method to improve the two-way shear capacity, it reduced the deformation capacity. Research needs to be conducted to study the effectiveness of a rehabilitation method in which a combination of CFRP stirrups and well-anchored CFRP sheets is evaluated.

4. Research should be conducted to study the effect of seismic-damage and the effectiveness of rehabilitation methods on the two-way shear strength of slab-column connections in post-tensioned flat-plate structures.

APPENDIX A

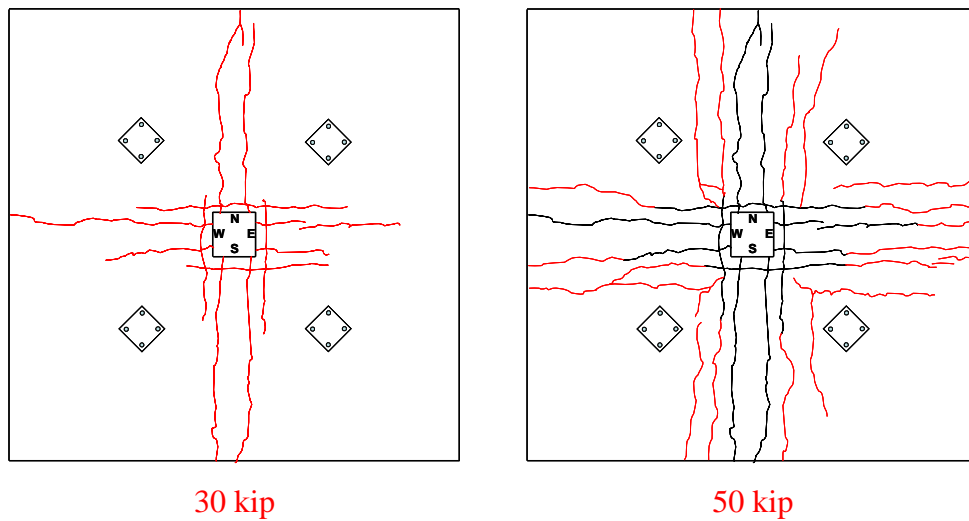
Crack patterns

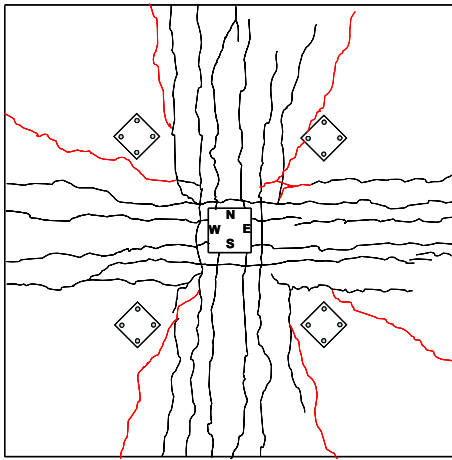
A.1 GENERAL

Crack patterns for all specimens at different loading stages are shown in Appendix A. Cracks shown in red color are the new cracks that form at the corresponding loading stage.

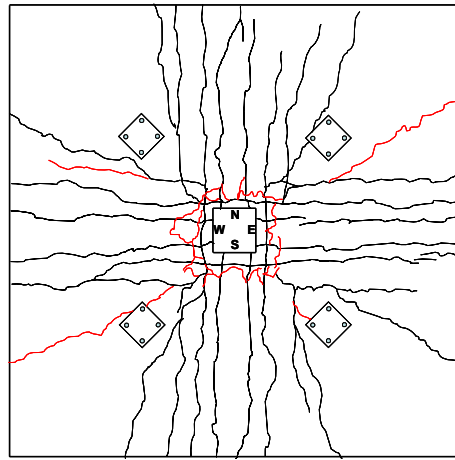
A.2 SPECIMEN G0.5

A.2.1 Top surface





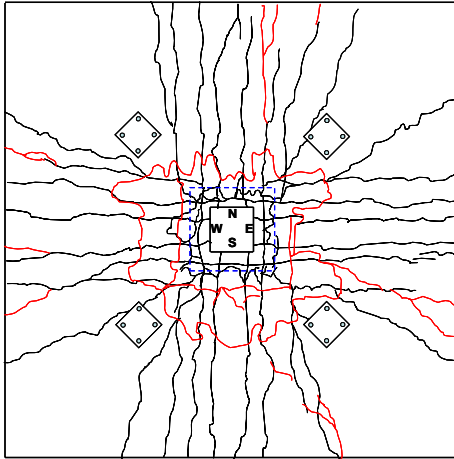
65 kip



Failure (69.9 kip)

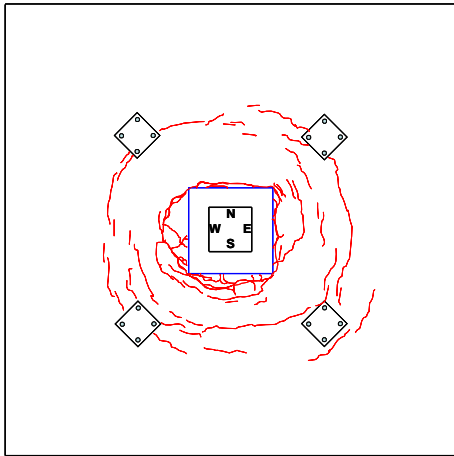
A.3 SPECIMEN RCG0.5

A.3.1 Top surface



Failure (101.3 kip)

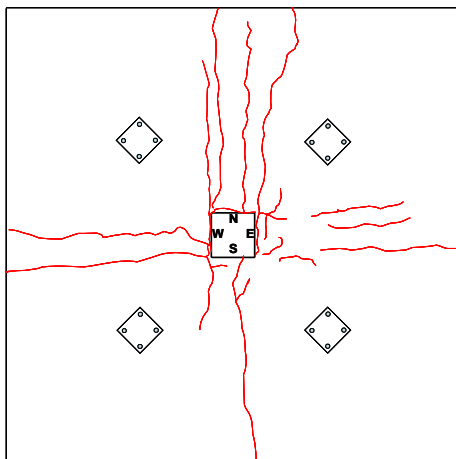
A.3.2 Bottom surface



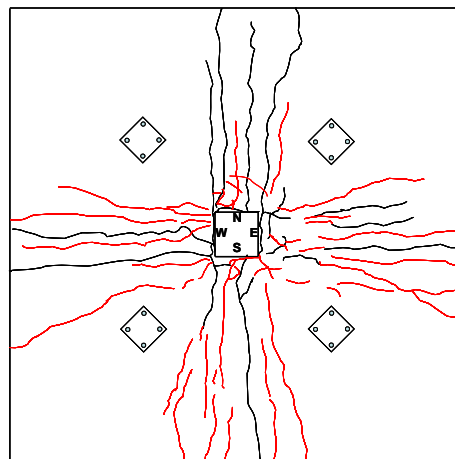
Failure (101.3 kip)

A.4 SPECIMEN G1.0

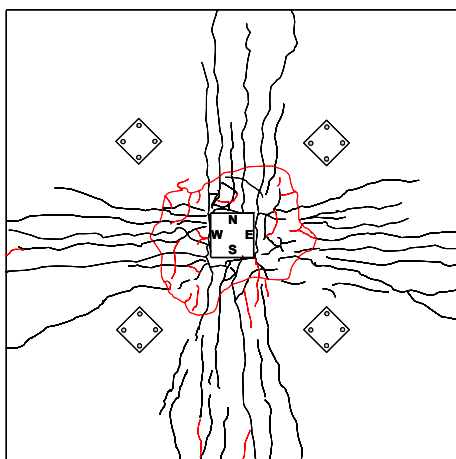
A.4.1 Top surface



60 kip



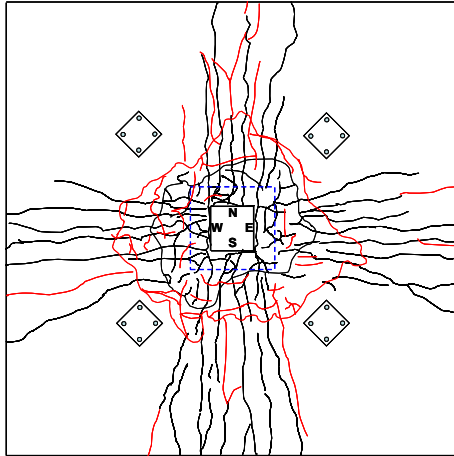
85 kip



Failure (90.2 kip)

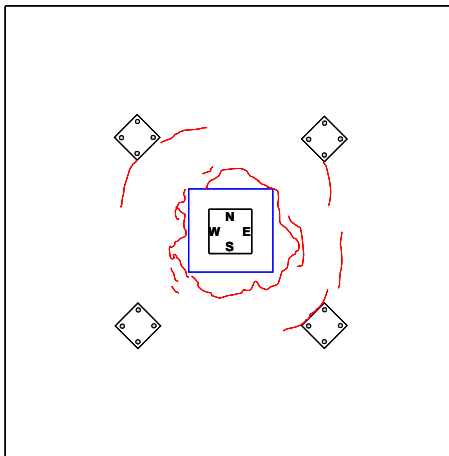
A.5 SPECIMEN RCG1.0

A.5.1 Top surface



Failure (128 kip)

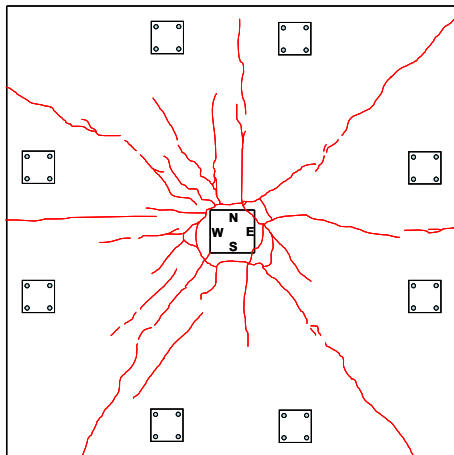
A.5.2 Bottom surface



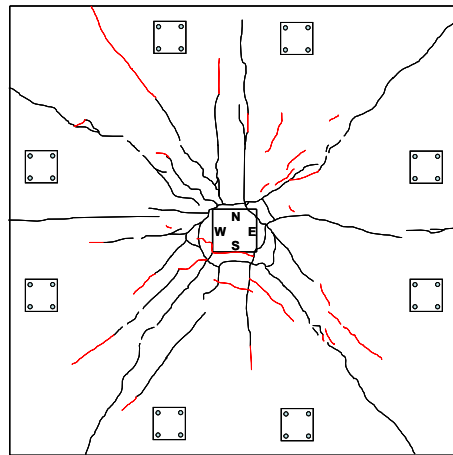
Failure (128 kip)

A.6 SPECIMEN L0.5

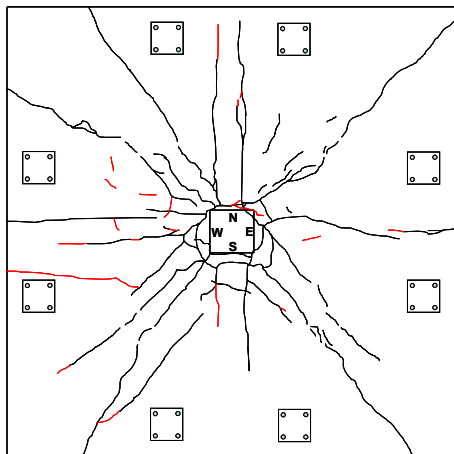
A.6.1 Top surface



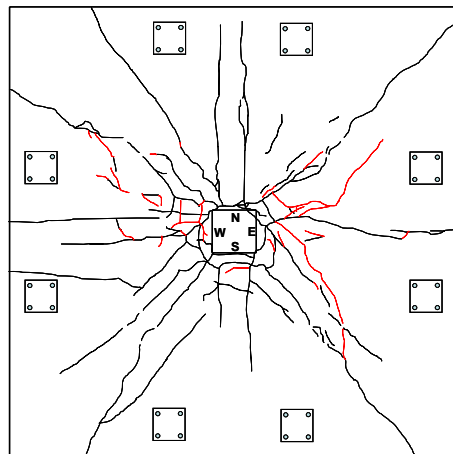
After gravity load (DL+25% LL)



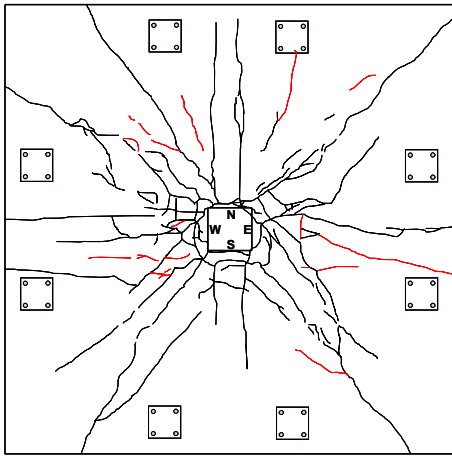
0.25% drift



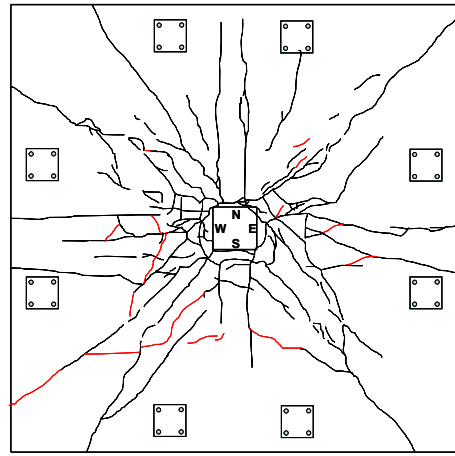
0.50% drift



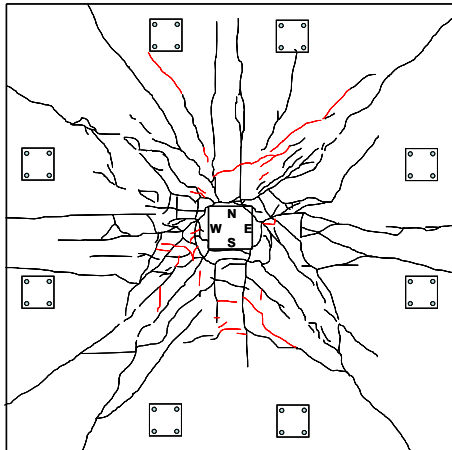
0.75% drift



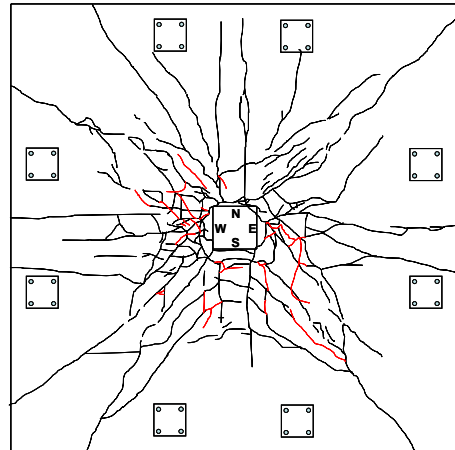
1.0% drift



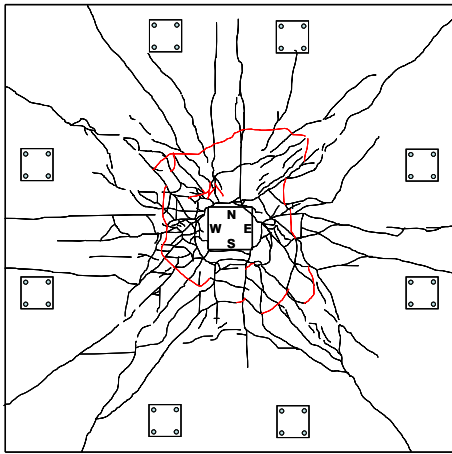
1.50% drift



1.75% drift

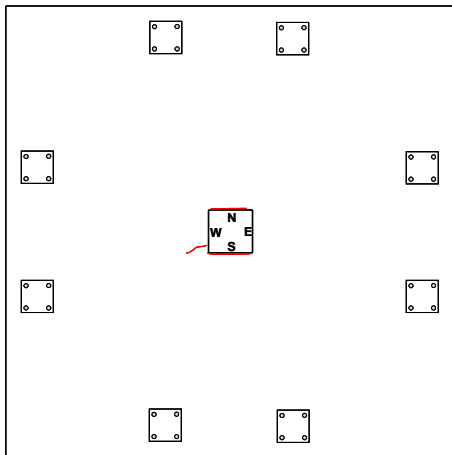


2.0% drift

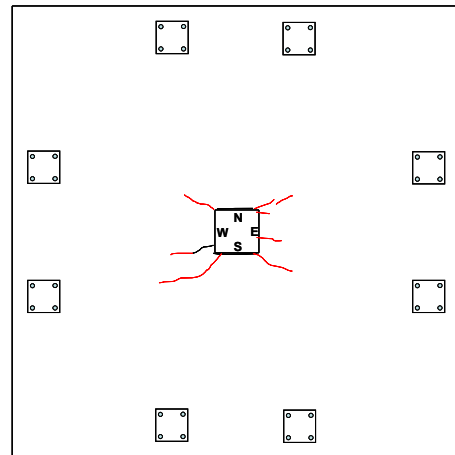


2.5% drift

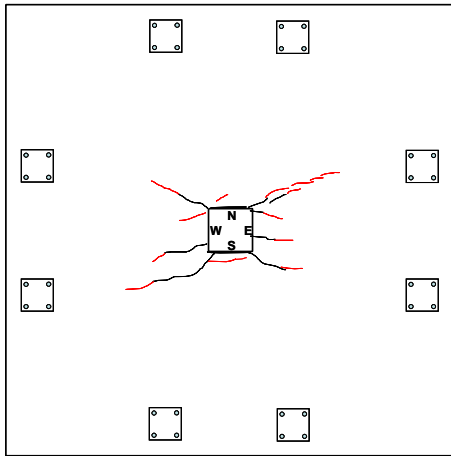
A.6.2 Bottom surface



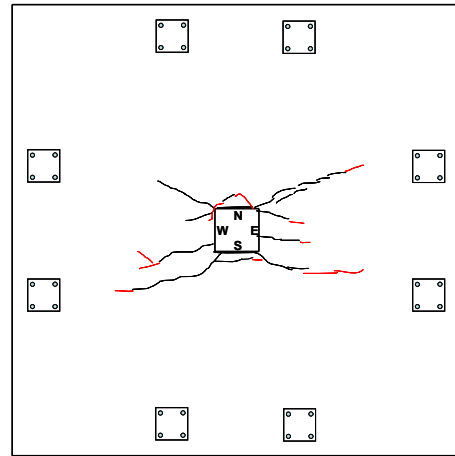
0.75% drift



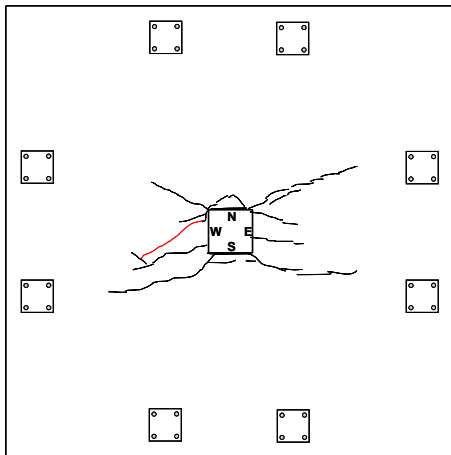
1.0% drift



1.5% drift



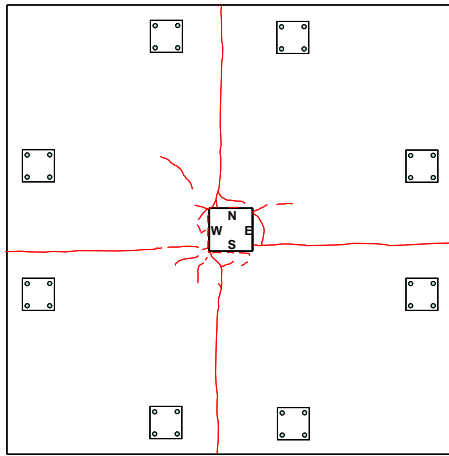
1.75% drift



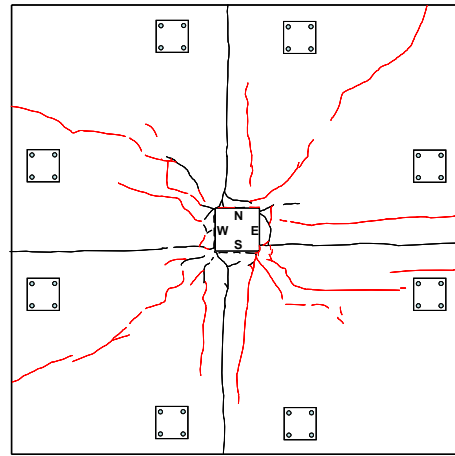
2.5% drift

A.7 SPECIMEN LG0.5

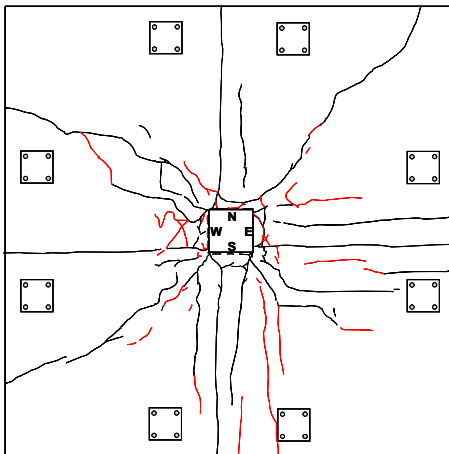
A.7.1 Simulated seismic test, top surface



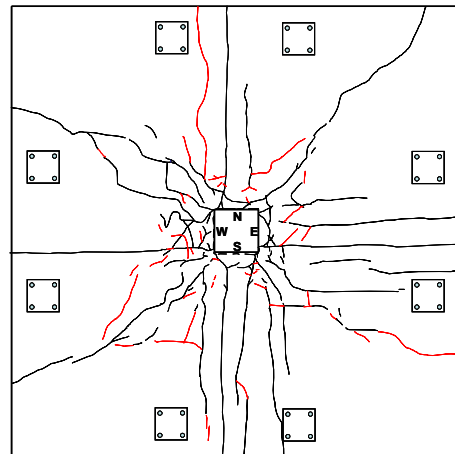
After gravity load (DL+25% LL)



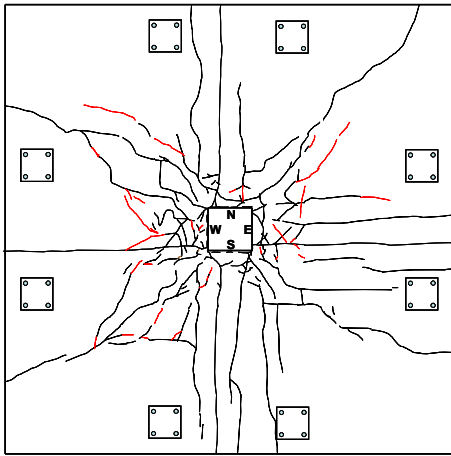
0.25% drift



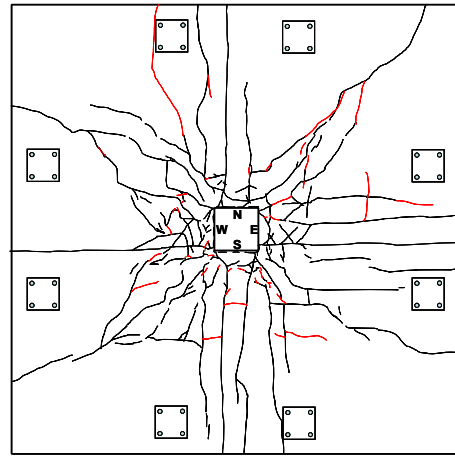
0.5% drift



0.75% drift

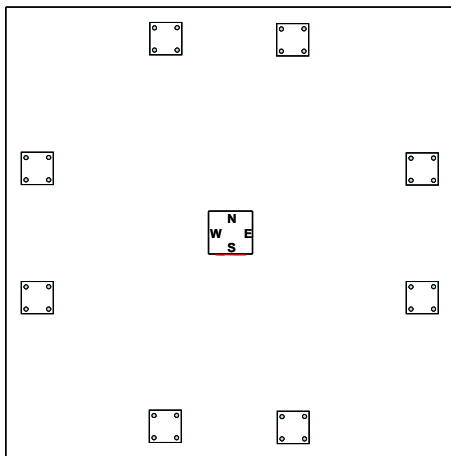


1.0% drift

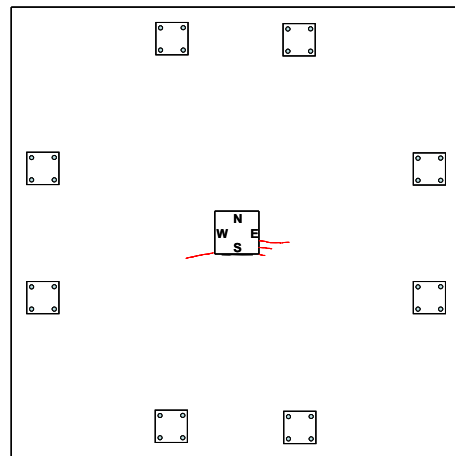


1.25% drift

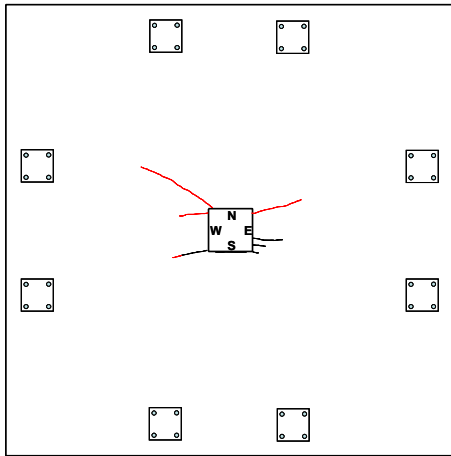
A.7.2 Simulated seismic test, bottom surface



0.75% drift

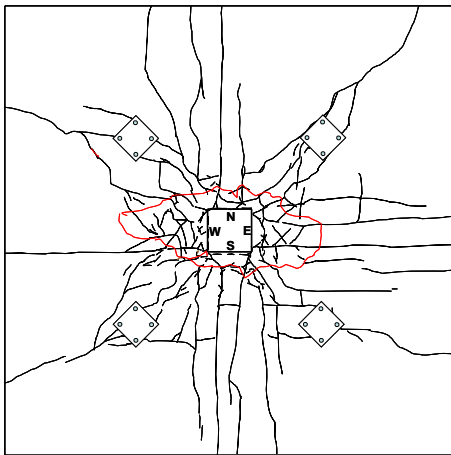


1.0% drift



1.25% drift

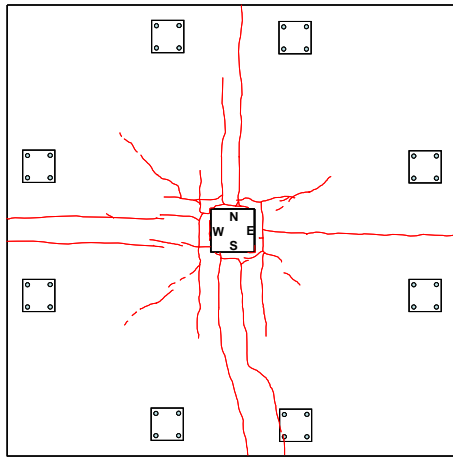
A.7.3 Punching shear test, top surface



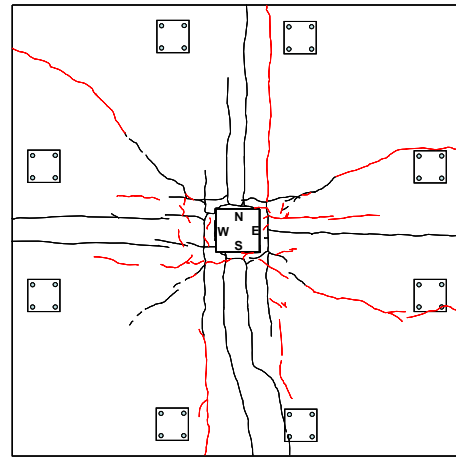
Failure (72.7 kip)

A.8 SPECIMEN LRSTG0.5

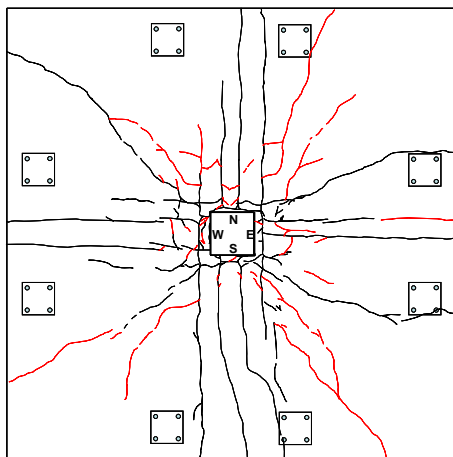
A.8.1 Simulated seismic test, top surface



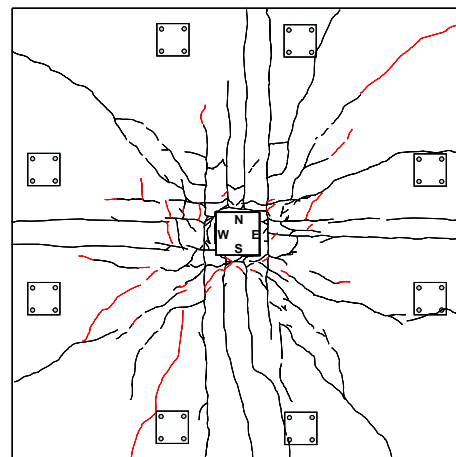
After gravity load (DL+25% LL)



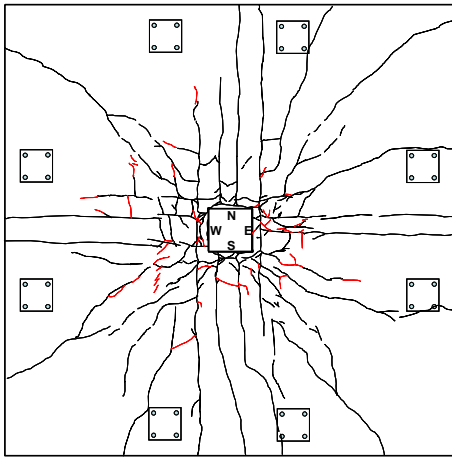
0.25% drift



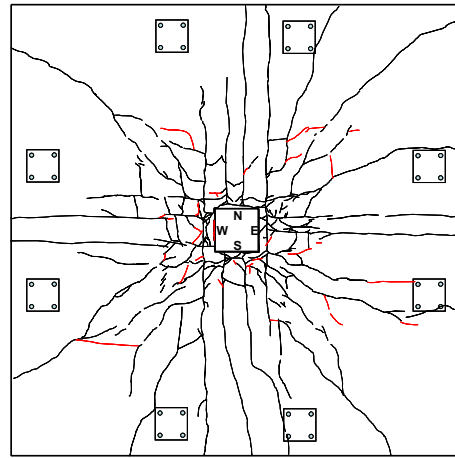
0.5% drift



0.75% drift

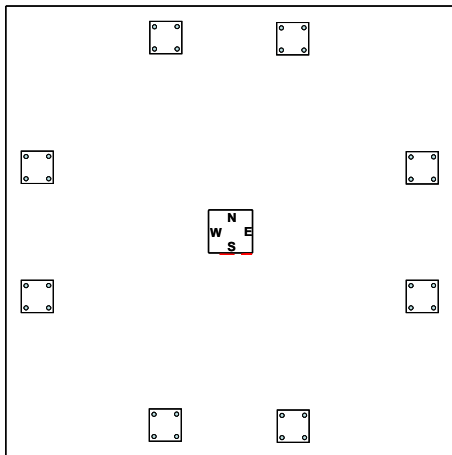


1.0% drift

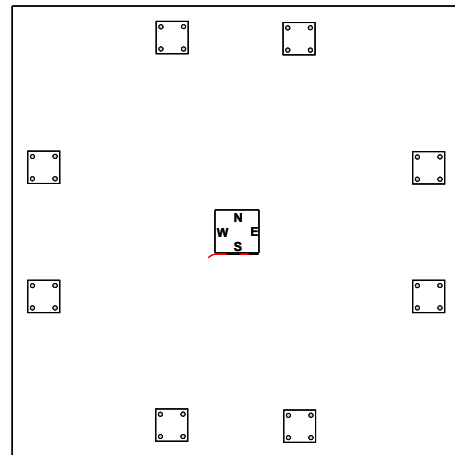


1.25% drift

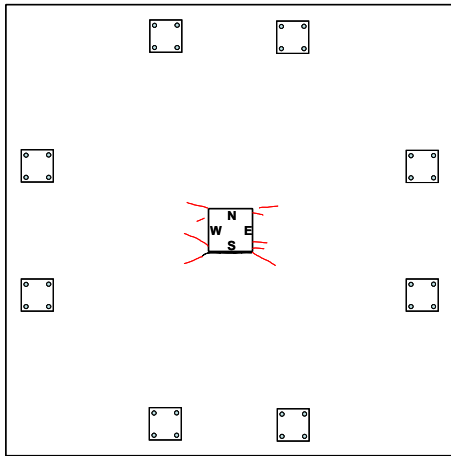
A.8.2 Simulated seismic test, bottom surface



0.75% drift

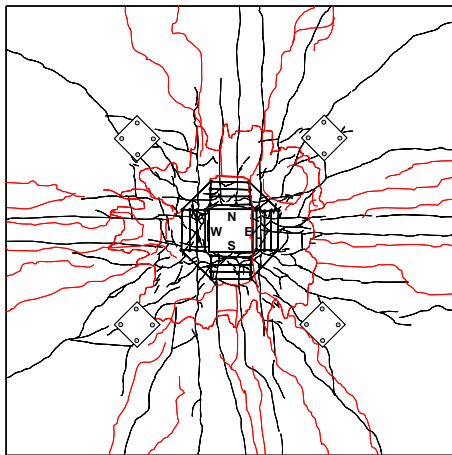


1.0% drift



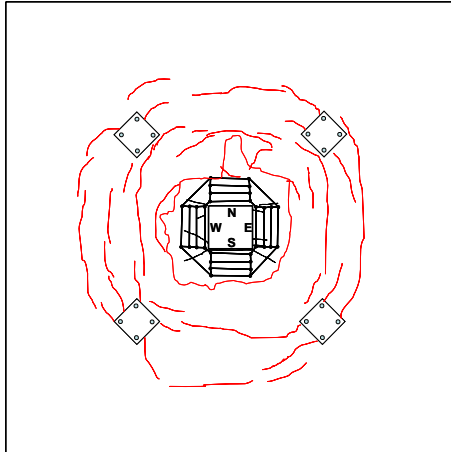
1.25% drift

A.8.3 Punching shear test, top surface



Failure (86.5 kip)

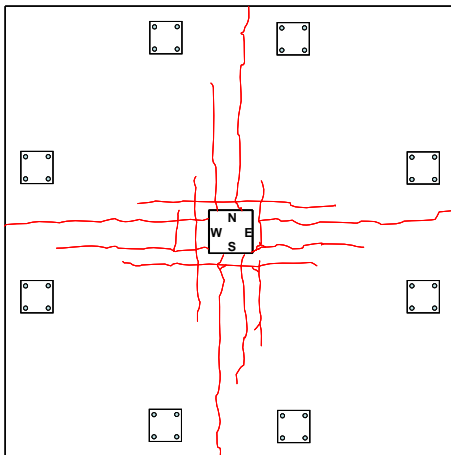
A.8.4 Punching shear test, bottom surface



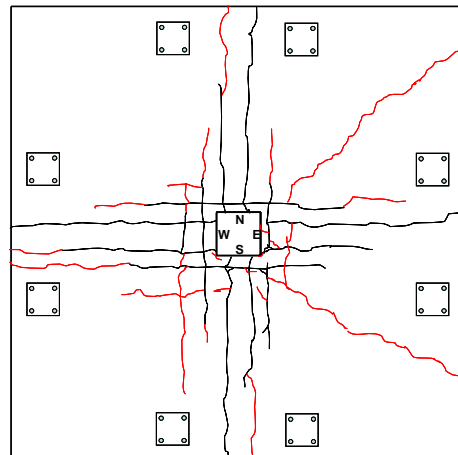
Failure (86.5 kip)

A.9 SPECIMEN LRSHG0.5

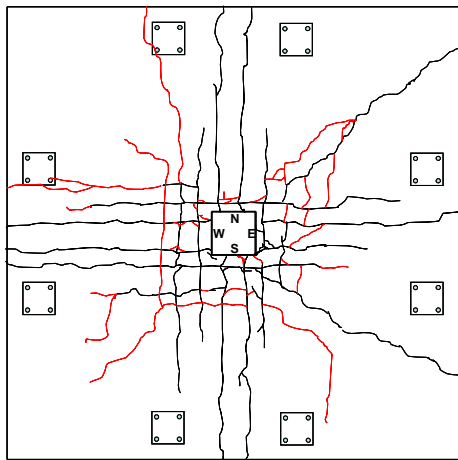
A.9.1 Simulated seismic test, top surface



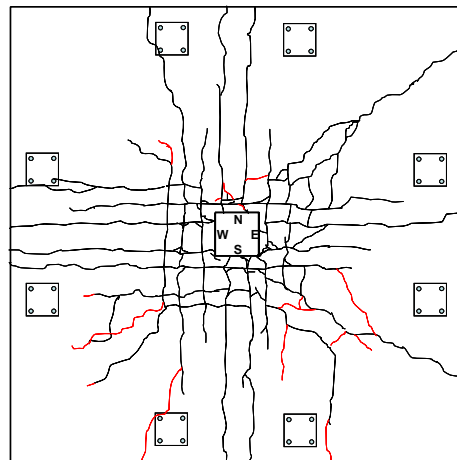
After gravity load (DL+25% LL)



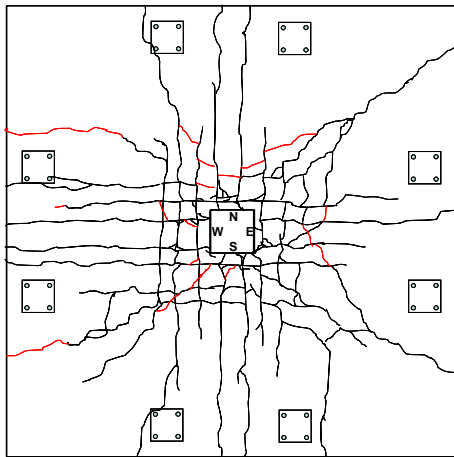
0.25% drift



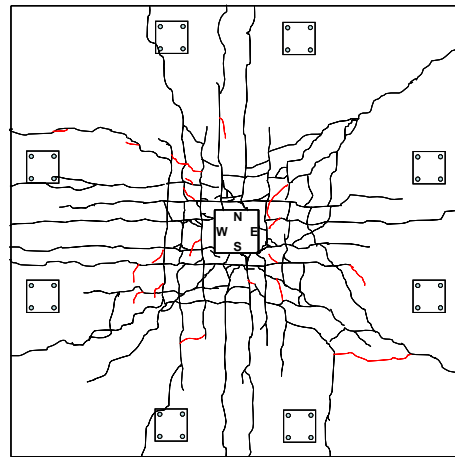
0.5% drift



0.75% drift

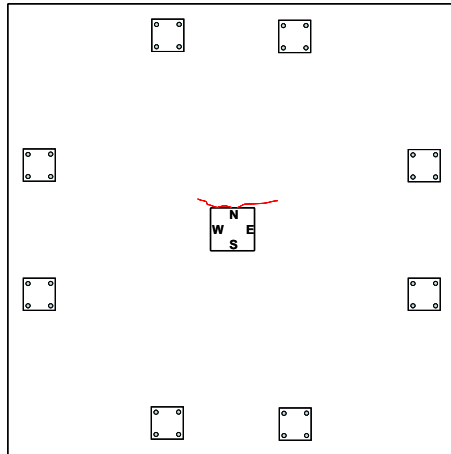


1.0% drift

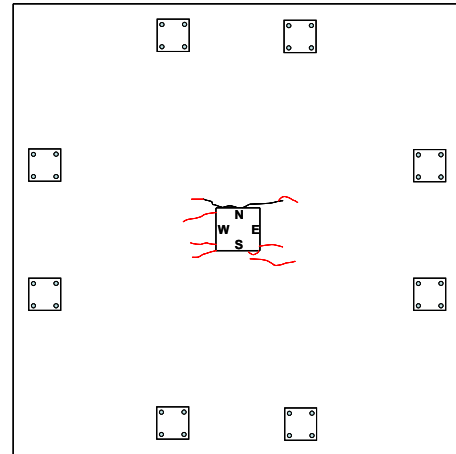


1.25% drift

A.9.2 Simulated seismic test, bottom surface

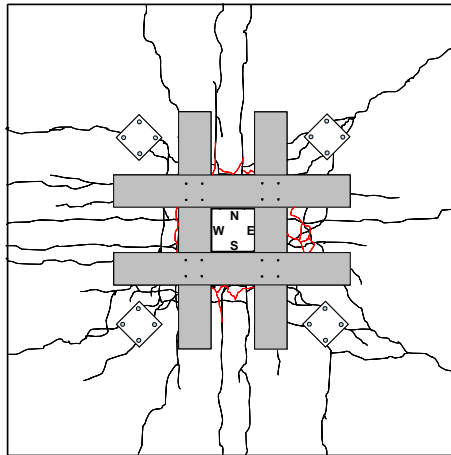


1.0% drift



1.25% drift

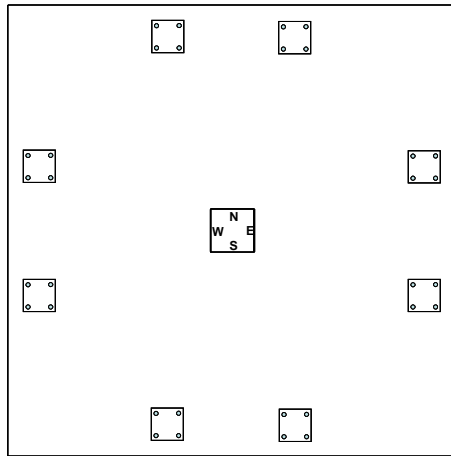
A.9.3 Punching shear test, top surface



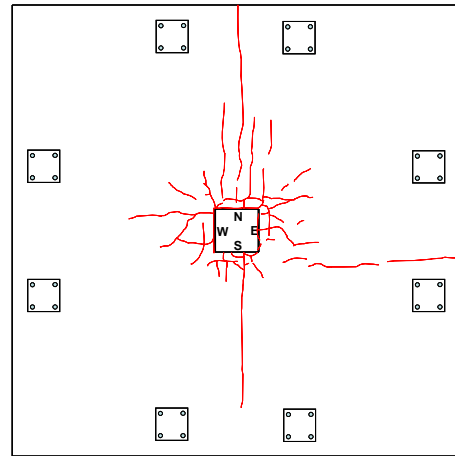
Failure (97.5 kip)

A.10 SPECIMEN LG1.0

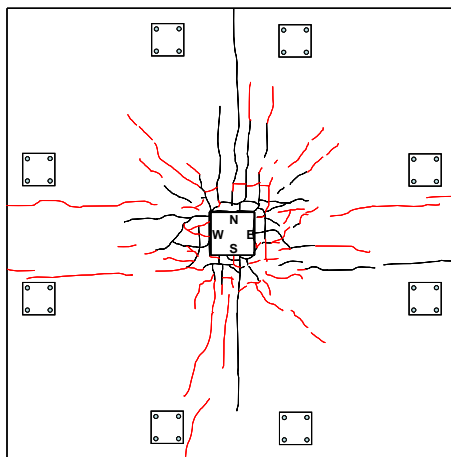
A.10.1 Simulated seismic test, top surface



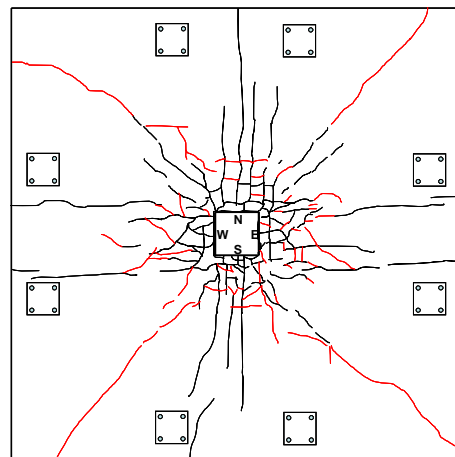
After gravity load (DL+25% LL)



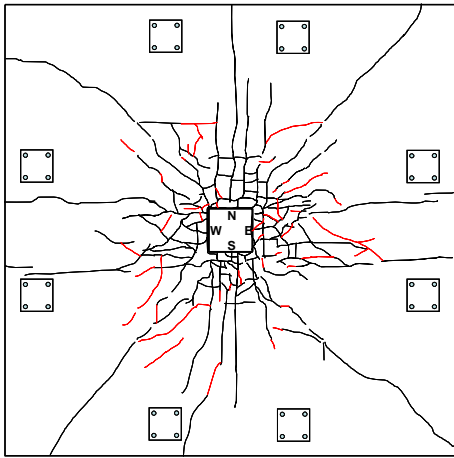
0.25% drift



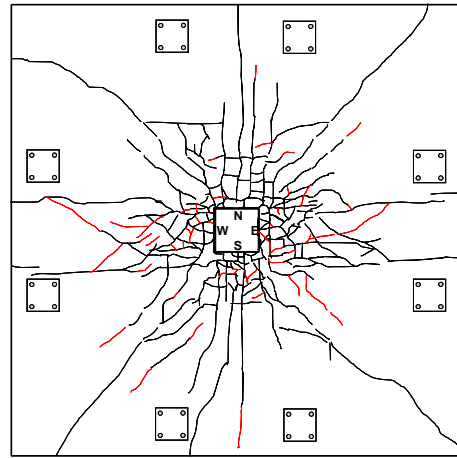
0.5% drift



0.75% drift

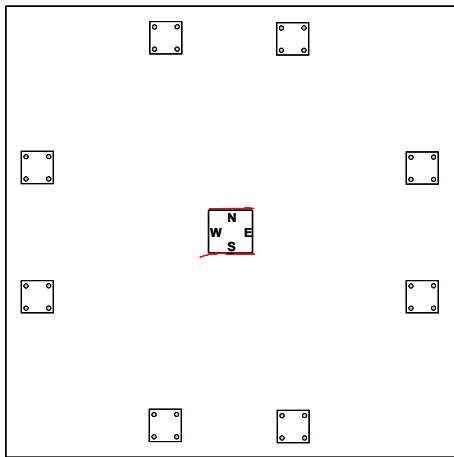


1.0% drift

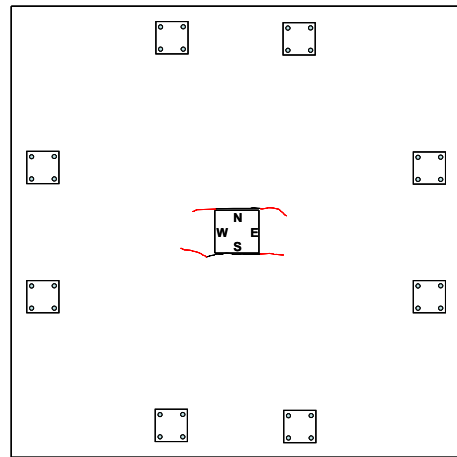


1.25% drift

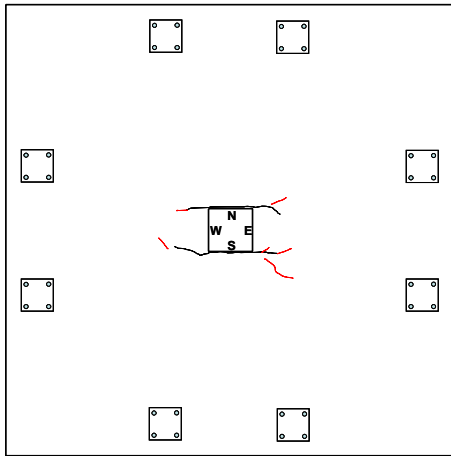
A.10.2 Simulated seismic test, bottom surface



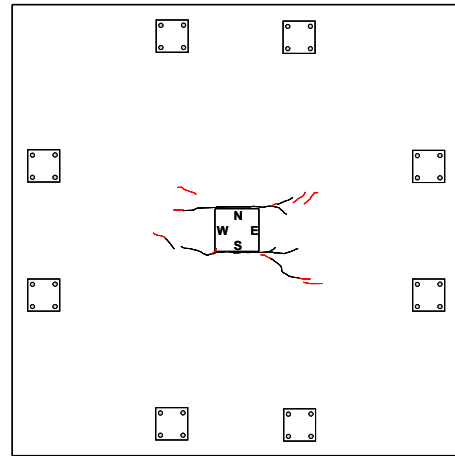
0.5% drift



0.75% drift

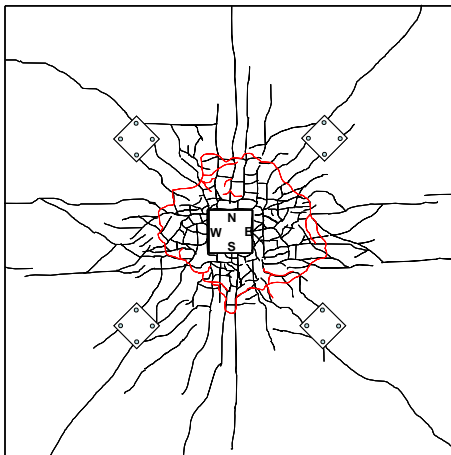


1.0% drift



1.25% drift

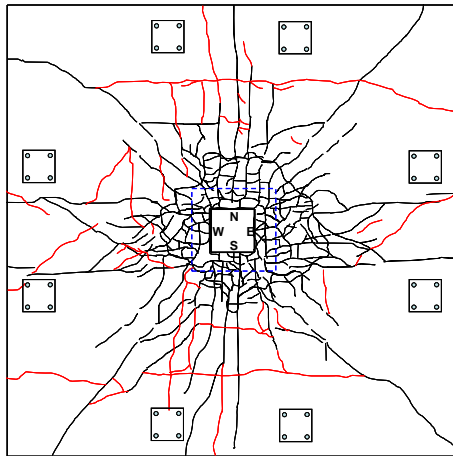
A.10.3 Punching shear test, top surface



Failure (89.8 kip)

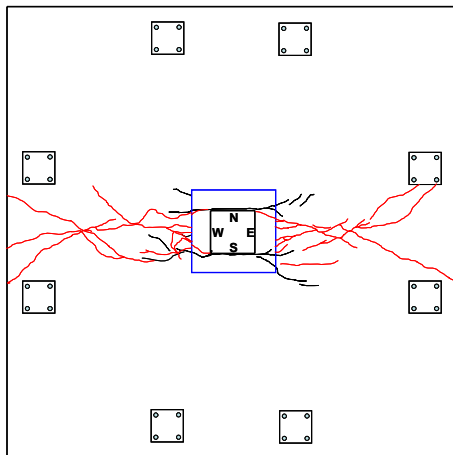
A.11 SPECIMEN RCL1.0

A.11.1 Simulated seismic test, top surface



Failure (3.0% lateral drift)

A.11.2 Simulated seismic test, bottom surface



Failure (3.0% lateral drift)

References

ACI Committee 318. (1941). *Building Regulations for Reinforced Concrete (ACI 318-41)*, American Concrete Institute, Detroit, Michigan, 63 pp.

ACI Committee 318. (1947). *Building Code Requirements for Reinforced Concrete (ACI 318-47)*, American Concrete Institute, Detroit, Michigan, 64 pp.

ACI Committee 318. (1951). *Building Code Requirements for Reinforced Concrete (ACI 318-51)*, American Concrete Institute, Detroit, Michigan, pp. 589-652.

ACI Committee 318. (1956). *Building Code Requirements for Reinforced Concrete (ACI 318-56)*, American Concrete Institute, Detroit, Michigan, pp. 913-986.

ACI Committee 318. (1963). *Commentary on Building Code Requirements for Reinforced Concrete (ACI 318R-63)*, Publication SP-10, American Concrete Institute, Detroit, Michigan, 91 pp.

ACI Committee 318. (1963). *Building Code Requirements for Reinforced Concrete (ACI 318-63)*, American Concrete Institute, Detroit, Michigan, 144 pp.

ACI Committee 318. (1971). *Commentary on Building Code Requirements for Reinforced Concrete (ACI 318R-71)*, American Concrete Institute, Detroit, Michigan, 96 pp.

ACI Committee 318. (1971). *Building Code Requirements for Reinforced Concrete (ACI 318-71)*, American Concrete Institute, Detroit, Michigan, 78 pp.

ACI Committee 318. (1973). *1973 Supplement to Building Code Requirements for Reinforced Concrete (ACI 318-71)*. American Concrete Institute, Detroit, Michigan, 9 pp.

ACI Committee 318. (1974). *1974 Supplement to Building Code Requirements for Reinforced Concrete (ACI 318-71)*. American Concrete Institute, Detroit, Michigan, 13 pp.

ACI Committee 318. (1975). *1975 Supplement to Building Code Requirements for Reinforced Concrete (ACI 318-71)*. American Concrete Institute, Detroit, Michigan, 18 pp.

ACI Committee 318. (1976). *1976 Supplement to Building Code Requirements for Reinforced Concrete (ACI 318-71)*. American Concrete Institute, Detroit, Michigan, 26 pp.

ACI Committee 318. (1977). *Commentary on Building Code Requirements for Reinforced Concrete (ACI 318R-77)*, American Concrete Institute, Detroit, Michigan, 132 pp.

ACI Committee 318. (1977). *Building Code Requirements for Reinforced Concrete (ACI 318-77)*, American Concrete Institute, Detroit, Michigan, 103 pp.

ACI Committee 318. (1980). *1980 Supplement to Building Code Requirements for Reinforced Concrete (ACI 318-77)*. American Concrete Institute, Detroit, Michigan, 10 pp.

ACI Committee 318. (1983). *Commentary on Building Code Requirements for Reinforced Concrete (ACI 318R-83)*, American Concrete Institute, Detroit, Michigan, 155 pp.

ACI Committee 318. (1983). *Building Code Requirements for Reinforced Concrete (ACI 318-83)*, American Concrete Institute, Detroit, Michigan, 111 pp.

ACI Committee 318. (1986). *1986 Supplement to Building Code Requirements for Reinforced Concrete (ACI 318-83) and (ACI 318M-83)*. American Concrete Institute, Detroit, Michigan, 14 pp.

ACI Committee 318. (1989). *Building Code Requirements for Reinforced Concrete (ACI 318-89) and Commentary-ACI 318R-89*, American Concrete Institute, Detroit, Michigan, 353 pp.

ACI Committee 318. (1995). *Building Code Requirements for Structural Concrete (ACI 318-95) and Commentary (ACI 318R-95)*, American Concrete Institute, Farmington Hills, Michigan, 369 pp.

ACI Committee 318. (1999). *Building Code Requirements for Structural Concrete (ACI 318-99) and Commentary (ACI 318R-99)*, American Concrete Institute, Farmington Hills, Michigan, 391 pp.

ACI Committee 318. (2002). *Building Code Requirements for Structural Concrete (ACI 318-02) and Commentary (ACI 318R-02)*, American Concrete Institute, Farmington Hills, Michigan, 443 pp.

ACI Committee 318. (2005). *Building Code Requirements for Structural Concrete (ACI 318-05) and Commentary (ACI 318R-05)*, American Concrete Institute, Farmington Hills, Michigan, 430 pp.

ACI Committee 440. (2002). *Guide for the Design and Construction of Externally Bonded FRP Systems for Strengthening Concrete Structures*, American Concrete Institute, Farmington Hills, Michigan, 45 pp.

ACI-ASCE Committee 326. (1962). "Shear and Diagonal Tension." *Journal of the American Concrete Institute, Proceedings*, V.59, pp. 1-30, pp. 277-334, pp. 353-396.

ACI-ASCE Committee 426. (1974). "The Shear Strength of Reinforced Concrete Members-slabs" *Journal of the Structural Division*, Vol. 100(ST8), pp. 1543-1591.

ACI-ASCE Committee 426. (1977). *Suggested Revisions to Shear Provisions for Building Codes (ACI 426.1R-77)*, American Concrete Institute, Farmington Hills, MI, 82 pp.

ACI-ASCE Committee 352. (1988). "Recommendations for Design of Slab-Column Connections in Monolithic Reinforced Concrete Structures." *ACI Structural Journal*, Vol. 85(6), pp. 675-696.

ACI ITG/T1.1, (2001). *Acceptance Criteria for Moment Frames Based on Structural Testing*, American Concrete Institute, Farmington Hills, Michigan.

Adetifa, B. and Polak, M.A. (2005). "Retrofit of Slab Column Interior Connections using Shear Bolts." *ACI Structural Journal*, Vol. 102(2), pp. 268-274.

Afhami, S., Alexander, S.D.B., and Simmonds, S.H. (1998). "Strip Model for Capacity of Slab-column Connection." *Structural Engineering Report No. 223*, University of Alberta.

Alander, C. (2000). "Punching Prevention in Flat Reinforced Concrete Slabs." *Proceedings*, International Workshop on Punching Shear Capacity of RC Slabs, Stockholm, TRITA-BKN: Bulletin 57, pp. 145-153.

- Albrecht, U. (2002). "Design of Flat Slabs for Punching – European and North American Practices." *Cement and Concrete Composites*, Vol. 24, pp. 531-538.
- Alexander, S.D.B. (1994). "Plastic Design of Column-Slab Connections." *Proceedings*, 1994 Annual Conference of the Canadian Society for Civil Engineering, Winnipeg, Man., June 1-4, pp. 214-223.
- Alexander, S.D.B. (1999). "Strip design for punching shear." *SP-183: The Design of Two-Way Slabs*, American Concrete Institute, pp. 161-179.
- Alexander, S.D.B. and Simmonds, S.H. (1992). "Bond Model for Concentric Punching Shear." *ACI Structural Journal*, Vol. 89(3), pp. 325-334.
- Alexander, S.D.B. and Hawkins, N.M. (2005). "A Design Perspective on Punching Shear." *SP-232: Punching Shear in Reinforced Concrete Slabs*, ACI, pp. 97-108.
- Argudo, J.F. (2006). "Non-destructive Evaluation of Gravity Load Carrying Capacity and Lateral Load Damage of Reinforced Concrete Slab-column Connections." *PhD dissertation*, Department of Civil and Environmental Engineering, University of Texas at Austin, Austin, Texas.
- Arya, C., Clarke, J.L., Kay, E.A., and O'Regan, P.D. (2002). "TR 55: Design Guidance for Strengthening Concrete Structures using Fibre Composite Materials: A Review." *Engineering Structures*, Vol. 24, pp. 889-900.
- AS 3600-1994. (1994). *Australian Standard: Concrete Structures*. Standards Association of Australia, Homebush, NSW 2140.
- ASTM D638. (2003). *Standard Test Method for Tensile Properties of Plastics*. ASTM International, 15 pp.
- ASTM D790. (2003). *Standard Test Method for Flexural Properties of Unreinforced and Reinforced Plastics and Electrical Insulating Materials*. ASTM International, 11 pp.
- ASTM C143. (2005). *Standard Test Method for Slump of Hydraulic-Cement Concrete*. ASTM International, 4 pp.
- ASTM E84. (2005). *Standard Test Method for Surface Burning Characteristics of Building Materials*. ASTM International, 19 pp.

- ASTM E119. (2005). *Standard Test Method for Fire Tests of Building Construction and Materials*. ASTM International, 22 pp.
- ASTM A706. (2006). *Standard Specification for Low-Alloy Steel Deformed and Plain Bars for Concrete Reinforcement*. ASTM International, 6 pp.
- ASTM D3039. (2006). *Standard Test Method for Tensile Properties of Polymer Matrix Composite Materials*. ASTM International, 13 pp.
- Bakis, C.E., Bank, L.C., Brown, V.L., Cosenza, E., Davalos, J.F., Lesko, J.J., Machida, A., Rizkalla, S.H., and Triantafillou, T.C. (2002). "Fiber-Reinforced Polymer Composites for Construction – State-of-the-Art Review." *Journal of Composites for Construction*, Vol. 6(2), pp. 73-87.
- Bari, M.S. (2000). "Punching shear strength of slab-column connections – a comparative study of different codes." *Journal of the Institution of Engineers (India)*. Civil Engineering Division, Vol.80, No.4, February 2000, pp.163-168.
- Bazant, Z.P. and Cao, Z. (1987). "Size Effect in Punching Shear Failure of Slabs." *ACI Structural Journal*, Vol. 84(1), pp. 44-53.
- Beutel, R. and Hegger, J. (2000). "Punching Behavior of Shear Reinforced Flat Slabs at Interior Columns – Effective and Economic Shear Systems." *Proceedings*, International Workshop on Punching Shear Capacity of RC Slabs, Stockholm, TRITA-BKN: Bulletin 57, pp. 171-179.
- Beutel, R. and Hegger, J. (2002). "The Effect of Anchorage on the Effectiveness of the Shear Reinforcement in the Punching Zone." *Cement & Concrete Composites*, Vol. 24, pp. 539-549.
- Binici, B. (2003). "Punching shear strengthening of reinforced concrete slabs using fiber reinforced polymers." *PhD dissertation*, Department of Civil and Environmental Engineering, University of Texas at Austin, Austin, Texas, 279 pp.
- Binici, B. and Bayrak, O. (2003). "Punching shear strengthening of reinforced concrete flat plates using carbon fiber reinforced polymers." *Journal of Structural Engineering*, Vol. 129(9), pp. 1173-1182.
- Binici, B. and Bayrak, O. (2005). "Use of fiber-reinforced polymers in slab-column connection upgrades." *ACI Structural Journal*, Vol. 102(1), pp. 93-102.
- Binici, B. and Bayrak, O. (2005). "Upgrading of slab-column connections using fiber reinforced polymers." *Engineering Structures*, Vol. 27, pp. 97-107.

- BNBC. (1993). *Bangladesh National Building Code (BNBC)*. HBRI and BSTI. Dhaka.
- Bonacci, J.F. and Maalej, M. (2001). "Behavioral Trends of RC Beams Strengthened with Externally Bonded FRP." *Journal of Composites for Construction*, Vol. 5(2), pp. 102-113.
- Broms, C.E. (2000). "Elimination of Flat Plate Punching Failure Mode." *ACI Structural Journal*, Vol. 97(1), pp. 94-101.
- Broms, C.E. (2000). "A Method to Avoid The Punching Failure Mode." *Proceedings*, International Workshop on Punching Shear Capacity of RC Slabs, Stockholm, TRITA-BKN: Bulletin 57, pp. 117-124.
- BS 8110. (1997). *Structural Use of Concrete, Part 1: Code of Practice for Design and Construction*. British Standards Institute, London.
- Burr, A.C. (2004). "Recent Developments in the Use of FRP Anchors and Masonry Wall Strengthening Techniques." *The Structural Engineer*, Vol. 82(8), pp. 20-21.
- Casadei, P., Nanni, A., and Ibell, T. (2003). "Experiments on Two-way RC Slabs with Openings Strengthened with CFRP Laminates." *CIES Report 03-39*, Center for Infrastructure Engineering Studies, University of Missouri-Rolla, Rolla, Missouri, 8 pp.
- CEB-FIP MC 90. (1993). *Design of Concrete Structures, CEB-FIP-Model-Code 1990*. Thomas Telford, 1993 construction. British Standard Institution, London.
- Chen, C.C. and Li, C.Y. (2000). "An Experimental Study on the Punching Shear Behavior of RC Slabs." *Proceedings*, International Workshop on Punching Shear Capacity of RC Slabs, Stockholm, TRITA-BKN: Bulletin 57, pp. 415-422.
- Chen, J.F. and Teng, J.G. (2001). "Anchorage Strength Models for FRP and Steel Plates Bonded to Concrete." *Journal of Structural Engineering*, Vol. 127(7), pp. 784-791.
- Chen, C.C. and Li, C.Y. (2005). "Punching Shear Strength of Reinforced Concrete Slabs Strengthened with Glass Fiber-Reinforced Polymer Laminates." *ACI Structural Journal*, Vol. 102(4), pp. 535-542.

Concrete Society. (2000). *Design Guidance for Strengthening Concrete Structures using Fibre Composite Materials*. Concrete Society Technical Report No. 55, Crowthorne, Berkshire, UK, 69 pp.

Cowel, A., Popov, E., and Bertero, V.V. (1980). "Repair of Bond in R/C Structures by Epoxy Injection." *Proceedings of the First Seminar on Repair and Retrofit of Structures*, Ann Arbor, Michigan, 1, pp. 234-240.

Criswell, M.E. (1970). "Strength and Behavior of Reinforced Concrete Slab-Column Connections Subjected to Static and Dynamic Loadings." *Technical Report N-70-1*, U.S. Army Engineer Waterways Experiment Station, Vicksburg, Mississippi.

Criswell, M.E. (1974). "Static and dynamic response of reinforced concrete slab-column connections." *Shear in Concrete*, Publication SP-42, American Concrete Institute, Detroit, Michigan, pp. 721-746.

CSA A23.3-04. (2004). *Design of Concrete Structure*. Canadian Standards Association, 214 pp.

Davies, J.M., Wang, Y.C., and Wong, P.M.H. (2004). "Polymer Composites in Fire." *Proceedings of the second international conference: Advanced Polymer Composites for Structural Applications in Construction*, University of Surrey, Guilford, UK, 20-22 April, pp. 3-17.

De Rose, D. (1997). "The Rehabilitation of a Concrete Structure using Fibre Reinforced Plastics." *MASc thesis*, Department of Civil Engineering, University of Toronto, Toronto, Ontario, Canada, 177 pp.

Diaz de Cossio, R. (1962). Discussion of a paper by ACI ASCE Committee 326: "Shear and Diagonal Tension", *Journal of the American Concrete Institute, Proceedings*, Vol. 59(9), pp. 1323-1332.

Dilger, W.H. and Sherif, A.G. (1993). "Full Scale Test of Flat Slab." *Proceedings, 1993 CSCE/CPCA Structural Concrete Conference*, Toronto, Ontario, 19-21 May. pp. 169-182.

Dilger, W., Birkle, G., and Mitchell, D. (2005). "Effect of Flexural Reinforcement on Punching Shear Resistance." *SP-232: Punching Shear in Reinforced Concrete Slabs*, ACI, pp. 57-74.

DIN 1045-1. (2001). *Tragwerke aus Beton, Stahlbeton, und Spannbeton, Teil 1: Bemessung und Konstruktion (Plain, Reinforced, and Prestressed Concrete*

Structures – Part 1: Design and Construction). Normenausschuss Bauwesen (NABau) im DIN Deutsches Institut für Normung e.V. Beuth Verl. Berlin, 148 pp.

Dovich, L. and Wight, J.K. (1996). “Lateral Response of Older Flat Slab Frames and the Economic Effect on Retrofit.” *Earthquake Spectra*, Vol. 12(4), pp. 667-691.

Dragosavic, M. and Van den Beukel, A. (1974). “Punching Shear.” *Heron*, Vol. 20(2), 48 pp.

Durrani, A.J, Du, Y., and Luo, Y.H. (1995). “Seismic Resistance of Nonductile Slab-Column Connections in Existing Flat-Slab Buildings.” *ACI Structural Journal*, Vol. 92(4), pp. 479-487.

Ebead, U.A.A. (2002). “Strengthening of Reinforced Concrete Two-Way Slabs.” *Doctoral thesis*, Memorial University of Newfoundland, St. John’s, Newfoundland, Canada, 245 pp.

Ebead, U. and Marzouk, H. (2002). “Strengthening of two-way slabs using steel plates.” *ACI Structural Journal*, Vol. 99(1), pp. 23-31.

Ebead, U. and Marzouk, H. (2002). “Strengthening of two-way slabs subjected to moment and cyclic loading.” *ACI Structural Journal*, Vol. 99(4), pp. 435-444.

Ebead, U. and Marzouk, H. (2004). “Fiber-reinforced polymer strengthening of two-way slabs.” *ACI Structural Journal*, Vol. 101(5), pp. 650-659.

EERI. (1997). “Annotated Slide Sets: A visual presentation of EERI slide sets on CD.” *CD-ROM*, Earthquake Engineering Research Institute, Committee on Continuing Education, Oakland, California.

El-Ghandour, A.W., Pilakoutas, K., and Waldron, P. (2003). “Punching Shear Behavior of Fiber Reinforced Polymers Reinforced Concrete Flat Slabs: Experimental Study.” *Journal of Composites for Construction*, Vol. 7(3), pp. 258-265.

Elnashai, A.S. (1997). “Seismic Capacity of Rehabilitation of RC Structures.” *Proceedings*, International Conference on Rehabilitation and Development of Civil Engineering Infrastructure Systems, June 9-11, American University of Beirut, Beirut, Lebanon, Vol. 1, pp. 1-14.

- Elstner, R.C. and Hognestad, E. (1956). "Shearing Strength of Reinforced Concrete Slabs." *Journal of the American Concrete Institute*, Vol. 28(1), pp. 29-58.
- El-Salakawy, E.F., Polak, M.A., and Soliman, M.H. (2000). "Reinforced concrete slab-column connections with shear studs." *Canadian Journal of Civil Engineering*, Vol. 27, pp. 338-348.
- El-Salakawy, E.F., Polak, M.A., and Soudki, K.A. (2003). "New strengthening technique for concrete slab-column connections." *ACI Structural Journal*, Vol. 100(3), pp. 297-304.
- El-Salakawy, E., Soudki, K.A., and Polak, M.A. (2004). "Punching shear behavior of flat slabs strengthened with fiber reinforced polymer laminates." *Journal of Composites for Construction*, Vol. 8(5), pp. 384-392.
- Erki, M.A. and Heffernan, P.J. (1995). "Reinforced concrete slabs externally strengthened with fibre-reinforced plastic materials." *Non-Metallic (FRP) Reinforcement for Concrete Structures*, Proceedings, Second International RILEM Symposium (FRPRCS-2), pp. 509-516.
- Eurocode 2-2003. (2003). *Eurocode 2: Design of Concrete Structures – Part 1-1: General Rules and Rules for Buildings*. European Committee for Standardization, Brussels.
- Farhey, D.N., Adin, M.A., and Yankelevsy, D.Z. (1995). "Repaired RC Flat Slab-Column Connection Subassemblages under Lateral Loading." *Journal of Structural Engineering*, Vol. 121(11), pp. 1710-1720.
- Faulkes, K.A. (1974). "The Design of Flat Slab Structures – An Historical Review" *UNICIV Report No. R-129*, University of New South Wales, Kensington, N.S.W., Australia.
- Feld, J. (1964). "Lessons from Failure of Concrete Structures." *Monograph No. 1*, American Concrete Institute Monograph Series, 179 pp.
- FEMA. (1997). "NEHRP Commentary on the Guidelines for the Seismic Rehabilitation of Buildings." *FEMA-274*, Federal Emergency and Management Agency (FEMA), Washington, D.C., chapter 6.
- Fib. (2001a). "Punching of Structural Concrete Slabs." *Bulletin No. 12*, International Federation for Structural Concrete (fib), Lausanne, Switzerland, 307 pp.

Fib. (2001b). "Externally Bonded FRP Reinforcement for RC Structures." *Bulletin* No. 14, International Federation for Structural Concrete (fib), Lausanne, Switzerland, 130 pp.

Fyfe Co LLC. (2000). "Tyfo FC/F Fire-resistance system." <http://www.fyfeco.com/products/finishcoats/fc-f.html>, accessed 28 April 2006.

Fyfe Co. LLC. (2002). Tyfo SCH-41S Composite using Tyfo S Epoxy. (<http://www.fyfeco.com/products/compositesystems/pdf/sch-41s-1.pdf>) (July 14 2005)

Gardner, N.J. (1995). "Discussion on Punching Shear Provisions for Reinforced and Prestressed Concrete Flat Slabs." *Proceedings*, 1995 Annual Conference of the Canadian Society for Civil Engineering, Ottawa, Ontario, June 1-3, pp. 247-256.

Gardner, N.J. and Shao, X.Y. (1996). "Punching Shear of Continuous Flat Reinforced Concrete Slabs." *ACI Structural Journal*, Vol. 93(2), pp. 218-228.

Gardner N.J., Huh J., and Chung L. (2002) "Lessons from Sampoong Department Store Collapse." *Cement and Concrete Composites*, Vol. 24(2), pp. 523-529.

Gardner, N.J. (2005). "ACI 318-05, CSA A23.3-04, Eurocode 2 (2003), DIN 1045-1 (2001), BS 8110-97 and CEB-FIP MC 90 Provisions for Punching Shear of Reinforced Concrete Flat Slabs." *SP-232: Punching Shear in Reinforced Concrete Slabs*, ACI, pp. 1-22.

Gesund, H. and Kaushik, Y.P. (1970). "Yield Line Analysis of Punching Failures in Slabs." *IABSE Publications*, Vol. 30-I, pp. 41-60.

Ghali, A. and Hammill, N. (1992). "Effectiveness of Shear Reinforcement in Slabs." *Concrete International*, Vol. 14(1), pp. 60-65.

Gomes R. and Regan, P. (1999). "Punching Strength of Slabs Reinforced for Shear with Cuts of rolled steel I-section beams." *Magazine of Concrete Research*, Vol. 51(2), pp. 121-129.

Gomes R. and Regan, P. (1999). "Punching Resistance of RC Flat Slabs with Shear Reinforcement." *Journal of Structural Engineering*, Vol. 125(6), pp. 684-692.

Graf, O. (1933). "Tests of Reinforced Concrete Slabs under Concentrated Load Applied Near One Support (Versuche uber die Widerstandsfahigkeit von

Eisenbetonplatten unter konzentrierter Last nahe einem Auflager).” *Deutscher Ausschuss für Eisenbeton*, No. 73, Berlin, Germany.

Granger, R.O., Peirce, J.W., Protze, H.G., Tobin, J.J., and Lally, F.J. (1971). “The Building Collapse at 2000 Commonwealth Avenue Boston, Massachusetts on January 25, 1971.” *Report of the Mayor’s Investigating Commission*, The City of Boston, Massachusetts.

Guralnick, S.A. and LaFraugh, R.W. (1963). “Laboratory study of a 45-foot square flat plate structure.” *Journal of the American Concrete Institute*, Vol. 60(9), pp. 1107-1185 ; also *Bulletin D70*, Portland Cement Association, Research and Development Laboratories, Skokie, Illinois.

Hallgren, M. (1996). “Punching Shear Capacity of Reinforced High Strength Concrete Beams without Stirrups.” *Doctoral Thesis*, TRITA-BKN, Bulletin 23, Royal Institute of Technology, KTH Stockholm.

Harajli, M.H. and Soudki, K.A. (2003). “Shear Strengthening of Interior Slab-Column Connections Using Carbon Fiber-Reinforced Polymer Sheets.” *Journal of Composites for Construction*, Vol. 7(2), pp. 145-153.

Harries, K.A., Porter, M.L., Busel, J.P. (2003). “FRP Materials and Concrete – Research Needs.” *Concrete International*, Vol. 25(1), pp. 69-74.

Hassanzadeh, G. and Sundqvist, H. (1998). “Strengthening of Bridge Slabs on Columns.” *Nordic Concrete Research*, The Nordic Concrete Federation, Publication no. 21, paper no.2.

Hawkins, N.M. (1974). “Shear strength of slabs with shear reinforcement.” *Shear in Concrete*, Publication SP-42, American Concrete Institute, Detroit, Michigan, pp. 785-815.

Hawkins, N.M., Mitchell, D., and Hanna, S.N. (1975). “The Effects of Shear Reinforcement on the Reversed Cyclic Loading Behavior of Flat Plate Structures.” *Canadian Journal of Civil Engineering*, Vol. 2(4), pp. 572-582.

Hawkins, N.M. and Mitchell, D. (1979) “Progressive Collapse of Flat Plate Structures,” *ACI Journal, Proceedings* Vol. 76(7), pp.775-808.

Hegger, J., Sherif, A., and Beutel, R. (2005). “Punching of Reinforced Concrete Flat Slabs – ACI and German Guidelines.” *SP-232: Punching Shear in Reinforced Concrete Slabs*, ACI, pp. 209-228.

- Hognestad, E. (1953). "Shearing Strength of Reinforced Concrete Column Footings." *Journal of the American Concrete Institute*, Vol. 25(3), pp. 189-208.
- Hognestad, E. (1953). "Yield Line Theory for the Ultimate Flexural Strength of Reinforced Concrete Slabs." *Journal of the American Concrete Institute*, Vol. 24(7), pp. 637-656.
- Hueste, M.B.D. and Wight, J.K. (1999). "Nonlinear Punching Shear Failure Model for Interior Slab-column Connections." *Journal of Structural Engineering*, Vol. 125(9), pp. 997-1008.
- Ibell, T., Nanni, A., and Eshwar, N. (2003). "The Effects of a Curved Soffit on FRP-Strengthening of Concrete Bridges." Report No. UTC R73, Center for Infrastructure Engineering Studies/UTC program, University of Missouri – Rolla, Rolla, Missouri, 10 pp.
- Iglesias, J. (1986). "Repairing and Strengthening of Reinforced Concrete Buildings Damaged in the 1985 Mexico City Earthquake." *The Mexico Earthquakes – 1985: Factors Involved and Lessons Learned*, Proceedings of the International Conference, September 19-21, edited by Cassaro, M.A. and Romero, E.M., ASCE, New York, New York, pp. 426-439.
- IS : 456 (1978). "Code of Practice for Plain and Reinforced Concrete." *Bureau of Indian Standards*, New Delhi.
- Islam, S. and Park, R. (1976). "Tests on slab-column connections with shear and unbalanced flexure." *Journal of the Structural Division*, 102(ST3), pp. 549-568.
- Johnson, G.P. and Robertson, I.N. (2004). "Retrofit of Slab-column Connections using CFRP." *Proceedings*, 13th World Conference on Earthquake Engineering, Vancouver, B.C., Canada, August 1-6, 2004, paper No. 142.
- Joint Committee of 1924. (1924). "Standard Specifications for Concrete and Reinforced Concrete. Joint Committee." *Proceedings, American Society for Testing Materials*, Vol.24, Part I, pp. 312-385.
- JSCE (1986). *Standard Specifications for Design and Construction of Concrete Structures, Part 1, Design*. JSCE (Japan Society of Civil Engineers), Tokyo, Japan.
- Kaminetzky, D. (1991). *Design and Construction Failures: Lessons from Forensic Investigations*. McGraw-Hill, Inc., USA.

- Karbhari, V.M. (2001). "Materials Considerations in FRP Rehabilitation of Concrete Structures." *Journal of Materials in Civil Engineering*, Vol. 13(2), pp. 90-96.
- Karbhari, V.M., Chin, J.W., Hunston, D., Benmokrane, B., Juska, T., Morgan, R., Lesko, J.J., Sorathia, U., and Reynaud, D. (2003). "Durability Gap Analysis for Fiber-Reinforced Polymer Composites in Civil Infrastructure." *Journal of Composites for Construction*, Vol. 7(3), pp. 238-247.
- Khalifa, A, Alkhrdaji, T., Nanni, A., and Lansburg, S. (1999). "Anchorage of Surface Mounted FRP Reinforcement." *Concrete International*, Vol. 21(10), pp. 49-54.
- Kinnunen, S and Nylander, H. (1960). "Punching of Concrete Slabs without Shear Reinforcement." *Transaction*, Royal Institute of Technology, Stockholm, No. 158.
- Kodur, V.R., Green, M.F., Bisby, L.A., and Williams, B. (2004). "Evaluating the Fire Performance of FRP-strengthened structures." *NRCC-47021*, National Research Council Canada, 5 pp.
- Lam, L. and Teng, J.G. (2001). "Strength of RC Cantilever Slabs Bonded with GFRP Strips." *Journal of Composites for Construction*, Vol. 5(4), pp. 221-227.
- Li, K.K.L. (2000). "Influence of size on punching shear strength of concrete slabs." *Master of Engineering thesis*, Department of Civil Engineering and Applied Mechanics, McGill University, Montreal, Canada.
- Liao, K., Schultheisz, C.R., Hunston, D.L., and Brinson, C.L. (1998). "Long-term Durability of Fiber-Reinforced Polymer-Matrix Composite Materials for Infrastructure Applications: A Review." *Journal of Advanced Materials*, Vol. 40(4), pp. 3-40.
- Limam, O., Foret, G., and Ehrlicher, A. (2003). "RC Two-way Slabs Strengthened with CFRP Strips: Experimental Study and a Limit Analysis Approach." *Composite Structures*, Vol. 60(4), pp. 467-471.
- Luo, Y. and Durrani, A.J. (1994). "Seismic Retrofit Strategy for Non-Ductile Flat-Plate Connections." *Proceedings*, 5th U.S. National Conference on Earthquake Engineering, Chicago, Illinois, July 1994, Vol.3, pp. 627-636.
- Magura, D.D. and Corley, W.G. (1969). "Tests to Destruction of a Multipanel Waffle Slab Structure." *Full-Scale Testing of New York World's Fair Structures*,

Volume II, The Rathskeller Structure, Publication 1721. Building Research Advisory Board, National Academy of Sciences, Washington, D.C., pp. 10-135.

Mahmood, K.F. (1978). "Bridge Slabs Supported on Columns." *MPhil. Thesis*, Polytechnic of Central London, London.

Martin, I. (1986). "Seismic Rehabilitation: Why, When, and How." *The Mexico Earthquakes – 1985: Factors Involved and Lessons Learned*, Proceedings of the International Conference, September 19-21, edited by Cassaro, M.A. and Romero, E.M., ASCE, New York, New York, pp. 396-408.

Martinez-Cruzado, J.A., Qaisrani, A.N., and Moehle, J.P. (1994). "Post-Tensioned Flat Plate Slab-Column Connections Subjected to Earthquake Loading." *Proceedings*, 5th U.S. National Conference on Earthquake Engineering, Chicago, Illinois, July 1994, pp. 139-148.

Marzouk, H. and Hussein, A. (1991). "Experimental Investigation on the Behavior of High-Strength Concrete Slabs." *ACI Structural Journal*, Vol. 88(6), pp. 701-713.

Marzouk, H. and Jiang, D. (1997). "Experimental Investigation on Shear Enhancement Types for High-Strength Concrete Plates." *ACI Structural Journal*, Vol. 94(1), pp. 49-58.

McHarg, P.J., Cook, W.D., Mitchell, D., and Yoon, Y.S. (2000). "Benefits of Concentrated Slab Reinforcement and Steel Fibers on Performance of Slab-column Connections." *ACI Structural Journal*, Vol. 97(2), pp. 225-234.

Megally, S. and Ghali, A. (2000). "Seismic Behavior of Slab-column Connections." *Canadian Journal of Civil Engineering*, Vol. 27(1), pp. 84-100.

Meier, U. (1997). "Post strengthening by continuous fiber laminates in Europe." *Non-metallic (FRP) Reinforcement for Concrete Structures, Proceedings of the Third International Symposium (FRPRCS-3)*, Sapporo, Japan, October 14-16, Vol. 1, pp. 41-56.

Meli, R. (1987). "Evaluation of Performance of Concrete Buildings Damaged by the September 19, 1985 Mexico Earthquake." *The Mexico Earthquakes – 1985: Factors Involved and Lessons Learned, Proceedings of the International Conference*, 19-21 September, edited by Cassaro, M.A. and Romero, E.M., ASCE, New York, New York, pp. 308-327.

- Meli, R. and Avila, J.A. (1989). "The Mexico Earthquake of September 19, 1985 – Analysis of Building Response." *Earthquake Spectra*, Vol. 5(1), pp. 1-17.
- Menetrey, P. (1995). "Simulation of Punching Failure: Failure Mechanism and Size-Effect." *Proceedings of Fracture Mechanics of Concrete Structures (FRAMCOS-2)*, ed. Folker H. Wittmann, Zurich, Switzerland, Vol. II, pp. 1229-1238.
- Menetrey, P. (1996). "Analytical Computation of the Punching Strength of Reinforced Concrete." *ACI Structural Journal*, Vol. 93(5), pp. 503-511.
- Mitchell, D., Tinawi, R., and Redwood, R.G. (1990). "Damage to Buildings Due to the 1989 Loma Prieta Earthquake – A Canadian Code Perspective." *Canadian Journal of Civil Engineering*, Vol. 17(5), pp. 813-834.
- Mitchell, D. Cook, W.D., and Dilger, W. (2005). "Effects of Size, Geometry and Material Properties on Punching Shear Resistance." *SP-232: Punching Shear in Reinforced Concrete Slabs*, ACI, pp. 39-56.
- Moe, J. (1961). "Shearing Strength of Reinforced Concrete Slabs and Footings under Concentrated Loads." *Bulletin D47*, Portland Cement Association Research and Development Laboratories, Skokie, Illinois, 130 pp.
- Moehle, J.P., Kreger, M.E., and Leon, R. (1988). "Background to recommendations for design of reinforced concrete slab-column connections." *ACI Structural Journal*, Vol. 85, pp. 636-644.
- Moehle, J.P. (1996) "Seismic Design Considerations for Flat Plate Construction." *Mete A. Sozen Symposium: A Tribute from his Students (SP-162)*, J.K. Wight and M.E. Kreger, eds., American Concrete Institute, pp. 1-34.
- Morrison, D.G., Hirasawa, I., and Sozen, M.A. (1983). "Lateral-load tests of R/C slab-column connections." *Journal of Structural Engineering*, Vol. 109(11), pp. 2698-2715.
- Mosallam, A.S. and Mosalam, K.M. (2003). "Strengthening of two-way concrete slabs with FRP composite laminates." *Construction and Building Materials*, Vol. 17(1), pp. 43-54.
- Mostafa, A.A.E.B. (2005). "Development of a New FRP Anchor for Externally Bonded CFRP Sheet/Laminate to Beams." *Master of Applied Science thesis*, Carleton University, Ottawa, Ontario, Canada, 201 pp.

- Nanni, A. (2003). "North American Design Guidelines for Concrete Reinforcement and Strengthening Using FRP: Principles, Applications, and Unresolved Issues." *Construction and Building Materials*, Vol. 17, pp. 439-446.
- Neale, K.W. (2000). "FRPs for Structural Rehabilitation: a Survey of Recent Progress." *Progress in Structural Engineering and Materials*, Vol.2, pp. 133-138.
- Nolting, D.M. (1984). "Das Durchstanzen Von Platten aus Stahlbeton – Tragverhalten, Berechnung, Bemessung." *Heft 62*, Institut für Baustoffe, Massivbau, und Brandschutz, Technischen Universität Braunschweig.
- Oller, E., Salcedo, J., Cobo, D., and Mari, A. (2001). "Flexural Strengthening of Reinforced Concrete Beams with Externally Bonded CFRP Laminates." *Proc. of Composite in Constructions*, Porto, Portugal, Figueiras et al. (eds.), pp. 473-478.
- Ospina, C.E., Alexander, S.D.B., and Cheng, J.J.R. (2001). "Behavior of concrete slabs with fibre-reinforced polymer reinforcement." *Structural Engineering Report No. 242*, Department of Civil and Environmental Engineering, University of Alberta, Edmonton.
- Pan, A.A. and Moehle, J.P. (1988). "Reinforced concrete flat-plates under lateral loading: An experimental study including biaxial effects" *Report No. UCB/EERC-88/16*, College of Engineering, University of California at Berkeley, 130 pp.
- Pan, A. and Moehle, J.P. (1989). "Lateral Displacement Ductility of Reinforced Concrete Flat Plates." *ACI Structural Journal*, Vol. 86(3), pp. 250-258.
- Pan, A.D. and Moehle, J.P. (1992). "An Experimental Study of Slab-column Connections." *ACI Structural Journal*, Vol. 89(6), pp.626-638.
- Park, R. and Gamble, W.L. (2000). *Reinforced Concrete Slabs*. 2nd edition, John Wiley & Sons, Inc.
- Pilakoutas, K. and Ioannou, C. (2000). "Verification of a Novel Punching Shear Reinforcement System for Flat Slabs." *Proceedings*, International Workshop on Punching Shear Capacity of RC Slabs, Stockholm, TRITA-BKN: Bulletin 57, pp. 135-143.
- Pilakoutas, K. and Li, X. (2003). "Alternative Shear Reinforcement for Reinforced Concrete Flat Slabs." *Journal of Structural Engineering*, Vol. 129(9), pp. 1164-1172.

- Pisanty, A. (2005). "Eurocodes and North American Codes Predictions of Punching Shear Capacity in View of Experimental Evidence." *SP-232: Punching Shear in Reinforced Concrete Slabs*, ACI, pp. 257-276.
- Polak, M.A. (2005). "Ductility of Reinforced concrete flat slab-column connections." *Computer-Aided Civil and Infrastructure Engineering*, Vol. 20, pp. 184-193.
- Polak, M.A., El-Salakawy, E., Hammill, N.L. (2005). "Shear Reinforcement for Concrete Flat Slabs." *SP-232: Punching Shear in Reinforced Concrete Slabs*, ACI, pp. 75-95.
- Ramos, A.M.P., Lucio, V.J.G., and Regan, P.E. (2000). "Repair and Strengthening Methods of Flat Slabs for Punching." *Proceedings*, International Workshop on Punching Shear Capacity of RC Slabs, Stockholm, Sweden, TRITA-BKN: Bulletin 57, pp. 125-133.
- Rankin, G.I.B. and Long, A.E. (1987). "Predicting the Punching Strength of Conventional Slab-column specimens" *Proceedings of the Institution of Civil Engineers*, Part 1 Design and Construction, Vol. 82, pp. 327-346.
- Rasmussen, B.H. (1963). "Betonindstobte tvaerbelastede boltes og dornes baereevne (Strength of transversely loaded bolts and dowels cast in concrete)." *Bygningsstatistiske Meddelelser*, Vol. 34(2).
- Regan, P.E. (1981). "Behavior of Reinforced Concrete Flat Slabs." *CIRIA Report 89*, Construction Industry Research and Information Association, London, 89 pp.
- Regan, P.E. (1985). "Shear Combs, Reinforcement Against Punching," *The Structural Engineer*, Vol. 63B(4), pp. 76-84.
- Regan, P.E., and Braestrup, M.W. (1985). "Punching Shear in Reinforced Concrete: A state of art report." *Bulletin d'information*, No.168, Comite Euro-International du Beton.
- Regan, P.E. and Samadian, F. (2001). "Shear Reinforcement Against Punching in Reinforced Concrete Flat Slabs." *The Structural Engineer*, Vol. 79(10), pp. 24-31.
- Richart, F.E. (1948). "Reinforced Concrete Wall and Column Footings, Part 1." *Journal of the American Concrete Institute*, Vol. 20(2), pp. 97-127.
- Richart, F.E. (1948). "Reinforced Concrete Wall and Column Footings, Part 2." *Journal of the American Concrete Institute*, Vol. 20(3), pp. 237-260.

Robertson, I.N and Durrani, A.J. (1992). "Gravity Load Effect on Seismic Behavior of Interior Slab-Column Connections." *ACI Structural Journal*, Vol. 89(1), pp. 37-45.

Robertson, I.N. and Johnson, G. (2001). "Repair of slab-column connections using CFRP." *Earthquake Resistant Engineering Structures III*, WIT Press, UK, pp. 505-514.

Robertson, I.N., Kawai, T., Lee, J., and Enomoto, B. (2002). "Cyclic Testing of Slab-Column Connections with Shear Reinforcement." *ACI Structural Journal*, Vol. 99(5), pp. 605-613.

Robertson, I.N. and Johnson, G. (2004). "Repair of slab-column connections using epoxy and Carbon Fiber Reinforced Polymer." *Journal of Composites for Construction*, Vol. 8(5), pp. 376-383.

Rodriguez, M. and Diaz, C. (1989). "The Mexico Earthquake of September 19, 1985 – Analysis of the Seismic Performance of a Medium Rise, Waffle Flat Plate Building." *Earthquake Spectra*, Vol. 5(1), pp. 25-40.

Rosenblueth, E. and Meli, R. (1986). "The 1985 Earthquake: Causes and Effects in Mexico City." *Concrete International*, Vol. 8(5), pp. 23-34.

Sabol, T.A. (1994). "Flat Slab Failure in Ductile Concrete Frame Building," *1994 Northridge Earthquake Buildings Case Studies Project*, Seismic Safety Commission, Sacramento, CA, pp. 167-187.

Salna, R., Marciukaitis, G., and Vainiunas, P. (2004). "Estimation of Factors Influencing the Punching Shear Strength of RC Floor Slabs." *Journal of Civil Engineering and Management*, Vol. 10(2), pp. 137-142.

Seible, F., Ghali, A., Dilger, W.H. (1980). "Preassembled shear reinforcing units for flat plates." *ACI Journal Proceedings*, Vol. 77(1), pp. 28-35.

Shehata, I.A.M. and Regan, P.E. (1989). "Punching in R.C Slabs." *Journal of Structural Engineering*, Vol. 115(7), pp. 1726-1740.

Sheikh, S.A. (2002). "Performance of Concrete Structures Retrofitted with Fibre Reinforced Polymers." *Engineering Structures*, Vol. 24, pp. 869-879.

Sherif, A.G. and Dilger, W.H. (1996). "Critical Review of the CSA A23.3-94 Punching Shear Strength Provisions for Interior Columns." *Canadian Journal of Civil Engineering*, Vol. 23, pp. 998-1101.

- Sozen, M.A. (2006). "The Building of a Building Code: The Tension between Theory and Observation." *Concrete International*, Vol. 28(5), pp. 45-50.
- Stark, A.D. (2003). "Seismic upgrade of flat-plate slab-column connections using carbon fiber reinforced polymer stirrups." *Master's thesis*, Department of Civil and Environmental Engineering, University of Texas at Austin, Austin, Texas, 216 pp.
- Stark, A., Binici, B., and Bayrak, O. (2005). "Seismic upgrade of reinforced concrete slab-column connections using carbon fiber-reinforced polymers." *ACI Structural Journal*, Vol. 102(2), pp. 324-333.
- Talbot, A.N. (1913). "Reinforced Concrete Wall Footings and Column Footings." *Bulletin No.67*, University of Illinois, Engineering Experiment Station, Urbana, Illinois, 114 pp.
- Tan, K.H. (2000). "Punching Shear Strength of RC Slabs Bonded with FRP Systems." *Proceedings*, Advanced Composite Materials in Bridges and Structures: 3rd International Conference, Ottawa, Ontario, Canada, August 15-18, 2000, pp. 387-394.
- Tankut, A.T. (1969). "The Behavior of the Reinforced Concrete Flat-plate Structures Subjected to Various Combinations of Vertical and Horizontal Loads." *PhD Thesis*, University of London.
- Teng, J.G., Lam, L., Chan, W., and Wang, J. (2000). "Retrofitting of Deficient RC Cantilever Slabs using GFRP Strips." *Journal of Composites for Construction*, Vol. 4(2), pp. 75-84.
- Teng, J.G., Chen, J.F., Smith, S.T., and Lam, L. (2002). *FRP-strengthened RC Structures*. John Wiley & Sons, Ltd., West Sussex, England.
- Teng, J.G., Smith, S.T., Yao, J., and Chen, J.F. (2003). "Intermediate crack-induced debonding in RC beams and slabs." *Construction and Building Materials*, Vol.17, pp.447-462.
- Tian, Y. (2006). "Behavior and Modeling of Reinforced Concrete Slab-column Connections." *PhD dissertation*, Department of Civil and Environmental Engineering, University of Texas at Austin, Austin, Texas.
- Triantafillou, T.C. (1998). "Strengthening of Structures with Advanced FRPs." *Progress in Structural Engineering and Materials*, Vol.1(2), pp. 126-134.

- Van der Voet, A.F., Dilger, W.H., and Ghali, A. (1982). "Concrete Flat Plates with Well-anchored Shear Reinforcement Elements." *Canadian Journal of Civil Engineering*, Vol. 9, pp. 107-114.
- Van Dusen, M.H. (1985). "Unbalanced Moment and Shear Transfer at Slab-Column Connections: Literature Review." *Master of Engineering thesis*, Department of Civil Engineering, University of Toronto, Toronto, Canada, September 1985.
- Vanderbilt, M.D. (1972). "Shear strength of continuous plates." *Journal of the Structural Division*, Vol. 98(ST5), pp. 961-973.
- Wey, E.H. and Durrani, A.J. (1992). "Seismic Response of Interior Slab-Column Connections with Shear Capitals." *ACI Structural Journal*, Vol. 89(6), pp. 682-691.
- Whitney, C.S. (1957). "Ultimate Shear Strength of Reinforced Concrete Flat Slabs, Footings, Beams, and Frame Members Without Shear Reinforcement" *Journal of the American Concrete Institute*, Vol. 29(4), pp. 265-298.
- Yagi, K., Tanaka, T., Sakai, H., and Otaguro, H. (1997). "Durability of Carbon Fiber Sheet for Repair and Retrofitting." *Non-metallic (FRP) Reinforcement for Concrete Structures, Proceedings of the Third International Symposium (FRPRCS-3)*, Sapporo, Japan, October 14-16, Vol. 2, pp. 259-266.
- Yamada, T., Nanni, A., and Endo, K. (1992). "Punching Shear Resistance of Flat Slabs: Influence of Reinforcement Type and Ratio." *ACI Structural Journal*, Vol. 89(4), pp. 555-563.
- Yitzhaki, D. (1966). "Punching Strength of Reinforced Concrete Slabs." *Journal of the American Concrete Institute*, Vol. 63(5), pp. 527-540.
- Zaghloul, A. (2002). "Behavior and Strength of CFRP Reinforced Flat Plate Interior Column Connections Subjected to Shear and Unbalanced Moments." *Master of Applied Science thesis*, Department of Civil and Environmental Engineering, Carleton University, Ottawa, Canada, 281 pp.